Atmospheric Environment 44 (2010) 4678–4734

Contents lists available at ScienceDirect

Atmospheric Environment

journal homepage: www.elsevier.com/locate/atmosenv

Transport impacts on atmosphere and climate: Aviation

D.S. Lee [a,*], G. Pitari [b], V. Grewe [c], K. Gierens [c], J.E. Penner [d], A. Petzold [c], M.J. Prather [e], U. Schumann [c], A. Bais [f], T. Berntsen [g], D. Iachetti [b], L.L. Lim [a], R. Sausen [c]

[a] Dalton Research Institute, Department of Environmental and Geographical Sciences, Manchester Metropolitan University, Chester Street, Manchester M1 5GD, UK
[b] Dipartimento di Fisica, University of L'Aquila, Vio Vetoio Località Coppito, 67100 l'Aquila, Italy
[c] Deutsches Zentrum für Luft- und Raumfahrt (DLR), Institut für Physik der Atmosphäre, Oberpfaffenhofen, D-82234 Wessling, Germany
[d] Department of Atmospheric, Oceanic and Space Sciences, University of Michigan, 2455 Hayward St., Ann Arbor, MI 48109-2143, USA
[e] Department of Earth System Science, University of California, Irvine, 3329 Croull Hall, CA 92697-3100, USA
[f] Laboratory of Atmospheric Physics, Aristotle University of Thessaloniki, Thessaloniki, Greece
[g] Department of Geosciences, University of Oslo, PO Box 1022 Blindern, 0315, Oslo, Norway

ARTICLE INFO

Article history:
Received 5 August 2008
Received in revised form
30 May 2009
Accepted 2 June 2009

Keywords:
Aviation
Climate
Ozone depletion
Radiative forcing

ABSTRACT

Aviation alters the composition of the atmosphere globally and can thus drive climate change and ozone depletion. The last major international assessment of these impacts was made by the Intergovernmental Panel on Climate Change (IPCC) in 1999. Here, a comprehensive updated assessment of aviation is provided. Scientific advances since the 1999 assessment have reduced key uncertainties, sharpening the quantitative evaluation, yet the basic conclusions remain the same. The climate impact of aviation is driven by long-term impacts from CO_2 emissions and shorter-term impacts from non-CO_2 emissions and effects, which include the emissions of water vapour, particles and nitrogen oxides (NO_x). The present-day radiative forcing from aviation (2005) is estimated to be 55 mW m^{-2} (excluding cirrus cloud enhancement), which represents some 3.5% (range 1.3–10%, 90% likelihood range) of current anthropogenic forcing, or 78 mW m^{-2} including cirrus cloud enhancement, representing 4.9% of current forcing (range 2–14%, 90% likelihood range). According to two SRES-compatible scenarios, future forcings may increase by factors of 3–4 over 2000 levels, in 2050. The effects of aviation emissions of CO_2 on global mean surface temperature last for many hundreds of years (in common with other sources), whilst its non-CO_2 effects on temperature last for decades. Much progress has been made in the last ten years on characterizing emissions, although major uncertainties remain over the nature of particles. Emissions of NO_x result in production of ozone, a climate warming gas, and the reduction of ambient methane (a cooling effect) although the overall balance is warming, based upon current understanding. These NO_x emissions from current subsonic aviation do not appear to deplete stratospheric ozone. Despite the progress made on modelling aviation's impacts on tropospheric chemistry, there remains a significant spread in model results. The knowledge of aviation's impacts on cloudiness has also improved: a limited number of studies have demonstrated an increase in cirrus cloud attributable to aviation although the magnitude varies: however, these trend analyses may be impacted by satellite artefacts. The effect of aviation particles on clouds (with and without contrails) may give rise to either a positive forcing or a negative forcing: the modelling and the underlying processes are highly uncertain, although the overall effect of contrails and enhanced cloudiness is considered to be a positive forcing and could be substantial, compared with other effects. The debate over quantification of aviation impacts has also progressed towards studying potential mitigation and the technological and atmospheric tradeoffs. Current studies are still relatively immature and more work is required to determine optimal technological development paths, which is an aspect that atmospheric science has much to contribute. In terms of alternative fuels, liquid hydrogen represents a possibility and may reduce some of aviation's impacts on climate if the fuel is produced in a carbon-neutral way: such fuel is unlikely to be utilized until a 'hydrogen economy'

* Corresponding author. Tel.: +44 161 247 3663.
E-mail address: D.S.Lee@mmu.ac.uk (D.S. Lee).

1352-2310/$ – see front matter
doi:10.1016/j.atmosenv.2009.06.005

develops. The introduction of biofuels as a means of reducing CO_2 impacts represents a future possibility. However, even over and above land-use concerns and greenhouse gas budget issues, aviation fuels require strict adherence to safety standards and thus require extra processing compared with biofuels destined for other sectors, where the uptake of such fuel may be more beneficial in the first instance.

1. Introduction

This report constitutes the aviation assessment component of the European 6th Framework project 'ATTICA', the '*European Assessment of Transport Impacts on Climate Change and Ozone Depletion*'. Partner assessments of surface transportation, shipping, and climate metrics are given by Uherek et al. (2009), Eyring et al. (2009), and Fuglestvedt et al. (2010), respectively.

Previously, the most complete and up to date assessment of aviation's impacts on climate change and ozone (O_3) depletion was that undertaken by the Intergovernmental Panel on Climate Change (IPCC) and published as a Special Report; '*Aviation and the Global Atmosphere*' (IPCC, 1999). The IPCC (1999) report had been preceded by a number of assessments of the effects of subsonic aviation on the atmosphere, e.g. Wahner et al. (1995), Friedl (1997) and Brasseur et al. (1998). Over the last 15 years or so, there has been considerable activity investigating aviation's effects on the global atmosphere in national and international research programmes, including dedicated efforts for the IPCC (1999) report. Shortly before the completion of the IPCC (1999) assessment, Boeing announced that it no longer intended to pursue development of a large supersonic aircraft, largely on grounds of economics and noise impacts. In addition, the aeronautics program at NASA was folded into the space shuttle program. The pioneering dedicated research programmes by NASA into effects from both potential future supersonic fleets and subsonic aviation were terminated.

In Europe, however, the main findings of the IPCC (1999) report, and in particular the magnitude of the non-CO_2 RF effects, estimated by the IPCC (1999) to be 63% of the total radiative effect from aviation in 1992 (excluding cirrus cloud enhancement), provided a springboard from which a number of research programmes into atmospheric science and 'green' aeronautical technology were initiated under the European Commission's Fifth Framework Programme. These programmes include: PartEmis, NEPAIR, TRADEOFF, INCA, AERO2K, METRIC, SCENIC and CRYOPLANE (see Appendix I). The bulk of the efforts of these programmes were directed at subsonic effects/technology, with the exception of SCENIC and minor components of TRADEOFF. CRYOPLANE focussed on the potential for future liquid hydrogen (LH_2) powered aircraft. In addition, a number of other related European Fifth Framework Projects were initiated studying the nitrogen budget in the upper troposphere from natural sources, especially lightning (LINOX, EULINOX, TROCCINOX), which have been summarized by Schumann and Huntrieser (2007). European Commission research efforts into aviation effects have continued through the Sixth Framework Integrated Project 'QUANTIFY', which runs until 2009.

By convention, the interest in aviation's impacts on climate change and ozone depletion are thought to date back some 40 years to the late 1960s when the US and UK were developing ideas for supersonic aircraft and concerns were raised over stratospheric O_3 depletion (Johnston, 1971). However, there is evidence dating back to the early 1960s of awareness that air traffic might modify climate through contrails (condensation trails) (Osmundsen, 1963). The possibility that aviation might affect tropospheric O_3 and climate appears to have been first considered during the early stratospheric assessments undertaken in the US, UK and France in the early to mid 1970s (e.g. the CIAP, COMESA and COVOS programmes) with the increasing recognition that tropospheric O_3 was a climate warming gas (Ramanathan and Dickinson, 1979; Wang et al., 1980; Lacis and WuebblesLogan, 1990). The earliest paper that identifies aircraft NO_x increasing tropospheric O_3 is not clear but early literature includes Hidalgo (1977), Hidalgo and Crutzen (1977) and Widhopf et al. (1977) following earlier recognition of a 'cross-over' from O_3 production from NO_x in the troposphere to O_3 destruction in the stratosphere by Johnston and Quitevis (1974).

After initial concerns over potential stratospheric O_3 depletion in the early 1970s from a proposed large fleet of supersonic aircraft (which was never developed), attention shifted in the early 1990s to O_3 enhancement in the upper troposphere and lower stratosphere (UT/LS) (where O_3 is a strong greenhouse gas) resulting from subsonic aircraft emissions of NO_x ($NO + NO_2$) (Johnston et al., 1991). Subsequently, much research has been focussed over the last 10 years on contrails and cirrus cloud enhancement. The IPCC (1999) report pointed out that the potential contribution from subsonic aviation for a range of 2050 scenarios could be between 3 and 7% of total radiative forcing, excluding cirrus cloud enhancement (Chapter 6; Prather et al., 1999). The IPCC Fourth Assessment Report considered aviation but only briefly: Working Group 1 (IPCC, 2007a) provided a short overview of literature on contrails and cirrus cloud enhancement (Chapter 2; Forster et al., 2007a) and Working Group 3 (IPCC, 2007b) reviewed technological mitigation potential (Chapter 5; Kahn-Ribeiro et al., 2007).

Sufficient concerns remain both in terms of the science and the policy (principally because of the historically strong growth rate of aviation and the fact that international aviation is not included in the Kyoto Protocol) over the potential magnitude of future aviation emissions and their contribution to climate change. Thus, a further state-of-the-art assessment updating that of IPCC (1999) was considered necessary, since much important material has been published since then.

The ATTICA aviation assessment focuses on the science: in terms of the policy, only the backdrop of aviation's impacts with respect to other sources and its potential growth in emissions will be addressed. Questions as to whether, why and how aviation emissions should be addressed through policy action are not covered here, although the metrics by which aviation emissions and their effects may be compared with those from other sources is an ongoing scientific debate, covered in more detail by the ATTICA climate metric assessment (Fuglestvedt et al., 2009) but also briefly dealt with here for completeness.

2. The effects of aviation on climate change and ozone depletion

The climate impact of current and potential future aviation is, by convention, quantified using the metric 'radiative forcing of climate', since many climate experiments have found an approximately linear relationship between a change in global mean radiative forcing (RF) and a change in global mean surface temperature (ΔT_s), when the system has reached a new equilibrium, with some proportionality constant, i.e.

$$\Delta T_s \approx \lambda \mathrm{RF} \quad (1)$$

where λ is the climate sensitivity parameter (K (W m^{-2})$^{-1}$), the value of which has been found to be model specific but stable across

forcings. However, a number of recent studies have shown that λ may vary between forcing agents and result in a stronger or weaker temperature change than for other climate gases (e.g. Hansen et al., 1997, 2005; Forster and Shine, 1997; Stuber et al., 2005). This is dealt with in more detail in Section 8.

According to the current consensus state of knowledge, subsonic aviation affects climate in the following ways, in terms of radiative forcing:

- emissions of CO_2 result in a positive RF (warming);
- emissions of NO_x result in the formation of tropospheric O_3 via atmospheric chemistry, with a positive RF (warming);
- emissions of NO_x result in the destruction of ambient methane (CH_4), also via atmospheric chemistry, with a negative RF (cooling), which is accompanied by a parallel, decadal loss of tropospheric O_3 (Wild et al., 2001);
- emissions of sulphate particles arising from sulphur in the fuel result in a negative (direct) RF (cooling);
- emissions of soot particles result in a (direct) positive RF (warming);
- the formation of persistent linear contrails that may form (depending upon atmospheric conditions) in the wake of an aircraft result in both positive and negative RF effects but overall, cause a positive RF effect (warming);
- the formation of contrail-cirrus cloud from spreading contrails similarly to line shaped-contrails results in both positive and negative RF effects but overall, is considered to cause a positive RF effect (warming);
- a sub-component of aviation-induced cirrus is a mechanism whereby soot particles seed cirrus clouds (or 'soot-cirrus[1]'; Jensen and Toon, 1997). This is different from the so-called 'Twomey effect' (Twomey, 1974, 1977) in that soot may either increase or decrease the number of ice particles and impact upon both the albedo and the emissivity of cirrus clouds. This effect may result in either positive or negative RF effects (warming/cooling) but is rather uncertain over the sign and proven existence of the effect (see section 7). (Penner et al., 2009).

In terms of supersonic aircraft flying in the stratosphere, the effects of emissions of NO_x have been investigated for a considerable period of time and found to deplete stratospheric O_3 (see section 6). The depletion of stratospheric O_3 is usually considered in terms of the 'column change' in O_3, measured in terms of Dobson Units (i.e. the thickness of a layer in units of 10^{-3} cm that would be formed by O_3 in a column at a pressure of 10^5 Pa and at 0 °C). Emissions from supersonic aircraft also have potential effects on climate, depending on a number of factors (e.g. cruise altitude) but particularly fleet size; effects on O_3 depletion and climate are summarized below:

- emissions of CO_2 result in a positive RF (warming);
- emissions of NO_x result in destruction or increase of stratospheric O_3 via atmospheric chemistry, depending upon altitude: above about 20 km, models always predict O_3 destruction (see Section 6.3). Using chemical kinetics data from Sander et al. (2000) or more recent (Sander et al., 2003), CTMs predict a net O_3 column decrease, larger than in IPCC (1999), with a global negative RF (cooling);
- emissions of H_2O result in a positive RF (warming): this is by far the dominant RF term for supersonic aircraft; an indirect (small) negative correction is obtained via O_3 chemistry (through additional formation of HO_x and consequent O_3 destruction);
- emissions of NO_x result in the destruction of ambient methane (CH_4), via atmospheric chemistry, with a negative RF (cooling) although this is negligible in the stratosphere;
- emissions of sulphate particles arising from sulphur in the fuel result in negative RF (cooling): an indirect effect occurs via heterogeneous chemistry; in this case more NO_x is lost towards nitric acid (HNO_3) and the O_3 destruction/increase is decreased in magnitude; in addition, the lower stratospheric O_3 increase due to NO_x emissions may change into destruction due to increasing Cl_x and Br_x (since chlorine and bromine nitrates will decrease): the net effect on O_3 is dependent upon altitude and model transport, as well as the sign of this indirect sulphate-related RF;
- emissions of soot result in positive RF (warming);
- the formation of persistent linear contrails that may form (depending upon atmospheric conditions) results in both positive and negative RF effects but overall, cause a positive RF effect (warming);
- the formation of contrail-cirrus cloud from spreading contrails is considered to result in a positive RF (warming).

These latter two effects of supersonic aircraft on contrails and cirrus cloudiness depend critically on cruise altitude: in the dry stratosphere, persistent contrails will not form, except possibly in the tropics where the tropopause is much higher and may therefore allow contrail formation at cruise altitudes of 18–20 km (Stenke et al., 2008).

3. Aviation emissions

3.1. Emission species

An aircraft exhaust plume contains species emitted by the engines, species formed in the plume from emitted species and atmospheric species that become entrained into the plume. The majority of the emitted species (gases and soot particles) are produced by combustion of kerosene with ambient air in the combustion chamber of the engine. In addition, some emitted species may originate from oil (Dakhel et al., 2005) and from the erosion of metal parts (Petzold et al., 1998; Demirdjian et al., 2007) and small amounts of metals (e.g. Fe, Cu, Zn) that may be present in the fuel (Lewis et al., 1999).

The fuel mostly used in civil aviation is kerosene. A number of types of kerosene are in common usage, the most common being Jet A-1which has a maximum freezing point of −47 °C, for which the mean C/H ratio is $C_{12}H_{23}$. Jet A, which has a maximum freezing point of −40 °C is in common usage in the US. All aviation fuels have stringent specifications that cover their physical properties, chemical composition, and performance (Lewis et al., 1999).

Combustion of kerosene produces mostly CO_2 and H_2O (see Table 1). These emissions are directly relevant as greenhouse gases (GHG), or the latter as a contrail precursor. Besides these gases, numerous trace species are formed including NO, NO_2, SO_2, CO, hydrocarbons (HCs), and soot particles. Nitrogen oxide emissions are relevant for photochemical O_3 formation. In the plume, large NO fractions cause initial local O_3 reductions, which then relax back to ambient values with mixing (Kraabøl et al., 2000a,b). Subsequently, the NO forms NO_2 via peroxy radicals which then may be photolysed, forming atomic oxygen which reacts with molecular O_2

[1] The concept of aviation seeding cirrus clouds, i.e. without initial spreading contrails has been discussed for some time (see SMIC, 1971): the expression 'soot cirrus' is a neologism of Schumann (2006); '*Climate change impact of air traffic*', paper presented at 25th International Congress of the Aeronautical Sciences, DGLR, Hamburg, proceedings available from DGLRhttp://www.icas2006.org/index2.php, paper number 199, 7 pp.

Table 1
Fuel consumption and emitted species, mean emission indices (mass of emissions per unit mass of burned fuel, for the fleet of aircraft in 2000) total emission rates due to aviation and for comparison emission rates from other sources (extended from IPCC, 1999). Fuel consumption is based on data from the International Energy Agency (IEA, 2007). Mean emission indices for NO_x, CO, soot and HC are taken from 2002 fleet averages computed within AERO2K (Eyers et al., 2005) and SAGE (Kim et al., 2007).

Species	Emission index, g kg^{-1} (ranges)	Emission rate (2004) in Tg yr^{-1}	Comparable emission rate, Tg yr^{-1}	Comparable emission source
Kerosene		224 (180–224)	3817	Total petrol production (IEA, 2007)
CO_2	3160	700	26,500	Total anthropogenic CO_2 emissions (Marland et al., 2006)
H_2O	1240	275	45	Methane oxidation in the stratosphere
			525,000	Evaporation of H_2O from Earth's surface
NO_x	14 (12–17)	3	2.9 ± 1.4	Stratospheric sources
			17 ± 10	Lightning (Schumann and Huntrieser, 2007)
			170 ± 20	Total source
Soot	0.025 (0.01–0.05)	0.006	12	Combustion of fossil fuels and biomass
SO_2	0.8 (0.6–1.0)	0.18	130	Total source from burning fossil fuels
			20–100	Natural sources
			5.4, 8.0	Non-eruptive, eruptive volcanoes
CO	3 (2–3)	0.67	1500	Total anthropogenic sources
HC	0.4 (0.1–0.6)	0.09	90	Total anthropogenic sources

to form O_3. Carbon monoxide and HC emissions from aircraft are of relevance to air quality, mainly near airports.

Among the emitted gases and gaseous products formed in the very young plume are condensable gases (Table 2). These may undergo condensation in the young plume leading to volatile aerosol particles and volatile coating of soot. Such particles, if large enough, may themselves act as condensation nuclei or may interact with soot to form condensation nuclei. The liquid droplets formed may freeze homogeneously and soot may act as nucleus for heterogeneous ice nucleation, and hence has an important role in the formation of contrails and perhaps even cirrus clouds. The ice nucleation properties of soot are sensitive to sulphuric acid coating (Möhler et al., 2005). Therefore, condensable gases present in a young exhaust plume are of considerable interest. Whereas contrail formation is insensitive to the particles and trace gases emitted (Schumann, 1996; Gierens, 2007a,b), the optical properties of the contrails and the resultant cirrus changes are expected to depend on particle and trace gas emissions (Kärcher et al., 2007).

3.2. Gas-phase species

3.2.1. Carbon containing species

The most abundant C-containing gas emitted from aircraft engines is CO_2 (3160 ± 60 g kg^{-1} for complete combustion; see Table 1). Minor C-containing gases include CO and various HCs (e.g Spicer et al., 1994; Slemr et al., 1998; Anderson et al., 2006), see Table 1.

Emissions of CO and HCs are generally the result of incomplete combustion and as such, their emission indices (EI, g kg^{-1} fuel) are greater at lower power conditions. Emissions of CO and HC are part of the International Civil Aviation Organization (ICAO) engine emissions certification testing regime but the HC measurements are total and not speciated (nor are they corrected for background). Hydrocarbon emissions from aircraft gas turbines have been measured in the context of air quality investigations, their potential role in tropospheric O_3 formation and their potential to form volatile particles.

Most measurements of HCs have been made at ground conditions (Anderson et al., 2006; Herndon et al., 2006; Knighton et al., 2007; Yelvington et al., 2007), whereas only a very limited number of measurements have been made at cruise conditions (Simpson et al., 2000; Slemr et al., 2001) or in test rigs (Kurtenbach et al., 2003). All studies, including older ones (e.g. Spicer et al., 1994) have found that HC emissions are a strong function of engine power, decreasing with increasing thrust. At ground conditions, Yelvington et al. (2007) found that HC emissions decreased with increasing ambient temperature (range approximately 11–30 °C). Measurements in engine exhaust have identified that HC emissions comprise a range of relatively light HCs (C_2–C_6), including alkanes and alkenes, and formaldehyde, methanol, ethylene, acetaldehyde, acetic acid, benzene, toluene, phenol, styrene, naphthalene and methylnaphthalenes (Slemr et al., 2001; Knighton et al., 2007; Yelvington et al., 2007). The EIs for the HC species measured tend to be quite variable even for the same approximate thrust conditions, depending upon engine and ambient temperature. There seems to be some evidence for a shift of speciation with thrust condition of the engine from a predominance of light HC species at lower thrust to heavier (C_4 plus) species at higher thrust (Anderson et al., 2006). Knighton et al. (2007) report a scaling of speciation with thrust but they measured mostly higher (C_4 plus) HCs so that this result is not necessarily at odds with those of Anderson et al. (2006).

Some of the low volatility hydrocarbons are thought to be involved in aerosol formation and even more pronounced in aerosol growth on existing particle nuclei (Yu and Turco, 1999). Low volatility hydrocarbons, including oxygenated hydrocarbons and organic acids have been identified (Kiendler et al., 2000a,b; Petzold et al., 2005a; Sorokin and Arnold, 2006). The importance of condensable organic matter for particle growth was deduced from the large volume of volatile aerosol found in aircraft plumes even when the aircraft burned fuel with very low sulphur content (Kärcher et al., 1998a; Yu and Turco, 1999; Schumann et al., 2002).

Table 2
Equivalent emission indices for condensable gases (excluding H_2O), soot and hydroxyl radicals emitted by aircraft engines or formed in the very young exhaust plume (Schumann and Ström, 2001; Eyers et al., 2005).

Species	Emission index ranges (g kg^{-1})[a]	Source
Soot	0.025 (0.01–0.1)[b]	Fuel carbon
H_2SO_4	0.04 (0.01–0.1)[c]	Fuel sulphur $SO_2 + OH$, $SO_2 + O$
HNO_2[d]	0.08–0.8	Fuel- and air-nitrogen passed through combustor, $NO + OH$
HNO_3[d]	0.003–0.3	Fuel- and air-nitrogen passed through combustor, $NO_2 + OH$
OH	0.1–0.5[e]	Combustion
Low volatility hydrocarbons	≈0.01–0.02[f]	Fuel carbon
Volatile aerosol particles	0.0065–0.05[g]	Condensable gases

[a] Equivalent emission index.
[b] Modern engines have a soot emission index of about 0.01 g soot kg^{-1} fuel.
[c] For a mean fuel sulphur content of 400 μg g^{-1} and a measured efficiency $\varepsilon = 0.033$ for fuel sulphur conversion to H_2SO_4. Commonly used fuel sulphur content values range from 10 to 1000 μg g^{-1} (upper limit 3000 μg g^{-1}).
[d] Condensable only in very cold, lower stratosphere (see text). ($T \leq 200$ K).
[e] Inferred from measurements with chemical plume models.
[f] Inferred from measurements (see text) and from Kärcher et al. (2000). Very uncertain.

3.2.2. Nitrogen containing species

The most abundant N-containing gases emitted are NO and NO_2 (see Tables 1 and 2). The ICAO emissions databank (ICAO ANNEX 16) provides $EINO_x$ (g NO_2 kg^{-1} fuel) data for in-production and older engines on certification for thrust settings representing idle, taxi, take-off and approach. Simple predictive algorithms according to fuel flow have been developed to represent these emissions at cruise by Boeing, DLR and others (Baughcum et al., 1996; DuBois and Paynter, 2006; Deidewig et al., 1996; Tsague et al., 2006). In addition, $EINO_x$ values have also been independently determined from ground tests and aircraft at cruise and compared with the ICAO data. Minor higher oxidized N species, such as nitrous and nitric acids (HNO_2, HNO_3) have been determined in specific experiments.

Emission factors for NO_x from aircraft at cruise and the NO/NO_x ratio have been derived from airborne measurements of NO and NO_2 and model analysis together with CO_2 measurements (Schulte and Schlager, 1996; Schulte et al., 1997; Schäfer et al., 2000). Ground measurements sampling directly behind an engine show that primary NO_2 (i.e. directly emitted) represents up to 80% of the total NO_x emissions for a modern engine at low powers, but this fraction decreases to 7% at the highest thrust setting (Wormhoudt et al., 2007). A study of airport operations indicated values of 28–35% (Herndon et al., 2004) but these values are subject to uncertainties of NO to NO_2 conversion in the plumes and an undefined range of operations at the airport. At cruise, a best-estimate of 0–15% was derived, and this value seems to be engine dependent (Schulte et al., 1997). A combustion modelling study indicated that primary NO_2 may be of the order 25–50% for idle, and 1–9% for higher thrust conditions of take-off and climb out (Garcia-Naranjo and Wilson, 2005).

A small fraction of the N gases emitted includes HNO_2 and HNO_3 (Table 2), which are formed via reaction of OH with NO and NO_2 respectively. Both HNO_2 and HNO_3 have been measured by chemical ionisation mass spectrometry in aircraft exhaust plumes at cruise altitudes (Arnold et al., 1992; Tremmel et al., 1998; Miller et al., 2003) and with optical methods at ground (Wormhoudt et al., 2007). The equivalent emission indices derived from these data are listed in Table 1. The emission index for HNO_2 depends on engine type and engine thrust (Wormhoudt et al., 2007). There is some evidence that the emission indices for HNO_2 and HNO_3 may be smaller for older military-type engines (Miller et al., 2003; Brundish et al., 2007) than for more modern civil engines (Wormhoudt et al., 2007).

Among the N gases, HNO_3 is a condensable gas under conditions of very low plume temperatures (<200 K) and when the humidity is low so that water-ice does not yet form (Meilinger et al., 2005) In addition, some HNO_3 may be taken-up by H_2SO_4/H_2O aerosols (Kärcher, 1996; Romakkaniemi et al., 2004) and by contrail particles at high relative humidity and at temperatures below 222 K (Gleitsmann and Zellner, 1999). Shonija et al. (2007) have also argued that HNO_3 may contribute to the activation of soot particles, which is usually considered to be mediated by H_2SO_4. Measurements in cirrus clouds indicate uptake of several percent of the HNO_3 by ice clouds depending on ambient temperature (Voigt et al., 2006, 2007). This uptake may impact the NO_x–O_3 chemistry and the cirrus properties.

3.2.3. Hydrogen-containing species

Besides H_2O (1230 ± 20 g kg^{-1} for completely burnt fuel), minor emitted H-containing gases include HCs, OH, HO_2 and H_2O_2, and possibly H_2. Most OH formed in the combustor is consumed by self-reaction or reactions with NO etc. before reaching the engine exit (Böckle et al., 1999). The emission index of OH has been deduced from measured HONO, HNO_3, NO, and NO_2 concentrations in exhaust plumes using a chemical model including plume dilution for a limited number of aircraft during the POLINAT campaigns (Schumann et al., 2000), see Table 2. The data include two cases of encounters with plumes of B747s at cruise, which were studied in detail by Tremmel et al. (1998) for which OH emission indices of 0.32–0.39 g kg^{-1} (fuel) which corresponds to an OH concentration at the combustor exit of 9.0–14.4 ppmv or 0.3–0.7 ppmv at the engine exit: these are similar to previous results obtained by measurements in the plume of a Concorde and ER-2 (Hanisco et al., 1997). Direct measurements of OH were made behind an engine simulator rig in the European PartEmis project (Wilson et al., 2004) using laser induced fluorescence (LIF) but yielded much lower values $\sim 2 \times 10^{10}$ molecules cm^{-3} (1.2 ppbv) than implied by the plume encounters. This large discrepancy may be caused by consumption of OH already between the combustor and the engine exit. This difference is important since the OH radical is indirectly involved in aerosol formation by producing gaseous H_2SO_4 (Gleitsmann and Zellner, 1999; Starik et al., 2004), which is an efficient aerosol precursor; and, the formation of HNO_3 and HNO_2 are the principle sink terms in the plume for emitted OH. Thus, estimates of the initial conversion of SO_2 to H_2SO_4 and the initial fraction of NO_z (HNO_3, HNO_2, PAN etc.) are dependent upon initial assumed OH emissions. This latter aspect may have implications for studies that attempt to estimate regional/global O_3 production, accounting for initial conversion of NO_x in the plume (e.g. Kraabøl et al., 2000a,b, 2002) since ppm levels of OH were assumed.

3.2.4. Sulphur-containing species

The most abundant S-containing gas in aircraft exhaust is SO_2 (see Tables 1 and 2). Measurements of SO_2 in aircraft exhaust plumes have been found to be consistent with average fuel sulphur contents (Arnold et al., 1998; Schumann et al., 1998; Hunton et al., 2000). According to models, fuel sulphur is oxidized mainly to SO_2 in the combustor (Brown et al., 1996). In the turbine, a small fraction, ε, of SO_2 experiences further oxidation by O atoms leading to SO_3 (Arnold et al., 1998). Additional SO_2 oxidation via OH radicals takes place downstream of the combustor exit but mostly still upstream of the engine exit plane (Tremmel and Schumann, 1999). Via reaction with water vapour, SO_3 becomes converted to gaseous H_2SO_4 mostly at plume ages of less than 10 ms (Reiner and Arnold, 1993). The consequences of more recent findings on the SO_x kinetics has still to be evaluated (Blitz et al., 2003; Somnitz et al., 2005; Yilmaz et al., 2006; Hindiyarti et al., 2007; Rasmussen et al., 2007). Gaseous H_2SO_4 has a very low vapour pressure and likely represents the most important aerosol precursor. Hence, the conversion fraction of fuel sulphur to H_2SO_4 is an important parameter. Gaseous H_2SO_4 was detected in fuel combustion experiments in the laboratory and in jet engine exhaust at ground-level (Frenzel and Arnold, 1994) and during combustor testing within PartEmis (Katragkou et al., 2004). Direct measurements of H_2SO_4 in aircraft exhaust plumes at cruising altitudes were performed using a chemical ionisation mass spectrometry instrument (Curtius et al., 1998, 2002). The various measurements yielded values of ε between 0.3 and $3.3 \pm 1.8\%$ (Curtius et al., 2002; Schumann et al., 2002; Katragkou et al., 2004; Petzold et al., 2005a). A model of OH-induced H_2SO_4 formation yielded $\varepsilon \approx 0.4$–0.6% (Tremmel et al., 1998). For O and OH-induced H_2SO_4 formation starting in the combustor of the engine, models predict ε values of 10% and more (Brown et al., 1996; Lukachko et al., 1998). A small fraction of the SO_3 is formed in the combustor but most is formed inside the engine between the combustor and engine exit (Starik et al., 2002; Sorokin et al., 2004). The H_2SO_4 is formed mainly at the end and outside of the engine. A budget analysis of S-containing species in particulate matter emitted from the PartEmis combustor yielded a partitioning of 97% SO_2, $\leq$2.7% gaseous H_2SO_4, and <0.3%

chemisorbed at soot particle surface (Petzold et al., 2005a). Upper bounds of ε of about 1.8–10% (depending on engine and the fuel sulphur content) can be derived from a combination of these direct measurements with aerosol measurements and models (Schumann et al., 2002). Model studies show that ε increases with temperature and pressure at combustor exit in the engine, and is, hence, engine dependent (Starik et al., 2002).

For a typical fuel sulphur content of 400 μg g^{-1}, and $\varepsilon = 3.3\%$, the engines emit 0.04g H_2SO_4 kg^{-1} (Table 2). This value exceeds the soot emission index of 0.01 g kg^{-1} of modern jet engines. The emission index for organic condensable material is about 0.01–0.03 g kg^{-1} (Table 2). Therefore sulphuric acid remains to be the most important precursor of volatile aerosols formed in aircraft exhaust plumes unless the fuel sulphur content decreases below about 100 μg g^{-1} (Schumann and Ström, 2001).

3.3. Particles – non-volatile

During combustion small non-volatile carbon soot particles are formed, which are nearly spherical with typical diameters of 30–60 nm and geometric standard deviation of the size distributions of about 1.55–1.7 (Petzold et al., 2003, 2005a; Popovicheva et al., 2004; Delhaye et al., 2007). Details are engine dependent (Brundish et al., 2007; Dakhel et al., 2007). Larger agglomerates may grow up to sizes larger than 100 nm in diameter. Soot emissions from aircraft engines are specified by ICAO in terms of smoke number measurements, which is a filter stain reference method. Correlations between smoke number and soot mass concentration were used to estimate the mean mass emission index of black carbon by the globally aircraft fleet in 1992 to be 0.04 g kg^{-1} (Petzold and Döpelheuer, 1998; Petzold et al., 1999). More modern engines such as the CFM56-3B1 on a B737 emit much less, 0.01 g soot kg^{-1} fuel. The average black carbon (BC) emission factor decreases with altitude from about 0.08 g kg^{-1} at altitudes near take-off and landing to 0.02 g kg^{-1} at 16 km (Hendricks et al., 2004). The 2002 fleet average computed from such correlations in AERO2K results in 0.025 g kg^{-1} (Eyers et al., 2005). Of the order of 10^{14}–10^{15} kg^{-1} soot particles are emitted depending on engine type and power setting (Petzold et al., 1999). In total, improvement of aircraft engine technology from 1960s technology to today results in a decrease of soot mass emissions by a factor of 40, see Fig. 1 (Petzold et al., 2003).

Soot[2] particles are composed of organic compounds (OC) and of graphitized elemental or black carbon. The split of organic and elemental carbon (EC) can be measured by thermal analysis methods (Petzold and Schröder, 1998; Petzold et al., 2003, 2005a). From the analysis of soot particles emitted from the PartEmis combustor, elemental carbon contributes 40–80% by mass to total carbon for an engine operating at cruise conditions. For take-off conditions, this fraction may increase up to > 90%, while for idle conditions it may be as low as 10% (Petzold and Schröder, 1998). Hence, the OC–EC split strongly depends on combustion temperature (Petzold et al., 2005a). Depending on the fuel sulphur content, these particles are coated by <5% by mass of volatile matter, mainly sulphuric acid (Petzold et al., 2003). Depending on the degree of coating, soot particles may act as ice nuclei (Kärcher et al., 2007).

An elemental analysis shows large (order 10%) mass fractions of O, S, and N, in soot exposed for some time to the exhaust stream. At the exit of several specific combustors, soot concentrations of 10^6–10^7 cm^{-3} with modal diameters ranging from 40 to 70 nm have been measured during the CHEMICON project (Zellner, 2000).

[2] In the literature relating to aircraft emissions, 'black carbon' is often used interchangeably with 'soot', although in the strictest sense they can be different.

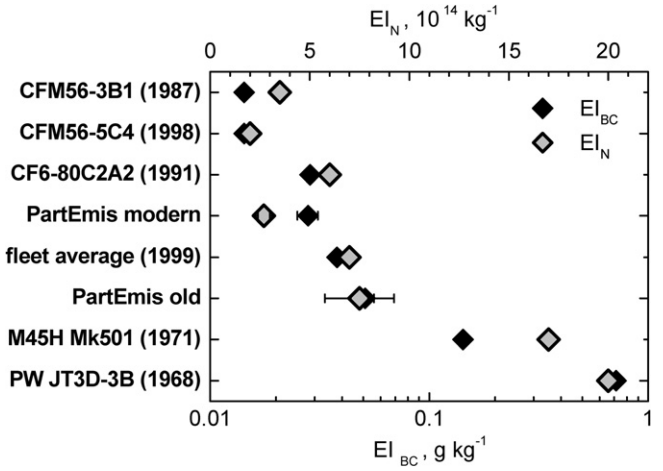

Fig. 1. Particle emission characteristics of the PartEmis combustor operated with medium fuel sulphur content, plotted in the context of emission characteristics measured for other aircraft engines at cruise conditions (adapted from Petzold et al., 2003; Copyright, 2003; American Geophysical Union. Modified by permission of American Geophysical Union).

PartEmis combustor exhaust studies yielded modal diameters of 40–50 nm (Petzold et al., 2003). Similar values were obtained from transmission electron microscopy analyses of CFM56 engine exhaust samples (Delhaye et al., 2007). The specific surface area of the microporous soot was 75 m^2 g^{-1} for combustor soot, and 64 m^2 g^{-1} for a laboratory prepared kerosene soot. Different from graphitic black carbon, combustor soot particles appear to be hydrophilic before reaching water saturation and may therefore serve as nuclei for water condensation without prior activation (Chughtai et al., 1999; Popovicheva and Starik, 2007). A joint analysis of hygroscopic growth measurements (Gysel et al., 2003), chemical analysis and cloud condensation activation measurements (Hitzenberger et al., 2003) obtained during PartEmis quantifies the increase in soot particle activation to cloud condensation nuclei from pure soot acting almost like an insoluble graphitic particle towards easily activated sulphuric acid coated particles (Petzold et al., 2005a,b). A sulphur coating of 3% by volume of soot particles reduces the diameter required for cloud condensation nuclei activation by a factor of 2 compared with pure graphite particles. The relationship between soot particle emission index and fuel sulphur content from a number of aircraft campaigns in contrail situations is shown in Fig. 2.

In the exhaust plume, the soot particles quickly build complex aggregates causing a second mode of larger particles between 100 and 500 nm (Sheridan et al., 1994; Petzold et al., 1998). Their size, however, is difficult to characterize due to the fractal or fluffy shape acquired during aggregation. The change of aviation soot properties in the atmosphere with increasing age (after a few minutes) has not yet been measured.

Aircraft soot particles are considerably smaller than particles containing BC from biomass burning sources, which tend to have number median diameters of close to 0.16 μm (Penner et al., 1998) while other sources can have either similar (0.03–0.1 μm, for coal, lignite; (Bond et al., 2002)) or larger (Chowdhury et al., 2001) size distributions. The diluting plume does not allow significant coagulation of these aircraft soot particles, so that most are expected to be found in the sizes ranges noted above in the ambient atmosphere (Kärcher et al., 2007). However, they are expected to coagulate with existing sulphate particles in the upper troposphere, rendering them possible immersion nuclei (Hendricks et al., 2004, 2005; Liu and Penner, 2005; Liu et al., 2005). The few existing

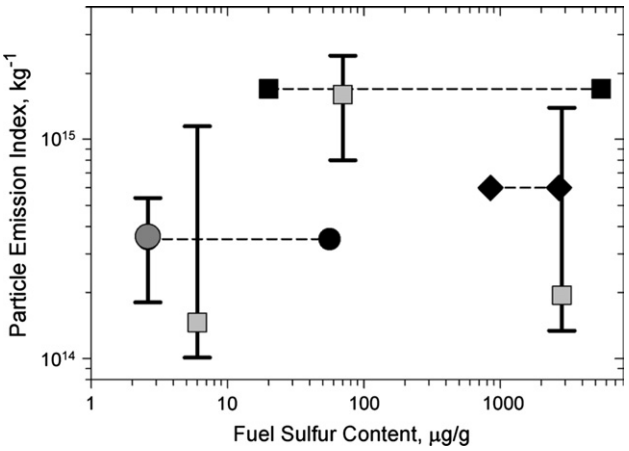

Fig. 2. Number of soot particles and ice particles per kg of fuel in contrails versus fuel sulphur content (FSC), behind various aircraft: ATTAS (squares), B737 (circles), and A310 (diamonds). The full symbols with dashed lines approximate the mean soot particle emission indices measured for the three aircraft in non-contrail plumes. The grey symbols with error bars denote the number of ice particles formed per kg of fuel burned in contrails for the B737 and the ATTAS (Schumann et al., 2002; Schumann, 2005).

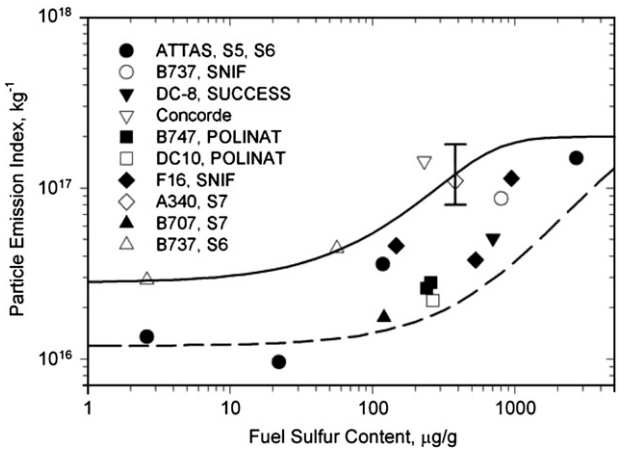

Fig. 3. Particle number emission index of detectable volatile particles in non-contrail plumes versus Fuel Sulphur Content (FSC) from various measurements, normalized to plume age 3 s, CNC cut-off 5 nm, and various sulphur conversion fractions ε and emission indices of condensable organic matter, EIOM (µg g^{-1} fuel). The curves emphasizing the trend of observed particle number emission index with increasing FSC are results computed with a model (Kärcher et al., 2000) at the same values of plume age, cut-off, and EI of CIs of 2×10^{17} kg^{-1}, and different EIOM and ε values: 20 µg g^{-1} fuel and 0.5% for dashed curve, and 30 µg g^{-1} fuel and 8% for full curve (Schumann et al., 2002; Copyright, 2002; American Geophysical Union. Reproduced by permission of American Geophysical Union).

measurements of soot and ice particles in fresh contrails suggest that the number of ice particles formed in the young contrail is essentially equal to the number of soot particles emitted (Schumann et al., 2002; Schumann, 2005).

3.4. Particles – volatile

3.4.1. Sulphur species

Previous measurements (Schröder et al., 1998) provided much progress in identifying the number of ultrafine particles. Once coagulated to larger particles, these particles are expected to affect the number of condensation nuclei and to cause volatile soot coating. Particle size spectra of aerosols particles with diameters from 3 to 60 nm were measured in young exhaust plumes, very close to the emitting aircraft (>30 m) at cruise during the SULFUR experiments. By normalization with the simultaneously measured CO_2 concentration, the apparent emission indices were determined (Brock et al., 2000; Schröder et al., 2000; Schumann et al., 2002).

Volatile aerosol particle concentrations in the aircraft plumes strongly increase as diameter decreases from 60 nm toward the sizes of large molecular clusters (diameter ≈3 nm), illustrating that apparent particle emissions are extremely sensitive to the smallest particle size detectable by the instrument used. Contrail formation and plume age alone can influence the number of detected ultrafine volatile particles within an order of magnitude, as well. The observed particle emissions decrease non-linearly with fuel sulphur content and become independent of fuel sulphur below 100 µg g^{-1} (Kärcher et al., 2000), see Fig. 3. The key controlling factors for liquid particle nucleation in the exhaust as identified during combustor exhaust studies are fuel sulphur content, availability of soot surface area which acts as an additional sink for condensable gases, and the temperature drop during exhaust gas dilution and mixing (Petzold et al., 2003; Vancassel et al., 2004; Schneider et al., 2006; Vatazhin et al., 2007).

3.4.2. Organic species

There are experimental indications that non-sulphate compounds – probably low-volatility hydrocarbons (Kiendler et al., 2000b; Wohlfrom et al., 2000) – dominate the volatile aerosol composition as the fuel sulphur content decreases below about 100 µg g^{-1}. For low fuel sulphur content, a sulphur conversion efficiency of even 50% is not enough to explain the large volume of volatile material measured with particle counters, and it has been therefore suggested that part of the volatile material results from condensable exhaust HCs (Kärcher et al., 1998b; Schröder et al., 1998, 2000; Yu and Turco, 1999). Variations in fuel aromatic content have no discernible impact on particle formation (Wey et al., 2007).

A model which explains the wide variance of apparent particle emission indices in exhaust plumes (not forming contrails) observed during various airborne experiments shows that this index depends on the lower cut-off size of the particle counters, the plume age, the fuel sulphur content, the conversion efficiency ε and the number of chemi-ions (CIs) available from the engine (Kärcher et al., 2000). The model assumes that the number of CIs available determines the number of volatile particles formed. The amount of sulphuric acid (depending on fuel sulphur content and the conversion efficiency, ε) and the amount of condensable organic matter together control the size of the particles formed. Coagulation and dilution control the time scales of particle growth. Using this model, the measured apparent emission indices can be normalized to a given plume age (3 s), emission index of low volatility hydrocarbons (20 µg g^{-1}), and cut-off size of the particle counters (5 nm). Consequentially, the data are consistent with volatile particle emissions of $1.5–4 \times 10^{17}$ kg^{-1}, independent of environmental conditions, engine type, and for fuel sulphur contents ranging between 2.6 and 2700 µg g^{-1} (Schumann et al., 2002).

3.4.3. Chemi-ions

Aircraft engines emit gaseous ions, so called chemi-ions (Arnold et al., 1998, 2000; Haverkamp et al., 2004) which are important as aerosol precursors (Frenzel and Arnold, 1994; Yu and Turco, 1998, 1999; Sorokin and Mirabel, 2001). Chemi-ions (CI) are formed during combustion in the engine (Starik et al., 2002) and may promote particle formation in two ways: through electrostatic forces the net charge stabilizes small molecular clusters and increases the flux of condensable gas molecules to the cluster. Primary CIs are formed in the combustor via radical–radical

reactions and subsequently undergo a rapid chemical evolution via ion–molecule reactions involving plume gases which leads to large cluster ions.

The concentration of charged particles formed by combustion-induced CIs is high at engine exit, about 10^9 cm^{-3} (Arnold et al., 2000); i.e. of the order 10^{17} kg^{-1} of fuel burned. Emission values found during the PartEmis combustor studies are of the same order of magnitude (Haverkamp et al., 2004). The CI concentration decreases steeply with increasing plume age due to ion-ion recombination in the early jet and due to dilution (Sorokin and Mirabel, 2001; Starik et al., 2002).

It was found that 'light' negative CIs are mostly of the type $HSO_4(H_2SO_4)_m(H_2O)_n$ ($m \leq 2$, $n \leq 3$) and that some negative CIs also contain HCs. Positive CIs are mostly composed of HCs, in agreement with theoretical arguments. Some of these HCs have been further identified as oxygenated HCs (Kiendler et al., 2000b). The positive and negative CIs can be very massive (exceeding 8500 atomic mass unit), even for nearly sulphur-free fuel (2 μg g^{-1}) (Wilhelm et al., 2004). The fractional abundances (in the range 0.2–0.7) of CIs with mass numbers >8500 atomic mass unit were found to increase with fuel sulphur content and to be larger for negative CIs than for positive ones. Probably the growth of these CIs involves organic trace gases. If composed mostly of an H_2SO_4/H_2O mixture, a CI with a mass number of 8500 would have a diameter of about 3 nm, which is comparable to the size-detection limit of present condensation nucleus particle counters. Hence, most of the smallest particles detected by such counters may actually have originated from CIs and their electrically neutral recombination products (Arnold et al., 2000).

There is good evidence to suggest that chemi-ions play a role in new particle formation, since they have been shown to exist under ground and in-flight conditions. The analysis of Kärcher et al. (1998a) demonstrated that ultrafine plume CN data can only be consistently explained when models include chemi-ion emissions and the associated nucleation pathways.

4. Future emissions trends and scenarios

4.1. Historical and current emissions

Most of the emissions from current civil aviation arise from modern high bypass ratio gas turbine engines. The first generation of lower-efficiency turbo-jets have been all but decommissioned, other than some remaining older aircraft in use in developing countries. Civil aviation is a strongly growing sector and has been steadily growing since the late 1960s when air travel started to become more widespread and economically accessible. Air traffic demand is usually expressed in Revenue Passenger Kilometres (RPK), or occasionally Revenue Tonne Kilometres (RTK), whereas air traffic capacity is expressed as Available Seat Kilometres (ASK). The absolute growth of aviation in terms of RPK is shown in Fig. 4. Various global-scale events such as the oil crises of the 1970s and early 1980s, the first Gulf crisis of 1991 and the WTC attack in 2001 etc. all affected passenger traffic but growth resumed shortly after each event, and in the case of post 2001–2007 period, very strongly with an overall increase in RPK of 38% (Lee et al., 2009). The effects of the current economic crisis are yet to be revealed in the global statistics: global air traffic data are available until 2007, which showed annual RPK growth rates of 5.9% yr^{-1} in 2006 and 6.6% yr^{-1} in 2007, which may be compared with the long-term growth rate of 6.23% yr^{-1} (1972–2007).

The year to year changes in growth rate are shown in Fig. 5. Clearly, there are strong year to year variations, with short-term declines occurring during the oil crises of the early 1970s, the Gulf War in the early 1990s, and the more recent events related to

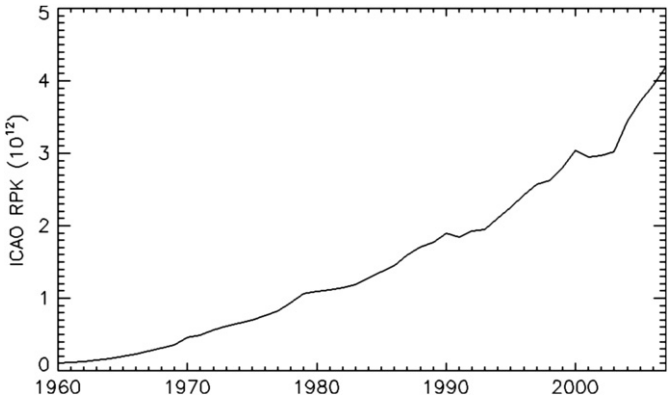

Fig. 4. Scheduled civil air traffic development from 1960 to 2007 in billions (10^{12}) of revenue passenger kilometres (RPK) (source: ICAO traffic statistics from http://www.airlines.org/economics/traffic/World+Airline+Traffic.htm accessed, 19 Sept. 2007).

September 11th, 2001, and the outbreak of severe acute respiratory syndrome (SARS). However, for all the strong declines, there has been almost equally strong recovery, demonstrating the resilience of the industry and the public's desire to travel.

Emissions from aviation have previously been assessed in terms of the construction of three-dimensional gridded inventories such as those constructed for early 1990s traffic and reviewed by Henderson et al. (1999). More recently, a number of other inventory models have been developed including AERO2K for 2002 (Eyers et al., 2005), FAST for 1990/2000 (Lee et al., 2005) and the SAGE modelling system which has produced results for 2000–2005 (Kim et al., 2007). The AERO2K and FAST models have also been used to produce forecast or scenario results for future years (Eyers et al., 2005; Owen and Lee, 2006), where here a 'forecast' is interpreted as an extrapolation of traffic and emissions, and a 'scenario' is a top-down calculation of traffic using some variable as a predictor; a similar definition to that used by Henderson et al. (1999). Some recent results from these and older models for early 1990s emissions are summarized in Table 3.

Such inventory models address movements of scheduled civil aviation and either ignore, or include some estimate of non-scheduled civil aviation, which can be important on regional scales, especially in summer months. Military aviation fleets and movements are much more difficult to estimate but have been calculated to be 18% of fuel usage in the early 1990s (Henderson et al., 1999) and 11% in 2002 (Eyers et al., 2005).

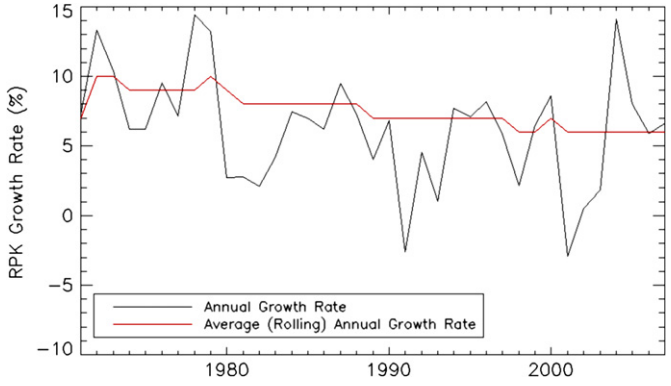

Fig. 5. Annual average growth rates in terms of revenue passenger kilometres (RPK) and long-term rolling average growth rate for scheduled civil aviation from 1970 to 2007 (source: ICAO traffic statistics from http://www.airlines.org/economics/traffic/World+Airline+Traffic.htm accessed, 19 Sept. 2007).

Table 3
Estimations of historical and current emissions from inventory models, 1990–2005.

Year	Inventory	Civil fuel ($Tg\ yr^{-1}$)	Military fuel ($Tg\ yr^{-1}$)	Total fuel ($Tg\ yr^{-1}$)	Total CO_2 ($Tg\ yr^{-1}$)	Distance (civil, 10^9 km)	NO_x ($Tg\ NO_2\ yr^{-1}$)	$EINO_x$ ($g\ NO_x/kg$ fuel)
1990	FAST	105	n.c.		331	15.7	1.42	
1992	NASA	114	25.5	139	359	n.c.	1.44	12.6(12.0)
1992	ANCAT/EC2	114	17.1	131	360	n.c.	1.60(1.81)	14.0(13.8)
1999	NASA	128 (134 inc. charter)	n.c.		404 (423 inc. charter)	25.8	1.69	13.2
2000	TRADEOFF	152	17.1[a]	169	480	25.1	1.95(2.15)	12.7(12.9)
2000	FAST	152	n.c.		480	26.9	2.03	13.4
2000	SAGE	181	n.c.		572	33.3	2.51	13.8
2001	SAGE	170	n.c.		536	31.9	2.35	13.8
2002	SAGE	171	n.c.		539	32.6	2.41	14.1
2002	AERO2K	156	19.5	176	492(553)	33.2	2.06(2.24)	13.2(12.7)
2003	SAGE	176	n.c.		557	34.5	2.49	14.1
2004	SAGE	188	n.c.		594	37.0	2.69	14.3
2005	SAGE	203	n.c.		641	40.7	2.90	14.2

References: 'FAST', Lee et al. (2005); 'NASA', Baughcum et al. (1996), Sutkus et al. (2001); 'ANCAT/EC2', Gardner et al. (1998); 'TRADEOFF', Gauss et al. (2006); 'SAGE', Kim et al. (2007); 'AERO2K', Eyers et al. (2005).
[a] Military emissions adopted from other study; n.c. not calculated; brackets include military emissions.

Gridded inventories are usually calculated for the purposes of providing input to chemical transport models (CTMs) or combined CTM/Global Climate Models (sometimes referred to as Chemistry Climate Models or CCMs). In addition, such inventories may be used for more policy-oriented analyses such as the calculation of allocation of international emissions under different assumptions (e.g. Lee et al., 2005; Owen and Lee, 2006). The emissions calculated may include NO_x, CO_2, SO_2, particles, H_2O, CO and HCs. In addition, gridded distance flown may be calculated as an input to contrail/cirrus models. Emissions of NO_x, CO and HCs do not scale directly with fuel usage and specific fuel-flow correlation algorithms are applied. For NO_x, the commonly used method is either the DLR-2 fuel flow method (Deidewig et al., 1996) or the Boeing Fuel Flow Method-2 (Baughcum et al., 1996). Whilst some inventories calculate CO and HCs, these have been shown to be unimportant for chemical impacts in the UT/LS, since the magnitude is so small compared with other sources (Hayman and Markiewicz, 1996).

The gridded inventories of aviation emissions still show some disagreement for estimates of the same year, even over fuel usage. There are a number of reasons for this: the core data for movements for all inventories is the OAG ('Official Airline Guide', www.oag.com) database of scheduled movements – non-scheduled movements need to be either estimated or calculated from 'real' (flight plan, radar) data. However, this is not a straightforward task, neither is the subtraction of the scheduled data from the total data. For regions where neither flight plan nor radar data are available, non-scheduled data are often estimated (Eyers et al., 2005; Kim et al., 2007). For some regions where there is significant aviation activity, e.g. Russia and China, there is anecdotal evidence that schedules are under-reported. Inventories may, or may not, include some estimation or explicit calculation of non-idealized routing, or simply use great-circle distances. The incorporation of the wide range of aircraft is often simplified, so that one aircraft may represent a number of others; for others, data may simply not be available. General aviation is usually excluded (i.e. small aircraft flying under visual flight rules). Comparative exercises are currently underway between the SAGE, FAST, AERO2K and AEM (a EUROCONTROL model) under the auspices of the activities of the International Civil Aviation Organization's Committee for Aviation Environmental Protection (ICAO-CAEP) and it is proving difficult to identify and quantify these sources of uncertainty. CAEP is attempting to provide a unified aircraft movements database (the Common Operational Database), as somewhat surprisingly, ICAO does not appear to quantify/record global aviation movements. However, even compiling the Common Operational Database is proving to be a challenge because of the sheer volume of data that need to be checked and verified.

Whilst such inventories are vital input to CTMs/GCMs, the data they provide are incomplete for calculations of aviation RF from CO_2, since this requires a time-history of emissions. The only published estimation of a time-series of aviation emissions dating back to the beginning of significant aviation activities (1940) is that of Sausen and Schumann (2000), whose estimations were also used in the IPCC (1999) assessment. Sausen and Schumann (2000) used International Energy Agency (IEA) statistics of kerosene fuel sales; this was recently updated from 1995 to 2005 by Lee et al. (2009). A comparison of IEA data with 'bottom up' inventory methodologies reveals a discrepancy which indicates a systematic underestimation of emissions by the inventories, which is the result of a number of assumptions and systematic biases, outlined above. This underestimation has been known for some time (Schumann, 1994) but it remains difficult to reconcile all the known differences (Owen and Lee, 2005). Nonetheless, it is critical that total historical CO_2 emissions are used in RF calculations, such that usage of the IEA data remains most suited to this purpose.

Future scenarios of aviation were constructed by Henderson et al. (1999) that included consideration of the growth in demand, change in fleet composition and aircraft size, and projected (and assumed) developments in technology. These were based on the GDP projections of the older IPCC IS92 scenarios. Recently, these have been updated using a similar methodology for two SRES GDP scenarios (A1 and B2) by Owen and Lee (2006), and a European Fifth Framework Project, 'CONSAVE' (Berghof et al., 2005). The predictions of CO_2 emission are shown in Fig. 6, along with the older IPCC 2050 aviation scenarios (Henderson et al., 1999) and other inventory results for past and present-day (Lee et al., 2009).

The production of scenarios always depends upon base year data. Thus, the uncertainties present within the range of base years available propagate through and introduce more uncertainty into the scenarios. By convention (although this is not necessary), scenarios usually use ICAO 20-year projections of traffic growth as a forecast as an intermediate point in the scenario modelling – however, ICAO's forecast is scheduled traffic only, which potentially introduces a systematic bias in the scenarios unless accounted for.

Despite the number of years that aviation emissions estimations and forecasts/scenarios have been worked on, there remain some significant obstacles in producing 'best' estimates that are usually limited by data availability. Here, ICAO could and should assist the modelling groups who produce these emissions estimations by provision of data.

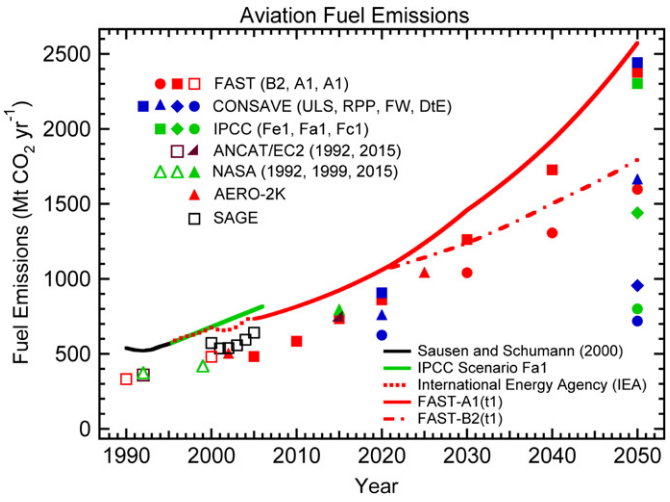

Fig. 6. Historical and present-day inventories, and future projections of civil aviation CO_2 emissions from a variety of sources: AERO2K (Eyers et al., 2005); ANCAT/EC2 (Gardner et al., 1998); CONSAVE (Berghof et al., 2005); FAST (Owen and Lee, 2006); IPCC (IPCC, 1999); NASA (Baughcum et al., 1996, 1998; Sutkus et al., 2001); SAGE (Kim et al., 2007). The open symbols indicate inventory analysis and the closed symbols indicate projections. Also shown are the CO_2 emissions implied by IEA fuel sales statistics (IEA, 2007). The IEA data represent the total of civil and military usage because all kerosene sales are included. The Sausen and Schumann (2000) data are also based on IEA. In the figure legend, the FAST, CONSAVE, and IPCC symbols are shown in an order that matches the scenario labels in the parentheses in each case (Lee et al., 2009).

4.2. Potential supersonic emissions and scenarios

The technology for a commercial supersonic aircraft – often referred to as 'High Speed Civil Transport' (HSCT) – is being developed in the United States, Europe, and Japan. However, to date, only two civil supersonic aircraft have been developed, the Concorde and the Tupolev 144, both of which have been withdrawn from service.

Previously, the goal has been to develop an aircraft that can carry approximately 300 passengers, with a 9260 km range, cruising at Mach 2.0–2.4 at altitudes of 18–20 km. The potential market for the HSCT is limited by economic and environmental considerations. The scenarios developed for HSCTs represent a technology that does not yet exist but one that might yet be developed and thus represent a quite different set of assumptions from other long-term scenarios, which only consider continued development of a subsonic fleet. For this reason, the range of emissions, fleet size, and cruise altitude covered by supersonic scenarios was larger than for subsonic aircraft. More recently, research has been initiated by a number of manufacturers to develop a supersonic business jet (SSBJ) although no prototype has yet been produced and concrete plans are scant in detail. Generally, the designs are for small aircraft, carrying between approximately 10 and 20 passengers with a possible fleet size of 250–300 aircraft.

In the IPCC (1999) assessment, the scenarios for supersonic aircraft in 2015 and 2050 were evaluated based upon the NASA Technology Concept Aircraft (TCA); 3-D emissions inventories of fuel burned, NO_x, CO, and unburned HC for fleets of 500 and 1000 active (high utilization) HSCTs were developed based on market penetration models and forecasts of air traffic in 2015 (Baughcum et al., 1994; Baughcum and Henderson, 1995, 1998). Projections of the HSCT fleets and their displacement of subsonic aircraft in the scenarios to 2050 were used (Baughcum et al., 1998; Baughcum and Henderson, 1998).

Over the past several years, manufacturers have proposed new designs that promise to increase transport speeds for the first time in over four decades. Boeing unveiled its Sonic Cruiser design in 2001 (and subsequently withdrew it in 2002). A variety of SSBJ proposals have also been made that may be able to take advantage of new technologies and changing market factors, transforming the aviation industry. The Boeing Sonic Cruiser proposals were considered to be aimed at competing with Airbus, specifically at the new 550-seat A380. If Boeing could have overcome the enormous hurdles and produce a 300-seat Mach 0.95–0.98 aircraft with greater than 6000 nautical mile range with only slightly higher direct operating costs, it would have transformed the economics of airline operations. However, the demise of this planned aircraft resulted from a lack of interest from airlines, who favoured reduced operating costs over increased speed.

The most recent set of HSCT scenarios based on the new technology concepts were used for most of the atmospheric impact calculations presented in the EU project 'SCENIC': 3-D distributions of combustion products (CO_2, H_2O, SO_x, NO_x, CO, HC, soot) emitted by sub- and supersonic aircraft fleets were developed for the years 2025 and 2050. For each date, two background scenarios were considered, one for a purely subsonic fleet, the other one for a mixed fleet where part of commercial subsonic traffic was replaced by supersonic traffic. In order to assist industry in designing a more environmental supersonic aircraft, several databases were produced, in which one of several parameters characterizing the supersonic aircraft were modified. These perturbation scenarios were different in number of routes, flights, supersonic market penetration on selected routes, number of aircraft and passengers transported, and traffic evaluation.

Here, a brief description of the SCENIC scenarios is given, considering the 2050 scenarios only (see Table 4). The S4 and S5 scenarios could be considered as 'background' scenarios that would serve as inputs for the scientific modellers. The S4 scenario provides a 3-D emissions distribution from a purely subsonic fleet; the S5 scenario provides a 3-D emissions distribution from a mixed fleet where part of commercial subsonic traffic is replaced by supersonic traffic. S6 is as S5 in terms of emissions; in this case, however, chemistry–transport models take into account in their chemistry codes the impact of sulphur and particle emissions on the rates of heterogeneous chemical reactions. The P2–P6 scenarios are 'perturbation' scenarios with respect to the base case S5, in which supersonic aircraft parameters were modified to evaluate the potential environmental impact of new supersonic designs as follows:

- scenario P2 is representative of emissions produced by the mixed fleet including the reference European Supersonic Civil Transport (ESCT) aircraft, for which the mean $EINO_x$ was increased to correspond to a lower technological-level maturity;
- scenario P3 is representative of emissions produced by the mixed fleet including the reference ESCT aircraft, where the demand for high-speed mean of transport is increased;
- scenario P4 is representative of emissions produced by the mixed fleet including a Mach 1.6 supersonic fleet in response to other industrial objectives;
- scenario P5 is representative of emissions produced by the mixed fleet including a Mach 2.0 supersonic aircraft, for which the range has been increased in response to traffic demand on longer distances;
- scenario P6 is representative of emissions produced by the mixed fleet including a Mach 1.6 supersonic fleet where cruise altitude has been reduced for environmental consideration.

The emission inventories were constructed on a resolution of $1^\circ \times 1^\circ$ in the horizontal and 1000 feet (305 m), in the vertical. The distribution of supersonic routes and the vertical distribution of the combined fleet for scenario S5 are shown in Fig. 7.

Table 4
Supersonic emissions scenarios for 2050 from EU 'SCENIC' project (Grewe et al., 2007).

Scenario	No of supersonic aircraft	Mach	Max range (nm)	Cruise altitude	RPK (10^{12})		Fuel (Tg yr^{-1})		NO_x (Tg NO_2 yr^{-1})		$EINO_x$		Distance 10^{10} km
					Total	Supersonic	Total	Supersonic	Total	Supersonic	Total	Supersonic	Total
S4-subsonic	0	–			17.82	0	677	0	7.35	0	10.9	–	11.7
S5-mixed	501	2.0	5400		17.84	0.73	721	60	7.45	0.27	10.3	4.6	11.8
P2-$EINO_x$	501	2.0	5400		17.84	0.73	721	60	7.75	0.57	10.7	9.6	11.8
P3-size	972	2.0	5400		17.87	1.41	762	115	7.54	0.53	9.9	4.6	12.0
P4-speed	544	1.6	6000		17.84	0.69	703	41	7.4	0.22	10.5	5.4	11.8
P5-range	558	2.0	5900		17.85	0.83	733	74	7.64	0.49	10.4	6.6	11.9
P6-height	561	1.6	5900		17.84	0.69	702	40	7.40	0.22	10.6	5.6	11.8

5. Impact on atmospheric composition–troposphere

5.1. Introduction

Commercial jet-engine aircraft fly at altitudes of around 8–12 km emitting a variety of species, which have an impact upon atmospheric composition either directly, or via chemical reactions. The interaction of atmospheric transport and chemistry plays a crucial role in determining the impact of aircraft emissions. At mid-latitudes, aircraft fly in the UT/LS region, where the general circulation transports air masses predominantly downwards into the troposphere on a timescale of weeks, with a pronounced seasonal cycle. The enhanced convective activity in summer largely reduces the turnover time of species in the upper troposphere. At lower latitudes, the Hadley circulation impacts the dispersion of emitted compounds, i.e. into the lower troposphere in the subsidence region and to higher altitudes in the convergence zone. In the subsidence region, clear sky-conditions enhance photochemistry, whereas the upwelling areas are characterized by deep convective clouds, where large fractions of soluble species are washed out.

5.2. Atmospheric transport of aircraft emissions

An understanding of the transport pathways of aircraft emitted species is important since they determine where compounds accumulate and hence control the chemical fate of species. Danilin et al. (1998) compared results from 2-D and 3-D global models, simulating an artificial 'aircraft-fuel' tracer, having an e-folding loss rate of 5 days in the troposphere. Rogers et al. (2002a) similarly investigated the transport characteristics of inert tracers localized in various UT/LS regions among models to understand better transport related model differences. Both studies indicated a large variability amongst the models. Schoeberl and Morris (2000) applied an experimental set-up comparable to that of Danilin et al. (1998) but applied a non-diffusive Lagrangian transport scheme. They concluded that a large fraction of the disagreement among models might arise from numerical diffusion by the transport scheme. Especially, a perturbation of the stratosphere above the emission region, i.e. in the 'middle world'[3] was not found. This finding was confirmed by Grewe et al. (2002a,b), who applied a Lagrangian transport scheme in a global chemistry–climate model. In this modelling study, 10,000 particles in the main aircraft emission region were released and showed that the predominant transport pathway is directed downward and an impact on the middle world was only found for trajectories directed towards the tropics followed by uplift. However, transport timescales were found to be greater than those of washout, implying a negligible impact from subsonic aircraft emissions upon the stratosphere.

[3] The extra-tropical stratosphere bounded by the local tropopause and the 380 K isentrope.

It has been shown by a number of model developers that detailed vertical model resolution is necessary in order to capture gradients of measured species in the UT/LS satisfactorily (Brasseur et al., 1998; Land et al., 2002; Roeckner et al., 2006). O'Connor et al. (2005) compared different vertical resolutions of a Eulerian CTM with measurements and demonstrated an improvement with better resolution; a Lagrangian scheme was also utilized but was not without its own problems and required a representation of mixing to reproduce the measurements. Similarly, Grewe et al. (2002a,b) showed that a sufficiently high model resolution at tropopause altitudes was necessary to maintain correct ozone gradients at the tropopause. With the higher vertical resolution, no stratospheric perturbation from subsonic aircraft emissions was found.

However, horizontal resolution may also have an impact on the representation of aircraft emissions in CTMs in the case of cross-tropopause transport. Kentarchos et al. (2000) increased the resolution of a coupled CTM/GCM from T30 to T63 resolution and compared results with T106-resolution results from the European Centre for Medium-Range Weather Forecasts (ECMWF) analysis fields. They found that 'streamers' (a filament of low-latitude air from a breaking Rossby wave event) and low specific humidity events were better represented at higher horizontal resolutions with a slightly improved vertical representation of O_3 profiles. A study of lightning NO_x chemistry and transport in the UT/LS similarly showed that a good representation of cross-tropopause transport was important for chemical budgets (Grewe et al., 2004). In a study of sensitivities to vertical and horizontal resolutions of the ECHAM5 climate model, Roeckner et al. (2006) found improvements from both changes and suggested that these should be made on a consistent basis. These aforementioned studies, although not applied to aircraft emissions, have potentially important implications for chemical budgets of perturbations brought about by such emissions.

Current subsonic aircraft, as already noted, fly in both the UT and LS depending upon factors including latitude, time of year, operational considerations. Using a set of case studies of conditions when aircraft flew directly in the LS in order to optimize flight conditions over head winds and adverse weather, Forster et al. (2003) showed that emissions in the North Atlantic Flight Corridor (NAFC) were transported polewards with a mean residence time of 23 days, using a Lagrangian dispersion model. However, Forster et al. (2003) noted that this was probably an upper bound. Morris et al. (2003) also examined the transport of subsonic emissions, using a trajectory model approach, showing little perturbation of the stratosphere by water vapour, it being confined to regions close to the tropopause.

In summary, according to recent model simulations, subsonic aircraft emissions (other than CO_2) are predominantly removed in the troposphere, and those emitted directly into the stratosphere (only at mid and high latitudes) are transported downward into the troposphere and do not seem to undergo significant upwards transport that would perturb the whole stratosphere. The atmospheric lifetime of an emitted compound is therefore dependent

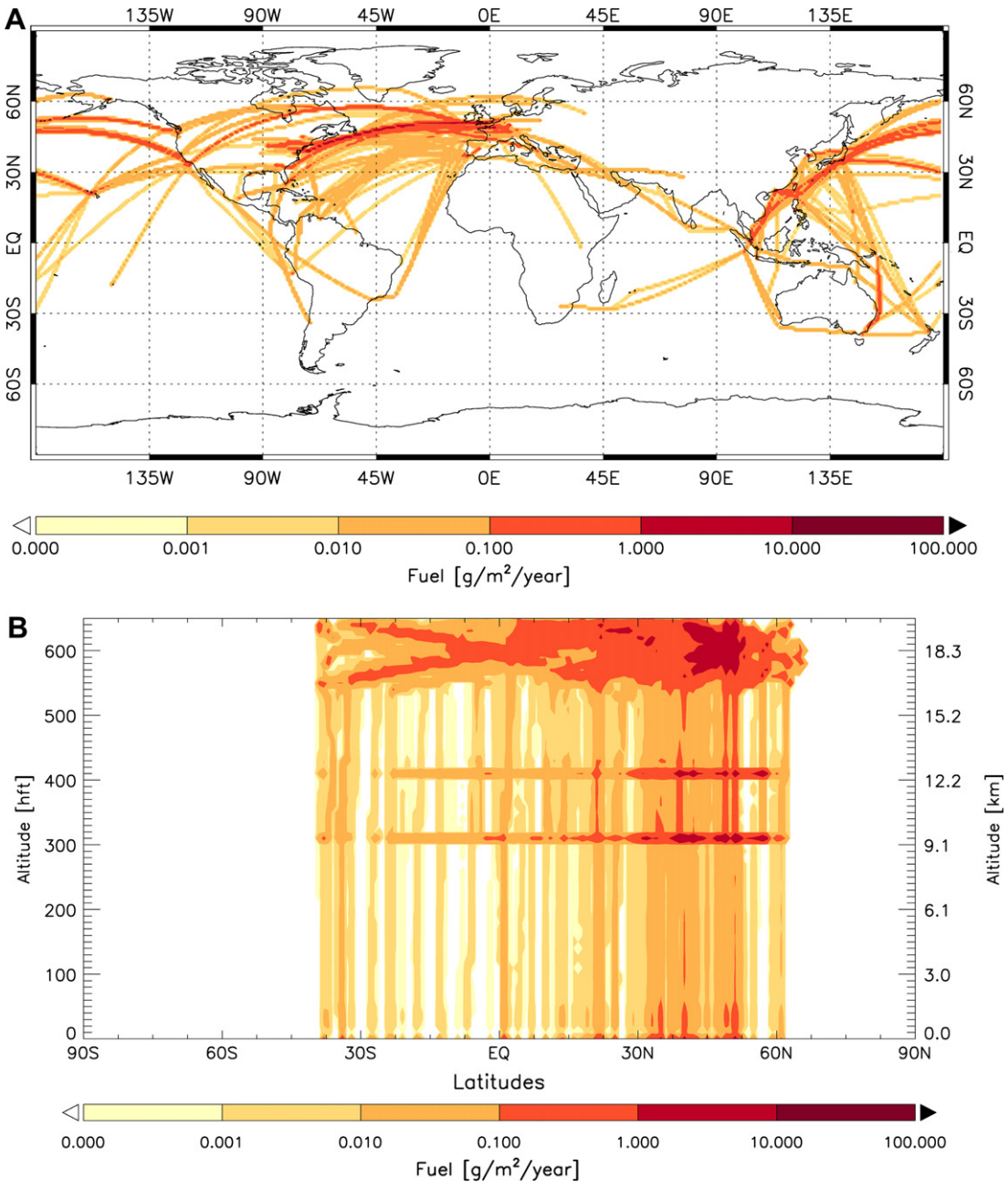

Fig. 7. Supersonic aircraft fuel consumption (g m^{-2} yr^{-1}) integrated over altitude (A) and (B) integrated over longitude.

upon the competing removal processes of chemical transformation and removal by wet and dry deposition. Fig. 8 shows the lifetime of a local water vapour perturbation, which also serves as a good indicator for wet deposition. (Grewe and Stenke, 2007).

5.3. Aircraft induced perturbations of the chemical composition of the atmosphere

5.3.1. Gas-phase chemistry

Emissions from current subsonic air traffic alter tropospheric chemistry and have an impact on the coupling of the NO_x–HO_x chemical reaction chains. Ozone is constantly being formed and photolysed in the cycle:

$$O(^3P) + O_2 + M \rightarrow O_3 + M \quad (2)$$

$$O_3 \xrightarrow{h\nu} O(^3P) + O_2 \quad (3)$$

where $O(^3P)$ is atomic oxygen in the ground state formed from the photodissociation of O_2 (mostly in the stratosphere > 16 km) where the wavelength of the incoming radiation is <243 nm (and M represents any third body). To form O_3 in the troposphere, O_2 has to undergo reactions in which CH_4, CO or other non-methane hydrocarbons (NMHC) react with OH (Fig. 9) to form HO_2. The reactions

$$HO_2 + NO \rightarrow NO_2 + OH \quad (4)$$

$$NO_2 \xrightarrow{h\nu} NO + O(^3P) \quad (5)$$

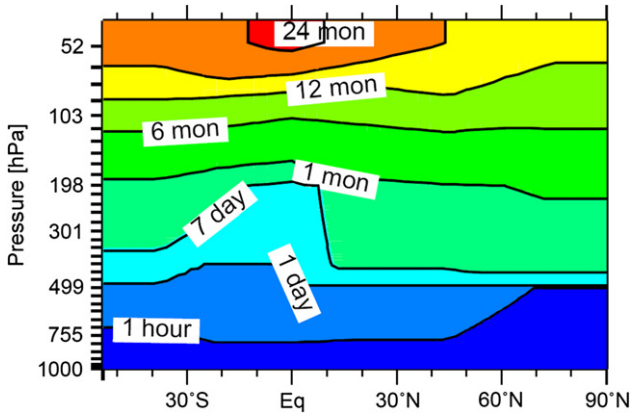

Fig. 8. Zonal and annual mean lifetime of an H_2O perturbation calculated with climate-chemistry model E39/C-ATTILA (from Grewe and Stenke, 2008).

lead to the formation of atomic oxygen, necessary to form O_3 (2). The main chemical O_3 loss processes are recombinations with OH or HO_2:

$$O_3 + HO_2 \rightarrow 2O_2 + OH \quad (6)$$

$$O_3 + OH \rightarrow O_2 + HO_2 \quad (7)$$

5.3.2. Impact on ozone

5.3.2.1. General impact. A general overview on the atmospheric composition changes due to air traffic emissions (here for 1991/92) is given in Fig. 10. An increase in concentrations of NO_x of 30–40% is found in the main flight corridors (for other model results see below). The additional NO_x in these regions lead to an enhancement of reaction (4). Hence, HO_2 decreases in that area, whilst O_3 production increases. Because of the greater insolation, the maximum O_3 production is shifted towards lower latitudes. Ozone production is also shifted to lower altitudes with respect to the NO_x changes, because HO_2 abundance, as one factor for O_3 production (eq. (3)) decreases with height between the UT/LS region and ~500 hPa. The shift in the HO_x partitioning towards OH from reaction (4) also leads to a decrease in the O_3 loss via reaction (6), which is not compensated by reaction (5). Both effects, i.e. the increase in O_3 production and the decrease in O_3 loss, lead to an increase of the net O_3 production rate resulting in an O_3 increase of approximately 3% in the Northern Hemisphere, which in turn leads to an increased O_3 loss rate via reactions (6) and (7). This secondary effect is visible especially in the lower atmosphere (Fig. 10).

Hence, three different regimes (R) may be distinguished with respect to air traffic induced O_3 changes (Grewe et al., 2002a,b): RNO_y, where O_3 production is controlled by increased NO_x and reaction (4); RHO_2, where O_3 loss is decreased due to a decrease in HO_2 via reaction (6) and RO_3, where O_3 loss is increased due to an increase in O_3 concentrations via reactions (5) and (6) (secondary effect). Köhler et al. (2008) found the same chemical regimes (their boxes A, B, C in their Fig. 5 match the regions RNO, RHO_2, RO_3). Additionally, Köhler et al. (2008) and Stevenson et al. (2004) point to a fourth regime close to the Earth's surface, where the additional HO_2 reacts with NO from other sources to form HNO_3, which is easily washed out. This reduces the O_3 production (Region RPO_3).

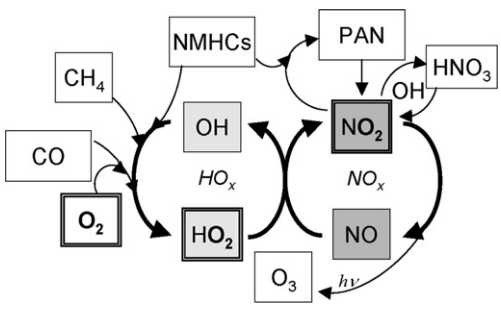

Fig. 9. Sketch of the main tropospheric O_3-related chemistry.

5.3.2.2. Impact of subsonic emissions of aircraft nitrogen oxides on stratospheric ozone. Current subsonic aviation emits NO_x directly into the stratosphere only at mid and high latitudes, where the general circulation is directed downwards (see Section 5.2). Hence, a significant impact on stratospheric O_3 may only occur via ascent of emitted NO_x at tropical tropospheric regions, where wash-out processes limit the lifetime of nitrogen species. Model studies suggest that air traffic emissions have a very limited impact on stratospheric NO_x and O_3, with O_3 reductions below 0.05% (Gauss et al., 2006; Grewe et al., 2002a,b; Köhler et al., 2008). Grewe et al. (2002a,b) pointed out that an impact on stratospheric O_3 occurred only in the case of a rather coarse vertical model resolution (>1.5 km).

5.3.2.3. Modelling capabilities. The application of atmosphere-chemistry models (ACM) is indispensable to estimation of the impact of air traffic emissions on the atmospheric composition since observational data by themselves are not suitable to detect air traffic induced changes. In the main emission regions of aircraft NO_x, the chemical lifetime of O_3 is of the order weeks, so that perturbations are dispersed zonally in the atmosphere. Their signal is too low compared with natural variability to be detected through measurements. However, for some circumstances, e.g. a stagnant high pressure system, the identification of air traffic induced ozone changes might be possible, since dispersion is reduced (Schlager et al., 1999). Note that the lifetime of atmospheric chemical perturbations depend on the times of the chemical modes excited by the perturbing species and not by the lifetime of that species (Prather, 1994, 1996). In this case, the NO_x perturbs the CH_4-like mode with a lifetime of 12 yr (Wild et al., 2001) and thus these perturbations are mixed globally.

The ACMs applied in recent years have been significantly improved over those used in the IPCC (1999) assessment, particularly with respect to the description of NMHC chemistry, stratospheric processes, model resolution, etc. A comprehensive validation of ACMs forms the basis of the assessment of calculated O_3 changes. In general, 2 types of ACMs are in use: CTMs, which are driven by meteorological data from forecast systems, and CCMs which calculate meteorological parameters by solving the primitive equations. For the first type, a direct comparison with measurements is applicable, whereas for the second a climatological approach is necessary.

Examples of recent multi-model validations on a climatological basis are given by Gauss et al. (2006) and Stevenson et al. (2006) for O_3 within the EU project ACCENT and for stratospheric-resolving CCMs by Eyring et al. (2006) and Waugh and Eyring (2008) within the Chemistry–Climate Model Validation (CCMVal) Activity for WCRP's (World Climate Research Programme) SPARC (Stratospheric Processes and their Role in Climate) project. Stevenson et al. (2006) compared output from 26 models with ozone sonde data showing that the mean model results closely resembled the observational data with a slight overestimation of O_3 in the northern hemisphere winter resulting in an underestimation of the amplitude of the northern hemisphere seasonal cycle. Brunner et al. (2003, 2005) utilized measurements from aircraft campaigns, integrated in the ETHmeg database (http://www.megdb.ethz.ch/),

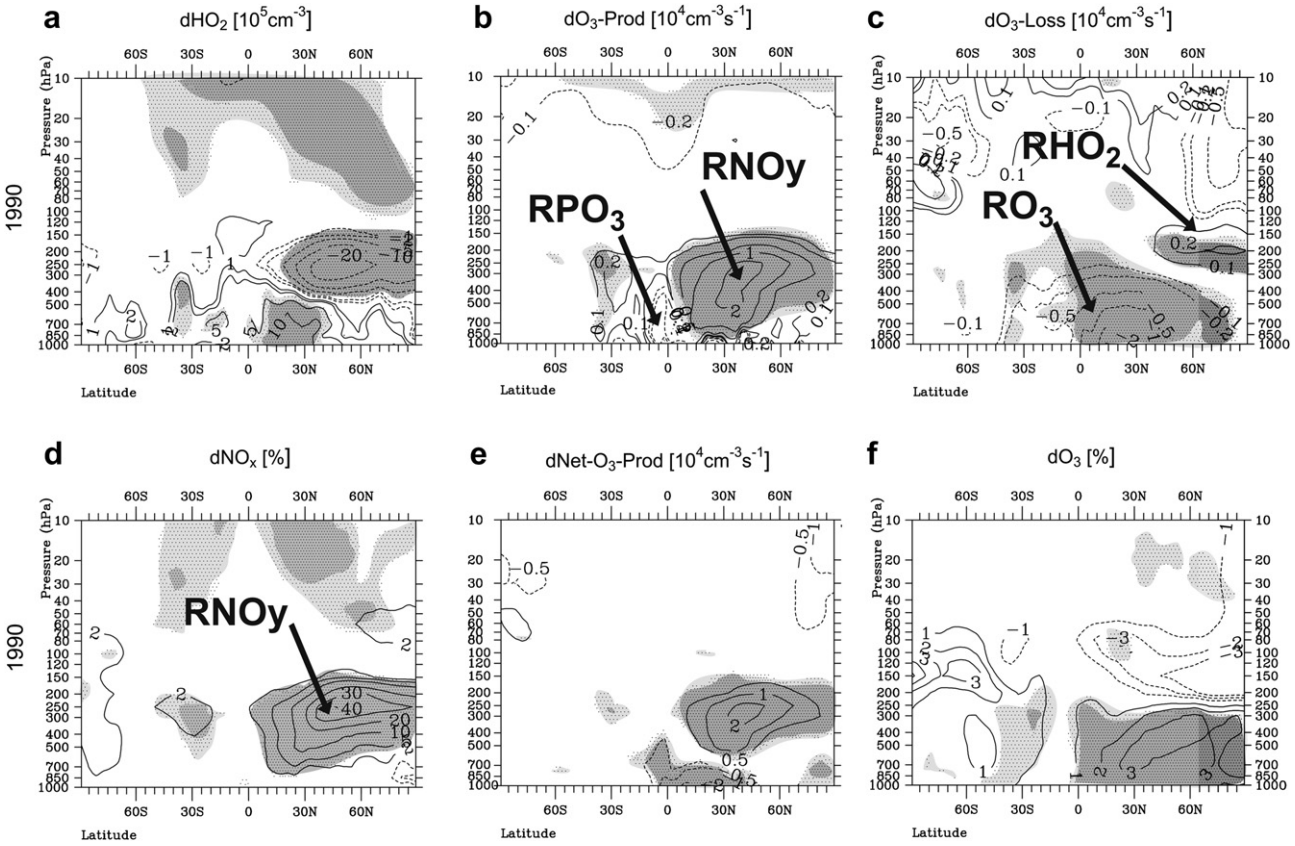

Fig. 10. Zonal and annual mean changes in (a) HO_2, (b) O_3 production, (c) O_3 loss, (d) NO_x, (e) net O_3 production, and (f) O_3 for 1991/92 air traffic emissions of 0.56 Tg N yr^{-1}. Regions are indicated where specific reactions occur, see text for details. Changes in production and loss rates are presented in a way that positive numbers indicate net O_3 production. Adapted from Grewe et al. (2002a).

for a direct point-by-point (in time and space) comparison with CTM model output. For the North Atlantic, the model results (Fig. 11) showed an underestimation of some species, e.g. NO. The overall correlation is around 0.7. However, models performing well in comparison with a certain campaign often failed with another campaign and vice versa (Brunner et al., 2005). This implies that whilst a single model may legitimately be used to calculate impacts of this nature, an ensemble of models will give more reliable results for an assessment (such as that of IPCC, 1999; Gauss et al., 2006; Stevenson et al., 2006). Similarly, the assessment of stratospheric-resolving CCMs (Eyring et al., 2006; Waugh and Eyring, 2008) shows that there is variability in the ability of CCMs to simulate different key processes, which may have ramifications for any assessments of HSCT scenarios requiring stratospheric models.

Another example for a CCM validation is given in Fig. 12, which shows a comparison of measurements taken on board a routinely flying Swiss Air aircraft (the 'NOXAR' project, Brunner et al., 1998) with results from a particular climate chemistry model (here E39/C). Clearly, the NO_x frequency distribution differs, since smaller-scale NO_x enhancements are not represented in coarse model distributions. However, the seasonal cycle of NO_x and O_3 is reproduced well by the E39/C model, with a broader distribution and the most frequent occurrence at larger mixing ratios. The most frequent NO_x mixing ratios are more important for O_3 production than the mean mixing ratio and those are in better agreement with the observational data.

An overview on the simulated tropospheric O_3 production, loss and budget terms is given in Table 5 (Stevenson et al., 2006). Generally, the standard deviation is in the range of 5% for O_3 production and loss terms, but differs more for O_3 deposition (15%)

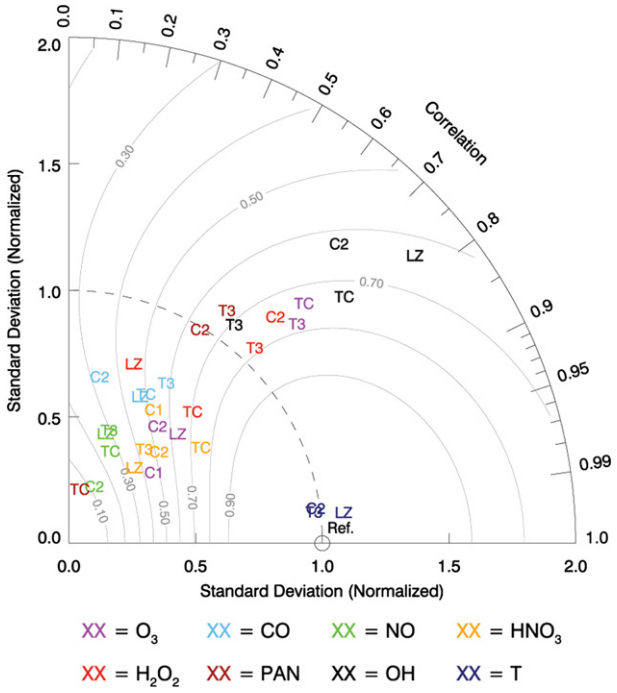

Fig. 11. Taylor diagram for 4 models: TM3(T3), OsloCTM2 (C2), TOMCAT (TC), and LMDz/INCA(LZ) applied in the TRADEOFF project in a comparison of model output for various species with measurements made between 1995 and 1998 in an altitude range between 5.5 km and 13 km over the North Atlantic (adapted from Brunner et al., 2003).

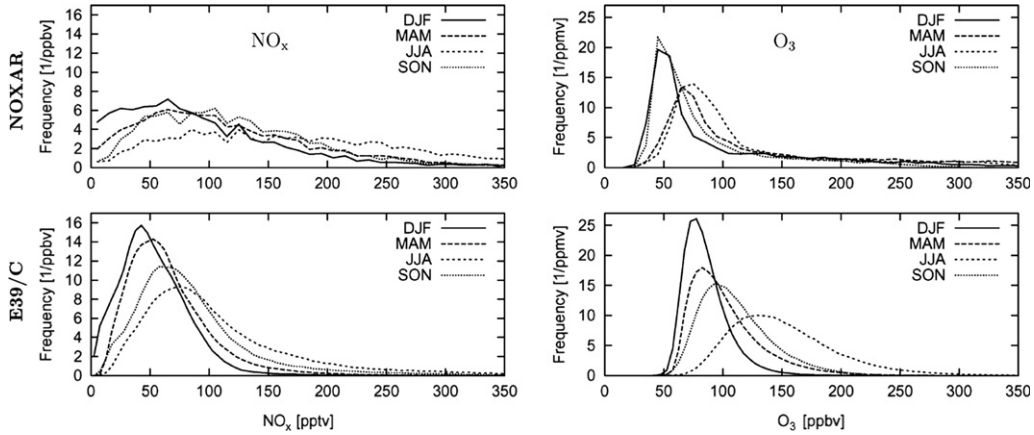

Fig. 12. Frequency distributions of NO_x (pptv, left) and O_3 (ppbv, right) derived from NOXAR measurements (top) and E39/C model data (bottom). Data are analysed in a region of 50 hPa below the local tropopause. NOXAR consists of a year of measurements made on board regular passenger aircraft flying between Europe and Eastern USA and Europe and the Far East (adapted from Grewe et al., 2001).

and O_3 influx (30%). Note that all models were run with identical boundary conditions, which reduced the model to model differences. Wu et al. (2007) similarly examined overall budgets of tropospheric O_3 in global models, noting that more recent modelling efforts have shown a systematic increase in the O_3 production term (35% greater than that reported in IPCC, 2001) although total burdens have only increased by about 10%, because of weaker stratosphere–troposphere exchange and shorter O_3 lifetimes.

5.3.2.4. Globally integrated impacts. Although there are significant differences in the details of how models simulate O_3 changes from air traffic NO_x emissions, e.g. in terms of seasonal cycle, local maximum perturbation, there are many consistencies found between the models, when examining globally integrated impacts.

The maximum O_3 increase is simulated approximately at the altitude of the flight corridors, i.e. in the main emission regions (Isaksen et al., 2001; Grewe et al., 2002a,b; Kentarchos and Roelofs, 2002; Berntsen et al., 2003; Rodriguez et al., 2003; Köhler et al., 2008; Hoor et al., 2009), which is consistent with previous studies (e.g. Isaksen et al., 1999). Similarly, an assessment of the globally integrated impact of aviation on column O_3 yields similar results (Fig. 13). Although the simulated response in O_3 ranges between 0.3 and 0.8 DU for an air traffic emission of around 0.55 Tg N yr^{-1}, the variability in the response is largely reduced, when applying identical background situations, i.e. NO_x emissions from biomass burning or industry as done within the projects TRADEOFF and QUANTIFY (but not during AEROCHEM II), with the exception of one model. The other model applied within TRADEOFF showed an increase of around 0.4 DU (0.33–0.44 DU) for an annual air traffic emission rate of 0.6 Tg N yr^{-1} and 0.6 DU (0.53–0.64 DU) per 0.76 Tg N yr^{-1} within QUANTIFY. The variability among these models is around 10–15%. Further model studies (Isaksen et al., 2001; Rodriguez et al., 2003; Grewe et al., 2002a,b) (including other background emissions) showed different responses ranging from 0.3 to 0.9 DU for an emission of around 0.6 Tg N yr^{-1}. Whilst the O_3 column change for an aircraft perturbation is reasonably consistent, it should be noted that total tropospheric O_3 column change amongst models still shows large variance, Gauss et al. (2006) noting a range of 7.9–13.8 DU in a comparison of seven CCMs and three CTMs.

A further consistency amongst some models is the tendency of lower O_3 production efficiencies for regions that have greater NO_x emission rates (both air traffic and other sources). This reflects a basic phenomenon that the net O_3 production rate (pO_3) increases rapidly with increasing NO_x, which was shown in UT measurements by Jaeglé et al. (1998). Early model comparisons showed that CTMs exhibited this behaviour when analysed on a large scale (Stevenson et al., 1997; Isaksen et al., 1999).

This phenomenon has been examined in a variety of ways. The IPCC (Isaksen et al., 1999) showed that global O_3 increases scaled almost linearly with increasing NO_x emission rates (from different emission scenarios). Rogers et al. (2002b) showed this phenomenon, with some evidence of a decline in pO_3 with greater emission rates. This behaviour was also in evidence, where pO_3 vs. NO_x emission was examined by latitude band showing that pO_3 increased at a much greater rate in low background NO_x environments. Grewe (2007) analysed a transient model simulation from 1960 to 1999 with increasing air traffic emissions along with changing background conditions, i.e. increasing background NO_x levels. The increase in O_3 relative to the air traffic emissions scaled almost linearly. However, a reduction in O_3 production efficiency can be observed (Fig. 13b), when comparing model simulations for different time horizons for consistent emission values. Table 6 gives a comparison of such model approaches (Isaksen et al., 2001; Grewe et al., 2002a,b; Grewe, 2007), by taking the 1990s ratio between O_3 increase and air traffic NO_x emissions on a relative basis

Table 5
Tropospheric ozone budget derived from a multi model analysis (Stevenson et al., 2006: S06) and from the IPCC Third Assessment Report (TAR), IPCC (2001). STE^{inf} describes the ozone influx from the stratosphere derived by $STE^{inf} = L + D - P$. The TAR best estimate of STE based on observations was much less than the model mean.

	Production	Loss	Deposition	STE^{inf}	Burden	τO_3	τCH_4[a]
	Tg O_3 yr^{-1}	Tg O_3 yr^{-1}	Tg O_3 yr^{-1}	Tg O_3 yr^{-1}	Tg O_3	days	yr
S06	4974 ± 223	4577 ± 291	953 ± 154	556 ± 154	336 ± 27	22.2 ± 2.2	8.45 ± 0.38
TAR (models)	3420	3470	770	770	300	24	8.4
TAR (analysis)				475			

[a] Note that this is the budget lifetime of CH_4 in the participating models and note the residence time of a CH_4 perturbation, which is estimated to be 12 yr.

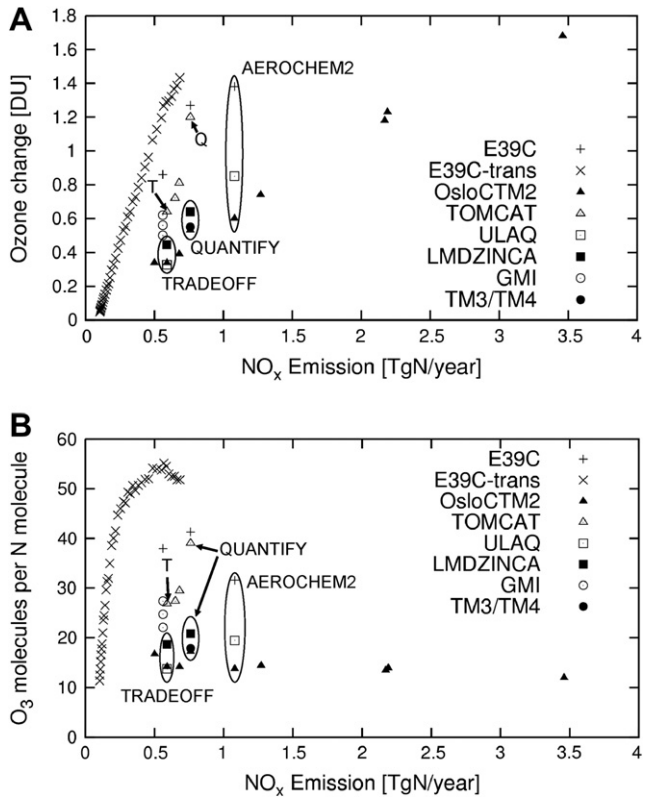

Fig. 13. Globally integrated ozone response [DU] relative to aircraft NO_x emissions (Tg N yr^{-1}) for a number of model simulations (A) and, the ozone production efficiency (OPE, the number of ozone molecules produced per emitted NO_x molecule) (B). Data from the AEROCHEM2 project (Berntsen et al., 2003), the TRADEOFF project (Sausen et al., 2005; Stordal et al., 2006; Gauss et al., 2006), the QUANTIFY project (Hoor et al., 2009); E39/C model runs (Grewe et al., 2002b; Grewe, 2007), the GMI project (Rodriguez et al., 2003), OsloCTM2 runs (Isaksen et al., 2001; Gauss et al., 2006). Since individual tropospheric ozone lifetimes were not available, this was assumed to be 28 days for all models (see discussion in text).

(=100%) and comparing relative changes in other time periods. The results in Table 6 indicate that the O_3 enhancement efficiency of air traffic emissions peaks at around 1990–2010 and decreases thereafter by 30% for larger air traffic emissions.

This efficiency in enhancing O_3 mass depends on the O_3 production efficiency and the O_3 lifetime. Grewe (2007) analysed the tropospheric O_3 lifetime between 1960 and 1999 and found a decrease from 30 to 26 days, which does not explain the low enhancement efficiency in the 1960s (Table 6). Assuming a constant O_3 lifetime of 28 days, one can derive the ozone production efficiency (OPE), which is defined as:

$$\mathrm{OPE} = \frac{\text{ozone enhancement [kg]}}{\mathrm{NO_x}\text{ emission }\left[\text{kg N yr}^{-1}\right]} \times \frac{\text{N molec. weight}}{\text{ozone molec. weight}} \times \frac{1}{\text{ozone lifetime [yr]}}$$

Table 6
Ozone increase efficiency (%) normalized to the 1990s, i.e. change in O_3 (DU) per emitted air traffic NO_x (Tg N yr^{-1}) relative to the 1990s. Results from the OsloCTM2 are based on Isaksen et al., 2001. Results for ECHAM/CHEM are based on Grewe (2007) for the 1960s, 1970s and 1980s; Grewe et al. (2002a) for 2015; and Grewe et al. (1999) for 2050.

Model	1960s	1970s	1980s	1990s	2015	2050-low	2050-high
OsloCTM2				100%	87%	81%	72%
ECHAM/CHEM	34%	71%	94%	100%	98%	81%	72%

It should be noted that the O_3 lifetime is not constant throughout the troposphere and can vary widely with latitude, season, and altitude. It could shorter in other models or future simulations (Table 5), which may lead to 25% larger OPEs. However, the general picture is unchanged. Fig. 13 shows the OPE for the various model experiments. The TRADEOFF simulations show an OPE in the range of 12–18 molecules of O_3 per emitted NO molecule. In the transient simulation from 1960 to 1999 (Grewe, 2007) a clear increase in the OPE from 11 molecules of O_3 per emitted NO molecule in 1960 to around 55 molecules around 1992 was observed. Afterwards, a clear decrease occurred, i.e. each additionally emitted NO molecule produced fewer O_3 molecules. The total O_3 production is largely determined by the background NO_x levels (Lin et al., 1988; Grooss et al., 1998; Jaeglé et al., 2000). With respect to global mean values, Fig. 14 shows a sketch of the relationship between NO_x concentration and net O_3 production with an inflexion around 1992. The 2050 values are still below the maximum O_3 production.

5.3.2.5. Seasonal effects. Some models show a 'double peak' structure in the air traffic O_3 perturbation, with maximum impacts in early summer (May) and autumn (October), whereas others only show one of those peaks (Hoor et al., 2009; Berntsen et al., 2003; Köhler et al., 2008). Mid latitude air traffic emissions have a weak maximum in summer/autumn and a minimum in winter (Schmitt and Brunner, 1997; Eyers et al., 2005). However, the accumulation of NO_x emitted by air traffic is largely reduced in summer because of intense vertical mixing (convection), which helps to explain the nature of the double peaks. Since the interaction between transport and chemistry varies amongst the models, these peaks are simulated differently. The atmospheric transport study of Rogers et al. (2002a) offers an explanation for these model differences: the model with the weakest vertical mixing for mid latitude emissions (their 'case T2', TOMCAT model) shows larger accumulations of NO_x during summer and hence maximum air traffic induced ozone changes in October, compared with the model with the largest vertical mixing (E39/C), which shows the peak in late spring.

5.3.2.6. Interannual variability. Natural climate variability also has an impact on atmospheric mixing, oxidation capacity, and chemical transformation rates, which leads to variations in the pattern of the O_3 increase from air traffic. However, only the impact on global O_3 has been analysed in more detail. Grewe et al. (1999) calculated an inter-annual variability of ±6%, ±8%, ±12%, ±16% for the O_3 response in 1992, 2015, and 2050 (low and high emission scenario) applying the ECHAM3/CHEM model. The revised model version E39/C led to lower values of around ±2% for 1992 and 2015 (Grewe et al., 2002a,b).

5.3.2.7. Impact of non-methane hydrocarbon and acetone chemistry. A number of studies have shown that the inclusion of NMHC chemistry in global models can significantly modify the net O_3

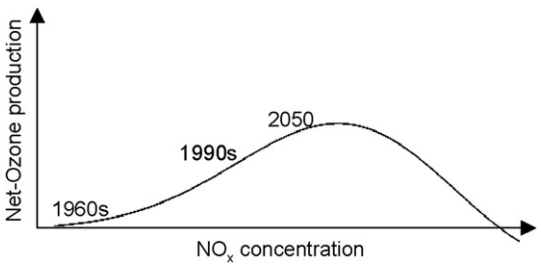

Fig. 14. Sketch of the relationship between background tropospheric NO_x abundance and net ozone production, showing development at particular points in time.

production rates in the lower and free troposphere (e.g. Roelofs and Lelieveld, 2000). Two effects are important with regard to NMHC chemistry: firstly, NMHC compounds react with OH and O_2 and enhance HO_2 formation (Fig. 9) and hence O_3 production. Secondly, the counteracting effect of peroxyacetyl radicals (from photolysed higher oxygenated NMHC compounds) is to react with NO_2 to form PAN, which can be transported over long distances in the upper troposphere until it subsides and thermally decomposes. Therefore, NO_x is converted into PAN, which reduces O_3 production via reaction (4).

Brühl et al. (2000) showed in box model simulations for the North Atlantic Flight Corridor that acetone concentrations significantly enhanced O_3 production induced by aircraft NO_x emissions. The consequences on global scales were investigated by Kentarchos and Roelofs (2002) by applying the climate chemistry model ECHAM4-CBM4, which in principle confirmed the findings of Brühl et al. They investigated the effect of the inclusion of NMHC chemistry on the calculated impact of current aircraft NO_x emissions on tropospheric O_3 levels. In the upper troposphere they found a decrease of NO_x owing to the formation of PAN and consequently an increase in HO_2 of 20%, which leads to a lower background O_3 formation since less NO_2 is produced via reaction (4). Globally, they concluded that when NMHC chemistry was included in their model chemistry, the aircraft-induced O_3 perturbations were greater by ~12% in summer and the aircraft-induced O_3 production efficiency per NO_x molecule increased by ~20% compared with a simulation without higher hydrocarbon chemistry. Thus, future evolution of surface NMHC emissions may have an impact on UT O_3 production from aircraft NO_x (Kentarchos and Roelofs, 2002).

The issue of NMHC effects on UT/LS O_3 production from aircraft NO_x emissions should be clearly separated from that of NMHC emissions from aircraft. The emissions of NMHC from aircraft are small (see Section 3.2.1) compared with background sources. A total NMHC emission index of 10.4 mg kg^{-1} fuel burnt has been measured during PartEmis (Kurtenbach et al., 2003) and hence is a factor of 1000 smaller than for NO. It has previously been found in plume modelling studies that the impact of including aircraft NMHC emissions is negligible on O_3 production (Hayman and Markiewicz, 1996; Pleijel et al., 1998).

5.3.2.8. Impact of particles and heterogeneous chemistry. In general, two mechanisms need to be distinguished. Firstly, the emission of particles from air traffic perturbs the chemical composition via heterogeneous reactions on those particles. Secondly, ice particles in the background (cirrus) or that induced by air traffic (contrails, contrail-cirrus) may alter the air traffic induced gas phase O_3 perturbation via heterogeneous reaction on these ice particles.

The most important particles produced by aircraft emissions that affect atmospheric chemistry are those of sulphuric acid (H_2SO_4) through heterogeneous reactions, converting NO_x into nitric acid, which reduces O_3 production via reaction (4). Because of the very small size of aircraft-generated particles and since emissions mostly occur at mid-latitudes, the relevant heterogeneous reactions are essentially hydrolysis of N_2O_5 and $BrONO_2$ (Meilinger et al., 2002). The main effect of these two reactions is twofold: (a) NO_x enhancements by NO_x aircraft emissions are partly counterbalanced by additional heterogeneous conversion of NO_x into HNO_3 on these particles in the flight corridors; (b) this reduced NO_x enhancement tends to increase the amount of reactive Cl and Br in the mid to high latitudes UT/LS region, since less Cl/Br can be stored into Cl and Br nitrates, which enhances O_3 depletion via catalytic Cl and Br cycles.

Aircraft emissions may perturb the global amount and the size distribution of H_2SO_4 aerosols in two ways: (a) the direct emission of ultrafine particles ($r \sim 5$ nm) (Pueschel et al., 1997; Curtius et al., 1998; Kärcher and Meilinger, 1998) and, (b) the release of gas phase SO_2 (Weisenstein et al., 1998). Direct particle emissions are estimated to account for 4–15% of the overall aircraft emitted sulphur (Curtius et al., 1998; Fahey et al., 1995). However, in these older studies much larger values of ε were estimated than are believed to be correct from more recent measurements and modelling studies (see Section 3.2). These direct particle emissions do not significantly change aerosol mass and extinction but may substantially increase surface area density (SAD) in the Northern Hemisphere UTLS. Release of gas phase SO_2, on the other hand, may increase the net production of H_2SO_4, thus enhancing the sulphate mass in the accumulation mode and consequently, the direct RF. It also may increase the gas phase contribution to SAD, in the range of 25% of the change produced by direct plume particle emission (Pitari et al., 2002b; Weisenstein et al., 1998).

Pitari et al. (2002b) quantified the subsonic aircraft impact on UT/LS H_2SO_4 aerosol SAD and its subsequent impact on aircraft induced O_3 perturbation. The calculated zonal mean aircraft SAD had a maximum of approximately 0.6–0.8 μm^2 cm^{-3} at current subsonic cruise altitudes and poleward of 30°N. This change is roughly consistent with that calculated by Kärcher and Meilinger (1998) under comparable conditions, i.e. assuming an average background SAD of 3 μm^2 cm^{-3} (Thomason et al., 1997), scaling their EI-SO_2 to 1.1 g kg^{-1}, and assuming a 25% additional aircraft contribution to SAD from gas phase SO_2 emissions; this results in an SAD of 0.7 μm^2 cm^{-3}. The model predicted a SAD increase above the source region which was qualitatively consistent with the results of the tracer fuel experiment described by Danilin et al. (1998).

The impact of these particle perturbations on air traffic induced O_3 changes was estimated by Pitari et al. (2002b) by applying two CTMs (ULAQ, TM3). Both models showed O_3 increases from air traffic NO_x emissions when gas phase chemistry and background heterogeneous chemistry were considered only. The inclusion of heterogeneous reactions on aircraft-induced aerosols led to O_3 losses in the lowermost stratosphere of about −4 to −6 ppbv, as an annual average at approximately 14 km altitude and poleward of about 50 °N, and to a reduction of the upper tropospheric O_3 increase (by about 2 ppbv). Pitari et al. (2002b) concluded that the lower stratosphere O_3 losses were caused by a decrease in NO_x via heterogenous reactions on aircraft perturbed SAD, followed by an increase in Br and Cl radicals, increasing O_3 destruction. The reduced O_3 levels were then transported downwards compensating to some extent the O_3 increase from aircraft NO_x emissions.

The impact of heterogeneous reactions on solid ice particles has been under discussion for time but there is no work directly addressing the impact of heterogeneous chemistry on cirrus/contrails on aircraft-induced O_3. Reichardt et al. (1996) noted low O_3 levels associated with mid-latitude tropospheric ice clouds. Peterson and Honrath (2001) made measurements of destruction of O_3 in snowpack interstitial air and suggested that this might be in operation in cirrus clouds. However, the general impact of these reactions on background O_3 can serve as an indicator as to how important these reactions may be. This was estimated by Von Kuhlmann and Lawrence (2006), who applied the CTM MATCH. They estimated a maximum O_3 reduction of 4% and 7% in the tropical upper troposphere in a case in which Langmuir theory was applied and a maximum HNO_3 uptake scenario (extreme case), respectively. However, in the region where maximum air traffic O_3 changes occur, those values were reduced to 3–5% O_3 reduction, implying that the impact of heterogeneous reactions on ice particles is likely to be of minor importance to air traffic O_3 changes. However, this depends critically on the distribution and abundance of cirrus clouds and this should be examined more carefully.

5.3.2.9. Impact of plume effects. Global atmospheric chemistry models have a spatial and temporal resolution that does not resolve chemical processes in the wake vortex and subsequent dispersion regime of an aircraft plume. Air traffic emissions are therefore treated as being instantaneously dispersed in a grid cell in global models. However, in reality, emitted species are confined in the plume and the composition may evolve differently. In order to account for this difference two approaches have been taken. Box or Gaussian plume models have been used to calculate either effective emissions indices (e.g. Karol et al., 1997; Petry et al., 1998) or emission conversion factors (Kraabøl et al., 2000a,b; Meijer, 2001; Plumb et al., 2003). In the first approach, factors are applied to the emission inventory to mimic concentration changes that occur resulting from the difference between a simulation with a plume model and one with instantaneous mixing. In the second approach, all relevant species (not only emitted once) experience changes which depend on the emission strength, atmospheric conditions (e.g. stability, shear, temperature, time of day etc.). These changes are pre-calculated as in the first approach with Gaussian plume models.

In general, the high OH concentrations in the plume lead to faster conversion into HONO and HNO_3, so that all applied plume models emit less NO_x and more $HONO/HNO_3$. Kraabøl et al. (2002a,b) estimated a decrease in the O_3 perturbation of 15–18% locally. Globally integrated (e.g. as in Fig. 13a), this leads to an O_3 decrease of around 10%, whereas in a similar approach, Plumb et al. (2003) found a decrease of less than 3%. However, it is not clear whether Plumb et al. (2003) accounted for initial plume chemistry, as their results refer to 'background atmosphere' effects. Meijer et al. (1997) reported similar plume impacts on aircraft induced O_3 perturbations to Kraabøl et al. (2002a,b); however, when they included O_3 conversion factors, i.e. similar to Kraabøl et al. the changes were reduced to 0–5% in January and −5 to 10% in July such that an increase in O_3 was found in summer. Hence, all studies concluded that the inclusion of plume processes reduce the annual and global mean O_3 increase from air traffic by maximum of approximately 10%. Where detailed chemical models are used (or data from underlying studies that use such models), the assumed initial emissions concentrations of OH are of the order 10 ppm (e.g. Kärcher, 1996; Tremmel et al., 1998). The emission of OH will strongly control the initial conversion of NO_x to NO_y species in the plume, particularly HNO_3. However, more recent measurements (see Section 3.2.3 and Wilson et al., 2004) do not support such large OH concentrations and suggest levels of the order 1–10 ppb. This will have an influence on the global model studies that attempt to account for this factor, probably reducing the O_3 reduction.

5.3.2.10. Impact of background emissions. As has been outlined above, background emissions (e.g. industry, lightning, etc.) have a large impact on the tropospheric NO_x concentrations and hence overall O_3 production since the chemistry is non-linear, as shown from measurements (e.g. Jaeglé et al., 1998). Grewe et al. (2002a) used surface NO_x emissions of 31.1 Tg N for 1992 and updated the surface emissions by using 40.0 Tg N for 1992, which increased the aircraft induced ozone perturbation by 50%. Similar sensitivities have been found previously (Isaksen et al., 1999) with regard to both strength and regional pattern of background emissions. This indicates the importance of accurately simulating the background atmospheric conditions. In the TRADEOFF and QUANTIFY projects, the emission scenarios were constrained for all models, which led to considerably lower model-to-model differences than for other multi-modelling studies (e.g. AEROCHEM2). Lightning emissions of NO_x are estimated to have a magnitude of the order 5 Tg N yr^{-1} (e.g. Schumann and Huntrieser, 2007: 5 ± 3 Tg N yr^{-1}; Boersma et al., 2005: 1.1–6.7 Tg N yr^{-1}) with large uncertainties (Labrador et al., 2005). However, they also partly occur, like air traffic emissions, in the UT, where they have a larger impact on O_3 than surface emissions of NO_x. Modelling studies suggest that an increase in lightning emissions from 5 to 10 Tg N yr^{-1} (the upper end of this range may be unrealistic), decreases the air traffic O_3 perturbation by between 15 and 50% (Isaksen et al., 1999; Brasseur et al., 1996) from the lower OPE at greater background levels of NO_x. Moreover, in a number of studies, it has been found that the type of parameterization and vertical lightning emission profile also has an impact on the O_3 perturbation (e.g. Tie et al., 2002; Grewe et al., 2002a,b; Labrador et al., 2005), which was found to be of the order 20% by Grewe et al. (2002a,b) but larger by others (Labrador et al., 2005).

5.3.2.11. Climate–chemistry interactions. Two aspects are of interest with regard to climate–chemistry interactions. Firstly, aviation-induced changes in the chemical composition lead to changes in radiative forcing and climate parameters, which in turn may change the aircraft-induced chemical perturbations. However, these changes are too small to produce a significant feedback on the perturbations (Grewe et al., 2002a). Note that this may change in the case of supersonic transport (see below). Secondly, future climate change (warming of the atmosphere) will alter atmospheric characteristics and may change the impact of aviation emissions: climate change is likely to result in greater H_2O and hence OH concentrations, but also different HNO_3 wash-out patterns and strengths (e.g. Johnson et al., 1999; Grewe et al., 2001). However, these results are affected by the climate sensitivity assumed (Gauss et al., 2006). Grewe et al. (1999) found that if the effects of climate change were included in a simulation, a decrease in air traffic (year 2015) induced O_3 perturbation of 10–15% resulted, mainly because of more efficient HNO_3 formation and removal.

5.3.3. Impact on methane

5.3.3.1. General impact. Emissions of NO_x lead (see Fig. 9) to a repartitioning of HO_x via reaction (6) in favour of OH, which enhances the oxidation of hydrocarbons, especially CH_4 by the reaction:

$$CH_4 + OH \rightarrow CH_3 + H_2O \quad (8)$$

This may be compensated by additional emission of NHMCs or CO, which in the case of air traffic is of minor importance, in contrast to road traffic (Uherek et al., 2009). Hence, as long as a substantial amount of NO_x is emitted in the troposphere, O_3 production is accompanied by CH_4 destruction. Changes in OH arise initially as a result of reaction (4) and as a second step a result from O_3 increases, e.g. by reaction (6) (Stevenson et al., 2004).

5.3.3.2. Methane lifetime changes. Methane atmospheric budget lifetimes are in the order of 8–9 yr (Table 5), and the effective residence time of a perturbation is 12 yr (Prather, 1994, 1996). Any changes in OH abundance, e.g. by air traffic emissions, thus generate decadal perturbation to atmospheric chemistry (Wild et al., 2001) and require multi-decade simulations to. Instead, changes in CH_4 loss are estimated by tropospheric OH changes. Methane lifetime changes are therefore subsequently deduced (see e.g. Fuglestvedt et al., 1999; Derwent et al., 1999). Modelled relative lifetime changes per unit aircraft NO_x emission are of the order $-1.9 \pm 0.9\%/(\text{Tg N yr}^{-1})$ (Table 7) on the basis of a number of 19 experiments from 7 models, shown in Fig. 13. A small part of the variability in CH_4 lifetime changes can be associated with the different O_3 responses: the response in CH_4 lifetime in relation to the O_3 increase ($\Delta\tau_{CH4}/\Delta O_3$) shows a variability amongst the models, which is reduced by 15%, i.e. from 0.49 to 0.42.

Table 7
Multi-model mean values for specific methane lifetime changes and related radiative forcings (Hoor et al., 2009).

Units	$\Delta\tau_{CH4/emission}$	$\Delta\tau_{CH4}/\Delta O_3$	RF O_3/emission	RF CH_4/emission	RF O_3/RF CH_4
	%/(Tg N yr^{-1})	%/DU	mW m^{-2}/Tg N yr^{-1}	mW m^{-2}/Tg N yr^{-1}	
Mean	−1.88	−2.21	36.9	−23.2	−1.65
Standard deviation	0.91	0.92	10.4	7.2	0.36
Norm. std. dev.	0.49	0.42	0.28	0.31	0.22
No. of experiments	19	17	10	10	10
No. of models	7	7	5	5	5

The effective residence time of O_3 and CH_4 perturbations differ considerably: one month vs. a decade. Therefore, the temporal evolution of O_3 and CH_4 changes due to air traffic emissions is very different. Stevenson et al. (2004) investigated the impact of an artificially magnified air traffic pulse emissions of 1-month-duration. The O_3 increases were found to be quite rapid, but declined in the third month (Fig. 15), whereas the CH_4 decrease was more persistent because of its longer lifetime. Stevenson et al. (2004) found that after approximately 6 months, O_3 changes were negligible but the CH_4 decreases persisted. This implies that less O_3 precursors are available and that the O_3 production decreases via reaction (4) leading to a slight O_3 decrease (Fig. 15).

5.3.4. Radiative forcing from ozone and methane changes

Table 7 gives a summary of the RF arising from changes in O_3 and CH_4 from aircraft NO_x emissions. Since model studies were based on different emission scenarios with differing total emissions, the specific RF is highlighted, i.e. that relative to the annual aircraft NO_x emissions, which focuses on the model's sensitivity between emission and RF rather than differences arising from different emission scenarios. The results show a specific RF of 36.9 ± 10.4 (mW m^{-2})/(Tg N yr^{-1}) for O_3 and −23.2 ± 7.2 (mW m^{-2})/(Tg N yr^{-1}) for CH_4, i.e. the standard deviation amounts to 30%. For all models, the absolute O_3 RF was larger than that for the CH_4 RF. The ratio is 1.65 ± 0.36 and shows a much smaller standard variation of around 20%, compared with individual forcings. Note that this number is dependent on the 3-D distribution of air traffic emissions and that regional changes could change this relationship. Specific RFs from the IPCC (1999) may be readily calculated, yielding 39.4 (mW m^{-2})/(Tg N yr^{-1}) for O_3 and −24.0 (mW m^{-2})/(Tg N yr^{-1}) for CH_4 with an absolute O_3/CH_4 ratio of 1.64 (all 1992 conditions). The picture is somewhat complicated by the evident non-linearity of response, since future scenarios (2015, 2050) yield different results, with a declining rate of response for O_3 with higher NO_x emissions, as might be expected. Results from the TRADEOFF project (Sausen et al., 2005) yielded 38.5 (mW m^{-2})/(Tg N yr^{-1}) for O_3 and 15.8(mW m^{-2})/(Tg N yr^{-1}) for CH_4. It appears that the specific RF for O_3 has decreased slightly over the last 10 years with model improvements; however, there is much variability in the results presented here (Table 7). In terms of specific forcing, O_3 RF from all sources (using IPCC, 2001 emissions and RF) is 6.7 (mW m^{-2})/(Tg N yr^{-1}) for O_3.

Fig. 16 shows the impact of regional normalized emissions of NO_x on O_3 and CH_4 RF; both show a clear latitudinal gradient with larger absolute RFs in the tropics (Grewe and Stenke, 2008). However, O_3 RF peaks for emissions in the upper troposphere, whereas CH_4 peaks in the mid troposphere. The ratio shows a maximum in the upper troposphere, with lower values at higher latitudes (Fig. 16c). Surface emissions of NO_x may even lead to a cooling (Wild et al., 2001), which is indicated by values <1 in Fig. 16c. Since future air traffic is expected to increase at a greater rate in tropical regions, e.g. South East Asia, the ratio may increase.

The above RFs from aircraft NO_x emissions do not take into account particle emissions (sulphate aerosols) and their impact on heterogeneous chemistry. Pitari et al. (2002b) calculated both the direct RF of sulphuric acid particles and their indirect RF via heterogeneous chemistry, the latter by applying 2 CTMs (ULAQ, TM3). The results showed that the O_3 radiative forcing almost halved from 27 to 15 mW m^{-2} (Fig. 17), whereas CH_4 RF remained almost unchanged. The ratio decreased in the ULAQ and TM3 models from 3.5 to 1.9.

6. Future impacts on stratospheric composition and changes in radiative forcing, mean surface temperature and UV flux

6.1. Supersonic scenarios – introduction

In the IPCC (1999) assessment, supersonic aircraft emissions of NO_x and H_2O were incorporated within six 2-D models and three 3-D models, using pre-calculated temperature and transport fields

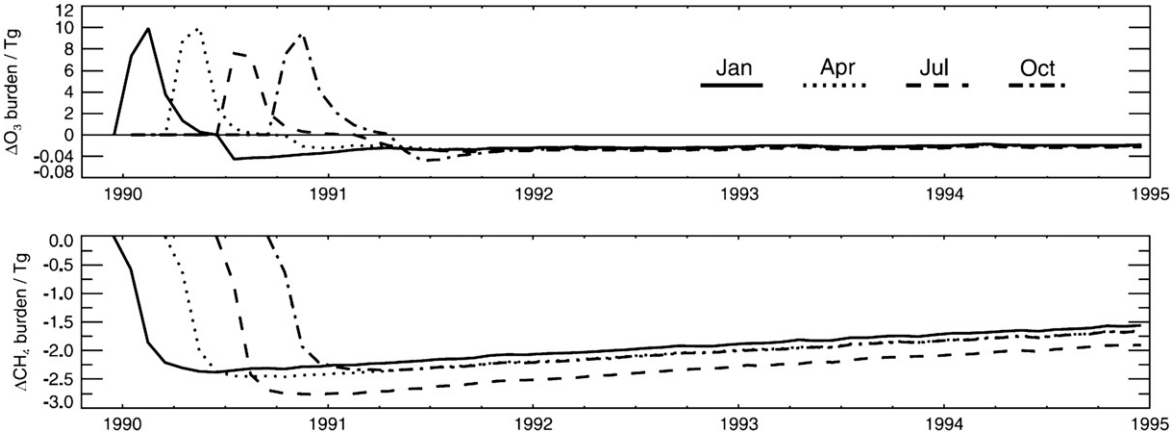

Fig. 15. Time evolution of perturbations in ozone and methane total burden from a 1-month-pulse of aircraft NO_x emissions. Note that negative scale for ozone has been expanded for clarity (adapted from Stevenson et al., 2004.Copyright, 2004; American Geophysical Union. Modified by permission of American Geophysical Union).

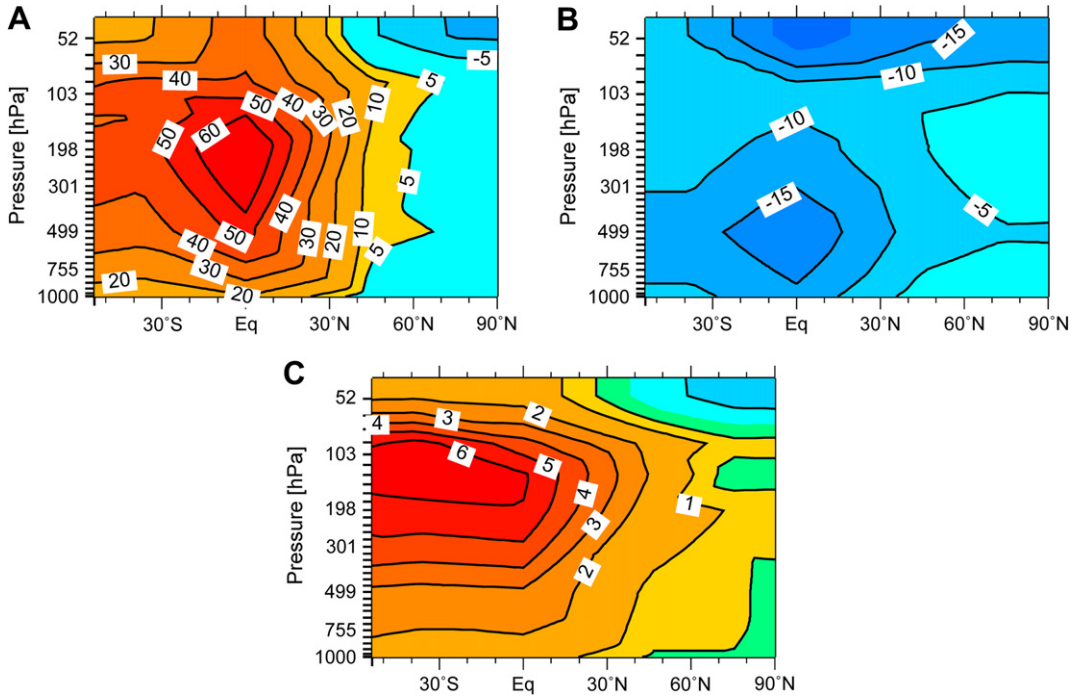

Fig. 16. Impact of the location of an emission on the RF of O_3 (panel A) and CH_4 (panel B) in mW m^{-2} ; the negative ratio of both is shown in (panel C). The RF values at a certain pressure level and latitude refer to a sustained emission of 1 Tg N yr^{-1} at that location.

(Isaksen et al., 1999). Below 25 km the calculated O_3 perturbation was found to be highly model dependent, resulting from the different transport and chemistry schemes incorporated in the individual models. The following sub-sections will discuss the major scientific updates since IPCC (1999), focusing on different aspects of modelling that are relevant for future supersonic aircraft impact studies.

6.2. Large-scale transport

An important sensitivity in the modelling of the potential impact of a future HSCT aircraft fleet was shown by Rogers et al. (2000). The model scenarios performed were identical to those used in IPCC (1999 – see Isaksen et al., 1999) but the importance of the background meteorological conditions in determining the potential impact of HSCTs was assessed by forcing the model with UK Meteorological Office analyses for the years 1992–1998. The use of annually varying meteorological analyses led to an inter-annual variability in the modelled transport of aircraft-emitted NO_x and H_2O from the North Atlantic flight corridor. The resulting O_3 perturbations exhibited an inter-annual variability of ~50 ppb in the middle stratosphere, which was of a similar magnitude to the differences between the O_3 perturbations calculated by models in Isaksen et al. (1999). This result highlighted both the importance of the chosen background meteorological conditions in aircraft assessments and the extent to which differences in meteorology can contribute to differences between model calculations.

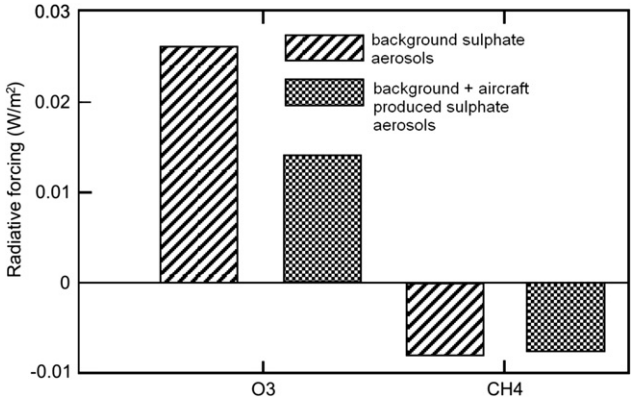

Fig. 17. Annual globally averaged radiative forcing of O_3 and CH_4 (W m^{-2}) for simulations with heterogeneous chemistry on background sulphate aerosols and simulations with heterogeneous chemistry on background plus aircraft produced sulphate aerosols (adapted from Pitari et al., 2002b; Copyright, 2004; American Geophysical Union. Modified by permission of American Geophysical Union).

To understand fully the inter-annual variability of the results, it is necessary to consider the global transport of aircraft emissions in the stratosphere. The zonal mean background distribution of N_2O, used as a dynamical tracer, at an altitude of 32 km was studied by Rogers et al. (2000) as a function of the meteorological year (Fig. 18, panel A). It should be noted that this altitude corresponds to the region of maximum potential O_3 loss from supersonic aircraft emissions. Large N_2O values indicate regions of ascent (e.g. tropics), while smaller N_2O values indicate regions of descent (e.g. high latitudes). Fig. 18 (panel A) shows the inter-annual variability of the N_2O distribution revealing the variation in dynamical circulation between different meteorological years such that larger N_2O values in the tropics suggest periods of stronger ascent. Stronger descent at the Poles was revealed by smaller N_2O values. As expected, periods of strong Polar descent are, in general, accompanied by large Polar O_3 values, from the transport of O_3-rich air from aloft. The zonal mean background distribution of NO_y, a dynamical tracer, at an altitude of 32 km is studied as a function of the meteorological year. The change in NO_y, from future supersonic aircraft, shows a pattern somewhat similar to that observed in the background N_2O distribution with increases in NO_y in the tropics particularly during 1994 meteorological conditions (Fig. 18, panel B). This study therefore suggests that the stronger ascent observed in the tropics for the meteorology in 1994 produced an enhanced upward

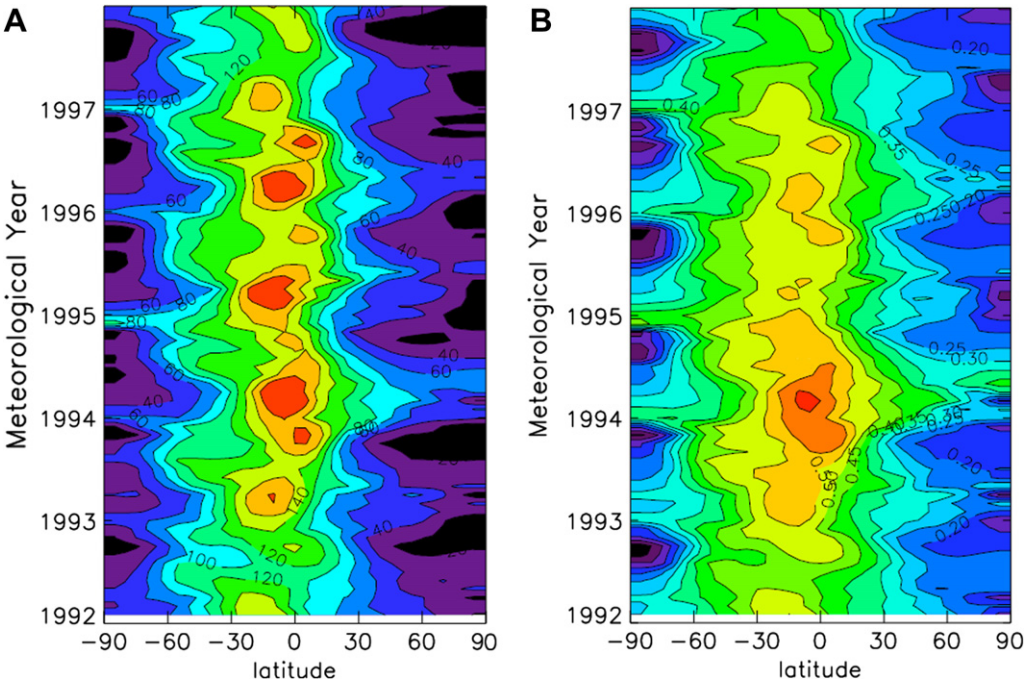

Fig. 18. SLIMCAT modelled background zonal mean N_2O (ppbv) at an altitude of 32 km as a function of meteorological year (A) and zonal mean NO_y differences (ppbv) (B) at an altitude of 32 km. Differences are calculated between the integration with both subsonic and supersonic aircraft and the integration with only subsonic aircraft, as a function of meteorological year (adapted from Rogers et al., 2000).

transport of aircraft emissions from the lower stratosphere (Rogers et al., 2000). The resulting increase in NO_y (and hence NO_x) in the middle stratosphere leads to reduced O_3 concentrations in the region where NO_x dominates the O_3 destruction.

A further study of Rogers et al. (2002a) focussed on the transport of aircraft-like emissions from sub- and supersonic aircraft. The results of this tracer study, a development of that of Danilin et al. (1998) with updated models, revealed that the transport of aircraft-like tracers was highly variable amongst models during a single two-year integration, highlighting the importance of reproducing the correct transport processes throughout the lower atmosphere in calculations of the atmospheric impact of aircraft.

6.3. Chemistry

After the IPCC (1999) Special Report, new studies have been undertaken using the various Jet Propulsion Laboratory (JPL) chemical kinetics updates (Sander et al., 2000, 2003), which resulted in different conclusions to those made by the IPCC (1999).

The NASA High Speed Research Program conducted an extensive evaluation of the effects of emissions from supersonic aircraft on the stratospheric O_3 layer. The study of Baughcum et al. (2003) evaluated the effect of fleet size, cruise altitude, NO_x emission levels, water vapour emissions and sulphate emissions on O_3. In their study, a two-dimensional model was used to evaluate parametrically the O_3 impact of supersonic aircraft as a function of fleet fuel use at cruise altitudes, $EINO_x$, and cruise altitude. In Baughcum et al. (2003) the sensitivity of the O_3 impact calculated with the CSIRO model (Randeniya et al., 2002) was evaluated as a function of the choice of reaction rate constants. The version of the model using the JPL 1997 chemical kinetics assessment (DeMore et al., 1997) predicted larger O_3 perturbations than did calculations presented by IPCC (1999). These differences arose both from changes in the model transport and the use of the updated JPL reaction rate coefficients and photolysis cross-sections. This resulted in a greater sensitivity of O_3 depletion to NO_x emission levels than in the previous assessment. Updating the reaction rate constants and photolysis cross sections in line with the JPL 2000 assessment of chemical kinetics (Sander et al., 2000), resulted in an increase the calculated O_3 dependence on $EINO_x$, because of the greater accumulation of exhaust emissions and the NO_x being transported to higher altitudes where NO_x chemistry dominates the O_3 removal process. The partial update to the JPL 2002 recommendations (Sander et al., 2003) resulted in a further increase in the impact, but not as large as that for the change from JPL 1997 to JPL 2000 chemistry (Fig. 19a).

The study of Wuebbles et al. (2003a) focussed on aircraft that would cruise primarily in the UTLS region, including the faster commercial aircraft that would primarily be used for intercontinental flights longer than 2500 nautical miles and a small fleet of Supersonic Business Jets (SSBJs). This study showed a much greater sensitivity to NO_x emissions from supersonic aircraft than was found the IPCC (1999) assessment, resulting from the new NASA chemistry recommendations.

In Fig. 19, the change in annual average Northern Hemisphere total O_3 column is shown as a function of $EINO_x$ in 2015 for a supersonic fleet of 500 HSCTs: the emissions were the same as those used in IPCC (1999 – see Isaksen et al., 1999), with fixed aerosol surface area density (SA0). The black line with the symbol "+" in Fig. 19 represents the SLIMCAT model calculation with updated reaction rates (Sander et al., 2000). This result contrasts with the IPCC assessment, which suggested that the impact of supersonic aircraft on the atmosphere was primarily through the role of water vapour emissions both on atmospheric O_3 and climate change. This significant difference results from the inclusion of new kinetic data in SLIMCAT atmospheric chemical transport model. With the inclusion of the updated rates, an increase in the $EINO_x$ has a significant effect on the O_3 column, with a reduction in the Northern Hemisphere O_3 column of −3.2% for an $EINO_x$ of 15. The reason for the large dependence of the column O_3 on the $EINO_x$ can be seen by considering that in the IPCC (1999) assessment, a cross-over point in the O_3 chemical production and destruction terms

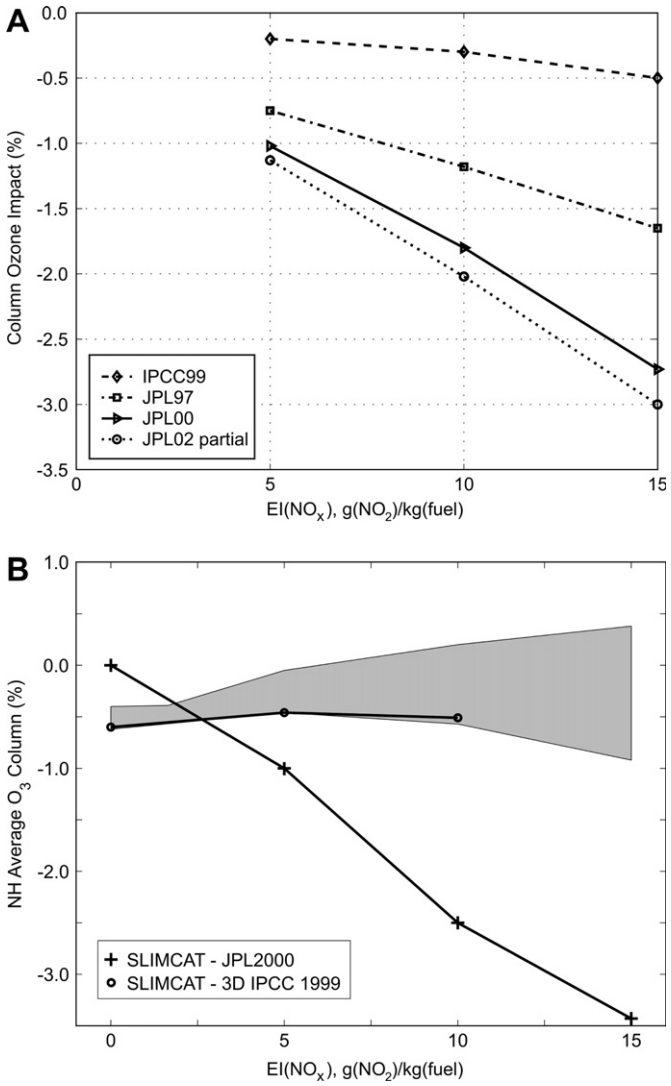

Fig. 19. Northern Hemisphere total ozone column change as a function of $EINO_x$ in 2015 for a supersonic fleet of 500 HSCTs (A) (adapted from Baughcum et al., 2003). Northern Hemisphere total ozone column change as a function of $EINO_x$ in 2015 for a supersonic fleet of 500 HSCTs (B). The shaded area represents the range of model variability in IPCC (1999) (adapted from IPCC, 1999). The black line with symbol "+" represents the SLIMCAT model calculation with updated reaction rates (B) (adapted from Dessens et al., 2007).

from NO_x chemistry, could be seen at an altitude of ~20 km. With the new kinetic data, the cross-over point is at a much lower altitude in the SLIMCAT calculations. With the injection of supersonic aircraft emissions at ~18 km almost all NO_x and H_2O emissions now take place in the region of O_3 chemical destruction. This has resulted in an O_3 decrease throughout the stratosphere and therefore in the O_3 column. This conclusion underlines the potential impact of a fleet of supersonic aircraft on the atmosphere and emphasises the necessity to continue to develop low NO_x combustion engines for the future, as well as the importance of maintaining state of the art kinetic data and updating assessments of impacts.

Sensitivity studies of supersonic aircraft emissions of H_2O and NO_x were carried out in the EU projects SCENIC and TRADEOFF. As a part of the SCENIC project, Søvde et al. (2007) investigated the impacts of NO_x, H_2O and aerosols using the OsloCTM2 model and SCENIC emission scenarios. They concluded that aerosol emissions in a projected future (2050) 'mixed fleet' of subsonic and supersonic aircraft are likely to increase stratospheric O_3 above 20 km in altitude, because of a lowered loss from NO_x. This mid-stratospheric O_3 increase was found to be larger than the O_3 decrease below 20 km, because of the reduced O_3 production from NO_x and more O_3 depletion by increasing ClO and BrO. However, the net effect of aircraft aerosol emissions on the O_3 column can be highly model-dependent, being a function of the NO_x removal efficiency from the aircraft emission region by large-scale transport (Rogers et al., 2002a). The faster is the removal rate, the larger is the mid-stratospheric impact on O_3.

A modelling study on potential ozone changes due to heterogeneous chemical reactions on black carbon soot particles emitted by aircraft has been undertaken by Wei et al. (2001). Before IPCC (1999), some studies had suggested that heterogeneous chemistry on soot emitted from high altitude aircraft could affect stratospheric ozone depletion (e.g. Bekki, 1997). However, these studies were limited because they did not adequately consider the decrease in reaction probability with time as the surface of the soot becomes 'poisoned' by its interactions with various gases. Wei et al. (2001) have shown that, even if active sites on soot surfaces are regenerated, upper troposphere and lower stratosphere ozone losses on aircraft emitted soot occurring through heterogeneous reactions are insignificant once poisoning effects are considered. This study was carried out for both subsonic and supersonic aircraft emissions.

6.4. Polar stratospheric clouds

Emissions from supersonic aircraft may influence the probability of formation and the properties of polar stratospheric clouds (PSCs). The cloud particles are composed of nitric acid and water, and stratospheric sulphate aerosols are believed to constitute the background particles, which serve as sites for PSC particle growth at low temperatures. New sulphate aerosol particles could be produced resulting from aircraft plume processing of SO_2/SO_3 and enhanced concentrations of SO_2, eventually oxidising to H_2SO_4, and increasing the stratospheric sulphate mass mixing ratios and background aerosol concentrations. More directly, aircraft emissions of water vapour and NO_x, converting into HNO_3, may lead to higher threshold temperatures for PSC formation and enhanced PSC particle surface area densities.

Perturbations in HNO_3 and H_2O arising from stratospheric supersonic aircraft emissions of NO_x and H_2O were investigated by Larsen et al. (2002). These perturbations were then used as input to a detailed microphysical model in order to study the effects on PSC formation. Microphysical simulations using domain-filling trajectories were performed in order to investigate the influence on Artic PSC formation and the properties of enhanced concentrations of HNO_3 and H_2O, caused by aircraft emissions in year 2015 scenarios. The results showed that increased concentrations of HNO_3 and H_2O, of the order of 5–10%, emitted from a combined fleet of subsonic and supersonic fleet, would have a direct influence on the thermodynamic threshold temperatures for the existence of nitric acid trihydrate (NAT), super-cooled ternary solutions (STS), and ice in the Northern Hemisphere Polar stratosphere (Fig. 20). This may cause the frequency of occurrence of temperatures below these thresholds to increase by 2–5% and may enhance Type 1b PSC equilibrium volumes by about 10%. Increased concentrations of water vapour, caused by stratospheric aircraft emissions, imply higher freezing temperatures for ice in PSC particles, required for the formation of solid type of PSC particles. These results show that the 'supersonic' aircraft emission-induced formation of solid type PSC particles may significantly increase the denitrification rate and lead to even larger relative increases in dehydration.

The impact of stratospheric H_2O increases on PSC abundance is also discussed by Stenke and Grewe (2005) who investigated two

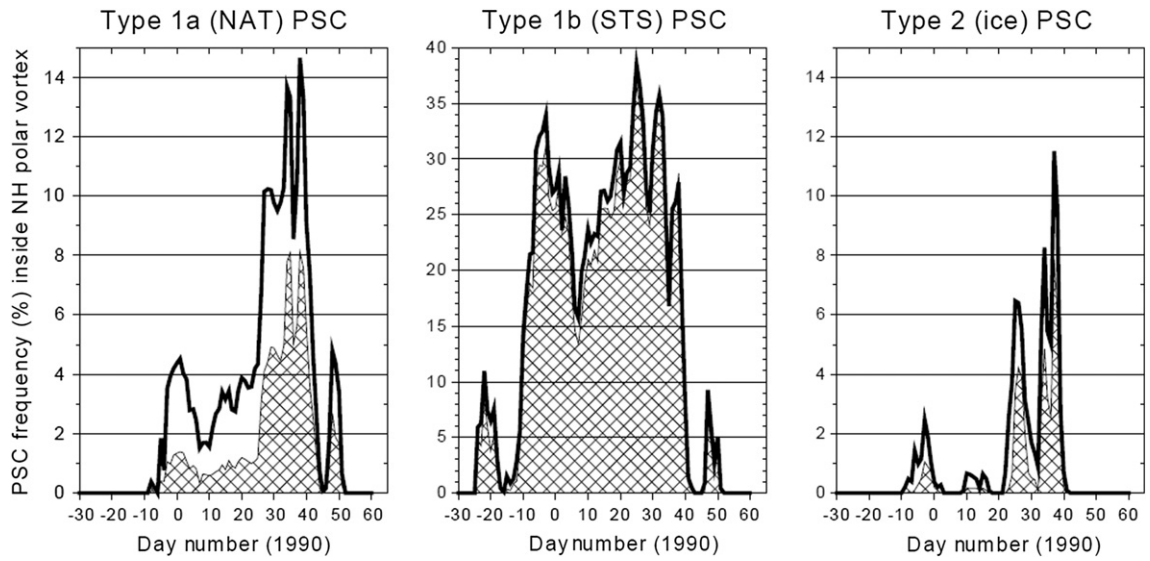

Fig. 20. Frequency of the occurrence of type 1a PSCs (left), type 1b PSCs (middle) and type 2 PSCs (right) at model level 5 (approx. 475 K potential temperature) in the 'no aircraft' emission scenario (hatched curves) and the 'supersonic' scenario (thick curves) using the University of Oslo aircraft induced perturbations in H_2O and HNO_3 concentrations (Larsen et al., 2002).

different long-term perturbations of lower stratospheric water vapour of +1 ppmv and +5 ppmv. They found that a long-term water vapour increase not only affected stratospheric gas-phase chemistry but also heterogeneous ozone chemistry in polar regions. The model results indicated an enhanced heterogeneous ozone depletion during Antarctic spring arising from a longer period in which PSCs can form. In the northern hemisphere polar vortex, ozone depletion during arctic spring was unaffected by the water vapour increases, because of the lesser PSC activity.

6.5. Radiative feedbacks

Pitari et al. (2001, 2002a) used a CCM to study the potential impact of H_2O and O_3 radiative feedbacks on the stratospheric composition changes produced by supersonic aircraft. They found that atmospheric tracers are significantly affected by H_2O and O_3 radiative feedbacks on the stratospheric circulation; one consequence is that dynamically driven O_3 changes have to be taken into account along with chemically produced ones. The spatial distribution of stratospheric H_2O and O_3 (as well as other long-lived tracers) was determined by the stratospheric residual circulation, which could be perturbed by upsetting the latitudinal gradients of radiatively active gases. This is the case of lower stratospheric in situ H_2O emissions from future supersonic aircraft: an increase of approximately 10% at Northern mid to high latitudes was predicted when treating H_2O as a passive tracer (see also IPCC, 1999). The consequently larger H_2O latitudinal gradient increases the pole-to-equator gradient of long-wave heating rates. Consequentially, the net effect may be that of a slight reinforcement of the stratospheric Brewer-Dobson circulation with enhanced tropical upwelling and mid-latitude subsidence. This change perturbs the O_3 distribution as well, producing more tracer accumulation in the extra tropical lowermost stratosphere. The globally averaged column O_3 change, was found to increase from +0.05% in the fixed circulation case to +0.6% in the radiatively interactive case. This net O_3 increase is a consequence of the enhanced mid-latitude downwelling branch of the Brewer-Dobson circulation, which transports more O_3 close to the tropopause, where the chemical loss is slower than at higher altitudes.

6.6. Radiative forcing

The IPCC (1999) also assessed the potential effects that supersonic aviation may have on climate change (Prather et al., 1999). The HSCT option of building a fleet beginning in 2015 and capping at 1000 aircraft in 2040 has a significant impact on total aviation RF: the HSCT aircraft themselves cause an RF of +0.10 W m^{-2}, which is offset only by −0.02 W m^{-2} from displaced subsonic aircraft. This large RF from HSCT aircraft was driven mainly by RF from increased stratospheric H_2O. This single component has a large uncertainty (at least a factor of 3) associated with the calculation of the stratospheric build up of H_2O and the value of its RF.

Further studies have been made in the last few years, in order to better estimate the potential HSCT RF contribution. Preliminary results of Wuebbles et al. (2003b) suggested that the stratospheric adjusted radiative forcing for perturbations to O_3 were within the range of the results presented by the IPCC (1999 – see Prather et al., 1999). However, their evaluation of the RF for the H_2O perturbation suggests that IPCC (1999) may have overestimated the stratospheric adjusted RF for the H_2O changes. Pitari et al. (2001) have shown that once H_2O and O_3 radiative feedbacks on the stratospheric circulation are accounted for, the dynamically interactive H_2O accumulation may be substantially different from that resulting from a passive tracer treatment. They found a reduction in H_2O accumulation at the tropical lower stratosphere, due to the above discussed stratospheric circulation reinforcement. This produced a significant reduction of the HSCT H_2O climate forcing. A different conclusion was reached in the SCENIC project when the E39/C CCM (Hein et al., 2001) was used: in this case the stratospheric accumulation of H_2O from supersonic aircraft was found to increase when the radiative feedbacks were included, because of a tropical tropopause layer (TTL) warming produced by the supersonic aircraft emissions net RF (a warming not predicted by Pitari et al., 2001). These findings support the earlier conclusions of Rind and Lonergan (1995) that the magnitude of the direct climate forcing produced by an HSCT aircraft fleet is sufficiently large that it is important to consider the effect of the feedbacks when estimating the climatic/dynamic response to such aircraft emissions.

Additional studies are currently underway to better evaluate the differences to the results of the IPCC (1999 – see Isaksen et al., 1999)

assessment of supersonic aircraft emissions. The study of Grewe et al. (2007) proposes a metric for the quantitative assessment of different options for supersonic transport with regard to the potential destruction of the O_3 layer and climate impacts. Options for fleet size, engine technology ($EINO_x$), cruising altitude, range, and cruising height were analysed, based on SCENIC emissions scenarios for 2050, which were to be as realistic as possible in terms of e.g., economic markets and profitable market penetration. Based on the CCM and CTM calculations for H_2O and O_3, the stratospheric adjusted RF has been calculated for the various cases (see Section 4.2 and Table 4). Table 8 gives the results for the base case from a set of models for H_2O, O_3 and CH_4, and from one model for contrails, black carbon and sulphate aerosols.

The results presented in Table 8 indicate that H_2O is the most important climate agent with respect to supersonic transport with values between 15 and 35 mW m^{-2} in 2050 and a mean value of 23 mW m^{-2}. The range of resultant forcings from the same emissions scenario can partly be explained by the variability in the differently simulated total water vapour increase: the CTM2, ULAQ and SLIMCAT models show the same response with 0.37 ± 0.02 mW m^{-2} Tg^{-1}, whereas the E39/C model shows 0.28 mW m^{-2} Tg^{-1}: this smaller response is likely to have resulted from the larger H_2O background in the E39/C model, leading to saturation effects (Forster et al., 2001). The ULAQ radiation scheme showed a factor of 2 higher values than the E39/C model, employing the same H_2O perturbation and background field (Table 8). These results are consistent with previous findings (IPCC, 1999), which showed an uncertainty of a factor of two in the calculation of the water vapour related RF, with lower values derived with E39/C model, compared with a narrow band model (Forster and Shine, 1997).

For O_3, the values ranged between −8.6 and +4.7 mW m^{-2}. The differences were the result of background O_3 concentrations, perturbation pattern, and magnitude of emissions. The changes in the lifetime of tropospheric CH_4 results in a mean change of the RF of −1.59 mW m^{-2} and may be of the same order of magnitude as the CO_2 RF perturbation. The change in contrails occurrence tends to reduce the climate impact, since more supersonic air traffic is replacing subsonic air traffic at higher latitudes (leading to fewer contrails) than lower latitudes (leading to additional contrails).

The total RF calculated ranged between 9 and 29 mW m^{-2}, with a mean value of 22 mW m^{-2} (see Table 8). The large range of uncertainty of a factor of three reflects the uncertainties in a number of processes which includes: stratospheric transport, chemistry, and radiation. Previous studies have shown that the uncertainty in the calculation of the RF is less than 10%, except for H_2O (Forster et al., 2001) and therefore smaller than those arising from differences in the transport and chemical calculations.

In the work of Pitari et al. (2008), based on the results of the EC project SCENIC, the RF impact of a future supersonic aircraft fleet was assessed in terms of perturbations of the chemical composition of the stratosphere and the potential climatic impact of aerosol particles, directly injected by the aircraft or formed after oxidation of SO_2. For the aerosols, both the direct forcing (i.e. scattering and absorption of incoming solar radiation) and indirect forcing produced by changes of chemical species (i.e. O_3) affected by heterogeneous chemical processes on the surface of aerosol particles were calculated. The direct impact of aircraft SO_4 aerosols on RF was negative from scattering of solar radiation; the direct RF in the long-wave spectrum, on the other hand, was found to be negligible because of the small size of these particles. The RF from supersonic aircraft emissions of SO_4 aerosols ranged from about −4 to −23 mW m^{-2}. Black carbon aerosols, on the other hand, normally give a positive RF since they effectively absorb incident solar radiation (the single scattering albedo is close to 0.7, whereas it is unity for SO_4 particles). As in the case of SO_4, the small size of aircraft particles produced a negligible RF in the long-wave spectrum. The calculated RF from aircraft emissions of BC from supersonic aircraft ranged from about 0.4 to 11 mW m^{-2}.

Fig. 21 shows the (S6-S4) net global RF per component. The bar indicates the range of model variability, since here O_3 and H_2O profile changes were taken from all four models participating in this work (SLIMCAT/UCAM, ULAQ, UiO, ECHAM3/DLR, see Pitari et al., 2008). Water vapour and SO_4 gave the largest contributions to RF (28 and −12 mW m^{-2}, respectively) (Grewe et al., 2007).

6.7. Perturbation to surface UV

The transfer of solar ultraviolet (UV) radiation through the atmosphere and its levels at the surface are controlled by a hierarchy of factors (e.g. Bais et al., 2007), the most important being the Sun–Earth geometry, clouds and ozone. Gaseous or particulate atmospheric constituents modify the solar UV radiation through absorption and scattering processes.

Emissions from civil aviation may influence the concentrations of these species, resulting in changes in the intensity of radiation reaching the earth's surface, or various altitudes in the troposphere. It is well known that aircraft emissions (either of the existing fleet or of potential future fleets) may affect ozone, cloudiness and aerosols (see sections 5 and 7, respectively). Although the underpinning mechanisms are well understood, quantification of these effects is still difficult because of the effects of other atmospheric processes (chemical or dynamical) which act in parallel. Similarly

Table 8
RF (mW m^{-2}) of the perturbations from the replacement by supersonic aircraft (Scenario S5-S4) on the basis of various model results. Calculations are based on the E39/C radiation code. Additionally, a calculation of the RF using the ULAQ radiation code and ULAQ perturbation pattern is used. The calculation of the totals includes the mean values for CH_4 for the SLIMCAT model. Abbreviations: Ctr: contrails; BC: Black carbon; Sulph: sulphate aerosol.

Model	CO_2	H_2O	O_3	CH_4	Total	Ctr	BC	Sulph.	Total
E39/C	3.3	17.7	0.3	−3.3	18.0	−0.6			17.4
CTM2	3.3	23.0	−7.4	−1.3	9.0				
ULAQ	3.3	15.8	4.7	−0.1	23.3				
SLIMCAT	3.3	35.9	−8.6	(−1.6)	29.0				
Total	3.3	23.1	−2.8	−1.6	21.9				
ULAQ	3.3	33.0	3.8		40.1		4.6	−11.4	33.3

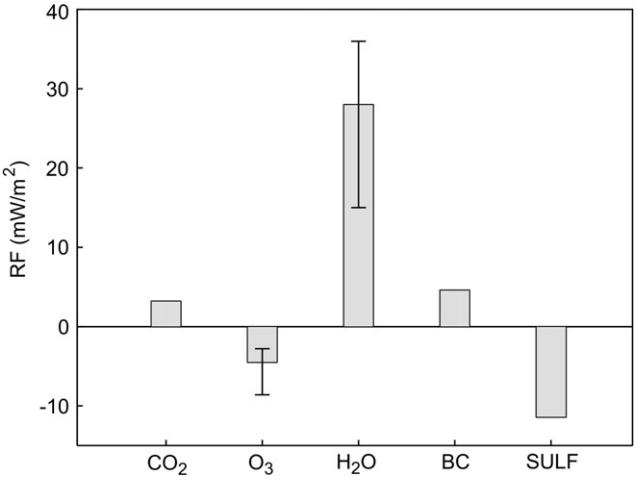

Fig. 21. Summary of radiative forcing per component in 2050 (mW m^{-2}), O_3 and H_2O radiative forcing average values and variability were calculated using the DLR model radiative code applied to O_3 and H_2O changes (S6-S4) calculated by UCAM, ULAQ, DLR and UiO CTMs (Pitari et al., 2008).

difficult is the prediction of these effects for future atmospheres. Once the changes in the aforementioned atmospheric factors (clouds, ozone and aerosols) are known, the calculation of changes in UV radiation levels at a given location and time is straightforward, through the use of radiative transfer models (RTMs). Such calculations have been made in the past (IPCC, 1999 – see Ryan et al., 1999), showing that surface erythemal irradiance around the middle of the 21st century may increase by less than 1% at all latitude bands as a result of introducing supersonic aircraft in the future fleet. Without supersonic aircraft the erythemal irradiance was predicted to decrease, also by less than 1%. Finally, the IPCC (1999) report concluded that the uncertainties in the calculated irradiance are in the range −2% to +3%.

Whilst the focus of the IPCC (1999) report was to assess the impact of changes in the future fleet with respect to the present situation, this work presents estimates of the surface UV changes due to changes in the composition of the fleet under the predicted atmospheric conditions around the middle of the 21st century. The UV calculations were based on predictions from the ULAQ CCM (Pitari and Mancini, 2001) which was run for the SCENIC project emission scenarios, specific for future supersonic aircraft emissions (Grewe et al., 2007). The ULAQ CCM provided ozone columns and profiles, profiles of aerosol optical properties (optical thickness and single scattering albedo), and temperature profiles for 2050, representing the average of simulations for the period 2046–2055. These estimates were used as inputs to the Libradtran RTM (Mayer and Kylling, 2005) to calculate the daily erythemal irradiance changes between different scenarios under cloud-free conditions. The effect from possible changes in cloudiness has not been considered since, presently, the aviation-induced changes in cirrus clouds could not be distinguished from changes arising from natural variability, climate change or other anthropogenic effects (IPCC, 2007a,b). The calculated monthly changes in erythemal UV irradiance at local noon for 6 scenarios relative to the base scenario, which includes only subsonic aircraft (SUB), are shown in Fig. 22. The changes are averaged over the extra-tropical latitudes of the Northern Hemisphere, where the bulk of the aircraft emissions occur. In all cases these changes are positive and smaller than 1%.

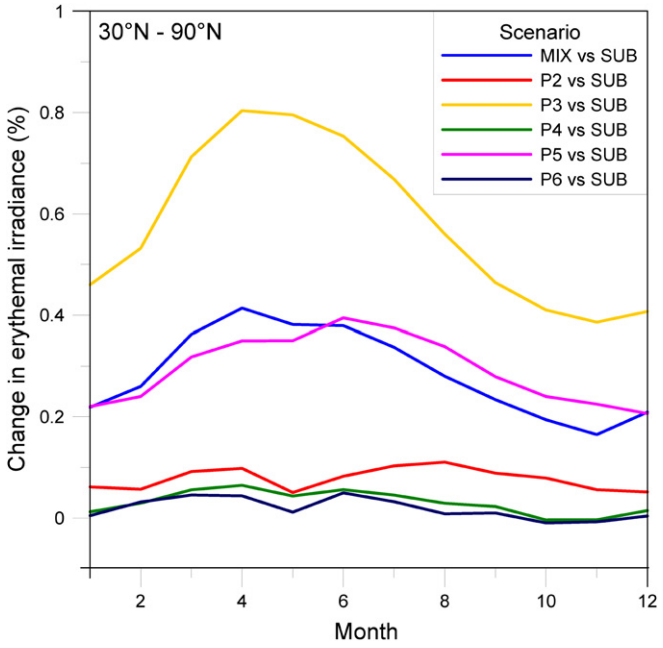

Fig. 22. Monthly changes in surface erythemal irradiance (percentage) for different emission scenarios defined in SCENIC (see Table 4) relative to the base scenario.

The largest differences, although still very small, appear in the P3 scenario with a maximum in the spring season. The P5 and MIX scenarios produce the second largest changes, with maxima in the spring-summer periods. Finally P2, P4 and P6, make little difference to surface erythemal irradiance. In the tropics and the Southern Hemisphere the changes (not shown) are even smaller.

6.8. Supersonic optimization studies

A combined metric is shown in Fig. 23 that captures the 2100 changes in surface temperature with respect to a base case HSCT fleet (filled bars) and the changes in the O_3 layer (dashed bars) for constant RPK (blue) and normalized to a constant HSCT RPK (red). The 'best' option would then be when both bars are minimal. With a constant RPK, the P4 (reduced speed) and the P6 (reduced cruise altitude) options offer the minimal impacts. The P5 scenario (range increase) also has a smaller impact for the combined effect (temperature and O_3 layer) than the base case. However, the increase in range leads to more air routes to South East Asia, which results in more emissions in the tropical tropopause layer and therefore a more intense transport of emitted NO_x into the stratosphere, so that O_3 destruction is enhanced in the scenario P5, compared with the base case. The error bars indicate the minimum and maximum values that can be obtained including all uncertainties discussed in the previous sections, such as model-dependent chemical perturbation, RF calculations and climate sensitivity. Accounting for this uncertainty, the scenarios P4 and P6 both minimize the environmental impact. Both measures can be combined by calculating the product (green bars), which better visualizes the results.

The uncertainty regarding the scenario P2 is largest since the increased $EINO_x$ leads to O_3 destruction and a decrease in surface temperature, which may compensate the H_2O-induced temperature changes, when assuming the lowest simulated water vapour RF and climate sensitivity, which is an extreme case. The lower the supersonic cruise altitude, or the lower the cruising speed, the smaller is the gain in time compared with subsonic flights. Therefore, such a scenario is less economical viable. However, increasing range may increase the viability with less environmental impacts compared with an increase in speed.

7. Effects on clouds and cloudiness

Aircraft effects on clouds may be associated with contrails, contrail-cirrus, and 'soot cirrus'[4]. Contrails are line-shaped cirrus produced when the hot and moist air from the aircraft exhaust mixes with ambient air that is below a critical temperature determined by the Schmidt–Appleman criterion (Schmidt, 1941; Appleman, 1953; Schumann, 1996). Contrail-cirrus is defined here as the cirrus formed from contrails after shear and/or uplift and mixing causes an increase in the areal extent of the contrail. The increase in areal coverage compared with that from contrails may be quantified by a 'spread factor'. 'Soot cirrus' is defined here as cirrus clouds induced by (or perhaps altered by) the addition of heterogeneous ice nuclei from aviation. Cirrus optical depth can decrease if heterogeneous nuclei are added to a region that is dominated by homogeneous ice nuclei (which require higher supersaturations to form ice). The formation of these cirrus clouds would typically have smaller ice number concentrations than those formed on homogeneous ice nuclei. Alternatively, if heterogeneous ice nuclei are added to a region where heterogeneous ice nuclei

[4] The term "soot cirrus" was first used in a paper presented at the 25th International Congress of the Aeronautical Sciences, DGLR, Hamburg (Schumann, 2006).

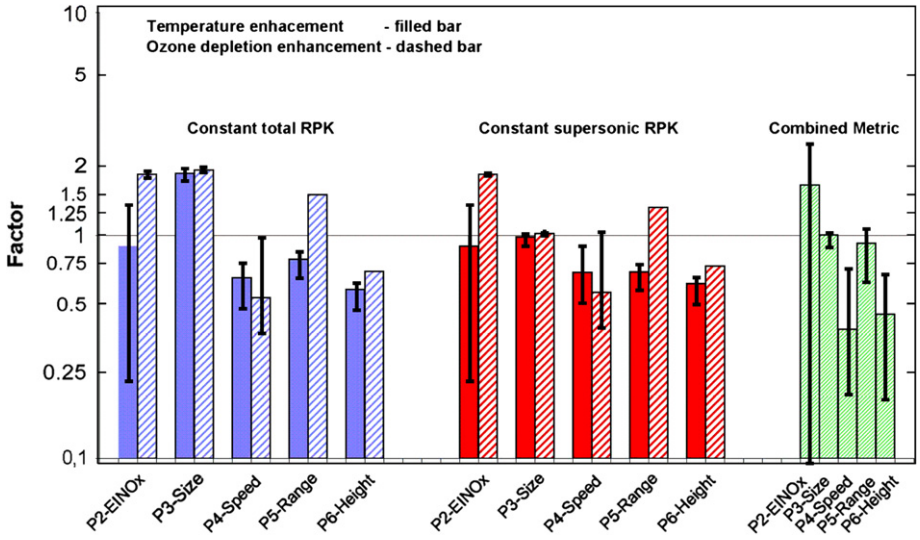

Fig. 23. Changes in global mean surface temperature for the year 2100 (solid bars) and for O_3 (dashed bars) for constant revenue passenger kilometres (RPK) of the total fleet (blue) and constant HSCT RPK (red). The product of both factors is added (green) for constant HSCT RPK. For each bar an uncertainty range is given, which represents minimum and maximum values. No bars are added when only one model has calculated chemical perturbations. In those cases the same uncertainty range has been assumed as for P4 for the calculation of the uncertainty of the product (Grewe et al., 2007).

already dominate ice formation, cirrus ice number concentrations can increase, similar to the "first indirect effect" in ambient water clouds (Penner et al., 2001).

7.1. Contrails and contrail-cirrus

7.1.1. Introduction

Aircraft produce persistent contrails in the upper troposphere in ice-supersaturated air masses and these are routinely observed to shear and spread, producing additional cloudiness termed contrail-cirrus, often forming 'fall streaks' (Heymsfield et al., 1998; Atlas et al., 2006). Contrails are thin line-shaped cirrus clouds, which reflect solar radiation and trap outgoing terrestrial radiation. The latter effect is expected to dominate for thin cirrus (Stephens and Webster, 1981; Hartmann et al., 1992; Meerkötter et al., 1999) which results in a net positive RF value for contrails. Persistent contrail cover has been calculated on a global basis from meteorological reanalysis data (Sausen et al., 1998) or by using a modified cirrus cloud parameterization in a GCM (Ponater et al., 2002; Marquart et al., 2003). Calculations of contrail cover depend upon the extent of supersaturated regions in the atmosphere. This extent is poorly known, but the probability of ice supersaturated regions has been characterized in regions where aircraft typically fly using data from MOZAIC by Gierens et al. (1999a,b) and a global climatology of ice-supersaturated regions has been developed using data from both MLS[5] and AIRS[6] (Spichtinger et al., 2003; Gettleman et al., 2006). Differences between these climatologies and the MOZAIC data are thought to be due to the characteristic sampling volumes for the satellite data as well as the inability of MLS to distinguish adequately between water vapour and thin cirrus. The recent extension of ice supersaturation in the ECMWF integrated forecast system allows the possibility of future assessments based on analysed data or forecast systems (Tompkins et al., 2007).

The spreading and shearing of contrails that produces additional cloudiness beyond line-shaped contrails has been documented in several studies (Schumann and Wendling, 1990; Minnis et al., 1998; Atlas et al., 2006), but estimates of the radiative impact of this additional cloudiness are uncertain. The large number of small ice crystals that are present in contrails may be heated by long-wave radiation from the ground, causing an instability that leads to uplift and causes further supersaturation with the consequent formation of additional cloudiness (Jensen et al., 1998a). Alternatively, the regions of depleted supersaturation in the contrail core may mix with supersaturated regions outside the contrail, allowing further growth of the contrail particles and their eventual precipitation out of the region, followed by further mixing of supersaturated areas and areas of the contrail core (Heymsfield et al., 1998). The ratio of the areal coverage of such cloudiness to that from line-shaped contrails, termed the 'spread factor', was estimated to be 1.8 by Minnis et al. (2004). The estimate of Mannstein and Schumann (2005) should no longer be cited since a similar increase in cirrus coverage with air traffic density has been estimated using the ECHAM4 climate model with natural cirrus only (Mannstein and Schumann, 2007). Estimates of the radiative effects of this additional cloudiness have also been attempted based upon trends in cirrus cloudiness (see Section 7.3 – Boucher, 1999; Fahey et al., 1999; Zerefos et al., 2003; Minnis et al., 2004; Stordal et al., 2005; Stubenrauch and Schumann, 2005; Eleftheratos et al., 2007).

7.1.2. Radiative forcing by contrails and contrail cirrus

Here, we discriminate between linear persistent contrails and contrail cirrus[7] in terms of their development. Discussions of contrails usually imply persistent linear contrails that can be discriminated in satellite imagery as having originated from aircraft, whereas contrail-cirrus is the result of spreading of linear contrails to form a cirrus-like coverage that cannot be necessarily related instantaneously to aircraft operations (in the absence of recording their development).

Estimates of contrail RF are available from a number of studies (Minnis et al., 1999; Marquart and Mayer, 2002; Marquart et al.,

[5] Microwave Limb Sounder, an instrument aboard the NASA Aura satellite.
[6] Atmospheric Infrared Sounder.

[7] The expression 'contrail cirrus' appears to have been first used by Nicodemus and McQuigg (1969), and has subsequently fallen into more popular usage, e.g. Schumann: '*Contrail Cirrus. Invited paper, Cirrus–Topical Meeting, Optical Society of America, Baltimore, October 6-8, 1998*', and Schumann (2002).

2003; Rädel and Shine, 2008; Stuber and Forster, 2007) that use coverage calculated either externally (e.g. Sausen et al., 1998) or internally within a GCM. Whilst the earliest studies assumed a specified optical depth of the contrails (e.g. Minnis et al., 1999), the most recent parameterizations within GCMs have allowed contrail optical depth to be predicted (Ponater et al., 2002), although some recent studies still prescribe an optical depth (e.g. Stuber and Forster, 2007; Rädel and Shine, 2008). Marquart et al. (2003) used this predicted optical depth within the ECHAM GCM to determine a radiative forcing in 1992, 2015, and 2050 of 3.5 mW m^{-2}, 9.4 mW m^{-2}, and 14.8 mW m^{-2}, respectively. These estimates did not include diurnal variations in traffic density but an estimate of this effect resulted in a 10% decrease in the net forcing for 1992. Other studies, however, have shown that the daily cycle of air traffic can be quite important (Meerkötter et al., 1999; Myhre and Stordal, 2001; Stuber et al., 2006; Stuber and Forster, 2007). For example, Stuber and Forster (2007) found that 60% of the global annual mean forcing is associated with night flights, even though only 40% of the distance travelled by aircraft is during the night. Myhre and Stordal (2001) used the Sausen et al. (1998) contrail coverage distribution and the diurnal variation from Schmitt and Brunner (1997) to estimate a reduced forcing of 9 mWm^{-2} compared with their estimate of 11 mW m^{-2} when diurnal variations were not included. Stuber and Forster (2007) used the ECMWF forecast fields to predict contrail cover (outside of the Bakan et al. (1994) region to which all studies tuned their predicted cover) and found an estimated forcing for 1992 of 2.0 mWm^{-2} (and 2.4 mWm^{-2} without the diurnal cycle) (Stuber and Forster, 2007). Both Myhre and Stordal (2001) and Stuber and Forster (2007) assume the contrail optical depth (0.3 and 0.1, respectively) whereas the optical depth in Marquart et al. (2003) is predicted. Contrail optical thickness has been found to be greater over the United States than over Western Europe (Palikonda et al., 2005; Meyer et al., 2002; Ponater et al., 2002), a feature that is captured in the Marquart et al. (2003) simulations.

Radiative forcing by spreading contrail cirrus is not included in the above estimates, since the contrail cover in all studies was tuned to fit the results of the line-shaped contrail cover detected by satellite over Europe (Bakan et al., 1994). The additional cirrus formation may increase cloud cover by as much as 1.8 times or more. Whether this additional spreading of contrail cover increases the RF by about the same amount is unknown. It is even conceivable that such spreading results in a decrease in forcing, if, for example, the increase in cloud cover is associated with a decrease in cloud optical depth or if the cloud cover that results from contrails replaces natural clouds with higher optical depth.

7.1.3. Uncertainties in contrail radiative forcing

The average effect of contrails on the earth's radiation budget, on RF and climate, depends in particular on their global coverage and mean optical thickness. Both quantities are not well known, although model-derived values of contrail cover seem to be similar. This, however, is a consequence of the adjustment of the modelled contrail cover to an observed value in the region 35–75°N and −30°W to 30°E (Bakan et al., 1994). Unfortunately, this observation (based on visual inspection of satellite scenes) is itself rather uncertain. Most striking is the decrease in contrail coverage between the periods 1979–1981 and 1989–1992 over Western Europe in that study, despite the *increase* in air traffic. The observed annual cycle has a maximum in spring/summer which is contrary to expectations based on the annual cycle of upper tropospheric relative humidity (Sausen et al., 1998) and is contrary to results from automatic contrail detection (Mannstein et al., 1999). Bakan et al. also reported a considerable interannual variability with root mean square values of contrail cover of the same magnitude as the average values themselves. The reported averages are often taken to refer to a base year of 1992, but actually, they are some mixture of base years one decade apart, over which period air traffic increased substantially. Later studies (e.g. Rädel and Shine, 2008) considered more recent years and accounted for the air traffic increase when using the Bakan et al. value for adjustment. However, even if the annual growth factor were known, it is not clear from which year onwards one should apply the growth factor. Last, but not least, visual inspection is a highly subjective method. Mannstein et al. (1999) found that contrail cover derived by various trained observers differed by a factor of 2.

Meyer et al. (2007) studied contrail cover over Europe and South East Asia (Thailand and Japan) from AVHRR[8] images and compared the results with contrail cover from the GCM ECHAM4 (Ponater et al., 2002), which was adjusted to the Bakan et al. value. While the GCM has twice as much contrail coverage over Europe than the contrail detection algorithm gives, the situation is the opposite over South East Asia where the contrail detection algorithm sees more than 50% greater contrail coverage than the GCM. Although part of this discrepancy is due to the different base years of the satellite observations and the GCM simulation, this shows that the normalization factor is not constant over the globe or that the GCM algorithm does not capture the correct regional variation. Gierens et al. (1999a,b) showed that the adjustment factor depends on whether fuel consumption or flown distance is used as a measure of air traffic. When flown distances are used instead of fuel use, the computed contrail coverage showed large regional differences from +15% over USA to −50% over SE Asia compared with the fuel-based parameterization.

Large uncertainties are also pertinent to the determination of the mean contrail optical thickness. Meyer et al. (2002) determined the visible optical thickness from the value at 11 μm. The ratio of optical depth at visible wavelengths to that at 11 μm depends sensitively upon the crystal size distribution, expressed as the effective diameter. The latter has values from 10 to 100 μm in the literature for contrails older than 30 min. From this assumption, Meyer et al. (2002) derived a range of 0.1–0.2 for the average optical thickness of contrails over Europe; contrails over USA are on the average optically thicker. Case studies of line-shaped contrails show optical thicknesses ranging from 0.05 to 0.5; values exceeding 1 are rarely observed (Meyer et al., 2002, and references therein). As noted above, the optical thickness of contrail-cirrus after being deformed from the linear shape is unknown.

Virtually all studies of contrail RF have used 'column' type radiative transfer models, which neglect any 3-D effects. Gounou and Hogan (2007) recently undertook a sensitivity study of the effect of horizontal transport of photons on RF from contrails. They found that in terms of horizontal transport, the short-wave effect was dependent on orientation of the Sun with the contrail; for the long-wave effect, the inclusion of horizontal transport increased the RF by ~10%. They also found dependencies of the 3-D effect on optical depth and aspect ratio of the vertical depth and width of the contrail.

7.2. Direct and indirect effects of aerosols

7.2.1. Introduction

Aerosols from aviation produce a small direct RF. The IPCC (1999) forcing estimate for sulphate aerosols was −3 mW m^{-2} in 1992, which was estimated assuming pure ammonium sulphate, a log-normal size distribution, with a dry geometric mean radius of 0.05 μm and standard deviation of 2.0, an ambient relative

[8] Advanced Very High Resolution Radiometer, flown on a variety of satellites.

humidity of 45% in the upper troposphere, and an effective conversion factor from fuel sulphur to optically active sulphate of 50%. The IPCC (1999) forcing estimate for soot aerosols was $+3$ mW m^{-2} for 1992, which was estimated assuming a log-normal size distribution for soot with a dry geometric mean radius of 0.0118 μm and standard deviation of 2.0. These aviation RFs were updated to 2000 by Sausen et al. (2005), but changes were minor. Such values should be revisited in light of the higher absorption optical depth associated with internally mixed sulphate/soot aerosols and the variations in upper tropospheric humidity.

The aerosols emitted by aircraft and formed within the plume that remain in the upper troposphere may also act as ice nuclei. Thus, in addition to the contrail-induced cloudiness discussed above, aircraft may form additional soot cirrus or modify ambient cirrus cloud properties.

Cirrus clouds are globally distributed and are composed almost exclusively of non-spherical ice crystals with an annual global and local frequency of occurrence of about 30% (e.g., Wylie and Menzel, 1999; Wang et al., 1996; Rossow and Schiffer, 1999). Cirrus clouds come in a variety of forms, ranging from optically thick anvil cirrus, closely associated with deep convection, to optically thin cirrus layers frequently observed near the tropopause. Thick anvil cirrus is created by the detrainment of condensate from cumulus updrafts. After the convection diminishes, the remaining detached anvil can evolve to form optically thin cirrus layers as the ice crystals with large radii precipitate out of the anvil (Prabhakara et al., 1993; Wang et al., 1996). The formation of thin cirrus layers can also occur resulting from the synoptic scale uplift of a humid layer (Jensen et al., 1996, 2005; Heymsfield and McFarquhar, 1996; Winker and Trepte, 1998).

7.2.2. Ice formation on ambient aerosols

An increase in ice particle concentrations has been measured in cirrus clouds with elevated soot concentrations that were assumed to be associated with aviation, which could indicate an aviation impact on ice particle formation (Ström and Ohlsson, 1998; Kristensson et al., 2000). However, the impact of aircraft particles on ambient cirrus depends upon the type of ice nuclei present in the ambient atmosphere without aircraft emissions. The particles that initiate ice formation include externally mixed sulphate aerosols, which may homogeneously freeze if temperatures are less than 235 K and supersaturations are greater than 45% with respect to ice (Koop et al., 1998). Heterogeneous nucleation involves aerosol particles that serve as some kind of substrate that matches the crystalline structure of ice. Heterogeneous mechanisms include direct deposition from vapour to ice on a suitable nucleus (deposition nucleation) and freezing of previously condensed supercooled cloud or haze droplets, with the freezing initiated either by contact of a nuclei with the cloud or haze droplet (contact nucleation) or by a nuclei immersed within the cloud or haze droplet (immersion nucleation). Condensation nucleation, where water freezes as it condenses on a particle is also possible. There is still a lack of data on the concentrations and properties of heterogeneous ice nuclei (IN) in the upper troposphere. Measurements during the NASA CRYSTAL-FACE mission confirmed that mineral dust and metallic particles are common heterogeneous IN (Sassen et al., 2003; DeMott et al., 2003a; Cziczo et al., 2004). Analyses of ice nucleating aerosols collected in the upper troposphere during the Subsonic Aircraft: Contrail and Cloud Effects Special Study (SUCCESS) showed that carbonaceous and crustal particles dominated the number fraction of IN (Chen et al., 1998).

Laboratory studies of cirrus ice formation that relate ice nucleation to aerosol properties show that heterogeneous ice nucleation on mineral dust (e.g., Zuberi et al., 2002; Hung et al., 2003; Archuleta et al., 2005; Field et al., 2006; Möhler et al., 2006; Salam et al., 2006), and on soot particles (DeMott, 1990; DeMott et al., 1999; Gorbunov et al., 2001; Möhler et al., 2005) requires lower relative humidity over ice (RHI) than homogeneous freezing on sulphate, while coating soot with sulphate can increase the nucleation thresholds from an ice saturation ratio of about 1.3 at 230 K to 1.5 at 185 K (Möhler et al., 2005). DeMott (2007) reported laboratory experiments with aircraft soot that showed that aircraft soot particles required RHI near 55% near -55 °C. Thus, these soot particles did not nucleate ice any easier than did sulphate aerosol when it freezes homogeneously. These conflicting results regarding the ability of soot to act as an IN make evaluation of the possible effects of aircraft soot on cirrus clouds highly uncertain.

In the upper troposphere, the importance of heterogeneous IN in cirrus cloud formation is largely unknown owing to a lack of information on the properties and abundances of IN, competition between different nucleation modes, and the dynamical factors that affect ice nucleation. Heymsfield and Miloshevich (1993) and Jensen and Toon (1994) concluded that homogeneous nucleation of supercooled drops is responsible for the occurrence of ice. However, DeMott et al. (1994) argued that even a small number of heterogeneous IN can initiate ice formation earlier at lower RHI, suppressing homogeneous nucleation, and changing cirrus cloud properties. DeMott et al. (1997) showed that if insoluble particles were at least 10% of the total number concentration and updrafts were less than 20 cm s^{-1}, they would determine the ice number concentration. On the other hand, Hoyle et al. (2005) demonstrated that the high ice crystal number concentrations (0.1–50 cm^{-3}) measured in cirrus clouds during the SUCCESS mission could only be explained by taking small-scale temperature fluctuations into account (which produce larger cooling rates equivalent to larger updrafts) and assuming that the freezing of ice occurs homogeneously. The formation of a tropopause cirrus cloud layer observed during CRYSTAL-FACE was reproduced using a model with ice nucleation via homogeneous freezing of sulphate aerosols that included the observed temperature perturbations (Jensen et al., 2005). It seems likely, based on the analysis of the Interhemispheric Differences in Cirrus Properties From Anthropogenic Emissions (INCA) project measurements of RHI, which show less frequent observation of RHI above about 130% outside of clouds in the Northern Hemisphere compared with the Southern Hemisphere, that a heterogeneous freezing mode occurs at least in some Northern mid-latitude cirrus clouds (Haag et al., 2003, see Fig. 24). Heterogeneous IN have a non-linear impact on the cirrus occurrence, optical extinction, and the fraction of clouds that are subvisible, due to the competition between the homogeneous and heterogeneous nucleation mechanisms (Haag and Kärcher, 2004).

If soot particles associated with sulphate and other soluble components such as those emitted by aircraft act as heterogeneous ice nuclei and initiate freezing at supersaturations of the order 120–130% (Haag et al., 2003), then it is possible that they may alter ambient cloud properties either by forming additional cirrus in regions that would not otherwise form cirrus clouds (because supersaturations are not high enough), or by altering the properties of cirrus that form on homogeneous or heterogeneous ice nuclei present in the UT from non-aircraft sources. In regions where homogenous freezing of solution droplets is the dominant formation pathway for cold cirrus without aircraft emissions, the addition of heterogeneous IN would be expected to decrease ice number concentrations or, possibly, to increase cirrus cloud coverage. But, if the ambient atmosphere is dominated by heterogeneous IN from sources other than aircraft, the addition of more heterogeneous IN would be expected to increase ice number concentrations (Hendricks et al., 2005). The former effect could lead to either a positive, or a negative RF. A negative RF would result if the areal coverage of cloud ice water path were undisturbed, but ice number

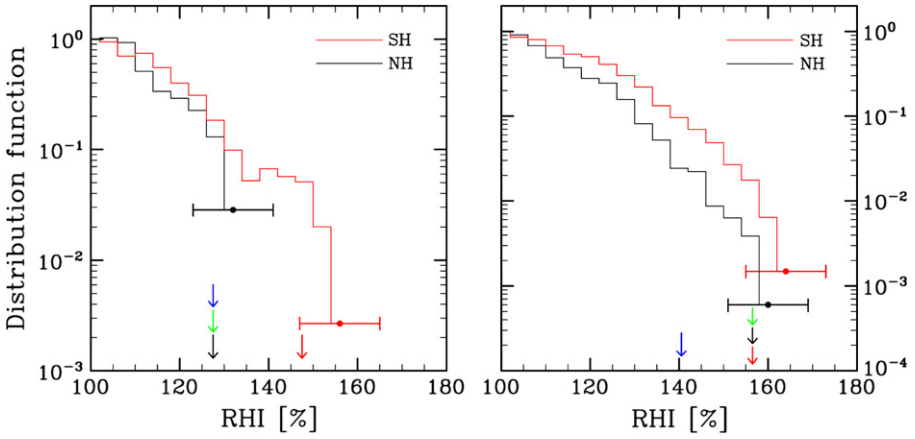

Fig. 24. Distribution of relative humidity over ice (RHI) outside of (left panel) and inside (right panel) cirrus clouds measured during the INCA project campaign in Punta Arenas (Southern Hemisphere – SH) and Prestwick (Northern Hemisphere – NH). The distributions are normalized with the number of data points in the respective 100% bin and all RHI values were binned into 4% intervals. The precision of RHI measurements is ±3% (1σ-limits), with horizontal bars depicting the 3σ-limits. The colored arrows mark the cut-offs derived from the modelled distributions (homogeneous – red; heterogeneous – blue; mixed homo-/heterogeneous for concentrations of total ice nuclei 0.1 cm^{-3} – black; mixed homo-/heterogeneous for concentrations of total ice nuclei 0.001 cm^{-3} – green) (Haag et al. (2003).

concentrations were decreased, while a positive RF may result if ice coverage increases. An increase in ice number concentrations, with no change in areal coverage of ice water path, would be expected in regions dominated by heterogeneous ice nucleation and would lead to a positive RF.

The observation that there are regions in the upper troposphere that have large supersaturations with respect to ice has been used to argue that homogeneous nucleation is the dominant process in cold cirrus (Heymsfield et al., 1998). Nevertheless, such regions do not, by any means, dominate the upper tropospheric probability distribution of relative humidity (Gierens et al., 1999a,b). Thus, it is possible that heterogeneous ice nuclei from surface sources dominate the formation of cirrus in some regions in the UT. Then, the addition of IN from aircraft, if they act to form ice at RHI below the threshold for sulphate, would produce a positive RF.

7.2.3. *Observations and modelling of ambient aerosol number concentrations*

Measurements of volatile and refractory aerosol concentrations in different size ranges in the upper troposphere have been summarized by Clarke and Kapustin (2002) and Minikin et al. (2003). Nucleation-mode aerosol concentrations are important, since these particles may determine the total aerosol number concentration and are able to grow to sizes that would act as homogeneous nuclei for cirrus formation through coagulation and condensation. Over the Pacific Ocean, Clarke and Kapustin (2002) found evidence of nucleation-mode (Dp $>$ 3 nm) particles ($\approx$10,000 cm^{-3} $\pm$ 25,000 at STP) when refractory particle concentrations were small relative to volatile concentrations. Some models that include binary nucleation of sulphate aerosols from gas phase H_2SO_4 capture the trends in these data, but with somewhat higher concentrations at some locations (Spracklen et al., 2005), while others predict smaller concentrations by about a factor of 10 (Lauer et al., 2005). By contrast, the nucleation-mode (Dp $>$ 5 nm) measurements by Minikin et al. (2003) near Punta Arenas in the Southern Hemisphere and near Scotland in the Northern Hemisphere and in the Southern Hemisphere LACE campaign (Petzold et al., 2002) were significantly smaller (median: 350 cm^{-3} with a 25 and 75 percentile range from 180 to 830 cm^{-3} and median: 1400 cm^{-3} with a 25 and 75 percentile range from 450 to 15,000 cm^{-3}, in the Northern Hemisphere and Southern Hemisphere INCA campaign, respectively, and median 800 cm^{-3} with a 25 and 75 percentile range from 400 to 1100 cm^{-3} at STP in the Northern Hemisphere European LACE campaign). The latter measurements are also significantly underestimated in the Lauer et al. (2005) model.

Aitken particle concentrations have also been characterized, with averages (for Dp $>$ 12 nm) ranging from 200 to 1200 cm^{-3} and from 350 to 1200 cm^{-3} at different Northern Hemisphere and Southern Hemisphere Pacific latitudes, respectively (Clarke and Kapustin, 2002) while the medians for the Northern Hemisphere and Southern Hemisphere INCA campaign were 770 cm^{-3} (range 450–15,000 cm^{-3}) and 240 cm^{-3} (range 130–400 cm^{-3}) for Dp $>$ 10 nm (Minikin et al., 2003).

The number concentrations of refractory particles (those that remain after heating to 300 °C) in the Aitken mode are significantly smaller than the total Aitken number concentrations. The average number of refractory particles over the Pacific (Dp $>$ 12 nm) ranges from 30 to 300 cm^{-3} at STP depending on latitude (with standard deviations of order a factor of 3), while that measured during the INCA campaign had medians of 37 cm^{-3} (range 12–75 cm^{-3}) and 105 cm^{-3} (range 24–840 cm^{-3}) at STP in the Southern Hemisphere and Northern Hemisphere, respectively. These refractory and volatile CN number concentrations are somewhat higher than those predicted using modelled soot concentrations with specified size distributions (Penner et al., 2009). Ström and Ohlsson (1998) found that the concentrations of absorbing material in ice could be as high as 0.1 μg m^{-3} (average 0.03 μg m^{-3}) which is 4000 times larger than observed concentrations of soot in the upper troposphere (Schwarz et al., 2006) and were probably associated with an aircraft plume age of about 1 h. Thus, it is only a small fraction of the ambient soot aerosol that acts as ice nuclei. Kristensson et al. (2000) report a decrease in effective diameter of 10–30% in cirrus clouds perturbed by aircraft, a finding which is not observed at temperatures warmer than −30 °C. This finding may imply that aircraft BC act as effective heterogeneous IN (i.e. at lower relative humidities than those required for ice formation on sulphate) in ambient cirrus that also form on IN or that the cirrus found in these corridors are aged contrail cirrus, where conditions are known to be such that aircraft soot does act as an IN.

Advancements in the measurement of heterogeneous ice nuclei (IN) have also been made over the past 10 years or so. Typically, measured IN concentrations are smaller than the total number of refractory particles. For example, DeMott et al. (2003b) and Richardson et al. (2007) report concentrations of $<$0.01 cm^{-3} at STP of IN at cirrus temperatures in April and May (2004) and November

Table 9
Summary of recent contrail RF studies, forcings given in mW m^{-2}.

Study	Diurnal cycle	Contrail visible optical depth	Contrail cover	Year	LW	SW	Net
Myhre and Stordal (2001)	Yes	0.3 (prescribed)	Sausen et al. (1998)	1992	20.0	−11.0	9.0
Marquart et al. (2003)	No	Predicted	ECHAM GCM	1992	4.9[a]	−1.4	3.5
Fichter et al. (2005)[a,b]	No	Predicted	ECHAM GCM				
			DLR-2 (dist/fuel)	1992	4.5/4.5	−1.3/−1.3	2.9/3.4
			TRADEOFF dist/fuel)		4.1/4.4	−1.2/−1.3	3.2/3.5
Stuber and Forster (2007)	Yes	0.1 (prescribed)	Based on ECMWF forecast	2002	3.34	−1.35	2.0
Rädel and Shine (2008)	Yes	0.1 (prescribed)	Based on ECMWF forecast	2002	10.1	−4.2	5.9

[a] Values adjusted for a 25% low bias in the ECHAM model.
[b] Details; personal communication, Christine Fichter, DLR, 2009.

(2001) in the free troposphere over the western US, indicating that not all refractory particles can act as ice nuclei (if those measured during the INCA campaign are also typical for the western U.S.). This is consistent with the report by Seifert et al. (2003) that scavenging ratios (fraction of ambient particles included in crystals) were <1% in the INCA campaign. Seifert et al. also showed that the ice crystal number density is dominated by residual particles with diameters of less than 0.1 μm, and, in this size range, high interstitial number concentrations are not necessarily associated with high ice crystal number concentrations. For particles larger than this, there is a correlation between crystal number concentration and interstitial number concentration.

7.2.4. Observations and modelling of cirrus ice number concentration and microphysical properties

Heymsfield and MacFarquhar (2002) summarized cirrus ice crystal number concentrations and microphysical properties prior to the INCA measurements. Number concentrations for particles with maximum dimension above 100 μm at temperatures below −40 °C ranged 10^{-4}–10^{4} L^{-1}, but were most often between 0.01 and 0.1 cm^{-3}. Unfortunately, the numbers of particles with sizes below 100 μm could not be reliably counted in these early experiments. Table 10 provides a summary of ice crystal concentrations and sizes for experiments since 1990. The microphysical properties of cirrus clouds have been studied by using satellite (Ou et al., 1998), ground-based remote sensing (Intrieri et al., 1993; Mace et al., 1998), and in situ measurements (Ström and Heintzenberg, 1994). However, only a few measurements have attempted to quantify total ice crystal number in cirrus clouds, and the number of small particles is still controversial, since particle shattering within the inlet of airborne probes may cause over-counting (Korolev and Isaac, 2005; McFarquhar et al., 2007). Available measurements of ice crystal number concentrations (N_i) have been made with a variety of instruments that do not always agree (Heymsfield and McFarquhar, 2002) and the temporal and spatial scatter of observed values is large. Measurements of ice crystal number concentration in cirrus clouds published since 1990 are summarized in Table 10. Notably, Gayet et al. (2004) found that the number concentration and size distribution of crystals in the Northern Hemisphere differs from that in the Southern Hemisphere. However, this finding should be confirmed given the wide spatial and temporal variations of these characteristics in cirrus.

We note that if ice nuclei concentrations are high enough (>10–50 cm^{-3}) most of the observed ice crystal concentrations must be produced as a result of homogeneous nucleation on volatile particles (e.g. DeMott et al., 1997). Even if only a small fraction of soot aerosols act as heterogeneous IN, nucleation on these IN may determine ice concentrations in many of the clouds with lower number concentrations. Model-predicted ice crystal number concentrations are within the ranges reported above (e.g. Lohmann et al., 2004; Hendricks et al., 2005), but the observed variability precludes distinguishing a dominant role for homogeneous nucleation versus heterogeneous nucleation.

7.2.5. Radiative forcing from indirect effects of aerosols on ambient cirrus

Penner et al. (2009) have implemented an off-line calculation of two recently developed physically-based ice nucleation

Table 10
Summary of ice crystal concentrations (N_i) and sizes for experiments since 1990.

Reference	Experiment (conditions)	Time	Place	N_i (cm^{-3})	Diameter (μm)
Ström and Ohlsson (1998)		Oct. 1996	Southern Germany (dense air traffic)	1–4 cm^{-3}, 1.2–7.6 cm^{-3} when perturbed by aircraft plume	
Ström et al. (1997)		March 1994	Southern Germany	2.5 at STP 0.5–13	16[d] 8–12[e]
Ström and Heintzenberg (1994)		January 1992, 2 flights	Austrian Alps	0.12 (0.060–0.38)[b] 0.38 (0.15–0.89)[b] Max: 3.8	32 (0–60)[b,c] 14 (10–17)[b,d]
Gallagher et al. (2005)	EMERALD-I	Sept., 2001	Southern Australia	0.49 (0.2–1.2)[a]	70–90[a]
Mace et al. (2001)	ARM	Annual 1997	Oklahoma	0.1 (0.01–0.4)	70 (20–200)
Schröder et al. (2000)	Highest number in "young cirrus"	1996–1997, various	Central Europe	0.3–5.0	25
Gayet et al. (2004)	INCA	September–October, 2000	Prestwick, Scotland (55°N)	2.23 (0.84–4.74)	36[e] (25–56)[b]
Gayet et al. (2004)	INCA	March–April, 2000	Punta Arenas (53°S)	1.45 (0.58–3.01)	42[e] (30–70)[b]

[a] Range of number concentration represents average from different flights, found up to 20–30 cm^{-3} on some flights. Maximum dimension of mean crystal size. Velocities of up to 1.5 m s^{-1} were recorded in 'frontal cirrus layers'.
[b] Range represents 25–75 percentile.
[c] Average crystal length (PMS probe – does not measure below 20 μm).
[d] Mass mean diameter.
[e] Effective diameter.

parameterizations (Liu and Penner, 2005; Kärcher et al., 2006) to calculate the ice crystal number concentration. Both parameterization methods are able to represent the competition between homogeneous and heterogeneous nucleation pathways, and to link the N_i to aerosol properties, thus allowing a nucleation simulation that accounts for the effects of different aerosol types (sulphate, soot, and mineral dust). This calculation requires assumptions regarding the small-scale velocity perturbations responsible for forming regions with supersaturation, but a probability distribution for these updrafts, with a mean of 0 cm s^{-1} and a standard deviation of 0.33 cm s^{-1} seems a reasonable choice (Haag and Kärcher, 2004; Kärcher and Ström, 2003). This off-line calculation did not include any feedbacks to the climate system, so does not provide any measure of the change in cloud coverage due to soot aerosols. Results show that changes in aerosol species can lead to large changes in ice number concentration ($\sim\pm5$ cm^{-3}) and in effective radius.

Results using two versions of the aerosol model were also estimated. In the first version, the sulphate number concentration from binary homogeneous nucleation and growth from the nucleation mode to the Aitken and accumulation modes was predicted. In the second version, only aerosol mass was predicted. In the latter model, aerosol number concentrations were diagnosed from the predicted sulphate and soot aerosol mass concentrations using an assumed size distribution whilst in the former, only soot size distributions were assumed. Since pure sulphate aerosol is highly soluble, it was assumed that it forms ice through homogeneous freezing after deliquescence. Soot particles are assumed to be efficient heterogeneous IN, with a freezing threshold RHI of ~130% in Liu and Penner (2005) and ~140% in Kärcher et al. (2006). Fig. 25 shows the annual mean values of in-cloud ice number density N_i at 140 hPa and 190 hPa. The two parameterization methods produced quite similar N_i patterns indicating good agreement between the two parameterization methods, but the Kärcher parameterization (KL) has higher ice number concentrations in the tropics and Southern Hemisphere since ice nucleation is dominated by homogeneous nucleation in this region. The Liu and Penner (LP) parameterization has lower ice concentrations at these levels since lower RHI must be achieved for heterogeneous nucleation to activate in the LP parameterization. In both parameterizations, homogeneous ice nucleation produces higher N_i and is a dominant mechanism for ice nucleation at high altitudes because of the very low temperature and high RHI there. At lower altitudes, heterogeneous ice nucleation becomes important and produces generally lower N_i. The higher N_i towards lower altitudes from the KL parameterization than those from the LP parameterization is caused by the higher freezing RHI threshold value for heterogeneous IN used in the KL parameterization.

These ice particle concentrations may be compared with those measured in recent aircraft campaigns. For example, Gayet et al. (2006) reported average crystal concentrations of 0.3–4 cm^{-3} in Southern Hemisphere mid-latitude cirrus, when Jet-stream cirrus and orographic-wave cloud cirrus (which form at greater vertical transport velocities) are excluded from the statistics. The median ice number concentrations decreased slightly as colder temperatures are reached, (from about 2 cm^{-3} at −25 °C down to about 0.8 cm^{-3} at −60 °C).

The potential effect of anthropogenic aerosol (sulphate and soot) on the ice effective radius was examined based on the calculated N_i. Aerosol concentrations were calculated from the coupled aerosol and climate models with present-day and pre-

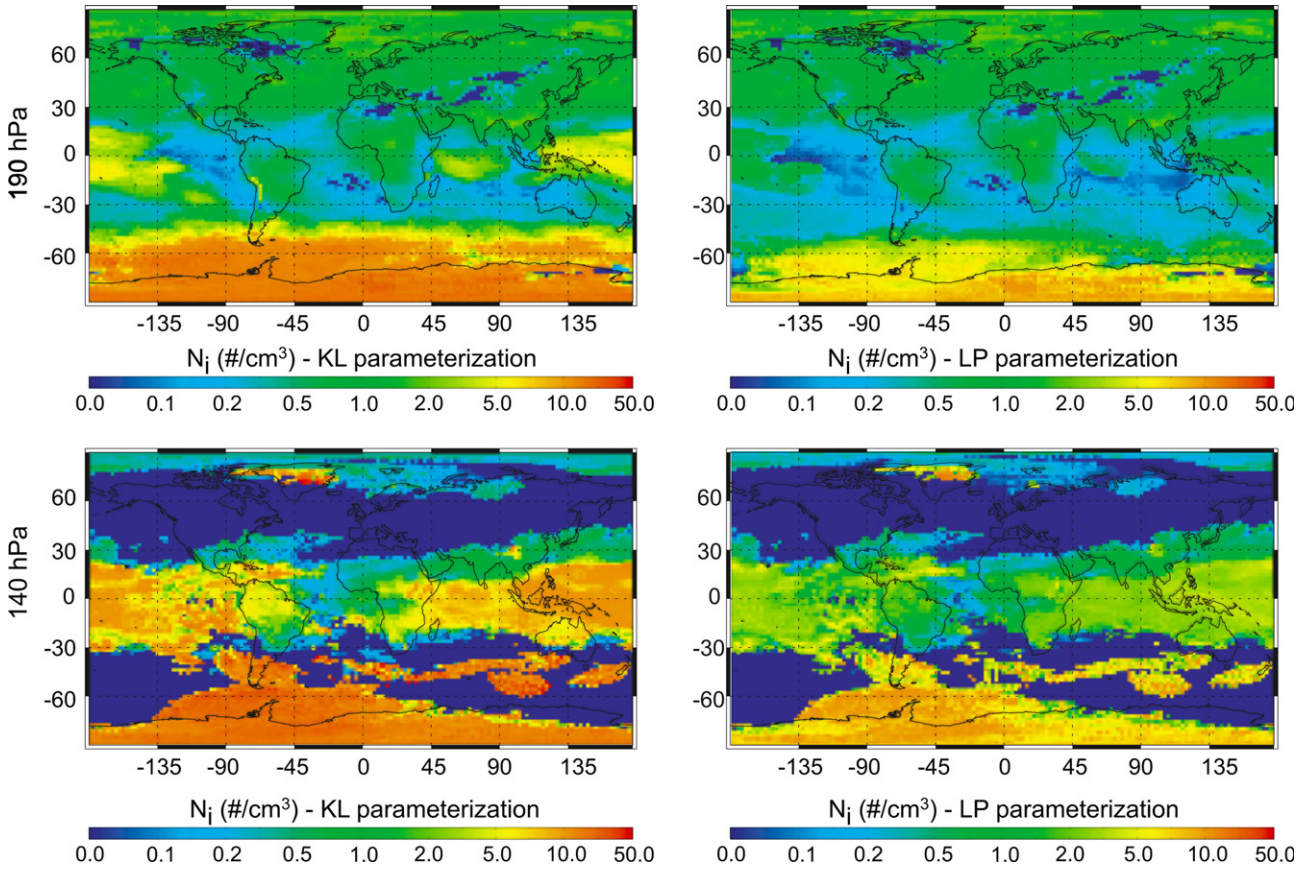

Fig. 25. In-cloud ice crystal number concentration (cm^{-3}) (N_i) calculated with the Kärcher et al. (2006) (KL, left) and with the Liu and Penner (2005) (LP, right) ice nucleation parameterization at 140 hPa (lower) and 190 hPa (upper). Aerosol and meteorological fields are from the coupled IMPACT-CAM3 model run.

industrial emissions. An analytical formulation relating the ice effective radius (r_e) to ice volume mean radius (r_v) was derived using combined ice crystal size distributions (a gamma distribution for length less than 20 μm and a power-law distribution for larger particles) (Wyser, 1998). The ice crystal shape was assumed to be hexagonal columns. The global statistics of N_i and r_e occurrence probability with different emission scenarios were examined. There are two modes in the probability distributions for N_i and r_e, one at larger ice number concentrations, which is associated with homogeneous nucleation, and one at smaller ice number concentrations, which is associated with heterogeneous nucleation. These are shifted by adding anthropogenic soot: for the mode where homogeneous nucleation dominates (with higher N_i and lower r_e), an increase in the heterogeneous IN (soot) inhibits the ice formation through homogeneous nucleation, lowers N_i and increases r_e. However, for the mode where the heterogeneous nucleation dominates (with lower N_i and higher r_e), an increase in soot particles increases N_i and lowers r_e. Thus, the combined effects narrow both the N_i and r_e probability distributions. The addition of anthropogenic sulphate (through homogeneous ice nucleation) has little effect on N_i and r_e except in the Southern Hemisphere.

Changes to the ice crystal effective radius can have important implications for both the short-wave (SW) and long-wave (LW) radiation in cirrus clouds. Penner et al. (2009) estimated the RF at the top of atmosphere (TOA) arising from anthropogenic aerosols (see Fig. 26). The net RF (SW plus LW) of anthropogenic aerosols through effects on cirrus cloud ice number and effective radius can be both positive (i.e., LW forcing dominates over SW forcing), or negative (i.e., SW forcing dominates over LW forcing). SW and LW forcing in the tropics is particularly sensitive to aerosol changes because of the low temperatures in the upper troposphere and high cirrus cloud fractions there. In many regions of the tropics and in the South Pole where homogeneous ice nucleation dominates, the net forcing from anthropogenic soot is negative because of a reduction of ice number by adding soot. In other regions where heterogeneous ice nucleation dominates, a net positive forcing is expected because of an increase of ice number, and a reduction of r_e. The global mean net TOA forcing ranges from −0.01 to +0.04 W m^{-2} from total anthropogenic sulphate for the KL and LP parameterizations, respectively and from −0.4 to −0.3 Wm^{-2} for soot from surface sources, and from −0.16 to −0.12 Wm^{-2} for aircraft soot (Penner et al., 2009). Calculated values based on the KL parameterization are shown in Fig. 26. These values were estimated using the version of the IMPACT model that predicts sulphate aerosol mass and number, but uses assumed size distributions for the other aerosol particles. When the version of the model that does not predict sulphate aerosol number concentration resulting from binary nucleation of H_2SO_4 vapour is used or when the relative humidity at which soot particles activate to form heterogeneous IN changes, the forcing may change. For example, the forcing

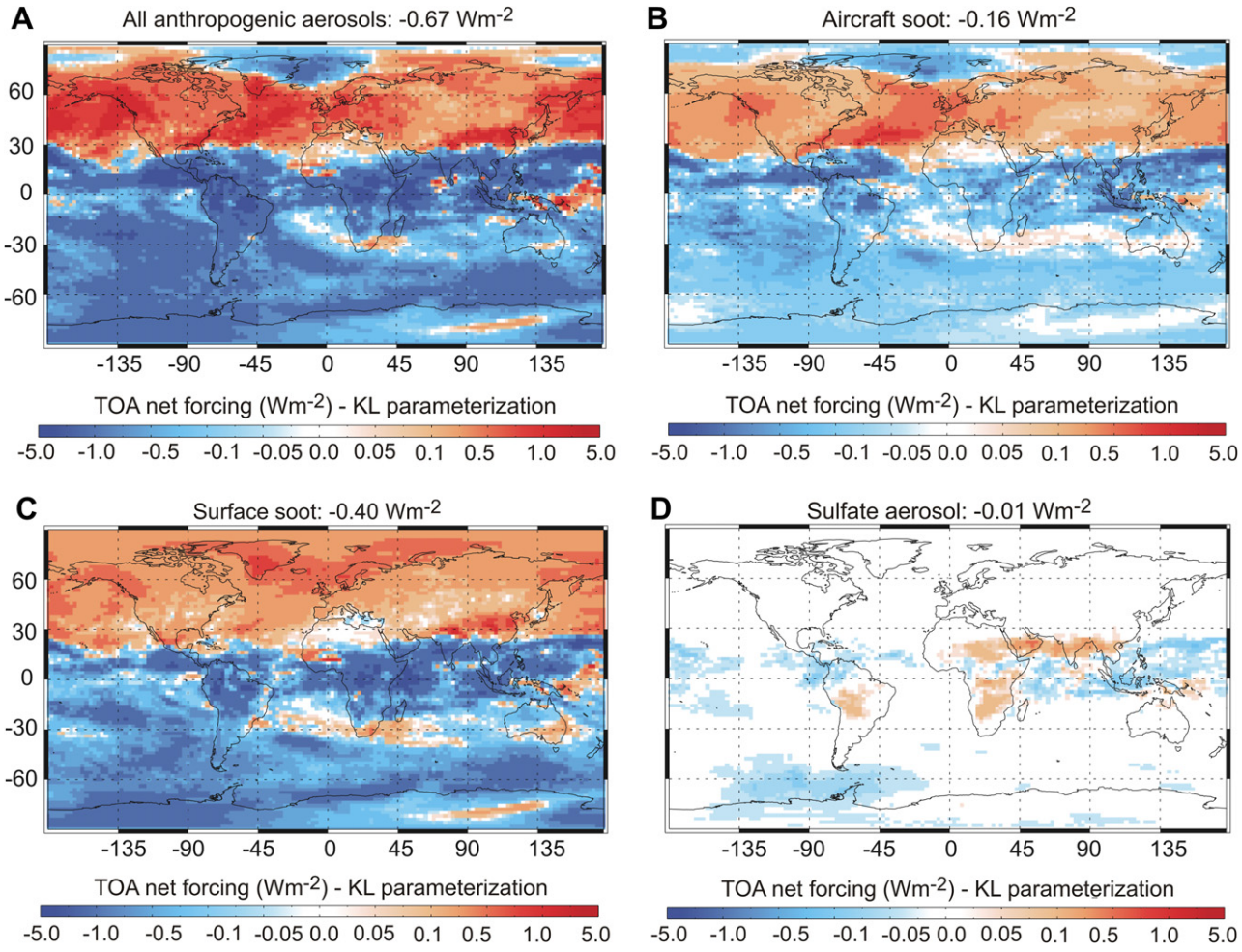

Fig. 26. Four month (January, April, July, October) average TOA net forcing (W m^{-2}) from all anthropogenic aerosols (A), aircraft generated soot (B), anthropogenic soot from surface sources (C) and anthropogenic sulphate (D). The Kärcher et al. (2006) parameterization together with the 3-mode sulfate aerosol model is used to calculate ice nucleation (adapted from Penner et al., 2009).

associated with aircraft soot becomes positive (but near zero) when the mass only version of the model with the LP parameterization is used. Clearly, there is a need to refine these values and to understand the effects of changing aerosol concentrations on ice number concentration and size.

We note that the above analysis is based on an offline calculation of N_i using an ice nucleation parameterization. Other ice microphysical processes (e.g., changes to the precipitation efficiency of ice clouds) are not considered. In addition, in the above calculations ice water content output from CAM3 did not include the contribution from anvil cirrus. Further changes might occur if anvil cirrus is included.

Very recent results with the same basic modelling system as Penner et al. (2009), investigating aerosol effects on cirrus clouds considering homogeneous and heterogeneous ice nucleation allowing for competition (HET), have been presented by Liu et al. (2009). Net cloud forcing for surface soot was +0.22 to +0.39 W m^{-2}, for sulphate was +0.01 to +0.31 W m^{-2} and for aircraft soot was −0.11 to +0.26 W m^{-2} (Liu et al., 2009).

Evidently, there is much work to be done to resolve both the sign and magnitude of the effect of aircraft soot on cirrus clouds.

7.3. Trends in cirrus clouds and relationship to aircraft

Estimates of the effects of additional cloudiness have been attempted based on determining trends in cirrus cloudiness (Boucher, 1999; IPCC, 1999; Fahey et al., 1999; Zerefos et al., 2003; Minnis et al., 2004; Stordal et al., 2005; Stubenrauch and Schumann, 2005; Eleftheratos et al., 2007, Nakanishi et al., 2001). Such studies have inherent uncertainty because they make use of observed correlations between aircraft fuel use/activity and cloudiness that may occur as a result of mechanisms that do not involve aircraft. Nevertheless, IPCC (1999 – see Fahey et al., 1999) used the difference in trend in cirrus coverage from surface-based observations (which are smaller than those from the then-current ISCCP data) inferred by Minnis et al. (2001) [proceedings referenced in Zerefos et al. (2003)] in regions predicted to have contrail coverage >0.5% (as inferred by Sausen et al., 1998) compared with the trend in regions predicted to have contrail coverage <0.5%, to place constraints on the forcing by the so-called 'aircraft-induced' cloudiness. The trend difference over land (where 84% of contrail coverage was expected) was 1.6%/decade for the period from 1971 to 1991, which implies an increase of 4.8% if extended over 30 years. This amounts to an increase of about 0.2% in total cirrus cloud cover. Assuming optical properties similar to those for contrails (i.e. optical depth 0.3, as assumed in IPCC (1999)), then the RF was estimated to be 40 mW m^{-2}.

The first analysis of cirrus formation induced by aviation made since the IPCC (1999) estimate (Fahey et al., 1999) was that of Zerefos et al. (2003). They used the ISCCP D2 data set over 1984–1998 to estimate changes in cirrus cloud cover. They first used regression analysis to remove the influence of ENSO, the QBO, the NAO, and any linear trend associated with tropopause temperature. This resulted in somewhat larger trend differences for ISCCP data for the same period as that based on Minnis et al. (2001) (as first reported in Fahey et al., 1999) in regions with high and low contrail coverage over land, but smaller differences over ocean regions (which were not statistically significant). These trend differences over land are decreased to 2.2%/decade when considering the extended time-period 1984 to 1998. However, this trend is still larger than that reported by Fahey et al. (1999) for surface-based observations, which may indicate an increase in the forcing due to these changes in cloud coverage of up to 55 mW m^{-2} (i.e. 0.2/4.8 = X/6.6 to give the change in cirrus, and 0.04 mW m^{-2} × X/0.2 to give the increase in forcing) associated with increasing cirrus cloudiness associated with air traffic.

Minnis et al. (2004) also used the ISCCP D2 data, but relied on a longer time period (1971–1995) to determine the trends in cloud cover. Data from the surface network cirrus trend relative to the air traffic increase was used to derive a spreading factor for trends in cloud cover relative to the trends inferred for linear contrails from the model study of linear contrail cover of Sausen et al. (1998). They excluded areas with significant changes in relative humidity at 300 hPa, which was expected to correlate with changes in natural cirrus cloud cover. This only left the United States as a possible study area. Applying the spreading factor to the estimated linear contrail cover from Sausen et al. (1998), and reducing the optical depth to between 0.15 and 0.25 from that assumed in IPCC, and considering an increase in the pressure at which contrails are considered from 200 to 225 hPa lead to a range in forcing of from 15.3 to 25.5 mW m^{-2}. They also applied the spreading factor of 1.8 to the forcing estimate for linear contrails from Marquart and Mayer (2002) of 3.2 mW m^{-2} to obtain a lower bound for the total cirrus cloudiness forcing from aircraft of 6 mW m^{-2}.

Stubenrauch and Schumann (2005) used data from TOVS Path-B satellite which provides an estimate of both temperature at 25 hPa intervals and precipitable water column between 300 and 100 hPa. These data allowed them to estimate relative humidity between 9 and 15 km as well as a criterion for the relative humidity in this layer associated with clear sky, general cirrus formation, and potential contrail formation. The difference in the trends in effective cloud amount (emissivity × coverage in percentage) in regions with potential contrails, and all situations or between regions with potential contrails and cirrus regions therefore allowed them to determine those trends specifically associated with air traffic. Weighted by the frequency of potential contrail occurrence (which is 7% and 5% for Europe and the North Atlantic flight corridor, respectively), they deduced an increase in cloud cover associated with air traffic of 0.2–0.25% decade^{-1} over Europe and an increase of 0.08–0.24% decade^{-1} over the North Atlantic flight corridor during the period 1987–1995. The authors considered these to be minimum values since TOVS is not sensitive to clouds with optical depth <0.1 in the visible.

Stordal et al. (2005) revisited the trends in cirrus associated with the ISCCP D2 data set from 1984 to 2000. They noted difficulties in determining trends using ISCCP because the different viewing angles can introduce discontinuities in the detection of high cloud and cloud trends. Moreover, the ISCCP algorithm is only sensitive to high clouds with optical depth >0.3. They attempted to minimize such problems by examining trends only in the regions seen by the METEOSAT satellites. The estimated trend in high cloud cover associated with air traffic density (distance flown per km^2 h^{-1}) in 2000 was estimated as 0.23% with a lower limit of 0.07% and an upper limit of 0.41%, giving a trend in cirrus of 1–2% decade^{-1}.

Mannstein and Schumann (2005) also correlated the trend in cirrus cloud cover with air traffic density, but using 2 months of cirrus data from METEOSAT and actual air traffic data from EUROCONTROL. For relating cirrus cover C and traffic density D they used an approach that takes overlapping of contrails and saturation effects (e.g. finite size of ice-supersaturated regions) into account: $C_{tot}(D) = C_0 + C_{pot}[1 - \exp(-D/D^*)]$, where C_0 is cover of natural cirrus, C_{pot} is the potential coverage of contrails and contrail cirrus (Sausen et al., 1998), and the term in square brackets is the fraction of C_{pot} that is actually covered by contrails. D^* denotes the mean air traffic density that would lead in an ice-supersaturated region to a total coverage by cirrus clouds without any overlap. It was shown that the relation between additional cirrus coverage and air traffic density indeed followed roughly the exponential model. The main result of this study was that over Europe aviation was determined

to be responsible for additional cirrus coverage of 3% (consistent with the result of Stordal et al.). This implies that the mean coverage of contrail cirrus over Europe exceeds the corresponding mean coverage of linear contrails by one order of magnitude. However, Mannstein and Schumann (2007) point out that the correlation found in Mannstein and Schumann (2005) was also found in some model simulations of natural cirrus, implying that the increase in cirrus with air traffic density is affected by spurious correlations of air traffic and natural cirrus coverage.

Krebs (2006) extended the study of Mannstein and Schumann, by analysing cirrus coverage and air traffic of 11 months in 2004, for Europe, North Africa, and the North Atlantic. Over this extended region he also found a significant correlation between cirrus coverage and air traffic density. The air traffic induced cirrus cover was smaller than that found in the Mannstein and Schumann (2005) study, namely $0.6 \pm 0.2\%$ as regions with essentially no air traffic, of course, leading to smaller mean additional cirrus coverage have been included. Krebs also investigated the effect of the additional cirrus on the radiation budget of the earth based on satellite data. He found a warming of 1.1 W m^{-2} for the region of interest, a value that is more than eight times larger than the value estimated by Boucher (1999). As noted above, it is currently not clear how much of the correlation in this work between air traffic and cirrus cloudiness is actually due to a causal relationship. Hence the determination of the RF from contrail cirrus is fraught with very large uncertainties; studies to resolve the differences and to constrain the error margins are certainly needed.

Finally, Eleftheratos et al. (2007) examined the ISCCP D2 data set from 1984 to 2004. After deseasonalizing the data and using regression to remove the NAO, they found a trend in the western part of the North Atlantic Flight Corridor of 1.6% $decade^{-1}$, while a trend of -0.5% $decade^{-1}$ was found in the eastern part of the North Atlantic.

All these aforementioned studies suggest that air traffic induces additional cirrus clouds, which seems plausible. It is of course difficult to prove a causal relationship from correlation statistics because of a number of factors, e.g natural variability, other climate change effects and cyclical influences (e.g. NAO). These other influences may be of the same magnitude or larger than the possible aviation effect. Some of the aforementioned studies have attempted to reduce the uncertainties arising from other factors by screening the data for them (e.g. Zerefos et al., 2003, 2007). Nonetheless, any correlation-type study will encounter such difficulties and it may be the case that little more can be learned from observational studies in the absence of process-type modelling that can be used to support the analysis. For example, a potentially serious limitation to the above studies that utilize data from the ISSCP project are artificial trends in the data set, e.g. due to changes in the satellite viewing geometry, as discussed by Evan et al. (2007).

8. Effects on climate

8.1. Short and long-term responses

The IPCC (1999) was the first assessment of the aviation sector that produced estimates of RF (defined specifically as the change in radiative forcing since the pre-industrial era) for all the forcing agents known to be pertinent to aviation, both for (what was then) current-day conditions (1992) and future scenarios (2050) (Prather et al., 1999). The main results were that in 1992, aviation RF was 3.5% of total anthropogenic forcing in 1992 and that this was from both CO_2 emissions and non-CO_2 effects. An update of aviation's RF for the year 2000 that included improvements in the modelling was given by Sausen et al. (2005).

The IPCC (1999) 'Summary for Policymakers' stated simply that over the period from 1992 to 2050, the overall RF by aircraft (excluding that from changes in cirrus clouds) for all scenarios was a factor of 2–4 larger than the forcing by aircraft CO_2 alone. The underlying Chapter 6 of the 1999 assessment presented a new measure, the radiative forcing index (RFI) for aviation, which was derived from the ratio of total instantaneous RF to that from CO_2 alone. Unfortunately, some commentators have misunderstood this as an *emission* metric, i.e. that total RF can be related directly to an annual rate of emissions of CO_2 – this is erroneous. The use of RFI for other sub-sectors would lead to nonsensical results. For example, dirty coal-fired power plants or maritime shipping is likely to have a zero or negative RFI in their first decade of growth because the direct and indirect cooling from the sulphate aerosols will offset the effect of CO_2 emissions, although the CO_2 will eventually emerge as the dominant RF. For this and other scientific reasons (Wit et al., 2005; Forster et al., 2006, 2007a,b; Fuglestvedt et al., 2009) this report rejects RFI as a suitable emissions index.

The use of RF or RFI as a measure of aviation's or any other sector's impact on climate also has other problems, although this is generic to the metric of RF. Firstly, the RF used in the ratio is the *instantaneous* RF and the history of aviation's forcing of climate evolves with CO_2, as it accumulates in the atmosphere, becoming relatively more important over time. The relationship between RF and global mean surface temperature change *only* applies in steady-state, when the RF is constant, and thus aviation's 1992 instantaneous RF is neither a measure of the climate change attributable to aviation up to 1992 nor that in the future. Secondly, the IPCC (1999) assessment of the aviation sector included non-Kyoto greenhouse gases. An equivalently thorough assessment of other sectors has not been performed until recently.

The previous usage, both legitimate and otherwise, of RF and RFI as a climate metric for aviation illustrates the difficulty of quantifying the net climate impact of an activity with numerous forcing agents, which is a basic property of all industrial sectors. Appropriate metrics depend entirely on the period of attribution (e.g., aviation's impact since 1940 *cf* emissions for a particular year) and the time frame considered for climate impact (e.g., climate change to date *cf* integrated climate damage to a time horizon of 2100, see analysis by den Elzen et al., 2005). For specific time horizons, the Kyoto metrics that adopt GWPs as emissions equivalences are appropriate. These usages have been discussed elsewhere in a more general sense by Fuglestvedt et al. (2003) and in relation to the aviation and other transport sectors in a companion assessment (Fuglestvedt et al., 2009).

By its very nature, RF relates different timescales of atmospheric constituents in its formulation. RF is useful as a first-order metric to quantify climate impacts because of its relationship to global mean surface temperature change through the linear equation (1). Nevertheless, this relationship is often misinterpreted since the studies that relate RF to global mean surface temperature are steady state: i.e., the RF is held fixed for more than a century as the climate system responds. Unfortunately, the RF from aviation is an increasing, evolving mix of components: CO_2 emissions accumulate in the atmosphere and its RF builds up while the RF from O_3, CH_4, aerosols, and contrails are in a quasi steady-state, reflecting only more recent emissions. The timescale for most of these atmospheric perturbations is less than a year, except for the 12-year response time of CH_4 (Stevenson et al., 2006; see also Table 5, IPCC, 2001 chapter for CH_4 feedback is needed here). For CO_2, the range of time scales reflect the equilibration times with the different carbon reservoirs and the history of its emissions needs to be taken into account. For example, 1940 can be considered the beginning of significant aviation activities (Sausen and Schumann, 2000), whereas significant shipping emissions began in the late 19th Century (Eyring et al., 2009; Lee et al., 2007). The climate response to changes in RF has its own time scales. Even short-lived RF

perturbations, such as that caused by Mt. Pinatubo, have decadal or longer impacts on climate. Thus, the complete history of RF, which includes shifts in the relative apportionment of different causes (e.g., O_3 vs. CO_2), is needed to attribute climate change both at present and in the near future.

The instantaneous RF is taken as a proxy for 'climate response', since climate responses (e.g. the specific patterns of mean surface temperature change) are sometimes difficult to detect. For example, it would either take large amounts of computing resources and massive ensemble climate simulations (e.g. Knight et al., 2007) to separate the relatively small signal of forced climate change due to aviation from the "noise" of natural climate variability. Global mean surface temperature change (ΔT) is a more satisfactory metric than RF since it is closer to the real impacts or possibly the potential damage (Fuglestvedt et al., 2003), and moreover it incorporates the history of RF and the time scales of the climate system's response.

The problem with using RF as a metric is that it does not account for the timescales of climate response (in terms of ΔT), which is related to the heat uptake of the oceans giving rise to the thermal inertia of the climate system. Thus, whilst a short-term forcing response may be removed quickly by cessation of the activity or emission, e.g. contrails, the *climate response* in terms of ΔT will only decay on much longer timescales if the atmosphere has been subjected to that forcing for some time. When the climate response timescale is coupled to the long lifetime of CO_2, this means that if the emission source were removed the temperature response from past emissions would actually increase after the cessation of emissions before damping very slowly. This phenomenon was illustrated for aviation CO_2 and O_3 effects by Sausen and Schumann (2000), and the concept of residual future warming from past emissions is often referred to as unrealized or committed warming (e.g. Hansen et al., 1985; Friedlingstein and Solomon, 2005; Meehl et al., 2005)[9]. This is illustrated in two ways in Fig. 27 using a simple model that treats all the aviation forcing components (Lim et al., 2007; Lee et al., 2009). Panel A of Fig. 27 shows the RF responses of CO_2, non-CO_2 effects and total RF to the historical development of aviation emissions to year 2000, after which, emissions are 'switched off' in the model simulation. The non-CO_2 RF goes negative after the cessation of emissions because of the lifetime of CH_4, whilst the CO_2 RF decays only slowly, in line with carbon sink timescales. The equivalent temperature responses of CO_2 and non-CO_2 forcing agents from aviation are shown in Fig. 27 panel B: here, because of the inertia of the climate system, the temperature response of the non-CO_2 forcings decay slowly, and the CO_2 temperature response decays even more slowly because of the timescales of response of carbon sinks, coupled with the response time of the climate system. Fig. 27 panel C shows an idealized pulse response case of RF, where a global aviation emissions are released for a year in proportion to those from the current-day fleet and the temperature decay response is followed (Fig. 27, panel D), showing the longer decay time for CO_2 vs. non-CO_2 forcings and the negative temperature response for the non-CO_2 forcings being driven by CH_4, switching to a positive long-term temperature response (many centuries) from the CO_2 forcing. The decay time for a metric like ΔT is extended because of the thermal inertia of the climate system, and even the total non-CO_2 short-lived RF shows the decadal-timescale decay time of the climate system.

[9] However, it should be noted that the usage of the term 'unrealized or committed warming' is very different to the concept of 'committed' scenarios in the 2007 IPCC assessment, in which CO_2 and other greenhouse gas emissions are continued at a trajectory that maintains constant abundances.

8.2. Aviation forcings and efficacy

At steady state, ΔT is found to be related almost linearly to RF by the climate sensitivity parameter, $\lambda(\mathrm{K(W\ m^{-2})^{-1}})$ (equation (1)). This relationship is evaluated by holding RF fixed for centuries, or by following a transient forcing with RF increasing at a regular exponential rate. At first, λ was considered to be constant for a given climate model, independent of the type of forcing (Cess et al., 1990, 1996), but further studies have shown that λ is dependent to an extent on the type of perturbation, in particular for non-homogeneously forcings (Forster and Shine, 1997; Hansen et al., 1997; Joshi et al., 2003; Stuber et al., 2005) and also for some aviation forcings, including O_3 and contrails (Ponater et al., 1999, 2006). In other words, the same *RF* may produce a different temperature (or other climate diagnostic) response. This is sometimes described as the '*efficacy*' (Hansen and Nazarenko, 2004; Hansen et al., 2005) and is defined as:

$$r_i = \frac{\lambda_i}{\lambda_{CO_2}}, \tag{9}$$

where λ_i and λ_{CO_2} are the climate sensitivity parameters associated with perturbations of the climate change agent i and of CO_2, respectively. Aviation-specific efficacies have only been extensively studied with the ECHAM climate model (Ponater et al., 2006), see Table 11. However, since r_i is a ratio, it should be relatively constant across different climate models. However, in the recent summary of results from the 2007 IPCC WG1 assessment (Forster et al., 2007a) this is not obvious and consistent values of r_i for aviation forcings are still undemonstrated.

Simple climate models (SCMs) are often used to analyse changes in mean global surface temperatures, which has been undertaken for aviation (e.g. Sausen and Schumann, 2000) and the transport sector as a whole and its components (Fuglestvedt et al., 2008). It is possible to incorporate aviation-specific efficacies into such modelling. However, whilst the usage of SCMs is instructive and can provide analyses not possible with GCMs, they have the serious disadvantage that they operate on global mean forcings and temperature responses. For aviation, as is the case for other sectors, some of these forcings may be positive and some negative (e.g. shipping, see Eyring et al., 2009). This can give the spurious impression of a net zero RF having no temperature impact. The most obvious example for aviation is the positive O_3 RF and negative CH_4 RF arising from NO_x emissions. For this example, IPCC (1999) showed that these forcings, although arising from the same emission, operated across different spatial scales and made the point that "…the latitudinal distribution of the radiative imbalance from these two perturbations does not cancel…" and that "*The response of the climate system to such geographically non-homogeneous forcing is unknown.*" (IPCC, 1999 – Prather et al., 1999 Section 6.5.1).

Some work has subsequently been undertaken over issues of non-homogeneous forcings in general. Forster et al. (2000) applied a range of idealized forcings with an intermediate GCM (IGCM) and found that forcing of the Northern Hemisphere (>30°N) gave a 40% greater climate sensitivity than at latitudes <30°N. In a study of climate sensitivity, Boer and Yu (2003a) found that the spatial structure of the temperature response to long-lived GHG (LLGHG) and sulphate forcings did not resemble the structure of the forcings, but the temperature response structure is rather driven by localized feedbacks. Boer and Yu (2003a) also note that forcings that occur in regions of positive feedbacks will produce comparatively large responses both locally and globally. However, elsewhere, Boer and Yu (2003b) also note that the global mean temperature response is proportional to global mean RF, broadly independent of the nature and pattern of the forcings in their simulations of LLGHG and

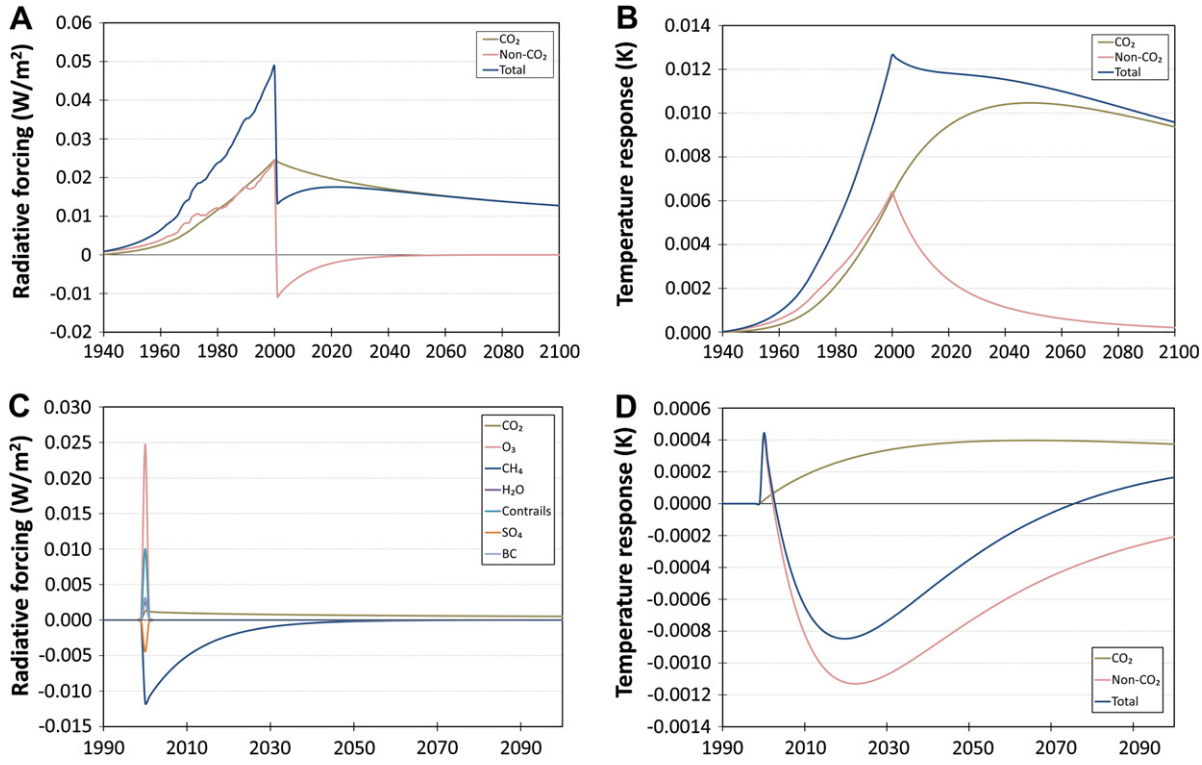

Fig. 27. Response of RF (W m^{-2}) and T (°K) to aviation emissions. (A &B) decay timescales of RF and T from different components following cessation of emissions in 2000. (C) An aviation fleet 'pulse' response of T assuming instantaneous fuel burn of 100 Tg C yr^{-1} and $EINO_x$ of 12 (from model of Lim et al. (2007), tuned to Stevenson et al. (2004)).

sulphates. The case for aviation forcings, however may be more complex as there is evidence that the temperature response, particularly to O_3, varies both by latitude and altitude in an idealized forcing experiment using three GCMs (Joshi et al., 2003).

In conclusion, while the CO_2 and CH_4 changes in abundance from aviation are globally uniform, the aviation forcings for O_3, aerosols and clouds are clearly heterogeneous in pattern. There is some evidence that the efficacy of some of these forcings deviates significantly from 1 but these are based on only limited experiments and principally from the ECHAM-4 GCM, such that other experiments are still needed. The issue of aviation forcings involving both positive and negative forcings and that some of them are heterogeneous in pattern makes the additivity – specifically the cancellation of climate impacts – a critical uncertainty in developing climate metrics to discuss control or mitigation strategies. There is added complexity for the impacts from NO_x, aerosols, and clouds in that these depend on the location and even conditions (day-night) of the flight path (Shine et al., 2005a, 2007; Bernsten et al., 2006)

8.3. Aviation radiative forcings for 2005 and 2050

Aviation RFs have recently been updated and quantified for 2005 over those for 2000 (Sausen et al., 2005) and reflect the strong growth in traffic since 2000 (Lee et al., 2009), see Fig. 28. Aviation traffic grew in terms of RPK by 22.5% over the period 2000–2005 with an increase in fuel usage of 8%, resulting in an increase in aviation RF of 14% (excluding AIC).

Lee et al. (2009) estimated that total aviation RF (excluding induced cirrus) in 2005 was ~55 mW m^{-2} (23–87 mW m^{-2}, 90% likelihood range), which was 3.5% (range 1.3–10%, 90% likelihood range) of total anthropogenic forcing. Including estimates for aviation-induced cirrus RF increased the total aviation RF in 2005–78 mW m^{-2} (38–139 mW m^{-2}, 90% likelihood range), which represents 4.9% of total anthropogenic forcing (2–14%, 90% likelihood range). These estimates are adopted for this assessment.

Lee et al. (2009) also estimated the RF for two SRES-based aviation emission scenarios (Owen and Lee, 2006, see also Fig. 6) were also calculated (A1 and B2), which adopted the same NO_x technology variants as did the IPCC (Henderson et al., 1999) in their 2050 scenarios, 'technology 1' and 'technology 2' (technology 1 assumes business-as-usual improvements in NO_x control technology, whereas technology 2 places more emphasis on NO_x control at some modest expense of fuel flow improvements: see Henderson et al., 1999). The results are presented in Table 12 and represent an increase in overall aviation RF in 2050 from 2000 for scenarios A1 and B2 by factors of 4 and 3, respectively, and represent 4–4.7% of total RF (excluding induced cirrus) for the matching SRES background scenarios. Note that this analysis differs to that of IPCC (1999), who calculated a range of aviation scenarios against a single background scenario (IS92a). A wider range of aviation scenarios for analysis is currently under preparation within the EU QUANTIFY project (Owen, personal communication).

Table 11
Efficacies, r_i, of aviation forcings.

Perturbation	Reference	r_i (range)
CO_2		1
Aviation O_3	Ponater et al., 2006	1.37 (1–2)
CH_4	Ponater et al., 2006	1.18 (1–1.2)
H_2O	Ponater et al., 2006	1.14
Contrails	Ponater et al., 2006	0.59
Cirrus		unknown

8.4. Other climate metrics

Whilst the different components of RF arising from aviation are useful for evaluating the present-day impact of historical emissions on climate, they do not necessarily reflect the impacts of present and future *emissions* on the future climate in terms of emissions

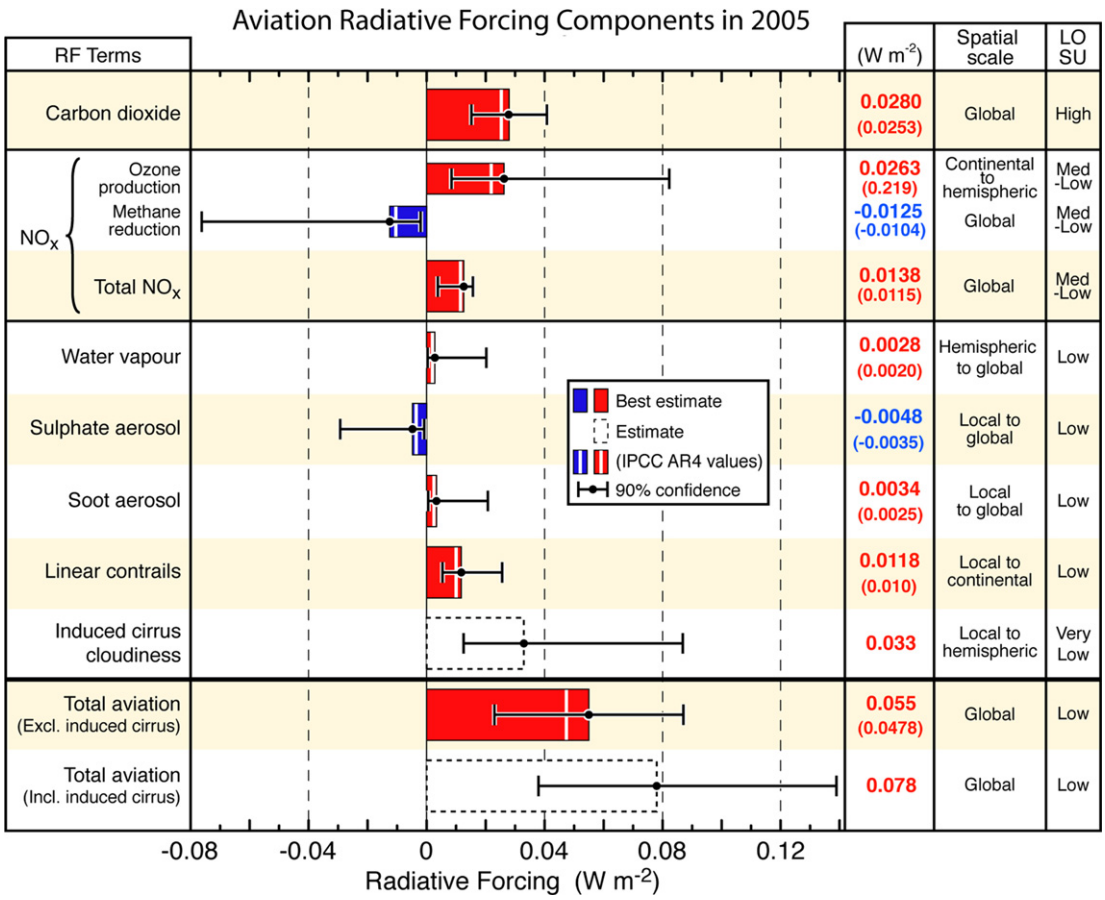

Fig. 28. Radiative forcing components from global aviation as evaluated from preindustrial times until 2005. Bars represent updated best estimates or an estimate in the case of aircraft-induced cirrus cloudiness (AIC). IPCC AR4 values are indicated by the white lines in the bars as reported by Forster et al. (2007a). The induced cloudiness (AIC) estimate includes linear contrails. Numerical values are given on the right for both IPCC AR4 (in parentheses) and updated values. Error bars represent the 90% likelihood range for each estimate. The median value of total radiative forcing from aviation is shown with and without AIC. The median values and uncertainties for the total NO_x RF and the two total aviation RFs are calculated using a Monte Carlo simulation. The Total NO_x RF is the combination of the CH_4 and O_3 RF terms, which are also shown here. The AR4 value noted for the Total NO_x term is the sum of the AR4 CH_4 and O_3 best estimates. Note that the confidence interval for 'Total NO_x' is due to the assumption that the RFs from O_3 and CH_4 are 100% correlated; however, in reality, the correlation is likely to be less than 100% but to an unknown degree (see text). The geographic spatial scale of the radiative forcing from each component and the level of scientific understanding (LOSU) are also shown on the right (Lee et al., 2009).

equivalency. Nor do calculations of present-day RF represent the forcing in terms of integrated RF.

As discussed by Fuglestvedt et al. (2009), there is not a uniquely correct way to do this, but it depends upon the goals of a particular climate policy. In the Kyoto Protocol to the UNFCCC it was decided to use the GWP with a 100-year time horizon (GWP_{100}) for this purpose (see Fuglestvedt et al., 2009, for definition and discussion of the GWP and other metrics). Recently Shine et al. (2005b, 2007) have proposed a new emission metric, the Global Temperature change Potential (GTP), that is designed to serve a policy consistent with a long-term climate target of constraining the global mean surface temperature increase below a threshold (e.g. the EU's target of keeping it below 2 °C above pre-industrial levels).

Because of the short-lived nature of many of the key components of emissions from aviation there are several fundamental problems of applying global and annual averaged metric values to these components. However, they can be readily calculated from the global model simulations (Sausen et al., 2005; Stevenson et al., 2004; Derwent et al., 2001; Wild et al., 2001; Köhler et al., 2008; Grewe and Stenke, 2008). Table 13 gives the GWP_{20}, GWP_{100}, GTP_{20},

Table 12
Aviation radiative forcings for 2000, 2005, 2020 and 2050 in units of mW m^{-2}. The 2050 scenarios utilize SRES (IPCC, 2000) GDP scenario assumptions of A1 and B2 and two levels of NO_x technology as described by IPCC (1999) and Lee et al. (2009), t1 and t2 (note that totals in all cases exclude cirrus). Key: Sa05 (Sausen et al., 2005); St05 (Stordal et al., 2005); L09 (Lee et al., 2009).

Year/study	RF (mW m^{-2})								
	CO_2	O_3	CH_4	H_2O	Contrails	SO_4	Soot	Cirrus (low, mean high)	Total (ex cirrus)
2000/Sa05/St05	25.3	21.9	−10.4	2.0	10.0	−3.5	2.5	10, 30, 80	47.8
2005/L09	28.0	26.3	−12.5	2.8	11.8	−4.8	3.5	11, 33, 87	55.0
2020/L09	40.8	40.6	−19.2	4.0	20.2	−7.0	5.0	16, 47, 125	84.4
2050 A1t1/L09	76.3	109.8	−52.0	9.7	55.4	−16.9	12.1	38, 114, 305	194.4
2050 A1t2/L09	77.7	85.3	−40.4	10.0	55.4	−17.5	12.5	39, 118, 315	183.0
2050 B2t1/L09	73.3	76.5	−36.3	6.7	37.2	−11.8	8.4	27, 80, 212	154.2
2050 B2t2/L09	74.5	59.4	−28.2	7.0	37.2	−12.2	8.7	27, 82, 220	146.5

Table 13
Emission metrics (GWP_{20}, GWP_{100}, GTP_{20}, GTP_{50}, GTP_{100}) and corresponding CO_2-equivalent emissions (in Tg (CO_2)/yr for all metrics) for the various components of 2005 aviation emissions.

	Metric values					Aviation emissions 2005	CO_2 equivalent emissions ($TgCO_2$/yr) for 2005					LOSU[b] (CO_2eq)
	GWP_{20}	GWP_{100}	GTP_{20}	GTP_{50}	GTP_{100}	Tg CO_2, N, H_2O	GWP_{20}	GWP_{100}	GTP_{20}	GTP_{50}	GTP_{100}	
CO_2	1	1	1	1	1	641	641	641	641	641	641	High
NO_x-lo	120	−2.1	−590	−210	−9.5	0.88	106	−1.9	−521	−185	−8.4	very low
NO_x-hi	470	71	−200	−59	7.6	0.88	415	63	−177	−52	6.7	very low
H_2O	0.49	0.14	0.14	0.023	0.02	252	123	35	35	5.8	5.0	
SO_4	−140	−40	−41	−6.9	−5.7	0.18	−25	−7	−7	−1.2	−1.0	
BC	1600	460	470	77	64	0.006	10	2.8	2.8	0.46	0.38	
contrail	0.74	0.21	0.21	0.036	0.03	641	474	135	135	23	19	Low
AIC[a]	2.2	0.63	0.64	0.11	0.089	641	1410	404	410	71	57	very low
Incl AIC												
Total NO_x-lo							2739	1208	696	554	713	very low
Total NO_x-hi							3048	1273	1040	688	728	very low
Ratio (lo) total/CO_2							4.3	1.9	1.1	0.86	1.1	very low
ratio (hi) total/CO_2							4.8	2.0	1.6	1.1	1.1	very low
Excl AIC												
Total NO_x-lo							1329	805	286	484	656	very low
Total NO_x-hi							1638	869	630	617	671	very low
Ratio (lo) Total/CO_2							2.1	1.3	0.45	0.75	1.0	very low
Ratio (hi) Total/CO_2							2.6	1.4	0.98	0.96	1.0	very low

[a] AIC = aircraft-induced cloudiness.
[b] LOSU = Level of Scientific Understanding (high, medium, low, very low).

GTP_{50}, GTP_{100} and CO_2-equivalent emissions for these metrics for the various components of the aircraft emissions and the range caused by uncertainties in the metric values. Different time-horizons were chosen in order to illustrate the variability of values of GWP and GTP for the shorter-lived climate forcing agents. The time horizon of 50 years (TH50) for the GTP metric is used as such a time horizon may be consistent with that for stabilizing global temperature increase. Details on the input data and the way in which the metrics are calculated are provided by Fuglestvedt et al. (2009). For BC and sulphate particles, detailed modelling of the radiative effects of emissions from aviation has not been performed and the metric values for surface emissions are used in Table 13. Also, indirect effects through modifications of clouds are not included in the metric values.

The CO_2 equivalent (CO_2eq) emissions are illustrated for the 2005 assessment of emissions, based on an IEA fuel usage for that year and using various recent emission indices from the literature. In the case of the NO_x GWP and GTPs – actually the sum of the positive short-term O_3 effect, long-term negative O_3 effect, and CH_4 negative effect all divided by an appropriate CO_2 emission AGWP – there is large uncertainty arising from the small number of studies available and the disparate results, in particular, one study by Stevenson et al. (2004) which provides a negative NO_x GWP_{100}. For contrails and aviation-induced cloudiness (AIC), they are referenced to CO_2 emissions as a proxy. It is known that fuel (CO_2) is not necessarily a good proxy or scalar for contrails and AIC as the former are physically related to movements, not fuel usage. However, detailed assessments of contrail forcing with movements rather than fuel have not yet been undertaken and validated; the relationship between aviation operations and AIC is as yet, unknown.

Some tentative total CO_2eq emissions are given, along with ratios of total CO_2eq to CO_2 emissions for both GWP and GTP metrics over sample time horizons. Such multipliers have been termed elsewhere (Forster et al., 2006) a 'CO_2 Emissions Weighting Factor' (EWF) for GWP values. Forster et al. (2007b: corrigendum to Forster et al., 2006) calculated a CO_2 EWF of 1.8 and 1.2 for TH20 and TH100, respectively. The equivalent ranges of values provided here are 4.3–4.8 (TH20) and 1.9–2.0 (TH100) for 2005, although it should be noted that our estimates include AIC and would have been 2.1–2.6 (TH20) and 1.3–1.4 (TH100) if AIC had been similarly excluded. The lower values for this work (excluding AIC) of 2.1, 1.3 (TH20, TH100) would be similar in basis (input data) to the calculations of Forster et al. (2006) (see Forster et al., 2007b corrigendum, also). Here, we have included AIC as we judge that the NO_x GWPs are just as uncertain as the AIC GWPs, given the switch in sign arising from different inputs (i.e. −2 for 'NO_x-lo' to 70 for 'NO_x-hi', both TH100, see Table 13).

Similarly, CO_2eq emissions for GTPs and a ratio of total CO_2eq emissions to CO_2 emissions have been calculated for 2005 (Table 13). These produce systematically lower ratios than GWPs.

In conclusion, the constraint on developing metrics further is clearly the quality of the input data: given improvements in this, one can be optimistic that a range of metrics (including a multiplier for aviation) can be developed for a variety of policy purposes. However, the particular metric and the particular policy purpose need to be matched carefully.

9. Mitigation options

9.1. Introduction: technological and operational context

It has been shown above that aviation affects the atmosphere via emission of radiatively and chemically active gases, and aerosols that also have the capacity to alter clouds. Indirect effects on cirrus and other cloud properties and their coverage can occur long after emission but since knowledge about this potential effect is so poor it will not be treated in this section.

Mitigation of aviation's effects on climate change and the ozone layer may be first understood as a technological problem, namely to reduce emissions of CO_2, NO_x, H_2O, and aerosols. Technological solutions generally have a long research and development lead time to being available to airlines (and the fleet has a turnover time of approximately 20–25 years), but new operational procedures may provide an additional possibility to reduce the climate impacts of aviation. The latter may become effective in the shorter term, although infrastructural changes can also have significant lead times, depending upon the complexity of the proposed changes,

such that generalizations over the timescales of changed operations are difficult.

The Advisory Council for Aeronautical Research in Europe (ACARE, Vision, 2020) published visionary goals in 2001 (ACARE, 2001) for a more environmentally friendly future air traffic system. The ACARE goals, for instance, comprise technology development that would result in emission reductions of 50% CO_2 per passenger km and even 80% for NO_x relative to year 2000 standards (although the 80% quantification is less clear as to what it refers). These are challenging objectives. Although they are principally achievable within the laws of physics, it requires important technological breakthroughs and new concepts of operation. It has been suggested that for the improvements in CO_2, 40% will come from the airframe, 40% from the engine and 20% from improved operations. Similarly, technology objectives with regard to environmental performance of aircraft have been published for the United States (Anonymous, 2007). In this, near term (<5 yr), mid-term (5–10 yr) and far term (>10 yr) goals and objectives have been set. In terms of fuel performance, the reference airframe/engine combination is a B737-800 with CFM56/7B engines, representative of 1998 entry into service technology: for NO_x, these are referenced against the CAEP2 NO_x standard. The relevant goals and objectives are presented in Table 14. It should be noted that these are extracted from a much wider set of energy and environment R&D objectives and goals; the fuel efficiency and NO_x standards are presented for comparison with the relevant ACARE Goals.

Medium and long-term technology goals for NO_x ('MTTG', 'LTTG', respectively) have also been set by ICAO's CAEP on NO_x emissions (LTTG, 2006). Similar to the recent US goals (Anonymous, 2007), these are referenced to the CAEP NO_x LTO regulatory metric. Whilst the environmental impacts being addressed were not specified (air quality was the raison d'être for the CAEP regulatory standard), it is implicitly assumed that reduction in LTO NO_x will result in a commensurate reduction in cruise NO_x, an assumption that has not been examined in detail in the setting of the CAEP MTTG/LTTG.

The CAEP MTTG and LTTG goals are illustrated in Fig. 29. These show the results of an exercise to project what may be possible in the future for the medium term (2020) and the long-term (2050) in terms of NO_x reductions.

Although such targets as described above have been set, very little work has been done on determining the impacts of such technology developments, either in terms of fleet emissions, or atmospheric impacts, other than the technology scenario variants of IPCC (1999 – see Henderson et al., 1999) within the body of that report. The turnover time of the global aviation fleet is of the order of 25 years and so any technology improvements are only taken up slowly. If airlines purchase new cleaner technology before the useful operable lifetime of the aircraft is over, these aircraft are generally sold on (commonly to developing nations or to be converted into freighters) rather than retired from the fleet. Also, the context of growth needs to be considered: in determining the emissions impact, the essential question is whether technology improvements can keep pace (or outpace) with growth in the fleet – IPCC (1999) was pessimistic over this issue, stating "*Although improvements in aircraft and engine technology and in the efficiency of the air traffic system will bring environmental benefits, these will not fully offset the effects of the increased emissions resulting from the projected growth in aviation.*" (IPCC, 1999, Summary for Policy Makers). This issue needs to be addressed in the future to properly quantify environmental benefits: initial work was presented by Sausen and Schumann (2000), using the IPCC (1999) scenarios (Henderson et al., 1999), and some limited work has been performed on the CAEP MTTG/LTTG goals (Owen, personal communication) and is in progress on the ACARE targets (Lee, Schumann, personal communication).

Any mitigation strategy, whether it is technical or operational, must be judged according to the total effect that it has. This means that tradeoffs have to be considered (e.g. less NO_x and fewer contrails could require higher fuel consumption, i.e. CO_2 emission). Calculating these tradeoffs is by no means simple, either technologically or in the atmospheric context. For the atmosphere, these effects occur over very different timescales (see Section 8). Examples of technological tradeoffs include: a higher bypass ratio to reduce fuel consumption and aircraft noise implies greater engine weight and diameter, which at some point will increase fuel consumption once more, moreover this makes NO_x control more difficult because of the higher temperatures and pressures at the combustor inlet. New operational procedures, e.g. a deviation to avoid an ice-supersaturated region for contrail avoidance, may increase travel time and fuel consumption. However, tradeoffs are also inherent in atmospheric physics and chemistry (e.g. flying in the stratosphere will reduce contrail and cirrus formation but the residence time of emissions will increase).

Other considerations necessary for each option are in particular safety, feasibility, and costs. As these considerations belong to engineering, air traffic management (ATM) and economics rather than atmospheric science, they are not covered in this assessment. However, before any measure is adopted it will be necessary that a holistic view is taken and all aspects of a measure will have to be considered.

Aircraft engineers and ATM currently see a need for atmospheric research in the following three areas (GbD, 2005): climate impact of contrails and contrail cirrus (and of indirect effects); the tradeoff between NO_x and CO_2 emissions; and metrics for impacts on climate. This latter topic is treated in Fuglestvedt et al. (2009), hence we concentrate here on contrails, NO_x and CO_2.

9.2. Contrail reduction

9.2.1. Contrail formation thermodynamics

Contrail avoidance strategies have recently been reviewed by Gierens et al. (2008). Contrail formation is determined almost

Table 14
Selected US technology goal for aviation and environment (from Aeronautics Science and Technology Subcommittee, Committee on Technology, National Science and Technology Council, Anonymous, 2007).

Goal	Near term (<5 yr)	Mid-term (5–10 yr)	Far term (>10 yr)
Advance development of technologies and operations to enable significant increases in the energy efficiency of the aviation system	Enable fuel efficient N + 1 aircraft and engines (33% reduction in fuel burn compared with a B737/CFM56)	Enable fuel efficient N + 2 aircraft and engines (at least 40% reduction in fuel burn compared with a B737/CFM56)	Enable fuel efficient N + 3 aircraft and engines to reduce fuel burn by up to 70% compared with a B737/CFM56)
Advance development of technologies and operational procedures to decrease the significant environmental impacts of the aviation system	Enable cleaner N + 1 aircraft and engines; LTO NO_x emissions reduction (70% below CAEP2 standard)	Enable cleaner N + 2 aircraft and engines; LTO NO_x emissions reduction (80% below CAEP2 standard)	Enable cleaner N + 3 aircraft and engines; LTO NO_x emissions reduction (better than 80% below CAEP2 standard)

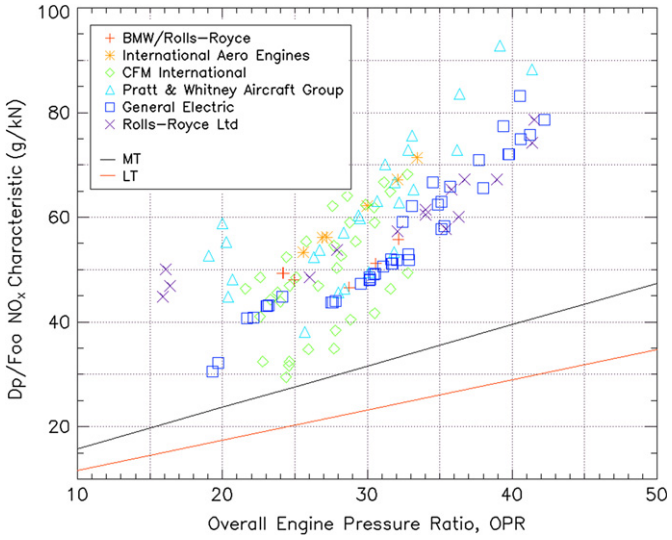

Fig. 29. Characterictic NO_x of in-service engines according to CAEP NO_x regulatory parameter, *Dp/foo* (g NO_x/kN thrust at static sea-level test conditions) vs overall pressure ratio of engine. The CAEP medium term (MT) and long term (LT) technology goals are shown as lines.

exclusively by principles of thermodynamics and the atmospheric conditions in which engine emissions are released. The theory of contrail formation can be cast into a simple equation, known as the Schmidt–Appleman criterion (Schmidt, 1941; Appleman, 1953). The validity of the Schmidt–Appleman theory has been demonstrated and confirmed on various research flights (Busen and Schumann, 1995; Kärcher et al., 1998a; Jensen et al., 1998b; IPCC, 1999; Schumann, 2000). This validation proves that thermodynamics is the controlling factor for contrail formation, not the physico-chemistry of the emitted particles. An in-depth derivation of the Schmidt–Appleman theory has been given by Schumann (1996).

The Schmidt–Appleman criterion only determines whether a contrail will form or not. It does not account for contrail persistency or whether a contrail can spread out into extended contrail cirrus. Persistency is only possible if the ambient air is supersaturated with respect to ice, which means that once ice crystals are formed in the plume they can grow until either the air becomes eventually subsaturated or until the ice crystals fall (due to their weight) into lower subsaturated atmospheric layers where they will then evaporate.

9.2.2. Technical options for suppressing contrails

Because of the thermodynamic control of contrail formation it is not possible to alter contrail formation conditions by changing the character of the emitted particles or particle precursor gases (SO_2, SO_3). A change in these emissions leads to changes in contrail composition and properties (e.g. particle number and size, contrail optical thickness, etc.), but not in formation conditions.

Technical mitigation options for contrails are only possible for those that lead to a decrease in the water vapour emission index, EI_{H_2O}, or lead to an increase in the specific heat content of the fuel, Q, or lead to a decrease of the overall propulsion efficiency, η.

The use of alternative fuels (e.g. CH_4, LH_2) could be an option for reducing contrails because they involved changes in EI_{H_2O} and Q. However, the so-called energy-specific emission index is 0.045 kg MJ^{-1} for CH_4, and 0.075 kg MJ^{-1} for LH_2, whereas it is 0.029 kg MJ^{-1} for kerosene (Lewis et al., 1999, Tables 7–11). Assuming equal η, it turns out that aircraft flying on these alternative fuels could potentially produce contrails at even higher ambient temperatures (hence at lower altitudes) than kerosene-fuelled aircraft.

Fuel additives have been considered by Gierens (2007a,b) as to whether they might be used as a contrail mitigation option. The basic idea explored was to consider a hypothetical additive that would potentially coat soot particles such that they would not be able to act as condensation nuclei for water vapour. Gierens (2007a,b) showed that it would be necessary to produce a soot coating with a threshold water saturation ratio of about 1.4 for water condensation in order to decrease the maximum temperature allowing for contrail formation by 4 K. Unfortunately, this would be balanced by changes in the overall airframe propulsion efficiency expected by 2050. Thus, Gierens concluded that fuel additives were not a useful approach for contrail suppression.

Technical measures for contrail suppression can potentially be applied to the engine architecture. One possibility is to cool the exhaust air with an additional heat exchange unit (cooled by bypass air) such that water vapour can condense in the unit. In this way the emission index of water vapour can be substantially reduced which helps to suppress contrails (Noppel et al., 2007). A fraction of the condensed water can be injected into the combustion chamber in order to reduce NO_x production. Haglind (2008) has investigated the idea to temporarily reduce the overall propulsion efficiency by using variable guide vanes in the engine fan when the aircraft flies through regions where persistent contrails are likely to form. Such a measure could decrease the threshold temperature for contrail formation by about 1.5 K, corresponding to a vertical distance of about 300 m, or 1000 ft (one flight level). In order to keep the price of such a contrail mitigation strategy low (increase in fuel consumption), such a method would have to be combined with operational measures as discussed below. Other technical possibilities to reduce contrail formation are discussed by Noppel and Singh (2007) but most of these are speculative and tend to ignore the overwhelming influence of the ambient atmosphere in contrail formation.

9.2.3. Changing contrail properties

As an alternative to contrail suppression one might aim at altering their optical and microphysical properties such that the radiative impact is reduced. An example is the cryoplane. Since no aerosol is formed by burning LH_2, cryoplane contrails form only on aerosol particles mixed in from the ambient air (Schumann, 1996) and potentially from reformed particles that have passed through the engine (Chen, 1999). Cryoplane contrails are predicted to have 1–2 orders of magnitude fewer ice crystals than contrails from equivalent kerosene-fuelled engines (Ström and Gierens, 2002). Ice crystals in cryoplane contrails are predicted to be 4–6 times larger (linear dimension) than those in kerosene contrails, which renders them optically thinner and of lower duration. Severe technical requirements for the introduction of a cryoplane fleet imply that the benefits of LH_2 technology will probably only appear in a timescale of 50 or more years (Ponater et al., 2006).

There has been some work in American laboratories on fuel additives suitable for reducing particulate emissions from aircraft, unfortunately with inconclusive results so far (Liscinsky et al., 2001; Bae and Avedisian, 2004; Montgomery et al., 2005). In any case, the number of particles would need to be reduced substantially (by orders of magnitude of $\sim$2) to reduce the number density of contrail ice crystals.

9.2.4. Operational means

A potential operational mitigation option to reduce contrail formation is to change flight altitudes. Because of the variation in the tropopause height by latitude, there is no universal solution. In the mid-latitudes a solution would be to fly slightly higher, namely in the extratropical lowermost stratosphere, which is generally too dry for contrail persistence (Schumann, 2005). Flying higher in the tropics would increase contrail formation (Sausen et al., 1998).

Fichter et al. (2005) conducted a parametric study using a climate model to determine potential responses to RF from changes in flight altitudes. Displacing overall cruise altitudes downwards, the global annual mean contrail coverage was reduced up to a maximum decrease of ~45% for a 6000 ft lower cruise altitude. The global mean radiative forcing by contrails was reduced almost proportionally to the contrail coverage, with strong seasonal and regional variability. Rädel and Shine (2008) showed that shifting the air traffic away from the most sensitive layers (10–12 km altitude) to either higher or lower levels would reduce the radiative impact from contrails. Reducing flight levels generally leads to an increase in fuel consumption, an effect that seems to be smaller for cryoplanes than for conventional planes due to different fuel storage configurations (Svensson et al., 2004).

Mannstein et al. (2005) found that relatively small changes in flight level can avoid a substantial fraction of contrails and contrail induced cirrus, due to the shallowness of the ice-supersaturation layers (which are the regions where contrails persist and spread into contrail-cirrus). A 14-month dataset of ice-supersaturated layers and their thickness distribution is shown in Fig. 30. New developments in the capability of meteorological models, such as the ECMWF operational model, to predict ice supersaturated regions (Tompkins et al., 2007) are required to realise such a flexible strategy. Equipping a number of commercial airliners with humidity probes that are designed especially for use in the upper troposphere (including AMDAR; Aircraft Meteorological Data Reporting to the weather centres) would help aviation weather forecasts to more accurately predict ice-supersaturated regions. The analysis of Mannstein et al. (2005) was based upon an analysis of upper air in a single region of Germany, for which the majority of ice-supersaturated layers were approximately 510 m in thickness (with a standard deviation of 600 m). Other radiosonde-based studies of ice-supersaturation layers (Treffeisen et al., 2007 for Svalbard, Sweden; Rädel and Shine, 2007, for southern England) found larger average thicknesses of ice-supersaturated regions (about 1 km), despite peak values of 100–200 m in their thickness distributions. Currently, a general conclusion that only minor changes in height are necessary to avoid contrails may be inappropriate and certainly this aspect requires further and more extensive data and investigation.

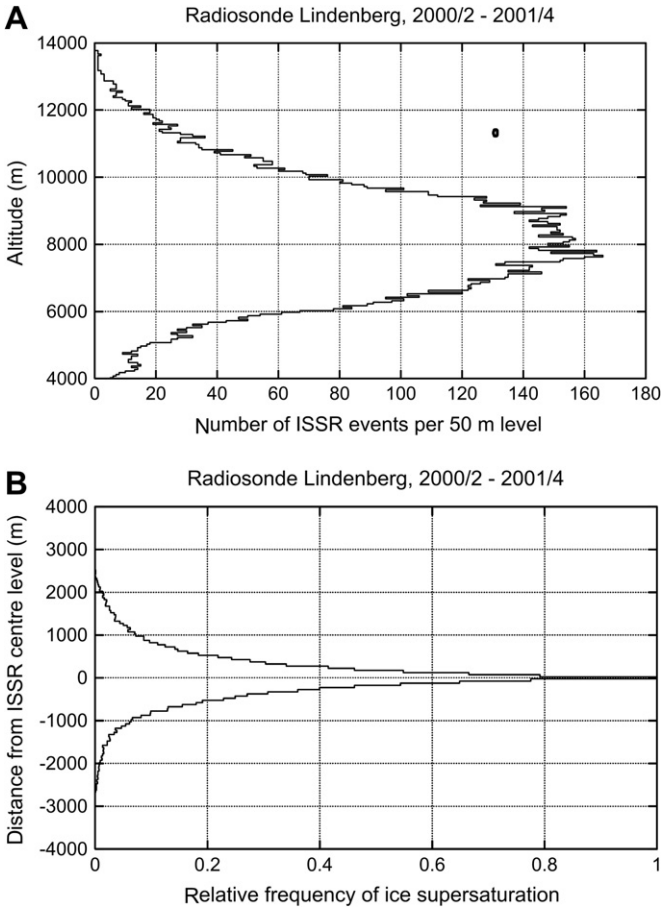

Fig. 30. Altitude distribution of ice supersaturated layers over Lindenberg, Germany, taken from corrected radiosonde humidity measurements (cf. Spichtinger et al., 2003) (A). A change in flight levels of at least ± 2 km would be needed to avoid half of the ice supersaturation. Probability of being in an ice supersaturated layer after an altitude change from the centre level of the ice-supersaturated region (B). A flight level change of ±300 m suffices to avoid ice-supersaturation on a case by case basis (analysis K. Gierens and U. Schumann).

A contrail mitigation study has been conducted by Jelinek et al. (2005) who examined the European air space and the potential to re-route, avoiding contrail formation. However, the study's results are doubtful because of a probable misinterpretation of the relative humidity values from a meteorological model output (MM5) since the areas of contrail coverage seem to be grossly overestimated. Such studies should probably be repeated paying more attention to meteorological data or using the recent ice supersaturation prediction capability of the ECMWF model (Tompkins et al., 2007).

There is also a potential operational mitigation option for reducing the climate impacts from contrails. Contrails heat the surface during the night but may cool the surface during the day (Meerkötter et al., 1999). In a case study presented by Myhre and Stordal (2001) it has been shown that "*assuming a limited persistence of contrails, any shift in the traffic density towards sunrise and sunset would reduce the RF due to contrails*". Most of the RF from contrails can be attributed to night-time flights (Stuber et al., 2006), which account for 60–80% of the contrail RF. Although 22% of annual air traffic movements in the limited study area of Stuber et al. (2006) were winter flights, they contributed about half of the annual mean RF from contrails. Therefore, rescheduling flight times to daylight hours could minimize the climate impact from contrails (Stuber et al., 2006).

A strategy, designed to achieve environmentally optimum flight routings (avoiding ice supersaturated air masses) especially for flights in the evening and night hours, is now being investigated as part of the German climate protection programme (http://www.pa.op.dlr.de/ufo/).

9.3. Nitrogen oxides and carbon dioxide reduction tradeoffs

There is a well-known tradeoff for technological developments in modern jet engines between fuel efficiency and NO_x production. Increased fuel efficiency has been achieved over the last few decades from a shift from turbojet engines to modern high bypass ratio turbofan engines. This tends to result in higher temperatures and pressures at the combustor inlet which optimizes for NO_x formation, such that extra efforts in combustor design are needed to keep NO_x levels down through additional cooling or changes in residence time (see Sehra and Whiltlow, 2004 for a comprehensive overview). The absolute NO_x production is a balance between the changes in fuel consumption (reducing NO_x) and the tendency for increased $EINO_x$ (increasing NO_x).

In his paper "Civil aviation and the environmental challenge" Green (2003) speculates on some potential technological solutions to simultaneously reduce aviation NO_x and CO_2 emissions. Fuel consumption can be reduced by several technical options, in particular drag and weight reductions are the two most promising technology options. However, radical changes in aircraft design are necessary to achieve substantial reductions in CO_2, e.g. laminar-

flow control and departure from the dominant swept-wing configuration. Propulsion efficiency can be enhanced by a transition to open rotor engines. However, open rotor engines (sometimes called 'unducted fans') have issues over safety (blade breakage) and noise impacts that would also have to be addressed. Thermal efficiency, however, can only be improved at the expense of increased NO_x production in the absence of additional efforts in combustor design. Fuel savings are also possible when long-haul flights are done in a series of stages, which would allow a reduction in the amount of fuel required to be loaded. However, there are time, ATM and potential air quality costs that make this option most unlikely.

Also, NO_x emissions might be reduced by the introduction of engines with ultra-low NO_x combustion technology. It is possible to design them in a way that only slightly more fuel is needed than in fuel optimized engines (Green, 2003). It is notable that the ACARE targets call for reductions in fuel consumption and NO_x, such that it should not necessarily be inferred that reduced NO_x always results in increased fuel: this is a tendency, rather than an inevitable fact. It will take quite some years for these novel technologies to come into service. Moreover, there is no reason that they would voluntarily be introduced by the sector in the absence of any regulatory pressure or financial incentive. Potential operational options to reduce the effects of NO_x (instead of reducing NO_x itself) have also been investigated. The EC project TRADEOFF investigated two kinds of options, rerouting of a part of the flights to the far north (where the tropopause is low and flights are mainly in the lower stratosphere; additionally, during polar night there is no photochemistry) and displacing the traffic up or down (+2000 ft, −2000 ft, −4000 ft, −6000 ft). Chemical perturbations, contrail coverage changes and the corresponding radiative forcings were computed with a range of CTMs and GCMs, and with a linear response model. Additionally the role of CO_2 vs. NO_x in terms of climate response from a technology tradeoff scenario was explored.

The effects on O_3 from changed flight routings and altitudes was investigated by Gauss et al. (2006) using the Oslo CTM2 model (a CTM). They first performed a model simulation without aviation, then added aviation corresponding to year 2000. A comparison of these simulations showed that inclusion of aviation leads to a globally averaged increase in the ozone column (expressed in Dobson units, DU) of 0.34 DU (base case), or 0.39 DU when military aircraft operations are considered as well. Most of the increase (about 90%) occurs in the troposphere. These changes provided a base case around which sensitivity studies were conducted, changing routes and lower/higher flight levels. The additional changes in O_3 column relative to the base case of most of these scenarios was of the order 0.01–0.03 DU (positive and negative), that is, at least ten times smaller than the effect of aviation itself, and even smaller than the effect of military operations. These relations are even more pronounced when the view is on the northern hemisphere only (see Gauss et al., 2006, their Table 3). Flying polar routes does not have an ozone penalty; during winter times when photochemistry is reduced or absent it even brings environmental benefits, *cf* lower latitude flights. The operational measures discussed would nevertheless cause spatial shifts in aircraft induced O_3 production with possible consequences for radiative forcing, since O_3 is a greenhouse gas with short lifetime. Preliminary studies (Stordal et al., 2006) indicate weak radiative effects. Hence we may conclude that, according to current knowledge, O_3 effects from aircraft NO_x emissions do neither favour any particular operational change in flight routings and altitudes, nor do they exclude them when for any reason (e.g. contrail avoidance) flying at different altitudes or Polar regions would turn out to be beneficial. Enhancing polar routes might have adverse climate effects for other reasons. The low tropopause at polar latitudes implies that a substantial fraction of emissions occur in the stratosphere where residence times are much longer than in the troposphere. Gauss et al. (2006) show how reactive nitrogen gases (NO_y) accumulate much more in the atmosphere when more polar routes are selected than with every other scenario investigated. As a large fraction of NO_y is HNO_3, which can be washed out by rain and falling ice crystals, such an effect can only be exploited by flying within the troposphere. Grewe et al. (2002b) found that if overall cruise altitudes were reduced, then NO_x emissions increased – however, less O_3 was formed because of increased rates of chemical removal and washout of NO_y species.

Within TRADEOFF, technology tradeoff studies were conducted using the linear response model of Sausen and Schumann (2000). Several scenarios were considered with reduced NO_x emissions at the expense of higher fuel consumption. The general tenor of the results was that greater benefits accrue from focussing upon NO_x rather than CO_2 reductions. This conclusion depends, yet, strongly upon the assumed equilibrium temperature response for aviation-generated O_3.

9.4. Cryoplanes and alternative fuels

'Alternative fuels' here, refers to fuels that are alternative energy sources to aviation than conventional kerosene. This might include LH_2, CH_4, kerosene manufactured by different processes, e.g. from the Fischer–Tropsch process, and lastly biofuels. The terminology 'alternative fuels' should be understood clearly, as it does not necessarily imply what might be understood a 'sustainable fuels' and some processes of alternative fuel production can be more carbon-intensive than conventional kerosene.

In terms of what are popularly referred to as 'biofuels', a distinction is sometimes made between first-, second- and third-generation biofuels. First-generation biofuels usually refers to fuels manufactured from sugar, starch, vegetable or even animal oils; second-generation biofuel usually refers to those manufactured from non-food crops including food-biomass waste; third-generation biofuels are usually referred to as those being derived from algae.

Saynor et al. (2003) investigated "*The potential for renewable energy sources in aviation*" considering biodiesel (e.g. oilseed rape or soybean methyl ester), ethanol, methanol, synthetic kerosene, nuclear power, liquid hydrogen, and liquefied biomethane. Of these fuels, ethanol and methanol were considered unsuitable, particularly because of their low energy density (both by mass and volume). At low power conditions, the combustion of alcohols produces organic acids and aldehydes, with attendant air quality health hazards (Saynor et al., 2003). Nevertheless, ethanol blended Jet-A fuels show marked reductions in CO_2, NO_x, and soot formation with increasing blend rates (Eiff et al., 1992). Biomethane was judged unsuitable by Saynor et al. (2003) because of its limited availability and uncertain quality. Nuclear power was deemed too dangerous in case of accidents or terrorist attacks. Thus, synthetic kerosene, biodiesel, and LH_2 were examined in Saynor et al.'s (2003) study, which discussed the corresponding production possibilities, costs, environmental considerations in production and transport, and advantages and disadvantages in use. The environmental advantages of these alternative fuels were deemed to be:

- Biodiesel as a partial substitute for kerosene would reduce fuel cycle carbon emissions. Since CO_2 is well mixed throughout the atmosphere, emission reductions in the fuel production process have the same benefit as emission reductions over the flight cycle.
- Synthetic kerosene, produced from biomass feedstock via the Fischer–Tropsch process, reduces fuel cycle carbon emissions as well. The fuel is virtually sulphur free, which would almost eliminate emissions of SO_2 and SO_3, which are precursors of

sulphuric acid solution droplets at cruise level-a form of particles that are important in cirrus formation.
- Burning LH_2 would eliminate emissions of all carbon bearing species including soot, and sulphur oxides. The only primary combustion products would be H_2O and NO_x.

Svensson and Singh (2004) showed the potential to design a combustion system using LH_2 fuel that produces less NO_x emissions than any system burning kerosene. The reason is the wider flammability range of the LH_2/air mixture compared with the kerosene/air mixture which allows combustion at an equivalence ratio, resulting in a lower flame temperature. Svensson and Singh (2005) discussed various engine cycles for LH_2 fuel, and showed that in relative terms, the potential to reduce NO_x emissions is greater than the potential to reduce fuel consumption and hence H_2O emission. In order to reduce mission NO_x emissions, engines with lower core power along with lower bypass ratios could be used. Lower core power means lower temperatures and pressures, such that less NO_x is formed. The reduced bypass ratio would limit decreases in fuel consumption.

The transition to LH_2 fuel would be a revolutionary step in aviation, since not only the engines would have to be redesigned but also the whole airframe which would have to carry larger fuel storage with cryogenic devices. Production, transport to the airport and storage there will be different from today's practice with kerosene. So the introduction of a significant cryoplane fleet will certainly be decades in the future. For the short- and mid-term future synthetic kerosene is the easiest to use for aviation, however, the production cost is considerably higher than that of mineral kerosene. Alternative fuels such as LH_2 might be useful to alter contrail properties that make them less detrimental to climate; however, for contrail suppression they are not applicable, as stated above. In the present section the potential of alternative fuels as a means of NO_x and CO_2 emission reduction is examined. For this purpose one has to firstly make a selection of potential fuels for aviation.

Biofuels are increasingly discussed as a means of mitigating climate change, often in the context of transportation fuels (Sims et al., 2006; Kahn-Ribeiro et al., 2007; Inderwildi and King, 2009). Aviation kerosene has a demanding specification because of safety requirements. The possibility of using biofuels as 'blends' with either conventional kerosene or synthetic fuels has been examined recently by Daggett et al. (2006, 2008). These authors note some of the difficulties associated with biofuels for kerosene blends, i.e. its lower freezing temperature at normal cruise conditions, its poorer thermal stability characteristics and storage stability over time. However, none of these difficulties were considered insurmountable. Suitable biofuels would require a large fraction of oil content, such as sunflower, soybeans or rapeseed. Daggett et al. (2006) illustrate that large areas of agricultural land would be required in order to supply demand on this basis, e.g. for a 15% biofuel kerosene blend, citing the US fleet consumption (year unspecified) of 13.6×10^9 US gallons, which at 15% blend would require 34 million acres of soybean production, approximating to the size of Florida State. They point out that cellulose-type feedstocks for ethanol for ground transportation purposes are far more efficient in yield per unit area.

More recently, the possibility of using algae as biofuel feedstock has been discussed as being more efficient than common biofuel terrestrial plants. Commonly, large-scale saltwater tanks or bioreactors are envisaged for the algal production but the feasibility of these methods and the production of a kerosene blend at a commercial scale remain to be properly investigated.

Wardle (2003) has also considered the usage of biofuel blends for aviation usage in a much broader context of feasibility, price, land-use, and ethics. Wardle argues that the potential large usage of agricultural land in developing nations would hamper development in terms of local agriculture and food supplies, thus bringing the ethics of a carbon-neutral flight vs. food supplies into question (see also Lovett, 2007). This is an issue clearly beyond the scope of this assessment but the issue is pointed out.

In terms of more general issues of biofuel production, it is possible that there are issues over extra N_2O released as a consequence of common agriculturally-based biofuel production, which may negate or exceed the biofuel-related CO_2 saving (Crutzen et al., 2008). This, if correct, brings the whole issue of biofuel viability into question on an atmospheric basis alone if carbon-neutrality is the goal. Recent work has called into question the usage of crop biofuels (as opposed to biowaste) (Searchinger et al., 2008), showing that land-use changes imply increases in net GHG emissions, as does conversion of rainforests, peatlands savannas and grasslands to biofuel-generating land (Fargione et al., 2008). These more complex questions over indirect effects are increasingly being addressed (e.g. Gallagher, 2008) and in the US, there is the CAAFI (Commercial Aviationn Alternative Fuels Initiative) initiative to provide a comprehensive life-cycle assessment[10].

What is necessary in assessing whether biofuels offer an advantage over conventional kerosene is a complete life-cycle analysis, including accounting for other potential associated GHG emissions (e.g. N_2O from fertilized land).

10. Summary and conclusions

10.1. Aircraft emissions – what are the principal effects on climate and ozone depletion, and have any 'new' effects been identified?

- The scope of current subsonic aviation effects on climate remain the same as those outlined in the IPCC (1999) report: positive RF (warming) arises from emissions of CO_2, soot, H_2O, NO_x as an O_3 precursor, contrails and cirrus cloud enhancement from spreading contrails; negative RF (cooling) arises from fuel S converted to sulphate particles and NO_x emissions that result in reductions of ambient CH_4. 'New' effects being investigated include the potential RF from 'soot cirrus' (i.e. seeding of new clouds from particles or the alteration of existing cirrus properties) which may have a positive or negative radiative effect.
- Current subsonic aviation is considered not to contribute towards O_3 depletion in the stratosphere.
- A future supersonic aviation fleet would overall cause a positive RF through emissions of CO_2 and H_2O, and the RF of the latter would dominate in magnitude. Emissions of NO_x result in either destruction or increases in O_3, depending critically upon the height of the emission. If O_3 destruction occurs, this will also result in a negative RF. What is new since IPCC is that the destruction of O_3 from supersonic emissions of NO_x appears to be more likely, since chemical reaction rates have been revised that result in the 'cross over' point between formation and destruction occurring at lower altitudes, approximately 16 km. Supersonic aircraft are unlikely to cause significant contrail formation or cirrus cloud enhancement except in the tropics.

10.2. What is the overall present-day and potential radiative forcing from subsonic aviation?

- Current-day (2005) traffic has been re-evaluated over the previous estimate for 2000. This has shown an increase in traffic (in RPK) of 22.5% with an increase in fuel usage of 8.4%

[10] http://www.caafi.org accessed 19-05-2009.

and RF of 14% over the period 2000–2005 (excluding AIC), Total aviation RF (excluding induced cirrus) in 2005 was ~55 mW m^{-2} (23–87 mW m^{-2}, 90% likelihood range), which was 3.5% (range 1.3–10%, 90% likelihood range) of total anthropogenic forcing. Including estimates for aviation-induced cirrus RF increases the total aviation RF in 2005–78 mW m^{-2} (38–139 mW m^{-2}, 90% likelihood range), which represents 4.9% of total anthropogenic forcing (2–14%, 90% likelihood range). Calculated future 2050 aviation RF for SRES scenarios B2 and A1, show an increase of RF (excluding cirrus) by factors of 3–4 over 2000 levels, representing 4–4.7% of total RF (excluding induced cirrus) for the relevant background scenarios.

10.3. How have individual estimates of forcing changed since the IPCC Aviation Special Report?

- The RFs from CO_2, H_2O, BC have increased with traffic growth and increased fuel usage. Estimates of RF from O_3 have not grown in proportion with traffic increases because the models have improved substantially and they predict a lesser global mean O_3 forcing per unit emission (36.9 ± 10.4 mW m^{-2}/Tg N yr^{-1}) than did the models used for the IPCC assessment (39.4 mW m^{-2}/Tg N yr^{-1}). However, the absolute ratio of the positive short-term O_3 forcing to the negative CH_4 forcing has not changed substantially since the IPCC (1999) exercise (IPCC = −1.64; −1.65 reported here). Note that this does not include the smaller, long-term negative tropospheric ozone RF that occurs in parallel with the decadal reduction in CH_4. Given the wide range of responses from the models reported here, it is not possible to say whether this change in specific O_3 forcing is significant and it is evident that more work is required to produce convergent results of aviation O_3 production and CH_4 destruction.
- The RF from contrails has been assessed as being smaller, despite increased traffic growth. This is primarily because of changed assumptions over the optical depth of contrails. This correction is uncertain and subject to further investigation.
- The RF from contrail-cirrus has been quantified from statistical observations of cirrus cloud trends. Whilst this has provided progress and the studies are in broad agreement of trends, there remain significant uncertainties over the attribution of such trends and the RF estimates made from them. In comparison with the IPCC (1999) results the upper estimate of potential RF from contrail-cirrus has increased from 40 mW m^{-2} to 80 mW m^{-2}. This assessment remains very uncertain and much more work is necessary.
- The RF arising from aircraft emissions of soot altering the physical and optical properties of cirrus clouds has been estimated for the first time, and this ranges from −160 to −120 mW m^{-2}, in one study (Penner et al., 2009) and from −110 to +260 W m^{-2} (Liu et al., 2009) in another, using the same basic modelling system but depending upon modelling assumptions and the particular parameterization used. The estimated values are highly uncertain since they depend on the mode of nucleation in the background atmosphere and the specific nucleation properties of aircraft soot emissions.

10.4. Aircraft CO_2 emissions: what are the global trends and potential future developments?

- Aircraft fuel usage and therefore CO_2 emissions have grown steadily over past decades (an increase of a factor of 1.8 in 2005 over 1980) and events such as the Gulf war of the early 1990s and the down-turn in aviation in the early 2000s have only offset one or two years of growth, with fast recovery of the global market. Currently, aviation represents 2.5% of global CO_2 emissions (2005), and was 2.7% in 2000.
- The construction of emission inventories and scenarios has become more refined with the incorporation of non-scheduled air traffic and better estimations of military emissions (although these remain a minor component). Nonetheless, challenges remain in these estimations because of the complexity of the data handling and some issues remain to be resolved. None of the bottom-up emissions inventories yet match the recorded sales of kerosene by the IEA. From IEA data, emissions of CO_2 from aviation were 733 Tg in 2005.
- A number of future (2050) scenarios have been constructed which are new since the IPCC (1999) report and utilize SRES-compatible assumptions of growth (GDP). According to these scenarios, CO_2 emissions will increase by factors of 2.7–3.9 over 2000 levels. These new scenarios generally match the older IPCC (1999) ones well, although the (IPCC and other) low-growth scenarios appear to be less plausible than the mid- to higher growth scenarios.

10.5. Aircraft non-CO_2 emissions: how has the characterization of emissions been improved and what are the implications?

- A great deal of progress has been made since the IPCC (1999) report on measuring and understanding the formation of emission species, particularly particles.
- It has been found that a significant fraction of NO_x emissions is primary NO_2 emitted at the ground for low power conditions (idle), of the order 50% or greater. However, this is not a climate impact issue but one of air quality. The estimated amount of primary NO_2 emitted at higher power settings relevant to cruise conditions has not changed since the IPCC (1999) report and remains of the order 1–10%.
- Emissions of OH, which control the rate of oxidation of NO_x to NO_y in the plume and the initial rate of conversion of S^{IV} to S^{VI}, are very difficult to measure and have previously been either estimated, or assumed to be of the order 10 ppm at the engine exit. Limited measurements during the PartEmis project indicate levels much lower than this at the engine exit, of the order 1 ppb. This may have implications for plume chemistry estimations and explains other estimations of S^{IV} to S^{VI} conversion if correct (see below).
- Good progress has been made on characterizing non-volatile particle emissions, i.e. soot. These typically have aerodynamic diameters of 30–60 nm and are largely spherical and may agglomerate, forming particles of 100 nm. Limited measurements show that the number of ice crystals in a young contrail is a direct function of the number of soot particles emitted. Soot may also interact with sulphate and organic species (see below) and be involved in the later formation of cirrus clouds, ('soot cirrus').
- Kerosene contains small amounts of sulphur (0.064%) which may be converted to SO_2 and H_2SO_4 and is the principle component of volatile particles. Gaseous H_2SO_4 is potentially an important aerosol precursor in the upper troposphere and it has been measured directly in plume encounters. The fraction of S^{VI} emitted from aircraft exhaust was previously thought to be of the order 10% or greater. Limited measurements and model studies have shown that this is rather lower, of the order 1–10%, with the higher values derived from model studies for modern engines with high

combustion pressure and temperature. Most of the conversion of S^{IV} to S^{VI} occurs within the engine itself.

- Measurements and modelling indicate that organic volatile compounds are emitted and can act as particle precursors. The precise nature and composition of these organic species is not yet known but particle measurements cannot be explained without this volatile material being present in the exhaust. Such organic species should be identified.
- Gaseous charged ions – chemi-ions – may also take part in the particle formation process and both positive and negative charged ions have been detected. It is possible that these ions form initial very small particles of a few nm in diameter.

10.6. How does aviation impact upon atmospheric composition in the upper troposphere and lower stratosphere?

- Approximately 60% of NO_x from aircraft are emitted between 9 km and 12 km, directly in the UT/LS region and result in changes in atmospheric composition either directly, or indirectly through chemical reactions.
- Aircraft emissions are a dominant source of NO_x in the UT/LS, along with lightning and result in production of O_3, which has a stronger radiative effect at these altitudes than at the ground such that the global mean forcing per unit N emission is much larger than all sources combined. The specific O_3 RF (mW m^{-2}/Tg N yr^{-1}) for O_3 from aviation is approximately 5.5 times greater than that from all NO_x sources combined.
- Aircraft NO_x emissions also result in the destruction of a small fraction of ambient CH_4. Ozone formation and CH_4 destruction from aircraft NO_x results in positive and negative RFs, respectively, with the CH4 response being accompanied by a decadal time-scale loss of O_3, but the primary O_3 and CH_4 responses to NO_x emissions occur on different temporal and spatial scales.
- The global modelling of aircraft emissions and their effect on chemistry and climate has improved greatly since the IPCC (1999) assessment. Models show similar enhancement of O_3 and destruction of CH_4 from NO_x emissions although the magnitude varies. Many models now include NMHC emissions which make a significant contribution to the overall O_3 budget: however, aviation has been shown to be an insignificant source of these emissions. It has also been shown that the inclusion of acetone and PAN chemistry is important in modelling aviation impacts.
- The inclusion of particles and heterogeneous chemistry in models results in an enhanced conversion of NO_x to HNO_3, which reduces the amount of O_3 formed.
- It has been speculated that the presence of cirrus clouds may reduce the O_3 by surface chemistry: this has not been directly investigated in terms of its potential impact on aviation-produced O_3 but there are indications that this is a minor effect, of the order 5%.
- Aircraft emit particles that have direct radiative effects by scattering (SO_4) solar radiation or absorbing (soot) terrestrial radiation.

10.7. What are the potential impacts of future supersonic emissions on the composition and chemistry of the stratosphere?

- Further hypothetical scenarios that include the development of supersonic aircraft have been developed for assessment studies, which include a number of parametric variants that have been used to study the effect of cruise altitude, aircraft size and speed, and $EINO_x$ (see below).
- *Interannual variability of effects arising from supersonic transport*: To fully understand the potential impact of a future HSCT aircraft fleet, it is necessary to consider the global transport of aircraft emissions in the stratosphere, taking into account the interannual variability of meteorological conditions on the model-calculated atmospheric perturbations. In fact, the interannual variability in calculated HSCT-induced O_3 changes in a global CTM may be of a magnitude comparable to the differences observed between calculations performed by various models within IPCC (1999). This result highlights both the importance of the chosen background meteorological conditions in aircraft assessments and the extent to which differences in meteorology can contribute to differences between model calculations.
- *JPL chemical updates*: Updates of the reaction rate constants and photolysis cross-sections in atmospheric chemical models to the recommendations of JPL 2000 and JPL 2002 (Sander et al., 2000, 2003) increased the calculated O_3 dependence on EI-NO_x, with respect to previous assessments, namely IPCC (1999). In fact, the cross-over point in the O_3 chemical production and destruction terms from NO_x chemistry is at altitudes of approximately 16 km, somewhat lower than deduced for the IPCC (1999) calculations. If NO_x and H_2O supersonic emissions take place in the region of O_3 chemical destruction, this causes an O_3 decrease throughout the stratosphere and therefore in the O_3 column. For this reason the potential impact on the atmosphere of a future fleet of supersonic aircraft may be highly dependent upon the amount of NO_x emitted from the fleet and the cruise altitude.
- *Polar stratospheric clouds*: Perturbations in HNO_3 and H_2O, arising from stratospheric supersonic aircraft emissions of NO_x and H_2O, would have a direct influence on the thermodynamic threshold temperatures for the existence of NAT, STS and ice particles in the Northern Hemisphere polar stratosphere. The 'supersonic' aircraft emission-induced perturbation in the formation of solid type PSC particles may significantly increase the denitrification rate in the Arctic lower stratosphere.
- *Radiative feedback*: The magnitude of the direct climate forcing produced by an HSCT aircraft fleet is such that it is important to consider the effect of the radiative feedbacks when estimating the climatic/dynamic response to such aircraft emission. The globally integrated amount of water vapour in the lower stratosphere would increase due to a TTL warming resulting from the net RF produced by the supersonic aircraft emissions, thus increasing the H_2O related RF (positive feedback). This effect may be balanced (or even overbalanced) when taking into account H_2O and O_3 radiative feedbacks on the stratospheric circulation: the latter would tend to reinforce, thus increasing the pole-to-equator gradient of the HSCT-accumulated H_2O in the lower stratosphere. In this case, one study found a reduction of the H_2O RF resulting from HSCT emissions (negative feedback). Additional numerical studies are needed to assess this effect.
- *UV*: Using EC-SCENIC emission scenarios of supersonic aircraft in 2050 and O_3 and aerosol changes calculated in a global CTM, the resulting calculated changes in erythemal UV with respect to the base (pure subsonic) scenario are generally positive at all latitudes and seasons and small, rarely exceeding 1%.
- *Climate forcing and sensitivity studies*: The quantitative assessment of different options for supersonic transport with

regard to the potential destruction of the O_3 layer and climate impacts is made analyzing options for fleet size, engine technology ($EINO_x$), cruising altitude, range, and cruising height. Based on EC-SCENIC emissions scenarios for 2050, considering both radiative forcing calculations and environmental options, the minimum impact was found for a supersonic scenario where speed and cruise altitude are reduced with respect to the base case, i.e. about Mach 1.6 and 16 km altitude, instead of Mach 2.0 and 20 km. An analysis of the different RF components in 2050 shows that the net forcing from aerosol particles is the largest component after water vapour.

10.8. What is the current status of knowledge of the effects of aviation on cloudiness?

- Aircraft have been known to make contrails for some considerable period of time; they are caused by the emission of water vapour and particles into cold ice-supersaturated air, and thus their occurrence is primarily controlled by environmental conditions. Contrails are initially linear and may result in an increase of cirrus cloud cover if they are persistent, depending upon the traffic density, and cause a local and global change in RF. The warming effect of persistent linear contrails exceeds the solar albedo (cooling) effect. The occurrence of contrails may be predicted with good accuracy. However, contrail coverage is still poorly quantified since the calculations of coverage involve normalization to observations by satellites, which do not 'see' contrails below a certain optical depth. Unfortunately, this normalization factor does not seem to be equal in all areas of the globe. Estimates of contrail RF indicate smaller values than the IPCC presented but this is largely a function of optical depth which has been reduced from 0.3 to 0.2, or less. Although some recent models compute the optical depth from the available IWC in contrails, it is prescribed in others. The values of optical depth in contrails are not well known and represent a significant uncertainty.
- Contrails may spread into non-linear structures that closely resemble cirrus clouds (contrail-cirrus). Progress has been made in quantifying the extent of contrail-cirrus but this has been from observations and a correlation between air traffic and increases in cirrus cloud coverage over e.g. timescales of more than 5 yr. Thus, a causal relationship cannot be established but a number of independent studies (that sometimes use the same underlying data) have indicated that there is an increase in cirrus cloud coverage in regions of heavy air traffic. However, recently, the usage of ISSCP data for long-term trend studies has been called into question, and if the data are corrected, studies on long-term trends in cirrus attributable to aviation should be repeated. The radiative properties of contrail cirrus are very poorly quantified but are currently considered to be similar to those of persistent linear contrails: these properties need to be confirmed.
- Modelling studies have been initiated that attempt to quantify the occurrence of soot-cirrus, which have utilized recent measurements and parameterizations of ice formation on particles. Cirrus cloud formation is believed to be dominated by homogeneous freezing of supercooled liquid droplets. However, heterogeneous ice nucleation may also occur, e.g. from aviation soot in the UT/LS and there is evidence of this from field campaigns and measurements comparing 'clean' cirrus with 'polluted' cirrus. The results from one modelling study were unequivocal in that both warming effects and cooling effects may theoretically occur but the 'real' occurrence is simply unknown. There is a lack of fundamental understanding over the mechanisms that are in operation in the atmosphere. Two physically-based ice-nucleation parameterizations have been developed and implemented into a global model. The two parameterizations provide good agreement with each other in terms of ice crystal number concentration. However, similarly to a previous study, the results may produce either positive or negative RFs (10–80 mW m^{-2} and -140 to -160 mW m^{-2}), depending upon the effects of aerosol concentrations on ice number concentration and size. A later study estimated the effect of aircraft soot on cirrus clouds to be in the range of -110 to $+260$ mW m^{-2}. Clearly, this is an aspect which requires much more work on both understanding the fundamental mechanisms and the implications for global mean RF.

10.9. What are the effects of aviation on climate and surface temperature response and what advances in understanding have been made?

- The effects of aviation on climate have mostly been assessed in terms of the RF metric. This is an acceptable and robust metric that quantifies the radiative effects of aviation to date, or under some particular emissions scenario, but underestimates the full consequences of historical emissions. It has been used in climate science in general because of the linear relationship between global mean RF and global mean surface temperature response.
- There is some recent evidence that different forcings may result in different temperature responses, when compared with the temperature response from CO_2 forcing. The ratio of these two sensitivities has been termed the 'efficacy'. Limited work on aviation forcings has indicated that there are significant deviations from unity in efficacy, both positive and negative.
- Since aviation results in both positive and negative RFs, it is important to understand the implications of this. These are usually quantified in terms of global mean RFs but the localized forcings may have different spatial patterns from one another, e.g. positive O_3 and negative CH_4 forcings. It has been found in some idealized GCM integrations that the global mean temperature response to the same O_3 forcing varies by latitude and altitude. More generally, some GCM experiments have shown that the pattern of temperature response to either homogeneous or heterogeneous forcing is *dissimilar* to the forcing and depends primarily on local feedbacks. However, forcings in these areas where local feedbacks operate may amplify the temperature response. The issue of quantification of the effects of homogeneous and heterogeneous aviation-induced forcings is an important area of work which requires further work. Such complex responses highlight the limitations of simple climate models to represent aviation forcings adequately in terms of global mean temperature response.
- Emission-based metrics such as the GWP and GTP have been reviewed and formulated into CO_2-equivalent emissions. The value of these depends on the time-horizon selected. Emissions weighting factors that represent the total effect of aviation as a ratio to that of CO_2 have been calculated and presented for GWPs and GTP metrics and different time-horizons. For GWPs, these range from 4.3 to 4.8 (GWP_{20}) and 1.9–2.0 (GWP_{100}) for 2005, including AIC; excluding AIC they are 2.1–2.6 (GWP_{20}) and 1.3–1.4 (GWP_{100}). In the context of these

calculations, AIC has a similar uncertainty to aviation NO_x GWPs, given that the few different estimates change in sign.

10.10. What are the mitigation options for aviation?

- Increasingly, mitigation options are being examined for aviation. This assessment has not considered policy options (e.g. market based options or regulatory regimes) but rather some technological and operational possibilities.
- Ambitious technology targets for fuel burn and NO_x emissions have been formulated in Europe, the US and at the international level through such bodies as ACARE, The US National Science and Technology Council, and ICAO. It is generally accepted that these targets will require technological breakthroughs and innovation: nonetheless, if achieved, market uptake is relatively slow because of the long lifetime of aircraft. Also, such targets need to be considered in terms of rate of growth when quantifying the effects of such improvements on aviation's impacts on climate change. Little work has yet been undertaken on assessing the impacts of such technology targets on global fleet emissions and their climate impacts (there are also potential technological tradeoffs with noise and emissions in the context of local air quality impacts). The climate impact tradeoffs are also complex, and have been considered in the companion assessment on transport-related climate metrics (Fuglestvedt et al., 2009).
- The formation of contrails is largely a function of environmental conditions, such that technological measures may change the contrail composition and properties but not the formation conditions. The only technological options that would lead to a reduction in contrail formation would require reductions in the emission index of H_2O, or an increase in the specific heat content of the fuel (Q), or a decrease in the overall propulsion efficiency. This latter prospect would be highly undesirable for a fuel efficiency point of view and invoke complex comparisons between short-term and long term climate responses from contrails and CO_2. Using either CH_4 or LH_2 as alternative fuels would result in contrails being formed at higher ambient temperatures than kerosene-powered aircraft and therefore increase the depth of the atmosphere over which contrails might be produced. Fuel additives are not a viable option.
- The main suggestion for reducing contrail formation has been operational avoidance. This has been shown in modelling studies to be quite effective, and would require avoidance of ice-supersaturated air. However, more work needs to be done on the feasibility (and cost) of implementation of this into the air traffic management system and the potential fuel penalties. Again, this invokes the complexity of assessing the impact of reducing a short-term climate impact against increasing a longer-term impact.
- Emissions of NO_x can be reduced by technological means by manipulation of the combustor conditions or the cooling air. There may be potential technological tradeoffs that impact upon fuel consumption, and potentially noise. The impact of NO_x on O_3 formation has been shown to be altitude dependent, along with the RF effect of the O_3 produced. Varying cruise altitudes can also change the NO_x impacts on O_3 formation. However, there is the complexity that O_3 production varies according to background conditions which may change in the future.
- Alternative fuels have been considered, mostly in terms of LH_2. Such 'cryoplanes' would result in reduced direct CO_2 emissions but the fuel production process would also have to be considered. Potentially, NO_x emissions from cryoplanes might also be reduced. However, it is only likely that such a fleet would be developed under a more general hydrogen economy. Biofuels have also been considered to a limited extent. Anything that reduces the release of 'locked carbon' from fossil fuels potentially reduces the CO_2 impact but there are other issues to be considered beyond the scope of this assessment that include; safety (in terms of kerosene specifications for aviation usage), carbon-budget and other GHG issues, and more general land-use issues (including ethical issues) over potential supply. Usage of biofuels in other sectors may yield more benefits than utilization in the transport sector.

Acknowledgements

This assessment has been funded by EU FP6 Specific Support Action ATTICA (European Assessment of Transport Impacts on Climate Change and Ozone Depletion, http://ssa-attica.eu) and has been supported by the EUFP6 Integrated Project QUANTIFY (Quantifying the Climate Impact of Global and European Transport Systems, http://ip-quantify.eu). We are grateful to the reviewers Prof. Christoph Zerefos (National Observatory, Athens, Greece), Dr Kostas Eleftheratos (National and Kapodistrian University of Athens) and Dr Helen Rogers (University of Cambridge, United Kingdom) for their detailed and constructive reviews, and Prof. Peter Brimblecombe (Atmospheric Environment) for his guidance in improving the manuscript. We would particularly like to thank ATTICA 'Shipping' and 'Metrics' coordinating lead authors Prof. Veronika Eyring (DLR), Prof. Ivar Isaksen (University of Oslo), Dr Jan Fuglestvedt (CICERO), Prof. Keith Shine (University of Reading) for fruitful discussions during the preparation of this assessment. JEP acknowledges support from the National Science Foundation under 0609836. We would also like to thank Dr Lourdes Maurice (Chief Scientific and Technical Advisor for Environment, US Federal Aviation Administration) and Mr Peter Newton (United Kingdom Department for Business, Enterprise and Regulatory Reform) for assistance on technology targets. We are also grateful to Prof. Bernd Kärcher and Dr Hermann Mannstein of DLR for comments on parts of the manuscript. Dr Jane Hurley and Jerome Hilaire of MMU are thanked for their assistance with the preparation of figures.

Appendix I. European Commission Framework Programme projects that relate to aviation emissions, impacts, or have published relevant studies

AERO2K (Global aviation emission inventories for 2000 and 2025) http://www.cate.mmu.ac.uk/aero2k.asp
CRYOPLANE (Liquid Hydrogen Fuelled Aircraft – System Analysis) http://www.aero-net.org/about/relproj/5-cryoplane.htm
CYPRESS (Future Engine Cycle Prediction and Emissions Study) http://www.aero-net.org/about/relproj/6-cypress.htm
INCA (Interhemispheric differences in cirrus properties from anthropogenic emissions) http://www.pa.op.dlr.de/inca/
METRIC (Metrics of climate change) http://www.pa.op.dlr.de/metric/
NEPAIR (New Emissions Parameter for aircraft) http://www.aeronet.org/lib/cr030440.pdf
PartEmis (Measurement and predictions of the emission of aerosols and gaseous precursors from gas turbine engines) http://www.aero-net.org/about/relproj/8-PartEmis.htm
SCENIC (Scenarios of aircraft emissions and impact studies on chemistry and climate) http://www-scenic.ch.cam.ac.uk/
TRADEOFF (Aircraft emissions: Contributions of various climate compounds to changes in composition and radiative forcing –

tradeoff to reduce atmospheric impact) http://www.geo.uio.no/forskning/atmosfare/prosjekter/TRADEOFF/

QUANTIFY (Quantifying the Climate Impact of Global and European Transport Systems) http://www.pa.op.dlr.de/quantify/

Appendix II. Very recent literature on aviation and climate

New literature is appearing all the time on this subject. The following list of papers – which is not intended to be exhaustive – comprises a selection of those that are relevant to this subject but appeared in the time between submission of this paper and its review and acceptance. These could not be incorporated into the paper but they are pointed out here, for completeness.

Burkhardt, U., Kärcher, B., 2009. Process-based simulation of contrail cirrus in a global climate model. J. Geophys. Res. (submitted).

Febvre G., Gayet, J.-F., Minikin, A., Schlager, H., Shcherbakov, V., Jourdan, O., Busen, R., Fiebig, M., Kärcher, B., Schumann, U., 2009. On optical and microphysical characteristics of contrails and cirrus. J. Geophys. Res. 114, D02204, doi: 10.1029/2008JD010184.

Gierens K., Kärcher, B., Mannstein, H., Meyer, B. 2009. Aerodynamic contrails: phenomenology and flow physics. J. Atmos. Sci. 66, 217–226.

Kärcher, B., Burkhardt, U., Unterstrasser, S., Minnis, P., 2009. Factors controlling contrail cirrus optical depth. Atmos. Phys. Chem. Dis.

Kärcher, B., Mayer, B., Gierens, K., Burkhardt, U., Mannstein, H., 2009. Aerodynamic contrails: microphysical and optical properties. J. Atmos. Sci. 66, 227–243.

Kärcher, B., Yu, F., 2009. Role of aircraft soot emissions in contrail formation. Geophys. Res. Lett. 36, L01804, doi: 10.1029/2008GL036649.

Liu, X., Penner, J.E., Wang, M., 2009. Influence of anthropogenic sulphate and black carbon on upper tropospheric clouds in the NCAR CAM3 model coupled to the IMPACT global aerosol model. J. Geophys. Res. 114, D03204, doi: 10.1029/2008JD010492.

Wang, M., Penner, J. E., Liu, X., 2009. Coupled IMPACT aerosol and NCAR CAM3 model: evaluation of predicted aerosol number and size distribution. J. Geophys. Res. 114, D06302, doi: 10.1029/2008JD010459.

References

ACARE, 2001. European Aeronautics: a Vision for 2020. Meeting Society's Needs and Winning Global Leadership. Report of the group of personalities. http://www.acare4europe.org/docs/Vision%202020.pdf (accessed 30.05.09).

Anderson, B.E., Chen, G., Blake, D.R., 2006. Hydrocarbon emissions from a modern commercial airliner. Atmos. Environ. 40, 3601–3612.

Anonymous, 2007. National Plan for Aeronautics Research and Devlopment and Related Infrastructure. Aeronautics Science and Technology Subcommittee, Committee on Technology, National Science and Technology Council, US. http://www.ostp.gov/aeroplans/pdf/aero_rd_plan_final_21_dec_2007.pdf (accessed 30.05.09).

Appleman, H., 1953. The formation of exhaust contrails by jet aircraft. Bull. Amer. Meteor. Soc. 34, 14–20.

Archuleta, C.M., DeMott, P.J., Kreidenweis, S.M., 2005. Ice nucleation by surrogates for atmospheric mineral dust and mineral dust/sulfate particles at cirrus temperatures. Atmos. Chem. Phys. 5, 2617–2634.

Arnold, F., Scheid, J., Stilp, Th., Schlager, H., Reinhardt, M.E., 1992. Measurements of jet aircraft emissions at cruise altitude. 1. The odd-nitrogen gases NO, NO_2, HNO_2 and HNO_3. Geophys. Res. Lett. 12 (24), 2421–2424.

Arnold, F., Wohlfrom, K.-H., Klemm, M.W., Schneider, J., Gollinger, K., Schumann, U., Busen, R., 1998. First gaseous ion composition measurements in the exhaust plume of a jet aircraft in flight: implications for gaseous sulfuric acid, aerosols, and chemiions. Geophys. Res. Lett. 25 (12), 2137–2140.

Arnold, F., Kiendler, A., Wiedemer, V., Aberle, S., Stilp, T., 2000. Chemiion concentration measurements in jet engine exhaust at the ground: implications for ion chemistry and aerosol formation in the wake of a jet aircraft. Geophys. Res. Lett. 27 (12), 1723–1726.

Atlas, D., Wang, Z., Duda, D.P., 2006. Contrails to cirrus—morphology, microphysics, and radiative properties. J. Appl. Meteor. Climatol. 45, 5–19.

Bae, J.H., Avedisian, C.T., 2004. Effect of TPGME blending on soot emissions from JP8 fuel droplets burning with spherical symmetry. In: AIAA 2004-5680, 2nd International Energy Conversion Engineering Conference, Providence, Rhode Island, Aug. 16–19, 2004.

Bais, A.F., Lubin, D., Arola, A., Bernhard, G., Blumthaler, M., Chubarova, N., Erlick, C., Gies, H.P., Krotkov, N., Lantz, K., Mayer, B., McKenzie, R.L., Piacentini, R.D., Seckmeyer, G., Slusser, J.R., Zerefos, C.S., 2007. Surface Ultraviolet Radiation: Past, Present, and Future. Chapter 7 in Scientific Assessment of Ozone Depletion: 2006, Global Ozone Research and Monitoring Project–Report No. 47. World Meteorological Organization, Geneva, Switzerland.

Bakan, S., Betancor, M., Gayler, V., Graßl, H., 1994. Contrail frequency over Europe from NOAA-satellite images. Ann. Geophysicae 12, 962–968.

Baughcum, S.L., Henderson, S.C., Hertel, P.S., Maggiora, D.R., Oncina, C.A., 1994. Stratospheric Emissions Effects Database Development. NASA-CR-4592. NASA, Langley Research Center, Hampton, VA, USA, pp. 1–156.

Baughcum, S.L., Henderson, S.C., 1995. Aircraft Emission Inventories Projected in Year 2015 for a High Speed Civil Transport (HSCT) Universal Airline Network. NASA, Langley Research Center, Hampton, VA, USA. NASA-CR-4659pp. 1–117.

Baughcum, S.L., Henderson, S.C., Tritz, T.G., Pickett, D.C., 1996. Schedules Civil Aircraft Emission Inventories for 1992: Database Development and Analysis. NASA-CR-4700. NASA, Langley Research Center, Hampton, VA, USA.

Baughcum, S.L., Henderson, S.C., 1998. Aircraft Emission Scenarios Projected in Year 2015 for the NASA Technology Concept Aircraft (TCA) High Speed Civil Transport Universal Airline Network. NASA-CR-1998–207635. NASA, Langley Research Center, Hampton, VA, USA, pp. 1–42.

Baughcum, S.L., Sutkus Jr., D.J., Henderson, S.C., 1998. Year 2015 Aircraft Emission Scenario for Scheduled Air Traffic. NASA-CR-1998-207638. NASA, Langley Research Center, Hampton, VA, USA, pp. 1–44.

Baughcum, S.L., Plumb, I.C., Vohralik, P.F., 2003. Stratospheric ozone sensitivity to aircraft cruise altitudes and NO_x emissions. In: Sausen, R., Fichter, C., Amanatidis, G. (Eds.), European Conference on Aviation, Atmosphere and Climate (AAC), Proceedings of an International Conference, Friedrichshafen, Germany, 30 June–3rd July 2003. European Commission, pp. 145–150. Air Pollution Research Report 83.

Bekki, S., 1997. On the possible role of aircraft-generated soot in the middlelatitude ozone depletion. J. Geophys. Res. 102, 10751–10758.

Berghof, R., Schmitt, A., Eyers, C., Haag, K., Middel, J., Hepting, M., Grübler, A., Hancox, R., 2005. CONSAVE 2050 Final Technical Report. DLR, Köln, Germany.

Berntsen, T.K., Gauss, M., Isaksen, I.S.A., Grewe, V., Sausen, R., Pitari, G., Mancini, E., Meijer, E., Hauglustaine, D., 2003. Sources of NO_x at cruise altitudes: implications for predictions of ozone and methane perturbations due to NO_x from aircraft. In: Sausen, R., Fichter, C., Amanatidis, G. (Eds.), European Conference on Aviation, Atmosphere and Climate (AAC), Proceedings of an International Conference, Friedrichshafen, Germany, 30 June–3rd July 2003. European Commission, pp. 190–196. Air Pollution Research Report 83.

Bernsten, T., Fuglestvedt, J., Myhre, G., Stordal, F., Berglen, T.F., 2006. Abatement of greenhouse gases: does location matter? Climatic Change 74, 377–411. doi:10.1007/s10584-006-0433-4.

Blitz, M.A., Hughes, K.J., Pilling, M.J., 2003. Determination of the high-pressure limiting rate coefficient and the enthalpy of reaction for OH + SO_2. J. Phys. Chem. A 107 (12), 1971–1978. doi:10.1021/jp026524y.

Böckle, S., Einecke, S., Hildenbrand, F., Orlemann, C., Schulz, C., Wolfrum, J., Sick, V., 1999. Laser-spectropscopic investigation of OH-radical concentrations in the exhaust plane of jet engines. Geophys. Res. Lett. 26 (13), 1849–1852.

Boer, G.J., Yu, B., 2003a. Climate sensitivity and response. Clim. Dynam. 20, 415–429. doi:10.1007/s00382-002-0283-3.

Boer, G.J., Yu, B., 2003b. Climate sensitivity and climate state. Clim. Dynam. 21, 167–176. doi:10.1007/s00382-003-0323-7.

Boersma, K.F., Eskes, H.J., Meijer, E.W., Kelder, H.M., 2005. Estimates of lightning NO_x production from GOME satellite observations. Atmos. Chem. Phys. 5, 2311–2331.

Bond, T.C., Covert, D.S., Kramlich, J.C., Larson, T.V., Charlson, R.J., 2002. Primary particle emissions from residential coal burning: optical properties and size distributions. J. Geophys. Res. 107 (D21), 8347. doi:10.1029/2001JD000571.

Boucher, O., 1999. Air traffic may increase cirrus cloudiness. Nature 397, 30–31.

Brasseur, G.P., Müller, J.-F., Granier, C., 1996. Atmospheric impact pf NO_x emissions by subsonic aircraft: a three-dimensional model study. J. Geophys. Res. 101 (D1), 1423–1428.

Brasseur, G.P., Cox, R.A., Hauglustaine, D., Isaksen, I., Lelieveld, J., Lister, D.H., Sausen, R., Schumann, U., Wahner, A., Wiesen, P., 1998. European scientific assessment of the atmospheric effects of aircraft emissions. Atmos. Environ. 32 (13), 2329–2418.

Brock, C.A., Schröder, F., Kärcher, B., Petzold, A., Busen, R., Fiebig, M., 2000. Ultrafine particle size distributions measured in aircraft exhaust plumes. J. Geophys. Res. 105 (D21), 26555–26567.

Brown, R.C., Anderson, M.R., Miake-Lye, R.C., Kolb, C.E., Sorokin, A.A., Buriko, Y.Y., 1996. Aircraft exhaust sulfur emissions. Geophys. Res. Lett. 23 (24), 3603–3606.

Brühl, C., Pöschl, U., Crutzen, P.J., Steil, B., 2000. Acetone and PAN in the upper troposphere: impact on ozone production from aircraft emissions. Atmos. Environ. 34, 3931–3938.

Brundish, K.D., Clague, A.R., Wilson, C.W., Miake-Lye, R.C., Brown, R.C., Wormhoudt, J., Lukachko, S.P., Chobot, A.T., Yam, C.K., Waitz, I.A., Hagen, D.E., Schmid, O., Whitefield, P.D., 2007. Evolution of carbonaceous aerosol and aerosol precursor emissions through a jet engine. J. Propul. Power 23 (5), 959–970. doi:10.2514/1.27502.

Brunner, D., Staehelin, J., Jeker, D., 1998. Large-scale nitrogen oxide plumes in the tropopause region and implications for ozone. Science 282, 1305–1309. doi:10.1126/science.282.5392.1305.

Brunner, D., Staehelin, J., Rogers, H.L., Köhler, M.O., Pyle, J.A., Hauglustaine, D., Jourdain, L., Berntsen, T.K., Gauss, M., Isaksen, I.S.A., Meijer, E., van Velthoven, P., Pitari, G., Mancini, E., Grewe, V., Sausen, R., 2003. An evaluation of the performance of chemistry transport models by comparison with research aircraft observations. Part 1: concepts and overall model performance. Atmos. Chem. Phys. 3, 1609–1631.

Brunner, D., Staehelin, J., Rogers, H.L., Köhler, M.O., Pyle, J.A., Hauglustaine, D.A., Jourdain, L., Berntsen, T.K., Gauss, M., Isaksen, I.S.A., Meijer, E., van Velthoven, P., Pitari, G., Mancini, E., Grewe, V., Sausen, R., 2005. An evaluation of the performance of chemistry transport models – part 2: detailed comparison with two selected campaigns. Atmos. Chem. Phys. 5, 107–129.

Busen, R., Schumann, U., 1995. Visible contrail formation from fuels with different sulfur contents. Geophys. Res. Lett. 22 (11), 1357–1360.

Cess, R.D., Potter, G.L., Blanchet, J.P., Boer, G.J., Del Genio, A.D., Déqué, M., Dymnikov, V., Galin, V., Gates, W.L., Ghan, S.J., Kiehl, J.T., Lacis, A.A., Le Treut, H., Li, Z.-X., Liang, X.-Z., McAvaney, B.J., Meleshko, V.P., Mitchell, J.F.B., Morcrette, J.-J., Randall, D.A., Rikus, L., Roeckner, E., Royer, J.F., Schlese, U., Sheinin, D.A., Slingo, A., Sokolov, A.P., Taylor, K.E., Washington, W.M., Wetherald, R.T., Yagai, I., Zhang, M.-H., 1990. Intercomparison and interpretation of climate feedback processes in 19 atmospheric general circulation models. J. Geophys. Res. 95 (D10), 16601–16615.

Cess, R.D., Zhang, M.H., Zhou, Y., Jing, X., Dvortsov, V., 1996. Absorption of solar radiation by clouds: interpretations of satellite, surface, and aircraft measurements. J. Geophys. Res. 101 (D18), 23299–23309.

Chen, J.-P., 1999. Particle nucleation by recondensation in combustion exhausts. Geophys. Res. Lett. 26 (15), 2403–2406.

Chen, Y., Kreidenweis, S.M., McInnes, L.M., Rogers, D.C., DeMott, P.J., 1998. Single particles analyses of ice nucleating aerosols in the upper troposphere and lower stratosphere. Geophys. Res. Lett. 25 (9), 1391–1394.

Chowdhury, Z., Hughes, L.S., Salmon, L.G., Cass, G.R., 2001. Atmospheric particle size and composition measurements to support light extinction calculations over the Indian Ocean. J. Geophys. Res. 106 (D22), 28597–28605.

Chughtai, A.R., Williams, G.R., Atteya, M.M.O., Miller, N.J., Smith, D.M., 1999. Carbonaceous particle hydration. Atmos. Environ. 33, 2679–2687.

Clarke, A.D., Kapustin, V.N., 2002. A Pacific aerosol survey. Part I: A decade of data on particle production, transport, evolution, and mixing in the troposphere. J. Atmos. Sci. 59, 363–382.

Crutzen, P.J., Mosier, A.R., Smith, K.A., Winiwarter, W., 2008. N_2O release from agro-biofuel production negates global warming reduction by replacing fossil fuels. Atmos. Chem. Phys. 8, 389–395.

Curtius, J., Sierau, B., Arnold, F., Baumann, R., Busen, R., Schulte, P., Schumann, U., 1998. First direct sulfuric acid detection in the exhaust plume of a jet aircraft in flight. Geophys. Res. Lett. 25 (6), 923–926.

Curtius, J., Arnold, F., Schulte, P., 2002. Sulfuric acid measurements in the exhaust plume of a jet aircraft in flight: implications for the sulphuric acid formation efficiency. Geophys. Res. Lett. 29 (7), 1113. doi:10.1029/2001GL013813.

Cziczo, D.J., Murphy, D.M., Hudson, P.K., Thomson, D.S., 2004. Single particle measurements of the chemical composition of cirrus ice residue during CRYSTAL-FACE. J. Geophys. Res. 109, D04201. doi:10.1029/2003JD004032.

Daggett, D., Hadaller, O., Hendricks, R., Walther, R., 2006. Alternative Fuels and their Potential Impact on Aviation NASA/TM-2006–214365, October 2006.

Daggett, D., Hendricks, R.C., Walther, R., Corporan, E., 2008. Alternate Fuels for Use in Commercial Aircraft NASA/TM-2008–214833, ISABE–2007–1196.

Dakhel, P.M., Lukachko, S.P., Waitz, I.A., Miake-Lye, R.C., Brown, R.C., 2005. Post-combustion evolution of soot properties in an aircraft engine. In: Proceedings of GT2005 ASME Turbo Expo 2005: Power for Land, Sea and Air 1, pp. 1–9.

Dakhel, P.M., Lukachko, S.P., Waitz, I.A., Miake-Lye, R.C., Brown, R.C., 2007. Post-combustion evolution of soot properties in an aircraft engine. J. Propul. Power 23 (5), 942–948. doi:10.2514/1.26738.

Danilin, M.Y., Fahey, D.W., Schumann, U., Prather, M.J., Penner, J.E., Ko, M.K.W., Weisenstein, D.K., Jackman, C.H., Pitari, G., Köhler, I., Sausen, R., Weaver, C.J., Douglass, A.R., Connell, P.S., Kinnison, D.E., Dentener, F.J., Fleming, E.L., Berntsen, T.K., Isaksen, I.S.A., Haywood, J.M., Kärcher, B., 1998. Aviation fuel tracer simulation: model intercomparison and implications. Geophys. Res. Lett. 25 (21), 3947–3950.

Deidewig, F., Döppelheuer, A., Lecht, M., 1996. Methods to assess aircraft engine emissions in flight. In: Proceedings of the 20th International Council of the Aeronautical Sciences, Sorrento, Italy, 8–13 September, 1996.

Delhaye, D., Ruiz, E., Ferry, D., Demirdjian, B., Suzanne, J., Penanhoat, O., Gouge, J., 2007. Physico-chemical characterization of soot emitted by a commercial aircraft engine: morphology, size, structure, and elemental composition. In: Sausen, R., Blum, A., Lee, D.S., Brüning, C. (Eds.), Proceedings of an International Conference on Transport, Atmosphere and Climate (TAC). Office for Official Publications of the European Communities, Luxembourg, ISBN 92-79-04583-0, pp. 22–26.

Demirdjian, B., Ferry, D., Suzanne, J., Popovicheva, O.B., Persiantseva, N.M., Shonija, N.K., 2007. Heterogeneities in the microstructure and composition of aircraft engine combustor soot: impact on the water uptake. J. Atmos. Chem. 56, 83–103. doi:10.1007/s10874-006-9043-9.

DeMore, W.B., Sander, S.P., Golden, D.M., Hampson, R.F., Kurylo, M.J., Howard, C.J., Ravishankara, A.R., Kolb, C.E., Molina, M.J., 1997. Chemical Kinetics and Photochemical Data for Use in Stratospheric Modeling, Evaluation Number 12. JPL Publication, pp. 97–104.

DeMott, P.J., 1990. An exploratory study of ice nucleation by soot aerosols. J. Appl. Meteor. 29, 1072–1079.

DeMott, P.J., Meyers, M.P., Cotton, W.R., 1994. Parameterization and impact of ice initiation processes relevant to numerical model simulations of cirrus clouds. J. Atmos. Sci. 51, 77–90.

DeMott, P.J., Rogers, D.C., Kreidenweis, S.M., 1997. The susceptibility of ice formation in upper tropospheric clouds to insoluble aerosol components. J. Geophys. Res. 102 (D16), 19575–19584.

DeMott, P.J., Chen, Y., Kreidenweis, S.M., Roger, D.C., Shermann, D.E., 1999. Ice formation by black carbon particles. Geophys. Res. Lett. 26 (16), 2429–2432.

DeMott, P.J., Sassen, K., Poellot, M.R., Baumgardner, D., Rogers, D.C., Brooks, S.D., Prenni, A.J., Kreidenweis, S.M., 2003a. African dust aerosols as atmospheric ice nuclei. Geophys. Res. Lett. 30 (14), 1732. doi:10.1029/2003GL017410.

DeMott, P.J., Cziczo, D.J., Prenni, A.J., Murphy, D.M., Kreidenweis, S.M., Thomson, D.S., Borys, R., Rogers, D.C., 2003b. Measurements of the concentration and composition of nuclei for cirrus formation. Proc. Nat. Acad. Sci. 100 (25), 14655–14660.

DeMott, P.J., 2007. In: Presentation at the 17th International Conference on Nucleation and Atmospheric Aerosols, Galway Ireland, August 2007.

Derwent, R., Friedl, R., Karil, I.I., Kelder, H., Kirchoff, V.W.J.H., Ogawa, T., Rossi, M.J., Wennberg, P., 1999. Impacts of aircraft emissions on atmospheric ozone. Chapter 2 of 'Aviation and the Global Atmosphere'. In: Penner, J.E., Lister, D.H., Griggs, D.J., Dokken, D.J., McFarland, M. (Eds.), Special Report of the Intergovernmental Panel on Climate Change. Cambridge University Press, Cambridge.

Derwent, R.G., Collins, W.J., Johnson, C.E., Stevenson, D.S., 2001. Transient behaviour of tropospheric ozone precursors in a global 3-D CTM and their indirect greenhouse effects. Climatic Change 49, 463–487.

Dessens, O., Rogers, H.L., Pyle, J.A., 2007. A change in the calculated impact of supersonic aircraft NO_x emissions on the atmosphere. Aeronaut. J. 111 (1119), 311–314.

DuBois, D., Paynter, G.C., 2006. Fuel flow method for estimating aircraft emissions. In: Non-Conference Specific Technical Papers – 2006, December 2006.

Eiff, G., Putz, S., Moses, C., 1992. Combustion properties of ethanol blended turbine fuels. In: Proceedings of 2nd Annual FAA/AIAA Symposium on General Aviation Systems, Wichita, KS, USA, March 1992.

Eleftheratos, K., Zerefos, C.S., Zanis, P., Balis, D.S., Tselioudis, G., Gierens, K., Sausen, R., 2007. A study on natural and manmade global interannual fluctuations of cirrus cloud cover for the period 1984–2004. Atmos. Chem. Phys. 7, 2631–2642.

Elzen, M.den, Fuglestvedt, J., Höhne, N., Trudinger, C., Lowe, J., Matthews, B., Romstad, B., de Campos, C.P., Andronova, N., 2005. Analysing countries' contribution to climate change: scientific and policy-related choices. Environ. Sci. Pol. 8, 614–636.

Evan, A.T., Heidinger, A.K., Vimont, D.J., 2007. Arguments against a physical long-term trend in global ISSCP cloud amounts. Geophys. Res. Lett. 34, L04701. doi:10.1029/2006GL028083.

Eyers, C.J., Addleton, D., Atkinson, K., Broomhead, M.J., Christou, R., Elliff, T., Falk, R., Gee, I., Lee, D.S., Marizy, C., Michot, S., Middel, J., Newton, P., Norman, P., Plohr, M., Raper, D., Stanciou, N., 2005. AERO2k Global Aviation Emissions Inventories for 2002 and 2025 QINETIQ/04/01113, Farnborough, Hants, UK.

Eyring, V., Butchart, N., Waugh, D.W., Akiyoshi, H., Austin, J., Bekki, S., Bodeker, G.E., Boville, B.A., Brühl, C., Chipperfield, M.P., Cordero, E., Dameris, M., Deushi, M., Fioletov, V.E., Frith, S.M., Garcia, R.R., Gettelman, A., Giorgetta, M.A., Grewe, V., Jourdain, L., Kinnison, D.E., Mancini, E., Manzini, E., Marchand, M., Marsh, D.R., Nagashima, T., Newman, P.A., Nielsen, J.E., Pawson, S., Pitari, G., Plummer, D.A., Rozanov, E., Schraner, M., Shepherd, T.G., Shibata, K., Stolarski, R.S., Struthers, H., Tian, W., Yoshiki, M., 2006. Assessment of temperature, trace species and ozone in chemistry–climate model simulations of the recent past. J. Geophys. Res. 111, D22308. doi:10.1029/2006JD007327.

Eyring, V., Isaksen, I.S.A., Berntsen, T., Collins, W.J., Corbett, J.J., Endresen, O., Grainger, R.G., Moldanova, J., Schlager, H., Stevenson, D.S., 2009. Transport impacts on atmosphere and climate: shipping. Atmos. Environ. doi:10.1016/j.atmosenv.2009.04.059.

Fahey, D.W., Keim, E.R., Woodbridge, E.L., Gao, R.S., Boering, K.A., Daube, B.C., Wofsy, S.C., Lohmann, R.P., Hintsa, E.J., Dessler, A.E., Webster, C.R., May, R.D., Brock, C.A., Wilson, J.C., Miake-Lye, R.C., Brown, R.C., Rodriguez, J.M., Loewenstein, M., Proffitt, M.H., Stimpfle, R.M., Bowen, S.W., Chan, K.R., 1995. In situ observations in aircraft exhaust plumes in the lower stratosphere at midlatitudes. J. Geophys. Res. 100 (D2), 3065–3074.

Fahey, D.W., Schumann, U., Ackerman, S., Artaxo, P., Boucher, O., Danilin, M.Y., Kärcher, B., Minnis, P., Nakajima, T., Toon, O.B., 1999. Aviation-produced aerosols and cloudiness. Chapter 3 of 'Aviation and the global atmosphere'. In: Penner, J.E., Lister, D.H., Griggs, D.J., Dokken, D.J., McFarland, M. (Eds.), Special Report of the Intergovernmental Panel on Climate Change. Cambridge University Press, Cambridge.

Fargione, J., Hill, J., Tilman, D., Polasky, S., Hawthorne, P., 2008. Land clearing and the biofuel carbon debt. Science 319, 1235–1238. doi:10.1126/science.1152747.

Fichter, C., Marquart, S., Sausen, R., Lee, D.S., 2005. The impact of cruise altitude on contrails and related radiative forcing. Meteorol. Z. 14 (4), 563–572.

Field, P.R., Möhler, O., Connolly, P., Krämer, M., Cotton, R., Heymsfield, A.J., Saathoff, H., Schnaiter, M., 2006. Some ice nucleation characteristics of Asian and Saharan desert dust. Atmos. Chem. Phys. 6, 2991–3006.

Forster, C., Stohl, A., James, P., Thouret, V., 2003. The residence times of aircraft emissions in the stratosphere using a mean emission inventory and emissions along actual flight tracks. J. Geophys. Res. 108 (D12), 8524. doi:10.1029/2002JD002515.

Forster, P.M.d.F., Shine, K.P., 1997. Radiative forcing and temperature trends from stratospheric ozone changes. J. Geophys. Res. 102 (D9), 10841–10855.
Forster, P.M., Blackburn, M., Glover, R., Shine, K.P., 2000. An examination of climate sensitivity for idealised climate change experiments in an intermediate general circulation model. Clim. Dyn. 16, 833–849.
Forster, P.M.d.F., Ponater, M., Zhong, W.-Y., 2001. Testing broadband radiation schemes for their ability to calculate the radiative forcing and temperature response to stratospheric water vapour and ozone changes. Meteorol. Z. 10 (5), 387–393.
Forster, P.M.d.F., Shine, K.P., Stuber, N., 2006. It is premature to include non-CO_2 effects of aviation in emission trading schemes. Atmos. Environ. 40, 1117–1121.
Forster, P., Ramaswamy, V., Artaxo, P., Berntsen, T., Betts, R., Fahey, D.W., Haywood, J., Lean, J., Lowe, D.C., Myhre, G., Nganga, J., Prinn, R., Raga, G., Schulz, M., Van Dorland, R., 2007a. Changes in atmospheric constituents and in radiative forcing. In: Solomon, S., Qin, D., Manning, M., Chen, Z., Marquis, M., Averyt, K.B., Tignor, M., Miller, H.L. (Eds.), Climate Change 2007: the Physical Science Basis. Cambridge University Press, Cambridge, United Kingdom and New York, NY, USA Contribution of Working Group I to the Fourth Assessment Report of the Intergovernmental Panel on Climate Change.
Forster, P.M.d.F., Shine, K.P., Stuber, N., 2007b. Corrigendum to "It is premature to include non-CO_2 effects of aviation in emission trading schemes. Atmos. Environ. 40, pp. 1117–1121". Atmos. Environ. 41, 3941.
Frenzel, A., Arnold, F., 1994. Sulfuric acid cluster ion formation by jet engines: implications for sulfuric acid formation and nucleation. In: Proceedings of the International Scientific Coll. On Impact of Emissions from Aircraft and Spacecraft upon the Atmosphere, Köln 1994, DLR-Mitt 94–06, pp. 106–112.
Friedl, R.R. (Ed.), 1997. Atmospheric Effects of Subsonic Aircraft: Interim Assessment Report of the Advanced Subsonic Technology Program. NASA Reference Publication 1400, National Aeronautics and Space Administration, Goddard Space Flight Center, Greenbelt, MD, USA, 168 pp.
Friedlingstein, P., Solomon, S., 2005. Contributions of past and present human generations to committed warming caused by carbon dioxide. Proc. Nat. Acad. Sci. 102 (31), 10832–10836.
Fuglestvedt, J.S., Bernsten, T.K., Isaksen, I.S.A., Mao, H., Liang, X.-Z., Wang, W.-C., 1999. Climatic forcing of nitrogen oxides through changes in tropospheric ozone and methane; global 3D model studies. Atmos. Environ. 33, 961–977.
Fuglestvedt, J.S., Berntsen, T.K., Godal, O., Sausen, R., Shine, K.P., Skodvin, T., 2003. Metrics of climate change: assessing radiative forcing and emission indices. Climatic Change 58, 267–331.
Fuglestvedt, J., Berntsen, T., Myhre, G., Rypdal, K., Bieltvedt Skeie, R., 2008. Climate forcing from the transport sectors. Proc. Nat. Acad. Sci. 105, 454–458.
Fuglestvedt, J.S., Shine, K.P., Berntsen, T., Cook, J., Lee, D.S., Stenke, A., Skeie, R.B., Velders, G.J.M., Waitz, I.A., 2009. Transport Impacts on Atmosphere and Climate: Metrics. doi:10.1016/j.atmosenv.2009.04.044.
Gallagher, M.W., Connolly, P.J., Whiteway, J., Figueras-Nieto, D., Flynn, M., Choularton, T.W., Bower, K.N., Cook, C., Busen, R., Hacker, J., 2005. An overview of the microphysical structure of cirrus clouds observed during EMERALD-1. Quart. J. Roy. Meteorol. Soc. 131, 1143–1169.
Gallagher, E., 2008. The Gallagher Review of the Indirect Effects of Biofuels Production. Renewable Fuels Agency, Ashdown House, East Sussex, UK.
Garcia-Naranjo, A., Wilson, C.W., 2005. Primary NO_2 from Aircraft Engines Operating over the LTO Cycle. Report RC110187/05/01. Department of Mechanical Engineering, University of Sheffield, Sheffield, UK.
Gardner, R.M., Adams, J.K., Cook, T., Larson, L.G., Falk, R.S., Fleuit, E., Förtsch, W., Lecht, M., Lee, D.S., Leech, M.V., Lister, D.H., Massé, B., Morris, K., Newton, P.J., Owen, A., Parker, E., Schmitt, A., Have, H.T., Vandenberghe, C., 1998. ANCAT/EC2 aircraft emissions inventories for 1991/1992 and 2015: final report. In: Produced by the ECAC/ANCAT and EC Working Group, European Civil Aviation Conference.
Gauss, M., Isaksen, I.S.A., Lee, D.S., Søvde, O.A., 2006. Impact of aircraft NO_x emissions on the atmosphere – tradeoffs to reduce the impact. Atmos. Chem. Phys. 6, 1529–1548.
Gayet, J.-F., Ovarlez, J., Shcherbakov, V., Ström, J., Schumann, U., Minikin, A., Auriol, F., Petzold, A., Monier, M., 2004. Cirrus cloud microphysical and optical properties at southern and northern midlatitudes during the INCA experiment. J. Geophys. Res. 109, D20206. doi:10.1029/2004JD004803.
Gayet, J.-F., Shcherbakov, V., Mannstein, H., Minikin, A., Schumann, U., Ström, J., Petzold, A., Ovarlez, J., Immler, F., 2006. Microphysical and optical properties of midlatitude cirrus clouds observed in the southern hemisphere during INCA. Quart. J. Roy. Meteorol. Soc. 132 (621), 2719–2748.
GbD, 2005. Air Travel – Greener by Design. The Technology Challenge. http://www.greenerbydesign.org.uk/_FILES/publications/GbD%20-%202003%20The%20Tech%20Challenge.pdf Report of the technology sub-group (accessed 30.05.09).
Gettleman, A., Fetzer, E.J., Eldering, A., Irion, F.W., 2006. The global distribution of supersaturation in the upper troposphere from the atmospheric infrared sounder. J. Clim. 19, 6089–6103.
Gierens, K., Sausen, R., Schumann, U., 1999a. A diagnostic study of the global distribution of contrails part II. Future air traffic scenarios. Theor. Appl. Climatol. 63, 1–9.
Gierens, K., Schumann, U., Helten, M., Smit, H., Marenco, A., 1999b. A distribution law for relative humidity in the upper troposphere and lower stratosphere derived from three years of MOZAIC measurements. Ann. Geophysicae 17, 1218–1226.
Gierens, K., 2007a. Are fuel additives a viable contrail mitigation option? Atmos. Environ. 41, 4548–4552.
Gierens, K., 2007b. Contrails, contrail cirrus, and ship tracks. In: Sausen, R., Blum, A., Lee, D.S., Brüning, C. (Eds.), Proceedings of an International Conference on Transport, Atmosphere and Climate (TAC). Office for Official Publications of the European Communities, Luxembourg, ISBN 92-79-04583-0, pp. 214–220.
Gierens, K., Lim, L., Eleftheratos, K., 2008. A review of various strategies for contrail avoidance. Open. Atmos. Sci. J. 2, 1–7.
Gleitsmann, G., Zellner, R., 1999. The aerosol dynamics of H_2O–H_2SO_4–HNO_3 mixtures in aircraft wakes. A modeling study. Phys. Chem. Chem. Phys. 1, 5503–5509.
Gorbunov, B., Baklanov, A., Kakutkina, N., Windsor, H.L., Toumi, R., 2001. Ice nucleation on soot particles. Aerosol Sci. 32, 199–215.
Gounou, A., Hogan, R.J., 2007. A sensitivity study of the effect of horizontal photon transport on the radiative forcing of contrails. J. Atmos. Sci. 64, 1706–1716.
Green, J.E., 2003. Civil aviation and the environmental challenge. Aeronaut. J. 107 (1072), 281–299.
Grewe, V., Dameris, M., Hein, R., Köhler, I., Sausen, R., 1999. Impact of future subsonic aircraft NO_x emissions on the atmospheric composition. Geophys. Res. Lett. 26 (1), 47–50.
Grewe, V., Brunner, D., Dameris, M., Grenfell, J.L., Hein, R., Shindell, D., Staehelin, J., 2001. Origin and variability of upper tropospheric nitrogen oxides and ozone at northern mid-latitudes. Atmos. Environ. 35, 3421–3433.
Grewe, V., Dameris, M., Fichter, C., Sausen, R., 2002a. Impact of aircraft NO_x emissions. Part 1: interactively coupled climate-chemistry simulations and sensitivities to climate-chemistry feedback, lightning and model resolution. Meteorol. Z. 11 (3), 177–186.
Grewe, V., Dameris, M., Fichter, C., Lee, D.S., 2002b. Impact of aircraft NO_x emissions. Part 2: effects of lowering the flight altitude. Meteorol. Z. 11 (3), 197–205.
Grewe, V., Shindell, D.T., Eyring, V., 2004. The impact of horizontal transport on the chemical composition in the tropopause region: lightning NO_x and streamers. Adv. Space Res. 33, 1058–1061.
Grewe, V., 2007. Impact of climate variability on tropospheric ozone. Sci. Total. Environ. 374, 167–181.
Grewe, V., Stenke, A., Ponater, M., Sausen, R., Pitari, G., Iachetti, D., Rogers, H., Dessens, O., Pyle, J., Isaksen, I.S.A., Gulstad, L., Søvde, O.A., Marizy, C., Pascuillo, E., 2007. Climate impact of supersonic air traffic: an approach to optimize a potential future supersonic fleet – results from the EU-project SCENIC. Atmos. Chem. Phys. 7, 5129–5145.
Grewe, V., Stenke, A., 2008. AirClim: an efficient tool for climate evaluation of aircraft technology. Atmos. Chem. Phys. 8, 4621–4639.
Grooss, J.-U., Brühl, C., Peter, T., 1998. Impact of aircraft emissions on tropospheric and stratospheric ozone. Part I: chemistry and 2-D model results. Atmos. Environ. 32, 3173–3184.
Gysel, M., Nyeki, S., Weingartner, E., Baltensperger, U., Giebl, H., Hitzenberger, R., Petzold, A., Wilson, C.W., 2003. Properties of jet engine combustion particles during the PartEmis experiment: hygroscopicity at subsaturated conditions. Geophys. Res. Lett. 30 (11), 1566. doi:10.1029/2003GL016896.
Haag, W., Kärcher, B., Ström, J., Minikin, A., Lohmann, U., Ovarlez, J., Stohl, A., 2003. Freezing thresholds and cirrus cloud formation mechanisms inferred from in situ measurements of relative humidity. Atmos. Chem. Phys. 3, 1791–1806.
Haag, W., Kärcher, B., 2004. The impact of aerosols and gravity waves on cirrus clouds at midlatitudes. J. Geophys. Res. 109, D12202. doi:10.1029/2004JD004579.
Haglind, F., 2008. Potential of lowering the contrail formation of aircraft exhausts by engine re-design. Aerosp. Sci. Technol. 12, 490–497.
Hanisco, T.F., Wennberg, P.O., Cohen, R.C., Anderson, J.G., Fahey, D.W., Keim, E.R., Gao, R.S., Wamsley, R.C., Donnelly, S.G., Del Negro, L.A., Salawitch, R.J., Kelly, K.K., Proffitt, M.H., 1997. The role HOx in super- and subsonic aircraft exhaust plumes. Geophys. Res. Lett. 24 (1), 65–68.
Hansen, J., Russell, G., Lacis, A., Fung, I., Rind, D., Stone, P., 1985. Climate response times: dependence on climate sensitivity and ocean mixing. Science 229, 857–859.
Hansen, J., Sato, M., Ruedy, R., 1997. Radiative forcing and climate response. J. Geophys. Res. 102 (D6), 6831–6864.
Hansen, J., Nazarenko, L., 2004. Soot climate forcing via snow and ice albedos. Proc. Nat. Acad. Sci. 101 (2), 423–428.
Hansen, J., Sato, M., Ruedy, R., Nazarenko, L., Lacis, A., Schmidt, G.A., Russell, G., Aleinov, I., Bauer, M., Bauer, S., Bell, N., Cairns, B., Canuto, V., Chandler, M., Cheng, Y., Del Genio, A., Faluvegi, G., Fleming, E., Friend, A., Hall, T., Jackman, C., Kelley, M., Kiang, N., Koch, D., Lean, J., Lerner, J., Lo, K., Menon, S., Miller, R., Minnis, P., Novakov, T., Oinas, V., Perlwitz, Ja., Perlwitz, Ju., Rind, D., Romanou, A., Shindell, D., Stone, P., Sun, S., Tausnev, N., Thresher, D., Wielicki, B., Wong, T., Yao, M., Zhang, S., 2005. Efficacy of climate forcings. J. Geophys. Res. 110, D18104. doi:10.1029/2005JD005776.
Hartmann, D.L., Ockert-Bell, M.E., Michelsen, M.L., 1992. The effect of cloud type on Earth's energy balance: global analysis. J. Clim. 5, 1281–1304.
Haverkamp, H., Wilhelm, S., Sorokin, A., Arnold, F., 2004. Positive and negative ion measurements in jet aircraft engine exhaust: concentrations, sizes and implications for aerosol formation. Atmos. Environ. 38, 2879–2884.
Hayman, G.D., Markiewicz, M., 1996. Chemical modeling of the aircraft exhaust plume. In: Schumann, U. (Ed.), Pollution from Aircraft Emissions in the North Atlantic Flight Corridor (POLINAT). European Commission, Brussels Air Pollution Research Report 58, report EUR 16978EN.
Hein, R., Dameris, M., Schnadt, C., Land, C., Grewe, V., Köhler, I., Ponater, M., Sausen, R., Steil, B., Landgraf, J., Brühl, C., 2001. Results of an interactively coupled atmospheric chemistry – general circulation model: comparison with observations. Ann. Geophysicae 19, 435–457.
Henderson, S.C., Wickrama, U.K., Baughcum, S.L., Begin, J.L., Franco, F., Greene, D.L., Lee, D.S., Mclaren, M.L., Mortlock, A.K., Newton, P.J., Schmitt, A., Sutkus, D.J.,

Vedantham, A., Wuebbles, D.J., 1999. Aircraft emissions: current inventories and future scenarios. Chapter 9 of 'Aviation and the Global Atmosphere'. In: Penner, J.E., Lister, D.H., Griggs, D.J., Dokken, D.J., McFarland, M. (Eds.), Special Report of the Intergovernmental Panel on Climate Change. Cambridge University Press, Cambridge.

Hendricks, J., Kärcher, B., Döpelheuer, A., Feichter, J., Lohmann, U., Baumgardner, D., 2004. Simulating the global atmospheric black carbon cycle: a revisit to the contribution of aircraft emissions. Atmos. Chem. Phys. 4, 2521–2541.

Hendricks, J., Kärcher, B., Lohmann, U., Ponater, M., 2005. Do aircraft black carbon emissions affect cirrus clouds on the global scale? Geophys. Res. Lett. 32, L12814. doi:10.1029/2005GL02274.

Herndon, S.C., Shorter, J.H., Zahniser, M.S., Nelson, D.D.J., Jayne, J., Brown, R.C., Miake-Lye, R.C., Waitz, I., Silva, P., Lanni, T., Demerjian, K., Kolb, C.E., 2004. NO and NO_2 emission ratios measured from in-use commercial aircraft during taxi and takeoff. Environ. Sci. Technol. 38, 6078–6084.

Herndon, S.C., Rogers, T., Dunlea, J.E., Jayne, J.T., Miake-Lye, R., Knighton, B., 2006. Hydrocarbon emissions from in-use commercial aircraft during airport operations. Environ. Sci. Technol. 40 (14), 4406–4413.

Heymsfield, A.J., Miloshevich, L.M., 1993. Homogeneous ice nucleation and supercooled liquid water in orographic wave clouds. J. Atmos. Sci. 50 (15), 2335–2353.

Heymsfield, A.J., McFarquhar, G.M., 1996. High albedos of cirrus in the tropical Pacific warm pool: microphysical interpretations from CEPEX and from Kwajalein, Marshall Islands. J. Atmos. Sci. 53 (17), 2424–2451.

Heymsfield, A.J., Lawson, R.P., Sachse, G.W., 1998. Growth of ice crystals in a precipitating contrail. Geophys. Res. Lett. 25 (9), 1335–1338.

Heymsfield, A.J., McFarquhar, G.M., 2002. Mid-latitude and tropical cirrus: microphysical properties. In: CirrusLynch, D.K., Sasson, K., Starr, D.O'C., Stephens, G. (Eds.). Oxford University Press, pp. 78–101.

Hidalgo, H., 1977. Study on the effects of atmospheric ozone of NO emissions from subsonic and supersonic aircraft using the Crutzen 2-D model. FAA-EQ-77-3. In: Oliver, R.C., Bauer, E., Hidalgo, H., Gardner, K.A., Wasylkiwskyj, W. (Eds.), Appendix A in 'Aircraft Emissions: Potential Effects on Ozone and Climate. A Review and Progress Report'. US Department of Transportation, Federal Aviation Administration, Washington DC, USA.

Hidalgo, H., Crutzen, P.J., 1977. The tropospheric and stratospheric composition perturbed by NO_x emissions of high-altitude aircraft. J. Geophys. Res. 82, 5833–5866.

Hindiyarti, L., Glarborg, P., Marshall, P., 2007. Reactions of SO_3 with the O/H radical pool under combustion conditions. J. Phys. Chem. A 111 (19), 3984–3991. doi:10.1021/jp067499p.

Hitzenberger, R., Giebl, H., Petzold, A., Gysel, M., Nyeki, S., Weingartner, E., Baltensperger, U., Wilson, C.W., 2003. Properties of jet engine combustion particles during the PartEmis experiment. Hygroscopic growth at supersaturated conditions. Geophys. Res. Lett. 30 (14), 1779. doi:10.1029/2003GL017294.

Hoor, P., Borken-Kleefeld, J., Caro, D., Dessens, O., Endresen, O., Gauss, M., Grewe, V., Hauglustaine, D., Isaksen, I.S.A., Jöckel, P., Lelieverld, J., Myhre, G., Meijer, E., Olivie, D., Prather, M., Schnadt Poberaj, C., Shine, K.P., Staehelin, J., Tang, Q., van Aardenne, J., van Velthoven, P., Sausen, R., 2009. The impact of traffic emissions on atmospheric ozone and OH: results from QUANTIFY. Atmos. Chem. Phys. 9, 3113–3136.

Hoyle, C.R., Luo, B.P., Peter, T., 2005. The origin of high ice crystal number densities in cirrus clouds. J. Atmos. Sci. 62, 2568–2579. doi:10.1175/JAS3487.1.

Hung, H.-M., Malinowski, A., Martin, S.T., 2003. Kinetics of heterogeneous ice nucleation on the surfaces of mineral dust cores inserted into aqueous ammonium sulfate particles. J. Phys. Chem. A 107 (9), 1296–1306. doi:10.1021/jp021593y.

Hunton, D.E., Ballenthin, J.O., Borghetti, J.F., Federico, G.S., Miller, T.M., Thorn, W.F., Viggiano, A.A., Anderson, B.E., Coffer III, W.R., McDougal, D.S., Wey, C.C., 2000. Chemical ionization mass spectrometric measurements of SO_2 emissions from jet engines in flight and test chamber operations. J. Geophys. Res. 105 (D22), 26841–26855.

IEA, 2007. Oil Information 2006, Table 9, 749 pp. International Energy Agency, Paris.

Inderwildi, O.R., King, D.A., 2009. Quo vadis biofuels? Energy & Environ. Sci. 2, 343–346. doi:10.1039/b822951c.

Intrieri, J.M., Stephens, G.L., Eberhard, W.L., Uttal, T., 1993. A method for determining cirrus cloud particle sizes using lidar and radar backscatter technique. J. Appl. Meteor 32, 1074–1082.

IPCC, 1999. Aviation and the global atmosphere. In: E Penner, J., Lister, D.H., Griggs, D.J., Griggs, D.J., Dokken, D.J., McFarland, M. (Eds.), Intergovernmental Panel on Climate Change. Cambridge University Press, Cambridge, UK.

IPCC, 2000. Emissions Scenarios. A Special Report of WG III of the Intergovernmental Panel on Climate Change. Cambridge University Press, UK.

IPCC, 2001. Climate change 2001: the scientific basis. In: Houghton, J.T., Ding, Y., Griggs, D.J., Noguer, M., van der Linden, P.J., Dai, X., Maskell, K., Johnson, C.A. (Eds.), Contribution of Working Group I to the Third Assessment Report of the Intergovernmental Panel on Climate Change. Cambridge University Press, UK.

IPCC, 2007a. Climate change 2007. The physical science basis. In: Solomon, S., Qin, D., Manning, M., Marquis, M., Averyt, K., Tignor, M.M.B., Miller, H.L., Chen, Z. (Eds.), Contribution of Working Group I to the Fourth Assessment Report of the Intergovernmental Panel on Climate Change. Cambridge University Press, UK.

IPCC, 2007b. Climate change 2007. Mitigation of climate change. In: Metz, B., Davidson, O.R., Bosch, P.R., Dave, R., Meyer, L.A. (Eds.), Contribution of Working Group III to the Fourth Assessment Report of the Intergovernmental Panel on Climate Change. Cambridge University Press, UK.

Isaksen, I., Jackman, C., Baughcum, S., Dentener, F., Grose, W., Kasibhatla, P., Kinnison, D., Ko, M.K.W., McConnell, J.C., Pitari, G., Wuebbles, D.J., 1999. Modeling the chemical composition of the future atmosphere. Chapter 4 of '*Aviation and the Global Atmosphere*'. In: Penner, J.E., Lister, D.H., Griggs, D.J., Dokken, D.J., McFarland, M. (Eds.), Special Report of the Intergovernmental Panel on Climate Change. Cambridge University Press, Cambridge.

Isaksen, I.S.A., Berntsen, T.K., Wang, W.-C., 2001. NO_x emissions from aircraft: its impact on the global distribution of CH_4 and O_3 and on radiative forcing. TAO 12 (1), 63–78.

Jaeglé, L., Jacob, D.J., Brune, W.H., Tan, D., Faloona, I., Weinheimer, A.J., Ridley, B.A., Campos, T.L., Sachse, G.W., 1998. Sources of HO_x and production of ozone in the upper troposphere over the United States. Geophys. Res. Lett. 25 (10), 1709–1712.

Jaeglé, L., Jacob, D.J., Brune, W.H., Faloona, I., Tan, D., Heikes, B.G., Kondo, Y., Sachse, G.W., Anderson, B., Gregory, G.L., Singh, H.B., Pueschel, R., Ferry, G., Blake, D.R., Shetter, R.E., 2000. Photochemistry of HO_x in the upper troposphere at northern midlatitudes. J. Geophys. Res. 105 (D3), 3877–3892.

Jelinek, F., Calrlier, S., Crook, I., Martin, K., Smith, J., Vo, M.N., 2005. ATM Contrail Mitigation Options Environmental Study. EEC/SEE/2005/015. EUROCONTROL Experimental Centre, Bretigny, France.

Jensen, E.J., Toon, O.B., 1994. Ice nucleation in the upper troposphere: sensitivity to aerosol number density, temperature, and cooling rate. Geophys. Res. Lett. 21 (18), 2019–2022.

Jensen, E.J., Toon, O.B., Selkirk, H.B., Spinhirne, J.D., Schoeberl, M.R., 1996. On the formation and persistence of subvisible cirrus clouds near the tropical tropopause. J. Geophys. Res. 101 (D16), 21361–21375.

Jensen, E.J., Toon, O.B., 1997. The potential impact of soot particles from aircraft exhaust on cirrus clouds. Geophys. Res. Lett. 24 (3), 249–252.

Jensen, E.J., Ackerman, A.S., Stevens, D.E., Toon, O.B., Minnis, P., 1998a. Spreading and growth of contrails in a sheared environment. J. Geophys. Res. 103 (D24), 31557–31567.

Jensen, E.J., Toon, O.B., Kinne, S., Sachse, G.W., Anderson, B.E., Chan, K.R., Twohy, C.H., Gandrud, B., Heymsfield, A., Miake-Lye, R.C., 1998b. Environmental conditions required for contrail formation and persistence. J. Geophys. Res. 103 (D4), 3929–3936.

Jensen, E., Pfister, L., Bui, T., Weinheimer, A., Weinstock, E., Smith, J., Pittman, J., Baumgardner, D., Lawson, P., McGill, M.J., 2005. Formation of a tropopause cirrus layer observed over Florida during CRYSTAL-FACE. J. Geophys. Res. 110, D03208. doi:10.1029/2004JD004671.

Johnson, C.E., Collins, W.J., Stevenson, D.S., Derwent, R.G., 1999. Relative roles of climate and emissions changes on future tropospheric oxidant concentrations. J. Geophys. Res. 104 (D15), 18631–18645.

Johnston, H., 1971. Reduction of stratospheric ozone by nitrogen oxide catalysts from supersonic transport exhaust. Science 173 (3996), 517–522. doi:10.1126/science.173.3996.517.

Johnston, H.S., Prather, M.J., Watson, R.T., 1991. The Atmospheric Effects of Stratospheric Aircraft: a Topical Review, NASA Reference Publication 1250, 36 pp.

Johnston, H.S., Quitevis, E., 1974. The Oxides of Nitrogen with Respect to Urban Smog, Supersonic Transports, and Global Methane. International Congress of Radiation Research, US Department of Transportation and US Atomic Energy Committee, Seattle, Washington. July 14–20, 1974.

Joshi, M., Shine, K., Ponater, M., Stuber, N., Sausen, R., Li, L., 2003. A comparison of climate response to different radiative forcings in three general circulation models: towards an improved metric of climate change. Clim. Dynam. 20, 843–854. doi:10.1007/s00382-003-0305-9.

Kahn-Ribeiro, S., Kobayashi, S., Beuthe, M., Gasca, J., Greene, D., Lee, D.S., Muromachi, Y., Newton, P.J., Plotkin, S., Wit, R.C.N., Zhou, P.J., 2007. Transportation and its infrastructure. In: 'Mitigation of Climate Change' Fourth Assessment Report Working Group III, Intergovernmental Panel on Climate Change. Cambridge University Press, UK.

Kärcher, B., 1996. Aircraft-generated aerosols and visible contrails. Geophys. Res. Lett. 23, 1933–1936.

Kärcher, B., Meilinger, S.K., 1998. Perturbation of the aerosol layer by aviation-produced aerosols: a parameterization of plume processes. Geophys. Res. Lett. 25 (24), 4465–4468.

Kärcher, B., Busen, R., Petzold, A., Schröder, F.P., Schumann, U., Jensen, E.J., 1998a. Physicochemistry of aircraft-generated liquid aerosols, soot, and ice particles. 2. Comparison with observations and sensitivity studies. J. Geophys. Res. 103 (D14), 17129–17147.

Kärcher, B., Yu, F., Schröder, F.P., Turco, R.P., 1998b. Ultrafine aerosol particles in aircraft plumes: analysis of growth mechanisms. Geophys. Res. Lett. 25 (15), 2793–2796.

Kärcher, B., Turco, R.P., Yu, F., Danilin, M.Y., Weisenstein, D.K., Miake-Lye, R.C., Busen, R., 2000. A unified model for ultrafine aircraft particle emissions. J. Geophys. Res. 105 (D24), 29379–29386.

Kärcher, B., Ström, J., 2003. The roles of dynamical variability and aerosols in cirrus cloud formation. Atmos. Chem. Phys. 3, 823–838.

Kärcher, B., Hendricks, J., Lohmann, U., 2006. Physically based parameterization of cirrus cloud formation for use in global atmospheric models. J. Geophys. Res. 111, D01205. doi:10.1029/2005JD006219.

Kärcher, B., Möhler, O., DeMott, P.J., Pechtl, S., Yu, F., 2007. Insights into the role of soot aerosols in cirrus cloud formation. Atmos. Chem. Phys. 7, 4203–4227.

Karol, I.L., Ozolin, Y.E., Rozanov, E.V., 1997. Box and Gaussian plume models of the exhaust composition evolution of subsonic transport aircraft in- and out of the flight corridor. Ann. Geophysicae 15, 88–96.

Katragkou, E., Wilhelm, S., Arnold, F., Wilson, C., 2004. First gaseous Sulfur (VI) measurements in the simulated internal flow of an aircraft gas turbine engine during project PartEmis. Geophys. Res. Lett. 31, L02117. doi:10.1029/2003GL018231.

Kentarchos, A.S., Roelofs, G.J., Lelieveld, J., 2000. Simulation of extratropical synoptic-scale stratosphere–troposphere exchange using a coupled chemistry GCM: sensitivity to horizontal resolution. J. Atmos. Sci. 57, 2824–2838.

Kentarchos, A.S., Roelofs, G.J., 2002. Impact of aircraft NO_x emissions on tropospheric ozone calculated with a chemistry-general circulation model: sensitivity to higher hydrocarbon chemistry. J. Geophys. Res. 107 (D13), 4175. doi:10.1029/2001JD000828.

Kiendler, A., Aberle, St, Arnold, F., 2000a. Negative chemiions formed in jet fuel combustion: new insights from jet engine and laboratory measurements using a quadrupole ion trap mass spectrometer apparatus. Atmos. Environ. 34, 2623–2632.

Kiendler, A., Aberle, S., Arnold, F., 2000b. Positive ion chemistry in the exhaust plumes of an air craft jet engine and a burner: investigations with a quadrupole ion trap mass spectrometer. Atmos. Environ. 34, 4787–4793.

Kim, B.Y., Fleming, G.G., Lee, J.J., Waitz, I.A., Clarke, J.-P., Balasubramanian, S., Malwitz, A., Klima, K., Locke, M., Holsclaw, C.A., Maurice, L.Q., Gupta, M.L., 2007. System for assessing Aviation's Global Emissions (SAGE), Part 1: model description and inventory results. Transport. Res. Transport. Environ. 12, 325–346.

Knight, C.G., Knight, S.H.E., Massey, N., Aina, T., Christensen, C., Frame, D.J., Kettleborough, J.A., Martin, A., Pascoe, S., Sanderson, B., Stainforth, D.A., Allen, M.R., 2007. Association of parameter, software, and hardware variation with large-scale behaviour across 57,000 climate models. Proc. Nat. Acad. Sci. 104 (30), 12259–12264.

Knighton, W.B., Rogers, T.M., Anderson, B.E., Herndon, S.C., Yelvington, P.E., Miake-Lye, R.C., 2007. Quantification of aircraft engine hydrocarbon emissions using proton transfer reaction mass spectrometry. J. Propul. Power 23 (5), 949–958. doi:10.2514/1.22965.

Köhler, M.O., Rädel, G., Dessens, O., Shine, K.P., Rogers, H.L., Wild, O., Pyle, J.A., 2008. Impact of perturbations to nitrogen oxide emissions from global aviation. J. Geophys. Res. 113, D11305. doi:10.1029/2007JD009140.

Koop, T., Ng, H.P., Molina, L.T., Molina, M.J., 1998. A new optical technique to study aerosol phase transitions: the nucleation of ice from H_2SO_4 aerosols. J. Phys. Chem. A 102 (45), 8924–8931. doi:10.1021/jp9828078.

Korolev, A., Isaac, G.A., 2005. Shattering during sampling by OAPs and HVPS. Part I: snow particles. J. Atmos. Oceanic Technol. 22, 528–542.

Kraabøl, A.G., Flatøy, F., Stordal, F., 2000a. Impact of NO_x emissions from subsonic aircraft: inclusion of plume processes in a three-dimensional model covering Europe, North America, and the North Atlantic. J. Geophys. Res. 105 (D3), 3573–3581.

Kraabøl, A.G., Konopka, P., Stordal, F., Schlager, H., 2000b. Modelling chemistry in aircraft plumes 1: comparison with observations and evaluation of a layered approach. Atmos. Environ. 34, 3939–3950.

Kraabøl, A.G., Berntsen, T.K., Sundet, J.K., Stordal, F., 2002. Impacts of NO_x emissions from subsonic aircraft in a global three-dimensional chemistry transport model including plume processes. J. Geophys. Res. 107 (D22), 4655. doi:10.1029/2001JD001019.

Krebs, W., 2006. Analyse des Einflusses des Flugverkehrs auf die natürliche Zirrusbewölkung über Europa, Nordafrika und dem Nordatlantik, dissertation, Ludwig-Maximilians Universität München, 211 pp (in German).

Kristensson, A., Gayet, J.-F., Ström, J., Auriol, F., 2000. In situ observations of a reduction in effective crystal diameter in cirrus clouds near flight corridors. Geophys. Res. Lett. 27 (5), 681–684.

Kurtenbach, R., Lörzer, J.C., Niedojadlo, A., Petrea, M., Weisen, P., Kapernaum, M., Wahl, C., 2003. Emission of non-methane volatile organic compounds (NMVOCs) from a jet engine combustor and a hot end simulator (HES) during the PartEmis Project. In: Sausen, R., Fichter, C., Amanatidis, G. (Eds.), European Conference on Aviation, Atmosphere and Climate (AAC), Proceedings of an International Conference, Friedrichshafen, Germany, 30 June–3rd July 2003. European Commission, pp. 52–58. Air Pollution Research Report 83.

Labrador, L.J., von Kuhlmann, R., Lawrence, M.G., 2005. The effects of lightning-produced NO_x and its vertical distribution on atmospheric chemistry: sensitivity simulations with MATCH-MPIC. Atmos. Chem. Phys. 5, 1815–1834.

Lacis, A., Wuebbles, D., Logan, J., 1990. Radiative forcing of climate by changes in the vertical distribution of ozone. J. Geophys. Res. 95, 9971–9981.

Land, C., Feichter, J., Sausen, R., 2002. Impact of vertical resolution on the transport of passive tracers in the ECHAM4 model. Tellus 54B, 344–360.

Larsen, N., Knudsen, B.M., Gauss, M., Pitari, G., 2002. Aircraft induced effects on Arctic polar stratospheric cloud formation. Meteorol. Z. 11 (3), 207–214.

Lauer, A., Hendricks, J., Ackermann, I., Schell, B., Hass, H., Metzger, S., 2005. Simulating aerosol microphysics with the ECHAM/MADE GCM – part I: model description and comparison with observations. Atmos. Chem. Phys. 5, 3251–3276.

Lee, D.S., Owen, B., Graham, A., Fichter, C., Lim, L.L., Dimitriu, D., 2005. Allocation of International Aviation Emissions from Scheduled Air Traffic – Present Day and Historical (Report 2 of 3). Manchester Metropolitan University, Centre for Air Transport and the Environment, Manchester, UK. http://www.cate.mmu.ac.uk/project_view.asp?chg¼;projects&chg2¼2&id¼2 CATE-2005-3(C)-2See (accessed 18.02.09).

Lee, D.S., Lim, L., Eyring, V., Sausen, R., Endresen, Ø, Behrens, H.-L., 2007. Radiative forcing and temperature response from shipping. In: Sausen, R., Blum, A., Lee, D.S., Brüning, C. (Eds.), Proceedings of an International Conference on Transport, Atmosphere and Climate (TAC). Office for Official Publications of the European Communities, Luxembourg, ISBN 92-79-04583-0, pp. 208–213.

Lee, D.S., Fahey, D.W., Forster, P.M., Newton, P.J., Wit, R.C.N., Lim, L.L., Owen, B., Sausen, R., 2009. Aviation and global climate change in the 21st century. Atmos. Environ.. doi:10.1016/j.atmosenv.2009.04.024.

Lewis, J.S., Niedzwiecki, R.W., Bahr, D.W., Bullock, S., Cumpsty, N., Dodds, W., DuBois, D., Epstein, A., Freguson, W.W., Fiorento, A., Gorbatko, A.A., Hagen, D.E., Hart, P.J., Hayashi, S., Jamieson, J.B., Kerrebrock, J., Lecht, M., Lowrie, B., Miake-Lye, R.C., Mortlock, A.K., Moses, C., Renger, K., Sampath, S., Sanborn, J., Simon, B., Sorokin, A., Taylor, W., Waitz, I., Wey, C.C., Whitefield, P., Wilson, C.W., Wu, S., 1999. Aircraft technology and its relation to emissions. Chapter 7 of '*Aviation and the Global Atmosphere*'. In: Penner, J.E., Lister, D.H., Griggs, D.J., Dokken, D.J., McFarland, M. (Eds.), Special Report of the Intergovernmental Panel on Climate Change. Cambridge University Press, Cambridge.

Lim, L.L., Lee, D.S., Sausen, R., Ponater, M., 2007. Quantifying the effects of aviation on radiative forcing and temperature with a climate response model. In: Sausen, R., Blum, A., Lee, D.S., Brüning, C. (Eds.), Proceedings of an International Conference on Transport, Atmosphere and Climate (TAC). Office for Official Publications of the European Communities, Luxembourg, ISBN 92-79-04583-0, pp. 202–207.

Lin, X., Trainer, M., Liu, S.C., 1988. On the nonlinearity of the tropospheric ozone production. J. Geophys. Res. 93 (D12), 15879–15888.

Liscinsky, D.S., Colket, M.B., Hautman, D.J., True, B., 2001. Effect of Fuel Additives on Particle Formation in Gas Turbine Combustors. AIAA paper 2001–3745. AIAA/ASME/SAE/ASEE Joint Propulsion Conference and Exhibit, 37th, Salt Lake City, UT, July 8–11, 2001.

Liu, X., Penner, J.E., 2005. Ice nucleation parameterization for global models. Meteorol. Z. 14 (4), 499–514.

Liu, X., Penner, J.E., Herzog, M., 2005. Global modeling of aerosol dynamics: model description, evaluation and interactions between sulfate and nonsulfate aerosols. J. Geophys. Res. 110, D18206. doi:10.1029/2004JD005674.

Liu, X., Penner, J.E., Wang, M., 2009. Influence of anthropogenic sulphate and black carbon on upper tropospheric clouds in the NCAR CAM3 model coupled to the IMPACT global aerosol model. J. Geophys. Res. 114, D03204. doi:10.1029/2008JD010492.

Lohmann, U., Kärcher, B., Hendricks, J., 2004. Sensitivity studies of cirrus clouds formed by heterogeneous freezing in the ECHAM GCM. J. Geophys. Res. 109, D16204. doi:10.1029/2003JD004443.

Lovett, J.C., 2007. Biofuels and ecology. Afr. J. Ecol. 45, 117–119.

LTTG, 2006. Report of the Long Term Technology Goals Sub Group, CAEP Working Group 3. Inernational Civil Aviation Organization.

Lukachko, S.P., Waitz, I.A., Miake-Lye, R.C., Brown, R.C., Anderson, M.R., 1998. Production of sulphate aerosol precursors in the turbine and exhaust nozzle of an aircraft engine. J. Geophys. Res. 103 (D13), 16159–16174.

Mace, G.G., Ackerman, T.P., Minnis, P., Young, D.F., 1998. Cirrus layer microphysical properties derived from surface-based millimeter radar and infrared interferometer data. J. Geophys. Res. 103 (D18), 23207–23216.

Mace, G.G., Clothiaux, E.E., Ackerman, T.P., 2001. The composite characteristics of cirrus clouds: bulk properties revealed by one year of continuous cloud radar data. J. Clim. 14, 2185–2203.

Mannstein, H., Meyer, R., Wendling, P., 1999. Operational detection of contrails from NOAA-AVHRR-data. Int. J. Remote Sensing 20 (8), 1641–1660.

Mannstein, H., Schumann, U., 2005. Aircraft induced contrail cirrus over Europe. Meteorol. Z. 14 (4), 549–554.

Mannstein, H., Spichtinger, P., Gierens, K., 2005. A note on how to avoid contrail cirrus. Transport. Res. Transport. Environ. 10, 421–426.

Mannstein, H., Schumann, U., 2007. Corrigendum to "Aircraft induced contrail cirrus over Europe". Meteorol. Z. 16 (1), 131–132.

Marland, G., Boden, T.A., Andres, R.J., 2006. Global, Regional, and National Annual CO_2 Emissions from Fossil-Fuel Burning, Cement Production, and Gas Flaring: 1751–2000. http://cdiac.ornl.gov/ndps/ndp030.html (accessed 30.05.09).

Marquart, S., Mayer, B., 2002. Towards a reliable GCM estimation of contrail radiative forcing. Geophys. Res. Lett. 29 (8). doi:10.1029/2001GL014075.

Marquart, S., Ponater, M., Mager, F., Sausen, R., 2003. Future development of contrail cover, optical depth and radiative forcing: impacts of increasing air traffic and climate change. J. Clim. 16, 2890–2904.

Mayer, B., Kylling, A., 2005. Technical note: the libRadtran software package for radiative transfer calculations – description and examples of use. Atmos. Chem. Phys. 5, 1855–1877.

McFarquhar, G.M., Um, J., Freer, M., Baumgardner, D., Kok, G.L., Mace, G., 2007. Importance of small ice crystals to cirrus properties: observations from the tropical warm pool international cloud experiment (TWP-ICE). Geophys. Res. Lett. 34, L13803. doi:10.1029/2007GL029865.

Meehl, G.A., Washington, W.M., Collins, W.D., Arblaster, J.M., Hu, A., Buja, L.E., Strand, W.G., Teng, H., 2005. How much more global warming and sea level rise? Science 307, 1769–1772. doi:10.1126/science.1106663.

Meerkötter, R., Schumann, U., Doelling, D.R., Minnis, P., Nakajima, T., Tsushima, Y., 1999. Radiative forcing by contrails. Ann. Geophysicae 17, 1080–1094.

Meijer, E.W., van Velthoven, P.F.J., Wauben, W.M.F., Beck, J.P., Velders, G.J.M., 1997. The effect of the conversion of nitrogen oxides in aircraft exhaust plumes in global models. Geophys. Res. Lett. 24 (23), 3013–3016.

Meijer, E., 2001. Modelling the impact of subsonic aviation on the composition of the atmosphere. PhD thesis, Technical University, Eindhoven.

Meilinger, S.K., Kärcher, B., Peter, Th., 2002. Suppression of chlorine activation on aviation-produced volatile particles. Atmos. Chem. Phys. 2, 307–312.

Meilinger, S.K., Kärcher, B., Peter, Th., 2005. Microphysics and heterogeneous chemistry in aircraft plumes – high sensitivity on local meteorology and atmospheric composition. Atmos. Chem. Phys. 5, 533–545.
Meyer, R., Mannstein, H., Meerkötter, R., Schumann, U., Wendling, P., 2002. Regional radiative forcing by line-shaped contrails derived from satellite data. J. Geophys. Res. 107 (D10), 4104. doi:10.1029/2001JD000426.
Meyer, R., Buell, R., Leiter, C., Mannstein, H., Pechtl, S., Oki, T., Wendling, P., 2007. Contrail observations over Southern and Eastern Asia in NOAA/AVHRR data and comparisons to contrail simulations in a GCM. Int. J. Remote Sensing 28 (9), 2049–2069. doi:10.1080/01431160600641707.
Miller, T.M., Ballenthin, J.O., Hunton, D.E., Viggiano, A.A., Wey, C.C., Anderson, B.E., 2003. Nitric acid emissions from the F100 jet engine. J. Geophys. Res. 108 (D1), 4032. doi:10.1029/2001JD001522.
Minikin, A., Petzold, A., Ström, J., Krejci, R., Seifert, M., van Velthoven, P., Schlager, H., Schumann, U., 2003. Aircraft observations of the upper tropospheric fine particle aerosol in the Northern and Southern Hemispheres at midlatitudes. Geophys. Res. Lett. 30 (10), 1503. doi:10.1029/2002GL016458.
Minnis, P., Young, D.F., Garber, D.P., Nguyen, L., Smith, W.L.J., Palikonda, R., 1998. Transformation of contrails into cirrus during SUCCESS. Geophys. Res. Lett. 25 (8), 1157–1160.
Minnis, P., Schumann, U., Doelling, D.R., Gierens, K.M., Fahey, D.W., 1999. Global distribution of contrail radiative forcing. Geophys. Res. Lett. 26 (13), 1853–1856.
Minnis, P., Ayers, J.K., Palikonda, R., Doelling, D.R., Schumann, U., Gierens, K., 2001. Changes in Cirrus Cloudiness and their Relationship to Contrails, No. 11.9. Proceedings of American Meteorology Society, Boston, USA, pp. 239–242.
Minnis, P., Ayers, J.K., Palikonda, R., Phan, D., 2004. Contrails, cirrus trends, and climate. J. Clim. 17, 1671–1685.
Möhler, O., Büttner, S., Linke, C., Schnaiter, M., Saathoff, H., Stetzer, O., Wagner, R., Krämer, M., Mangold, A., Ebert, V., Schurath, U., 2005. Effect of sulfuric acid coating on heterogeneous ice nucleation by soot aerosol particles. J. Geophys. Res. 110, D11210. doi:10.1029/2004JD005169.
Möhler, O., Field, P.R., Connolly, P., Benz, S., Saathoff, H., Schnaiter, M., Wagner, R., Cotton, R., Krämer, M., Mangold, A., Heymsfield, A.J., 2006. Efficiency of the deposition mode of ice nucleation on mineral dust particles. Atmos. Chem. Phys. 6, 3007–3021.
Montgomery, C.J., Sarofim, A.F., Preciado, I., Marsh, N.D., Eddings, E.G., Bozzelli, J.W., 2005. Experimental and Numerical Investigation Soot-reducing Fuel Additives. AIAA 2005-4472. In: 41st AIAA/ASME/SAE/ASEE Joint Propulsion Conference and Exhibit, Tucson, Arizona, July 10–13, 2005.
Morris, G.A., Rosenfield, J.E., Schoeberl, M.R., Jackman, C.H., 2003. Potential impact of subsonic and supersonic aircraft exhaust on water vapor in the lower stratosphere assessed via a trajectory model. J. Geophys. Res. 108 (D3), 4103. doi:10.1029/2002JD002614.
Myhre, G., Stordal, F., 2001. On the tradeoff of the solar and thermal infrared radiative impact of contrails. Geophys. Res. Lett. 28 (16), 3119–3122.
Nakanishi, S., Curtis, J., Wendler, G., 2001. The influence of increased jet airline traffic on the amount of high level cloudiness in Alaska. Theor. Appl. Climatol. 68, 197–205.
Nicodemus, L.L., McQuigg, J.D., 1969. A simulation method for studying possible modification of surface temperature,. J. Appl. Meteorol. 8, 199–204.
Noppel, F., Singh, R., 2007. Overview on contrail and cirrus cloud avoidance technology. J. Aircraft 44 (5), 1721–1726. doi:10.2514/1.28655.
Noppel, F., Singh, R., Taylor, M., 2007. Novel engine concept to suppress contrail and cirrus cloud formation. In: Sausen, R., Blum, A., Lee, D.S., Brüning, C. (Eds.), Proceedings of an International Conference on Transport, Atmosphere and Climate (TAC). Office for Official Publications of the European Communities, Luxembourg, ISBN 92-79-04583-0, pp. 221–227.
O'Connor, F.M., Carver, G.D., Savage, N.H., Pyle, J.A., Methven, J., Arnold, S.R., Dewey, K., Kent, J., 2005. Comparison and visualisation of high-resolution transport modelling with aircraft measurements. Atmos. Sci. Let. 6, 164–170.
Osmundsen, J.A., 1963. Weather Scientists are Optimistic that New Findings are Near. New York Times, September 23, p 1.
Ou, S.C., Liou, K.N., Caudill, T.R., 1998. Remote sounding of multilayer cirrus cloud systems using AVHRR data collected during FIRE-II-IFO. J. Appl. Meteor. 37, 241–254.
Owen, B., Lee, D.S., 2005. Allocation of International Aviation Emissions – Allocation Options 2 and 3 (Report 1 of 3). CATE-2005-3(C)-1. Centre for Air Transport and the Environment, Manchester Metropolitan University, UK. http://www.cate.mmu.ac.uk/documents/projects/mmuallocationsreport1v14a.pdf (accessed 30.05.09).
Owen, B., Lee, D.S., 2006. Allocation of International Aviation Emissions from Scheduled Air Traffic – Future Cases, 2005 to 2050. CATE-2006-3(C)-3. See. Centre for Air Transport and the Environment, Manchester Metropolitan University, UK. http://www.cate.mmu.ac.uk/project_view.asp?chg¼;projects&chg2¼2&id¼2 (accessed 18.02.09).
Palikonda, R., Minnis, P., Duda, D.P., Mannstein, H., 2005. Contrail coverage derived from 2001 AVHRR data over the continental United States of America and surrounding area. Meteorol. Z. 14 (4), 525–536.
Penner, J.E., Chuang, C., Grant, K., 1998. Climate forcing by carbonaceous and sulfate aerosols. Clim. Dyn. 14, 839–851.
Penner, J.E., Andreae, M., Annegarn, H., Barrie, L., Feichter, J., Hegg, D., Jayaraman, A., Leaitch, R., Murphy, D., Nganga, J., Pitari, G., 2001. Aerosols, their direct and indirect effects. Climate change 2001: the scientific basis. In: Houghton, H.T., Ding, Y., Griggs, D.J., Noguer, M., van der Linden, P.J., Dai, X., Maskell, K., Johnson, C.A. (Eds.). Cambridge University Press, United Kingdom and New York, NY, USA Contribution of Working Group I to the Third Assessment Report of the Intergovernmental Panel on Climate Change.
Penner, J.E., Chen, Y., Wang, M., Liu, X., 2009. Possible influence of anthropogenic aerosols on cirrus clouds and anthropogenic forcing. Atmos. Chem. Phys. 9, 879–896.
Peterson, M.C., Honrath, R.E., 2001. Observations of rapid photochemical destruction of ozone in snowpack interstitial air. Geophys. Res. Lett. 28, 511–514.
Petry, H., Hendricks, J., Möllhoff, M., Lippert, E., Meier, A., Ebel, A., Sausen, R., 1998. Chemical conversion of subsonic aircraft emissions in the dispersing plume: calculation of effective emission indices. J. Geophys. Res. 103 (D5), 5759–5772.
Petzold, A., Döpelheuer, A., 1998. Reexamination of black carbon mass emission indices of a jet engine. Aerosol Sci. Tech. 29, 355–356. doi:10.1080/02786829808965575.
Petzold, A., Schröder, F.P., 1998. Jet engine exhaust aerosol characterization. Aerosol Sci. Tech. 28, 62–76. doi:10.1080/02786829808965512.
Petzold, A., Ström, J., Ohlsson, S., Schröder, F.P., 1998. Elemental composition and morphology of ice-crystal residual particles in cirrus clouds and contrails. Atmos. Res. 49, 21–34.
Petzold, A., Döpelheuer, A., Brock, C.A., Schröder, F., 1999. In situ observation and model calculations of black carbon emission by aircraft at cruise altitude. J. Geophys. Res. 104 (D18), 22171–22181.
Petzold, A., Fiebig, M., Flentje, H., Keil, A., Leiterer, U., Schröder, F., Stifter, A., Wendisch, M., Wendling, P., 2002. Vertical variability of aerosol properties observed at a continental site during the Lindenberg Aerosol Characterization Experiment (LACE 98). J. Geophys. Res. 107 (D21), 8128. doi:10.1029/2001JD001043.
Petzold, A., Stein, C., Nyeki, S., Gysel, M., Weingartner, E., Baltensperger, U., Giebl, H., Hitzenberger, R., Döpelheuer, A., Vrchoticky, S., Puxbaum, H., Johnson, M., Hurley, C.D., Marsh, R., Wilson, C.W., 2003. Properties of jet engine combustion particles during the PartEmis experiment: microphysics and chemistry. Geophys. Res. Lett. 30 (13), 1719. doi:10.1029/2003GL017283.
Petzold, A., Gysel, M., Vancassel, X., Hitzenberger, R., Puxbaum, H., Vrochticky, S., Weingartner, E., Baltensperger, U., Mirabel, P., 2005a. On the effects of organic matter and sulphur-containing compounds on the CCN activation of combustion particles. Atmos. Chem. Phys. 5, 3187–3203.
Petzold, A., Fiebig, M., Fritzsche, L., Stein, C., Schumann, U., Wilson, C.W., Hurley, C.D., Arnold, F., Katragkou, E., Baltensperger, U., Gysel, M., Nyeki, S., Hitzenberger, R., Giebl, H., Hughes, K.J., Kurtenbach, R., Wiesen, P., Madden, P., Puxbaum, H., Vrchoticky, S., Wahl, C., 2005b. Particle emissions from aircraft engines – a survey of the European project PartEmis. Meteorol. Z. 14 (4), 465–476.
Pitari, G., Mancini, E., 2001. Climatic impact of future supersonic aircraft: role of water vapour and ozone feedback on circulation. Phys. Chem. Earth (C) 26 (8), 571–576. not used in text?
Pitari, G., Mancini, E., Bregman, A., Rogers, H.L., Sundet, J.K., Grewe, V., Dessens, O., 2001. Sulphate particles from subsonic aviation: impact on upper tropospheric and lower stratospheric ozone. Phys. Chem. Earth (C) 26 (8), 563–569.
Pitari, G., Mancini, E., Rizi, V., Shindell, D.T., 2002a. Impact of future climate and emission changes on stratospheric aerosols and ozone. J. Atmos. Sci. 59, 414–440.
Pitari, G., Mancini, E., Bregman, A., 2002b. Climate forcing of subsonic aviation: indirect role of sulfate particles via heterogeneous chemistry. Geophys. Res. Lett. 29 (22), 2057. doi:10.1029/2002GL015705.
Pitari, G., Iachetti, D., Mancini, E., Montanaro, V., De Luca, N., Marizy, C., Dessens, O., Rogers, H., Pyle, J., Grewe, V., Stenke, A., Søvde, O.A., 2008. Radiative forcing from particle emissions by future supersonic aircraft. Atmos. Chem. Phys. 8, 4069–4084.
Pleijel, H., Sild, J., Danielsson, H., Klemedtsson, L., 1998. Nitrous oxide emissions from a wheat field in response to elevated carbon dioxide concentration and open-top chamber enclosure. Environ. Pollut. 102 (S1), 167–171.
Plumb, I.C., Randeniya, L.K., Vohralik, P.F., Baughcum, S.L., 2003. The effect of plume processes on aircraft impact. In: Sausen, R., Fichter, C., Amanatidis, G. (Eds.), European Conference on Aviation, Atmosphere and Climate (AAC), Proceedings of an International Conference, Friedrichshafen, Germany, 30 June–3rd July 2003. European Commission, pp. 79–84. Air Pollution Research Report 83.
Ponater, M., Sausen, R., Feneberg, B., Roeckner, E., 1999. Climate effect of ozone changes caused by present and future air traffic. Clim. Dynam. 15, 631–642.
Ponater, M., Marquart, S., Sausen, R., 2002. Contrails in a comprehensive global climate model: parameterization and radiative forcing results. J. Geophys. Res. 107 (D13), 4164. doi:10.1029/2001JD000429.
Ponater, M., Pechtl, S., Sausen, R., Schumann, U., Hüttig, G., 2006. Potential of the cryoplane technology to reduce aircraft climate impact: a state-of-the-art assessment. Atmos. Environ. 40, 6928–6944.
Popovicheva, O.B., Persiantseva, N.M., Lukhovitskaya, E.E., Shonija, N.K., Zubareva, N.A., Demirdjian, B., Ferry, D., Suzanne, J., 2004. Aircraft engine soot as contrail nuclei. Geophys. Res. Lett. 31, L11104. doi:10.1029/2003GL018888.
Popovicheva, O.B., Starik, A.M., 2007. Aircraft-generated soot aerosols: physicochemical properties and effects of emission into the atmosphere. Izvestiya Atmos. Ocean. Phys. 43 (2), 125–141.
Prabhakara, C., Kratz, D.P., Yoo, J.-M., Dalu, G., Vernekar, A., 1993. Optically thin cirrus clouds: radiative impact on the warm pool. J. Quantitative Spectrosc. Radiative Transfer 49 (5), 467–483.
Prather, M.J., 1994. Lifetimes and eigenstates in atmospheric chemistry. Geophys. Res. Lett. 21, 801–804.
Prather, M.J., 1996. Natural modes and time scales in atmospheric chemistry: theory, GWPs for CH_4 and CO, and runaway growth. Geophys. Res. Lett. 23, 2597–2600.
Prather, M., Sausen, R., Grossmann, A.S., Haywood, J.M., Rind, D., Subbaraya, B.H., 1999. Potential climate change from aviation. Chapter 6 of '*Aviation and the*

global atmosphere'. In: Penner, J.E., Lister, D.H., Griggs, D.J., Dokken, D.J., McFarland, M. (Eds.), Special Report of the Intergovernmental Panel on Climate Change. Cambridge University Press, Cambridge.

Pueschel, R.F., Hallett, J., Strawa, A.W., Howard, S.D., Ferry, G.V., Foster, T., Arnott, W.P., 1997. Aerosol and cloud particles in tropical cirrus anvil: importance to radiation balance. J. Aerosol. Sci. 28 (7), 1123–1136.

Rädel, G., Shine, K.P., 2007. Evaluation of the use of radiosonde humidity data to predict the occurrence of persistent contrails. Quart. J. Roy. Meteorol. Soc. 133, 1413–1423.

Rädel, G., Shine, K.P., 2008. Radiative forcing by persistent contrails and its dependence on cruise altitudes. J. Geophys. Res. 113, D07105. doi:10.1029/2007JD009117.

Ramanathan, V., Dickinson, R.E., 1979. The role of stratospheric ozone in the zonal and seasonal radiative energy balance of the Earth–troposphere system. J. Atmos. Sci. 36, 1084–1104.

Randeniya, L.K., Vohralik, P.F., Plumb, I.C., 2002. Stratospheric ozone depletion at northern mid latitudes in the 21st century: the importance of future concentrations of greenhouse gases nitrous oxide and methane. Geophys. Res. Lett. 29 (4), 1051. doi:10.1029/2001GL014295.

Rasmussen, C.L., Glarborg, P., Marshall, P., 2007. Mechanisms of radical removal by SO_2. Proc. Combustion Inst. 31 (I), 339–347.

Reichardt, J., Ansmann, A., Serwazi, M., Weitkamp, C., Michaelis, W., 1996. Unexpectedly low ozone concentration in midlatitude tropospheric ice clouds: a case study. Geophys. Res. Lett. 23 (15), 1929–1932.

Reiner, Th., Arnold, F., 1993. Laboratory flow reactor measurements of the reaction $SO_3 + H_2O + M -> H_2SO_4 + M$: implications for gaseous H_2SO_4 and aerosol formation in the plumes of jet aircraft. Geophys. Res. Lett. 20 (23), 2659–2662.

Richardson, M.S., DeMott, P.J., Kreidenweis, S.M., Cziczo, D.J., Dunlea, E.J., Jimenez, J.L., Thomson, D.S., Ashbaugh, L.L., Borys, R.D., Westphal, D.L., Casuccio, G.S., Lersch, T.L., 2007. Measurements of heterogeneous ice nuclei in the western United States in springtime and their relation to aerosol characteristics. J. Geophys. Res. 112, D02209. doi:10.1029/2006JD007500.

Rind, D., Lonergan, P., 1995. Modeled impacts of stratospheric ozone and water vapor perturbations with implications for high-speed civil transport aircraft. J. Geophys. Res. 100 (D4), 7381–7396.

Rodriguez, J.M., Logan, J.A., Rotman, D.A., Bergmann, D.J., Baughcum, S.L., Friedl, R.R., Anderson, D.E., 2003. Activities of NASA's Global Modeling Initiative (GMI) in the assessment of subsonic aircraft impact. In: Sausen, R., Fichter, C., Amanatidis, G. (Eds.), European Conference on Aviation, Atmosphere and Climate (AAC), Proceedings of an International Conference, Friedrichshafen, Germany, 30 June–3rd July 2003. European Commission, pp. 134–139. Air Pollution Research Report 83.

Roeckner, E., Brasseur, G.P., Giorgetta, M., Jacob, D., Jungclaus, J., Reick, C., Sillmann, J., 2006. Climate Projections for the 21st Century. Max Planck Institute for Meteorologie, Hamburg. Internal Report, 1–28.

Roelofs, G.J., Lelieveld, J., 2000. Tropospheric ozone simulation with a chemistry-general circulation model: influence of higher hydrocarbon chemistry. J. Geophys. Res. 105, 22697–22712.

Rogers, H.L., Chipperfield, M.P., Bekki, S., Pyle, J.A., 2000. The effects of future supersonic aircraft on stratospheric chemistry modeled with varying meteorology. J. Geophys. Res. 105 (D24), 29359–29367.

Rogers, H., Teyssedre, H., Pitari, G., Grewe, V., van Velthoven, P., Sundet, J., 2002a. Model intercomparison of the transport of aircraft-like emissions from sub- and supersonic aircraft. Meteorol. Z. 11 (3), 151–159.

Rogers, H.L., Lee, D.S., Raper, D.W., Forster, P.M.D., Wilson, C.W., Newton, P.J., 2002b. The impact of aviation on the atmosphere. Aeronaut. J. 106 (1064), 521–546.

Romakkaniemi, S., Kokkola, H., Petzold, A., Laaksonen, A., 2004. Growth of upper tropospheric aerosols due to uptake of HNO_3. Atmos. Chem. Phys. 4, 549–556.

Rossow, W.B., Schiffer, R.A., 1999. Advances in understanding clouds from ISCCP. Bull. Amer. Meteor. Soc. 80 (11), 2261–2287.

Ryan, K.R., Frederick, J.E., Bais, A.F., Kerr, J.B., Wu, B., 1999. Solar ultraviolet irradiance at the ground. Chapter 5 of '*Aviation and the Global Atmosphere*'. In: Penner, J.E., Lister, D.H., Griggs, D.J., Dokken, D.J., McFarland, M. (Eds.), Special Report of the Intergovernmental Panel on Climate Change. Cambridge University Press, Cambridge.

Salam, A., Lohmann, U., Crenna, B., Lesins, G., Klages, P., Rogers, D., Irani, R., MacGillivray, A., Coffin, M., 2006. Ice nucleation studies of mineral dust particles with a new continuous flow diffusion chamber. Aerosol Sci. Tech. 40 (2), 134–143. doi:10.1080/02786820500444853.

Sander, S.P., DeMore, W.B., Golden, D.M., Hampson, R.F., Kurylo, M.J., Howard, C.J., Ravishankara, A.R., Kolb, C.E., Molina, M.J., 2000. Chemical Kinetics and Photochemical Data for Use in Stratospheric Modeling, Eval. 13. JPL, Pasadena, California. JPL Publ. 00-3.

Sander, S.P., Friedl, R.R., Golden, D.M., Kurylo, M.J., Huie, R.E., Orkin, V.L., Moortgat, G.K., Ravishankara, A.R., Kolb, C.E., Molina, M.J., Finlayson-Pitts, B., 2003. Chemical Kinetics and Photochemical Data for Atmospheric Studies. JPL, Pasadena, California. e-Publication, 02–25.

Sassen, K., DeMott, P.J., Prospero, J.M., Poellot, M.R., 2003. Saharan dust storms and indirect aerosol effects on clouds: CRYSTAL-FACE results. Geophys. Res. Lett. 30 (12), 1633. doi:10.1029/2003GL017371.

Sausen, R., Gierens, K., Ponater, M., Schumann, U., 1998. A diagnostic study of the global distribution of contrails part I: present day climate. Theor. Appl. Climatol. 61, 127–141.

Sausen, R., Schumann, U., 2000. Estimates of the climate response to aircraft CO_2 and NO_x emissions scenarios. Climatic Change 44, 27–58.

Sausen, R., Isaksen, I., Grewe, V., Hauglustaine, D., Lee, D.S., Myhre, G., Köhler, M.O., Pitari, G., Schumann, U., Stordal, F., Zerefos, C., 2005. Aviation radiative forcing in 2000: an update of IPCC (1999). Meteorol. Z. 14 (4), 555–561.

Saynor, B., Bauen, A., Leach, M., 2003. The Potential for Renewable Energy Sources in Aviation. Imperial College Centre for Energy Policy and Technology, Imperial College, London.

Schäfer, K., Heland, J., Lister, D.H., Wilson, C.W., Howes, R.J., Falk, R.S., Lindermeir, E., Birk, M., Wagner, G., Haschberger, P., Bernard, M., Legras, O., Wiesen, P., Kurtenbach, R., Brockmann, K.J., Kriesche, V., Hilton, M., Bishop, G., Clarke, R., Workman, J., Caola, M., Geatches, R., Burrows, R., Black, J.D., Hervé, P., Vally, J., 2000. Nonintrusive optical measurements of aircraft engine exhaust emissions and comparison with standard intrusive techniques. Appl. Optic 39 (3), 441–455.

Schlager, H., Schulte, P., Flatoy, F., Slemr, F., van Velthoven, P., Ziereis, H., Schumann, U., 1999. Regional nitric oxide enhancements in the north Atlantic flight corridor observed and modeled during POLINAT 2-A case study. Geophys. Res. Lett. 26 (20), 3061–3064.

Schmidt, E., 1941. Die Entstehung von Eisnebel aus den Auspuffgasen von Flugmotoren. Schriften der Deutschen Akademie der Luftfahrtforschung, Verlag R. Oldenbourg, Muenchen und Berlin, Heft 44, pp. 1–15.

Schmitt, A., Brunner, B., 1997. Emissions from aviation and their development over time. Pollutants from air traffic—results of atmospheric research 1992–1997. In: Schumann, U. (Ed.), BMBF-Förderzeichen 01 LL 9207/0, DLR-Mitteilungen 97-04. Deutsches Zentrum für Luft-und Raumfahrt e.V. (DLR), pp. 37–52.

Schneider, J., Hings, S.S., Hock, B.N., Weimer, S., Borrmann, S., Fiebig, M., Petzold, A., Busen, R., Kärcher, B., 2006. Aircraft-based operation of an aerosol mass spectrometer: measurements of tropospheric aerosol composition. J. Aerosol. Sci. 37, 839–857.

Schoeberl, M.R., Morris, G.A., 2000. A Lagrangian simulation of supersonic and subsonic aircraft exhaust emissions. J. Geophys. Res. 105 (D9), 11833–11839.

Schröder, F.P., Kärcher, B., Petzold, A., Baumann, R., Busen, R., Hoell, C., Schumann, U., 1998. Ultrafine aerosol particles in aircraft plumes: in situ observations. Geophys. Res. Lett. 25 (15), 2789–2792.

Schröder, F., Brock, C.A., Baumann, R., Petzold, A., Busen, R., Schulte, P., Fiebig, M., 2000. In situ studies on volatile jet exhaust particle emissions: impacts of fuel sulfur content and environmental conditions on nuclei mode aerosols. J. Geophys. Res. 105 (D15), 19941–19954.

Schulte, P., Schlager, H., 1996. In-flight measurements of cruise altitude nitric oxide emission indices of commercial jet aircraft. Geophys. Res. Lett. 23 (2), 165–168.

Schulte, P., Schlager, H., Ziereis, H., Schumann, U., Baughcum, S.L., Deidewigm, F., 1997. NO_x emission indices of subsonic long-range jet aircraft at cruise altitude: in situ measurements and predictions. J. Geophys. Res. 102 (D17), 21431–21442.

Proc. of a DLR Intern. Coll., Bonn, Nov. 15/16, 1990, Lecture Notes in Engrg Schumann, U., Wendling, P., 1990. Determination of Contrails from Satellite Data and Observational Results, vol. 60. Springer-Verlag., Berlin. 138–153.

Schumann, U., 1994. On the effect of emissions from aircraft engines on the state of the atmosphere. Ann. Geophysicae 12, 365–384.

Schumann, U., 1996. On conditions for contrail formation from aircraft exhausts. Meteorol. Z. 5, 4–23.

Schumann, U., 1998. Contrail Cirrus. Invited Paper, Cirrus–Topical Meeting. Optical Society of America, Baltimore. October 6–8, 1998.

Schumann, U., Schlager, H., Arnold, F., Baumann, R., Haschberger, P., Klemm, O., 1998. Dilution of aircraft exhaust plumes at cruise altitudes. Atmos. Environ. 32 (18), 3097–3103.

Schumann, U., 2000. Influence of propulsion efficiency on contrail formation. Aerosp. Sci. Technol. 4, 391–401.

Schumann, U., Schlager, H., Arnold, F., Ovarlez, J., Kelder, H., Hov, Ø., Hayman, G., Isaksen, I.S.A., Staehelin, J., Whitefield, P.D., 2000. Pollution from aircraft emissions in the North Atlantic flight corridor: overview on the POLINAT projects. J. Geophys. Res. 105 (D3), 3605–3631.

Schumann, U., Ström, J., 2001. Aviation impact on atmospheric composition and climate. In: European Research in the Atmosphere 1996–2000: Advances in Our Understanding of the Ozone Layer during THESEO. European Commission, Brussels, pp. 257–307.

Schumann, U., 2002. Contrail cirrus. In: Lynch, D.K., Sassen, K., Starr, D.O'C, Stephens, G. (Eds.), Cirrus. Oxford University Press, pp. 231–255.

Schumann, U., Arnold, F., Busen, R., Curtius, J., Kärcher, B., Kiendler, A., Petzold, A., Schlager, H., Schröder, F., Wohlfrom, K.-H., 2002. Influence of fuel sulfur on the composition of aircraft exhaust plumes: the experiments SULFUR 1–7. J. Geophys. Res. 107, D15. doi:10.1029/2001JD000813.

Schumann, U., 2005. Formation, properties and climatic effects of contrails. C.R. Physique 6, 549–565.

Schumann, 2006. Climate change impact of air traffic. In: Paper Presented at 25th International Congress of the Aeronautical Sciences. DGLR, Hamburg proceedings available from DGLR. http://www.icas2006.org/index2.php, paper number 199, 7 pp.

Schumann, U., Huntrieser, H., 2007. The global lightning-induced nitrogen oxides source. Atmos. Chem. Phys. 7, 3823–3907.

Schwarz, J.P., Gao, R.S., Fahey, D.W., Thomson, D.S., Watts, L.A., Wilson, J.C., Reeves, J.M., Darbeheshti, M., Baumgardner, D.G., Kok, G.L., Chung, S.H., Schulz, M., Hendricks, J., Lauer, A., Kärcher, B., Slowik, J.G., Rosenlof, K.H., Thompson, T.L., Langford, A.O., Loewenstein, M., Aikin, K.C., 2006. Single-particle measurements of midlatitude black carbon and light-scattering

aerosols from the boundary layer to the lower stratosphere. J. Geophys. Res. 111, D16207. doi:10.1029/2006JD007076.
Searchinger, T., Heimlich, R., Houghton, R.A., Dong, F., Elobeid, A., Fabiosa, J., Tokgoz, S., Hayes, D., Yu, T.-H., 2008. Use of U.S. croplands for biofuels increases greenhouse gases through emissions from land use change. Science 319, 1238–1240. doi:10.1126/science.1151861.
Sehra, A.K., Whitlow, W., 2004. Propulsion and power for 21st century aviation. Prog. Aerospace Sci. 40, 199–235.
Seifert, M., Ström, J., Krejci, R., Minikin, A., Petzold, A., Gayet, J.-F., Schumann, U., Ovarlez, J., 2003. In-situ observations of aerosol particles remaining from evaporated cirrus crystals: comparing clean and polluted air masses. Atmos. Chem. Phys. 3, 1037–1049.
Sheridan, P.J., Brock, C.A., Wilson, J.C., 1994. Aerosol particles in the upper troposphere and lower stratosphere: elemental composition and morphology of individual particles in northern midlatitudes. Geophys. Res. Lett. 21 (23), 2587–2590.
Shine, K.P., Berntsen, T.K., Fuglestvedt, J.S., Sausen, R., 2005a. Scientific issues in the design of metrics for inclusion of oxides of nitrogen in global climate agreements. Proc. Nat. Acad. Sci. 102, 15768–15773.
Shine, K.P., Fuglestvedt, J.S., Hailemariam, K., Stuber, N., 2005b. Alternatives to the global warming potential for comparing climate impacts of emissions of greenhouse gases. Clim. Change 68, 281–302.
Shine, K.P., Berntsen, T.K., Fuglestvedt, J.S., Skeie, R.B., Stuber, N., 2007. Comparing the climate effect of emissions of short – and long-lived climate agents. Phil. Trans. R. Soc. A 365, 1903–1914. doi:10.1098/rsta.2007.2050.
Shonija, N.K., Popovicheva, O.B., Persiantzeva, N.M., Savel'ev, A.M., Starik, A.M., 2007. Hydration of aircraft engine soot particles under plume conditions: effect of sulfuric and nitric acid processing. J. Geophys. Res. 112, D02208. doi:10.1029/2006JD007217.
Simpson, I.J., Sive, B.C., Blake, D.R., Blake, N.J., Chen, T.-Y., Lopez, J.P., Anderson, B.E., Sachse, G.W., Vay, S.A., Fuelberg, H.E., Kondo, Y., Thomson, A.M., Rowland, F.S., 2000. Nonmethane hydrocarbon measurements in the north Atlantic flight corridor during the subsonic assessment ozone and nitrogen oxide experiment. J. Geophys. Res. 105 (D3), 3785–3793.
Sims, R.E.H., Hastings, A., Schlamadinger, B., Taylors, G., Smith, P., 2006. Energy crops: current status and future prospects. Global Change Biol. 12, 2054–2076. doi:10.1111/j.1365-2486.2006.01163.x.
Slemr, F., Giehl, H., Slemr, J., Busen, R., Schulte, P., Haschberger, P., 1998. In-flight measurements of aircraft non-methane hydrocarbon emission indices. Geophys. Res. Lett. 25 (3), 321–324.
Slemr, F., Giehl, H., Habram, M., Slemr, J., Schlager, H., Schulte, P., Haschberger, P., Lindermeir, E., Döpelheuer, A., Plohr, M., 2001. In-flight measurements of aircraft CO and nonmethane hydrocarbon emission indices. J. Geophys. Res. 106 (D7), 7485–7494.
SMIC, 1971. Inadvertent Climate Modification. Report of the Study of Man's Impact on Climate. MIT Press, Cambridge, Mass, US.
Somnitz, H., Gleitsmann, G.G., Zellner, R., 2005. Novel rates of OH induced sulfur oxidation. Implications to the plume chemistry of jet aircraft. Meteorol. Z. 14 (4), 459–464.
Sorokin, A., Mirabel, P., 2001. Ion recombination in aircraft exhaust plumes. Geophys. Res. Lett. 28 (6), 955–958.
Sorokin, A., Katragkou, E., Arnold, F., Busen, R., Schumann, U., 2004. Gaseous SO_3 and H_2SO_4 in the exhaust of an aircraft gas turbine engine: measurements by CIMS and implications for fuel sulfur conversion to sulfur (VI) and conversion of SO_3 to H_2SO_4. Atmos. Environ. 38, 449–456.
Sorokin, A., Arnold, F., 2006. Organic positive ions in aircraft gas-turbine engine exhaust. Atmos. Environ. 40, 6077–6087.
Søvde, O.A., Gauss, M., Isaksen, I.S.A., Pitari, G., Marizy, C., 2007. Aircraft pollution – a futuristic view. Atmos. Chem. Phys. 7, 3621–3632.
Spicer, C.W., Holdren, M.W., Riggin, R.M., Lyon, T.F., 1994. Chemical composition and photochemical reactivity of exhaust from aircraft turbine engines. Ann. Geophysicae 12, 944–955.
Spichtinger, P., Gierens, K., Read, W., 2003. The global distribution of ice-supersaturated regions as seen by the microwave limb sounder. Q. J. Roy. Meteorol. Soc. 129 (595), 3391–3410.
Spracklen, D.V., Pringle, K.J., Carslaw, K.S., Chipperfield, M.P., Mann, G.W., 2005. A global off-line model of size-resolved aerosol microphysics: II. Identification of key uncertainties. Atmos. Chem. Phys. 5, 3233–3250.
Starik, A.M., Savel'ev, A.M., Titova, N.S., Schumann, U., 2002. Modeling of sulfur gases and chemiions in aircraft engines. Aerosp. Sci. Technol. 6, 63–81.
Starik, A.M., Savel'ev, A.M., Titova, N.S., Loukhovitskaya, E.E., Schumann, U., 2004. Effect of aerosol precursors from gas turbine engines on the volatile sulfate aerosols and ion clusters formation in aircraft plumes. Phys. Chem. Chem. Phys. 6, 3426–3436.
Stenke, A., Grewe, V., 2005. Simulation of stratospheric water vapor trends: impact on stratospheric ozone chemistry. Atmos. Chem. Phys. 5, 1257–1272.
Stenke, A., Grewe, V., Pechtl, S., 2008. Do supersonic aircraft avoid contrails? Atmos. Chem. Phys. 8, 955–967.
Stephens, G.L., Webster, P.J., 1981. Clouds and climate: sensitivity of simple systems. J. Atmos. Sci. 38, 235–247.
Stevenson, D.S., Collins, W.J., Johnson, C.E., Derwent, R.G., 1997. The impact of aircraft nitrogen oxide emissions on tropospheric ozone studied with a 3D Lagrangian model including fully diurnal chemistry. Atmos. Environ. 31 (12), 1837–1850.
Stevenson, D.S., Doherty, R.M., Sanderson, M.G., Collins, W.J., Johnson, C.E., Derwent, R.G., 2004. Radiative forcing from aircraft NO_x emissions: mechanisms and seasonal dependence. J. Geophys. Res. 109, D17307. doi:10.1029/2004JD004759.
Stevenson, D.S., Dentener, F.J., Schultz, M.G., Ellingsten, K., van Noije, T.P.C., Wild, O., Zeng, G., Amann, M., Atherton, C.S., Bell, N., Bergmann, D.J., Bey, I., Butler, T., Cofala, J., Collins, W.J., Derwent, R.G., Doherty, R.M., Drevet, J., Eskes, H.J., Fiore, A.M., Gauss, M., Hauglustaine, D.A., Horowitz, L.W., Isaksen, I.S.A., Krol, M.C., Lamarque, J.-F., Lawrence, M.G., Montanaro, V., Müller, J.-F., Pitari, G., Prather, M.J., Pyle, J.A., Rast, S., Rodriguez, J.M., Sanderson, M.G., Savage, N.H., Shindell, D.T., Strahan, S.E., Sudo, K., Szopa, S., 2006. Multimodel ensemble simulations of present-day and near-future tropospheric ozone. J. Geophys. Res. 111, D08301. doi:10.1029/2005JD006338.
Stordal, F., Myhre, G., Stordal, E.J.G., Rossow, W.B., Lee, D.S., Arlander, D.W., Svendby, T., 2005. Is there a trend in cirrus cloud cover due to aircraft traffic. Atmos. Chem. Phys. 5, 2155–2162.
Stordal, F., Gauss, M., Myhre, G., Mancini, E., Hauglustaine, D.A., Köhler, M.O., Berntsen, T., Stordal, E.J.G., Iachetti, D., Pitari, G., Isaksen, I.S.A., 2006. TRADEOFFs in climate effects through aircraft routing: forcing due to radiatively active gases. Atmos. Chem. Phys. Discuss. 6, 10733–10771.
Ström, J., Heintzenberg, J., 1994. Water vapor, condensed water, and crystal concentration in orographically influenced cirrus clouds. J. Atmos. Sci. 51 (16), 2368–2383.
Ström, J., Strauss, B., Schröder, F., Anderson, T., Heintzenberg, J., 1997. In-situ observations of microphysical properties of young cirrus clouds. J. Atmos. Sci. 54, 2542–2553.
Ström, J., Ohlsson, S., 1998. In situ measurements of enhanced crystal number densities in cirrus clouds caused by aircraft exhaust. J. Geophys. Res. 103 (D10), 11355–11361.
Ström, L., Gierens, K., 2002. First simulations of cryoplane contrails. J. Geophys. Res. 107 (D18), 4346. doi:10.1029/2001JD000838.
Stubenrauch, C.J., Schumann, U., 2005. Impact of air traffic on cirrus coverage. Geophys. Res. Lett. 32, L14813. doi:10.1029/2005GL022707.
Stuber, N., Ponater, M., Sausen, R., 2005. Why radiative forcing might fail as a predictor of climate change. Clim. Dynam. 24, 497–510. doi:10.1007/s00382-004-0497-7.
Stuber, N., Forster, P., Rädel, G., Shine, K., 2006. The importance of the diurnal and annual cycle of air traffic for contrail radiative forcing. Nature 441, 864–867. doi:10.1038/nature04877.
Stuber, N., Forster, P., 2007. The impact of diurnal variations of air traffic on contrail radiative forcing. Atmos. Chem. Phys. 7, 3153–3162.
Sutkus, D.J., Baughcum, S.L., DuBois, D.P., 2001. Scheduled Civil Aircraft Emission Inventories for 1999: Database Development and Analysis. National Aeronautics and Space Administration, Glenn Research Centre. NASA CR-2001/211216.
Svensson, F., Singh, R., 2004. Effects of using hydrogen on aero gas turbine pollutant emissions, performance and design. In: Proceedings of ASME Turbo Expo 2004, 14–17 June 2004, Vienna, Austria.
Svensson, F., Hasselrot, A., Moldanova, J., 2004. Reduced environmental impact by lowered cruise altitude for liquid hydrogen-fuelled aircraft. Aerosp. Sci. Technol. 8, 307–320.
Svensson, F., Singh, R., 2005. Design of Hydrogen-fuelled Aero Gas Turbines for Low Environmental Impact. ISABE-2005-1231. American Institute for Aeronautics and Astronautics.
Thomason, L., Poole, L., Deshler, T., 1997. A global climatology of stratospheric aerosol surface area density deduced from stratospheric aerosol and gas experiment II measurements: 1984–1994. J. Geophys. Res. 102 (D7), 8967–8976.
Tie, X., Zhang, R., Brasseur, G., Lei, W., 2002. Global NO_x production by lightning. J. Atmos. Chem. 43, 61–74.
Tompkins, A.M., Gierens, K., Rädel, G., 2007. Ice supersaturation in the ECMWF integrated forecast system. Q. J. Roy. Meteorol. Soc. 133 (622), 53–63.
Treffeisen, R., Krejci, R., Ström, J., Engvall, A.C., Herber, A., Thomason, L., 2007. Humidity observations in the Arctic troposphere over Ny-Ålesund, Svalbard based on 15 years of radiosonde data. Atmos. Chem. Phys. 7, 2721–2732.
Tremmel, H.G., Schalger, H., Konopka, P., Schulte, P., Arnold, F., Klemm, M., Droste-Franke, B., 1998. Observations and model calculations of jet aircraft exhaust products at cruise altitude and inferred initial OH emissions. J. Geophys. Res. 103 (D9), 10803–10816.
Tremmel, H.G., Schumann, U., 1999. Model simulations of fuel sulfur conversion efficiencies in an aircraft engine: dependence on reaction rate constants and initial species mixing ratios. Aerosp. Sci. Technol. 3, 417–430.
Tsague, L., Tsogo, J., Tatietse, T.T., 2006. Prediction of the production of nitrogen oxide (NO_x) in turbojet engines. Atmos. Environ. 40, 5727–5733.
Twomey, S., 1974. Pollution and the planetary albedo. Atmos. Environ. 8, 1251–1256.
Twomey, S., 1977. The influence of pollution on the shortwave albedo of clouds. J. Atmos. Sci. 34, 1149–1152.
Uherek, E., Halenka, T., Balkanski, Y., Berntsen, T., Borken-Kleefeld, J., Borrego, C., Gauss, M., Hoor, P., Juda-Rezler, K., Lelieveld, J., Melas, D., Rypdal, K., Schmid, S., 2010. Transport impacts on atmosphere and climate: land transport. Atmos. Environ 40, 4772–4816.
Vancassel, X., Sorokin, A., Mirabel, P., Petzold, A., Wilson, C., 2004. Volatile particles formation during PartEmis: a modelling study. Atmos. Chem. Phys. 4, 439–447.
Vatazhin, A.B., Kozlov, V.E., Starik, A.M., Kholshchevnikova, E.K., 2007. Numerical modeling of the formation of aerosol particles in jet engine plumes. Fluid Dynam. 42 (1), 33–43.
Voigt, C., Schlager, H., Ziereis, H., Kärcher, B., Luo, B.P., Schiller, C., Krämer, M., Popp, P.J., Irie, H., Kondo, Y., 2006. Nitric acid in cirrus clouds. Geophys. Res. Lett. 33, L05803. doi:10.1029/2005GL025159.
Voigt, C., Kärcher, B., Schlager, H., Schiller, C., Krämer, M., de Reus, M., Vössing, H., Borrmann, S., Mitev, V., 2007. In-situ observations and modeling of small nitric acid-containing ice crystals. Atmos. Chem. Phys. 7, 3373–3383.

Von Kuhlmann, R., Lawrence, M.G., 2006. The impact of ice uptake of nitric acid on atmospheric chemistry. Atmos. Chem. Phys. 6, 225–235.
Wahner, A., Geller, M.A., Arnold, F., Brune, W.H., Cariolle, D.A., Douglass, A.R., Johnson, C., Lister, D.H., Pyle, J.A., Ramaroson, R., Rind, D., Rohrer, F., Schumann, U., Thompson, A.M., 1995. Subsonic and supersonic aircraft emissions. In: 'Scientific Assessment of Ozone Depletion: 1994' World Meteorological Organization Global Ozone Research and Monitoring project—Report No. 37, Geneva.
Wang, P.-H., Minnis, P., Patrick McCormick, M., Kent, G.S., Skeens, K.M., 1996. A 6-year climatology of cloud occurrence frequency from Stratospheric Aerosol and Gas Experiment II observations (1985–1990). J. Geophys. Res. 101 (D23), 29407–29429.
Wang, W.C., Pinto, J.P., Yung, Y.L., 1980. Climatic effects due to halogenated compounds in the Earth's atmosphere. J. Atmos. Sci. 37, 333–338.
Wardle, D.A., 2003. Global sale of green air travel supported using biodiesel. Renew. Sustain. Energ. Rev. 7, 1–64.
Waugh, D.W., Eyring, V., 2008. Quantitative performance metrics for stratospheric-resolving chemistry–climate models. Atmos. Chem. Phys. 8, 5699–5713.
Wei, C.-F., Larson, S.M., Patten, K.O., Wuebbles, D.J., 2001. Modeling of ozone reactions on aircraft-related soot in the upper troposphere and lower stratosphere. Atmos. Environ. 35, 6167–6180.
Weisenstein, D., Ko, M., Dyominov, I., Pitari, G., Ricciardulli, L., Visconti, G., Bekki, S., 1998. The effects of sulfur emissions from HSCT aircraft: a 2-D model intercomparison. J. Geophys. Res. 103 (D1), 1527–1547.
Wey, C.C., Anderson, B.E., Wey, C., Miake-Lye, R.C., Whitefield, P., Howard, R., 2007. Overview on the aircraft particle emissions experiment. J. Propul. Power 23 (5), 898–905. doi:10.2514/1.26406.
Widhopf, G.F., Glatt, L., Kramer, R.F., 1977. Potential ozone column increase resulting from subsonic and supersonic aircraft NO_x emissions. AIAA J. 15, 1322–1330.
Wild, O., Prather, M.J., Akimoto, H., 2001. Indirect long-term global radiative cooling from NO_x emissions. Geophys. Res. Lett. 28 (9), 1719–1722.
Wilhelm, S., Haverkamp, H., Sorokin, A., Arnold, F., 2004. Detection of very large ions in aircraft gas turbine engine combustor exhaust: charged small soot particles? Atmos. Environ. 38, 4561–4569.
Wilson, C.W., Petzold, A., Nyeki, S., Schumann, U., Zellner, R., 2004. Measurement and prediction of emissions of aerosols and gaseous precursors from gas turbine engines (PartEmis): an overview. Aerosp. Sci. Technol. 8, 131–143.
Winker, D.M., Trepte, C.R., 1998. Laminar cirrus observed near the tropical tropopause by LITE. Geophys. Res. Lett. 25 (17), 3351–3354.
Wit, R.C.N., Boon, B.H., van Velzen, A., Cames, M., Deuber O., Lee D.S., 2005. Giving wings to emission trading. Inclusion of aviation under the European emission trading system (ETS): design and impacts. CE-Delft, No. ENC.C.2/ETU/2004/0074r, the Netherlands.
Wohlfrom, K.-H., Eichkorn, S., Arnold, F., Schulte, P., 2000. Massive positive and negative ions in the wake of a jet aircraft: detection by a novel aircraft-based Large Ion Mass Spectrometer (LIOMAS). Geophys. Res. Lett. 27 (23), 3853–3856.
Wormhoudt, J., Herndon, S.C., Yelvington, P.E., Lye-Miake, R.C., Wey, C., 2007. Nitrogen oxide (NO/NO2/HONO) emissions measurements in aircraft exhausts. J. Propul. Power 23 (5), 906–911. doi:10.2514/1.23461.
Wu, S., Mickley, L.J., Jacob, D.J., Logan, J.A., Yantosca, R.M., Rind, D., 2007. Why are there large differences between models in global budgets of tropospheric ozone? J. Geophys. Res. 112, D05302. doi:10.1029/2006JD007801.
Wuebbles, D.J., Dutta, M., Patten, K.O., Baughcum, S.L., 2003a. Parametric study of potential effects of aircraft emissions on stratospheric ozone. In: Sausen, R., Fichter, C., Amanatidis, G. (Eds.), European Conference on Aviation, Atmosphere and Climate (AAC), Proceedings of an International Conference, Friedrichshafen, Germany, 30 June–3rd July 2003. European Commission, pp. 140–144. Air Pollution Research Report 83.
Wuebbles, D.J., Dutta, M., Jain, A.K., Baughcum, S.L., 2003b. Radiative forcing on climate from stratospheric aircraft emissions. In: Sausen, R., Fichter, C., Amanatidis, G. (Eds.), European Conference on Aviation, Atmosphere and Climate (AAC), Proceedings of an International Conference, Friedrichshafen, Germany, 30 June–3rd July 2003. European Commission, pp. 184–189. Air Pollution Research Report 83.
Wylie, D.P., Menzel, W.P., 1999. Eight years of high cloud statistics using HIRS. J. Clim. 12, 170–184.
Wyser, K., 1998. The effective radius in ice clouds. J. Clim. 11, 1793–1802.
Yelvington, P.E., Herndon, S.C., Wormhoudt, J.C., Jayne, J.T., Miake-Lye, R.C., Berk Knighton, W., Wey, C., 2007. Chemical speciation of hydrocarbon emissions from a commercial aircraft engine. J. Propul. Power 23 (5), 912–918. doi:10.2514/1.23520.
Yilmaz, A., Hindiyarti, L., Jensen, A.D., Glarborg, P., Marshall, P., 2006. Thermal dissociation of SO_3 at 1000–1400 K. J. Phys. Chem. A 110 (21), 6654–6659. doi:10.1021/jp0557215.
Yu, F., Turco, R.P., 1998. Contrail formation and impacts on aerosol properties in aircraft plumes: effects of fuel sulfur content. Geophys. Res. Lett. 25 (3), 313–316.
Yu, F., Turco, R.P., 1999. Evolution of aircraft-generated volatile particles in the far wake regime: potential contributions to ambient CCN/IN. Geophys. Res. Lett. 26 (12), 1703–1706.
Zellner, R., 2000. Chemistry and Microphysics of Contrail Formation, CHEMICON. Univ. Essen, 194 pp, Final Report, June 1998–May 2000, Contract No. ENV4-CT97-0620.
Zerefos, C.S., Eleftheratos, K., Balis, D.S., Zanis, P., Tselioudis, G., Meleti, C., 2003. Evidence of impact of aviation on cirrus cloud formation. Atmos. Chem. Phys. 3, 1633–1644.
Zerefos, C.S., Eleftheratos, K., Zanis, P., Balis, D.S., Tselioudis, G., 2007. Search for man-made cirrus contrails over Southeast Asia. TAO 18, 459–474.
Zuberi, B., Bertram, A.K., Cassa, C.A., Molina, L.T., Molina, M.J., 2002. Heterogeneous nucleation of ice in $(NH_4)_2SO_4$–H_2O particles with mineral dust immersions. Geophys. Res. Lett. 29 (10), 1504. doi:10.1029/2001GL014289.

Acronyms and abbreviations
Abbreviation–Full

AAC: Aviation, Atmosphere and Climate conference
ACARE: Advisory Council for Aeronautical Research in Europe
ACCENT: Atmospheric Composition Change the European Network of Excellence
ACM: Atmosphere–Chemistry Model
AEM: Advanced Emission Model
AERO2K: Global aviation emission inventories for 2000 and 2025
AEROCHEM: Project to study effect of aircraft emissions on ozone
AIC: Aviation-Induced Cirrus
AIRS: Atmospheric Infrared Sounder
AMDAR: Aircraft Meteorological Data Reporting
ASK: Available Seat Kilometres
ATM: Air Traffic Management
ATTAS: Advanced Technologies Testing Aircraft System
ATTICA: Assessment of Transport Impacts on Climate Change and Ozone Depletion
AVHRR: Advanced Very High Resolution Radiometer
BC: Black Carbon
CAEP: Committee on Aviation Environmental Protection
CAM: Community Atmosphere Model
CCM: Chemistry–Climate Model
CCMVal: Chemistry–Climate Model Validation (CCMVal) activity for WCRP's (World Climate Research Programme) SPARC (Stratospheric Processes and their Role in Climate) project
CHEMICON: Chemistry And Microphysics Of Contrail Formation
CI: Chemi-Ions
CIAP: Climatic Impact Assessment Program
CICERO: Centre for International Climate and Environmental Research (Norway)
CN: Condensation Nuclei
CO_2eq: CO_2 equivalent
COMESA: Committee on Meteorological Effects of Stratospheric Aircraft
CONSAVE: Constrained Scenarios on Aviation and Emissions
COVOS: Comite sur les Consequences des Vols Stratospheriques
CRYOPLANE: Liquid Hydrogen Fuelled Aircraft - System Analysis
CRYSTAL-FACE: The Cirrus Regional Study of Tropical Anvils and Cirrus Layers – Florida Area Cirrus Experiment
CSIRO: Commonwealth Scientific and Industrial Research Organisation (Australia)
CTM: Chemical Transport Model
CYPRESS: Engine Cycle Prediction and Emissions Study
DGLR: Deutsche Gesellschaft für Luft- und Raumfahrt (Germany)
DLR: Deutsches Zentrum für Luft- und Raumfahrt (Germany)
DU: Dobson Units
EC: European Commission
ECHAM: ECMWF Hamburg GCM
ECMWF: European Centre for Medium-Range Weather Forecasts
EI: Emission Index
EI_{H2O}: Emission Index (Water Vapour)
EI_{NOx}: Emission Index (Nitrogen Oxides)
EIOM: Emission Index (Organic Matter) $\mu g\ g^{-1}$ fuel
EI_{SO2}: Emission Index (Sulphur Dioxide)
EMERALD-I: Egrett Microphysics Experiment, with radiation, Lidar and Dynamics
ENSO: El Nino Southern Oscillation
ESCT: European Supersonic Civil Transport
ETHmeg: Database for CTM model validation studies
EU: European Union
EULINOX: European Lightning Nitrogen Oxides Project
EUROCONTROL: European Organisation for the Safety of Air Navigation
EWF: CO_2 Emissions Weighting Factor
FP6: Sixth Framework Program
FSC: Fuel Sulphur Content
GCM: General Circulation Model
GDP: Gross Domestic Product
GHG: Greenhouse Gas
GMI: Global Modeling Initiative
GTP: Global Temperature Change Potential
GTP_{20}: GTP with a 20 year time horizon
GTP_{50}: GTP with a 50 year time horizon
GTP_{100}: GTP with a 100 year time horizon
GWP: Global Warming Potential
GWP_{100}: GWP with a 100 year time horizon
GWP_{20}: GWP with a 20 year time horizon
HALOE: Halogen Occultation Experiment
HET: Heterogeneous
HOM: Homogeneous
HSCT: High Speed Civil Transport
ICAO: International Civil Aviation Organization
IEA: International Energy Agency

IGCM: Intermediate GCM
IN: Ice Nuclei
INCA: Interhemispheric Differences in Cirrus Properties From Anthropogenic Emissions
IPCC: Intergovernmental Panel on Climate Change
ISCCP: International Satellite Cloud Climatology Project
ISSR: Ice-Supersaturated Regions
IWC: Ice Water Content
JPL: Jet Propulsion Laboratory (US)
KL: Kärcher parameterization
LACE: Lindenberg Aerosol Characterization Experiment
LH_2: Liquid Hydrogen
LIF: Laser Induced Fluorescence
LINOX: Lightning Nitrogen Oxides
LLGHG: Long Lived Greenhouse Gas
LMDz: Laboratoire de Météorologie Dynamique (France)
LOSU: Level of Scientific Understanding
LP: Liu and Penner parameterization
LTO: Landing-Takeoff Cycle
LTTG: Long-Term Technology Goals for NO_x
LW: Long-wave
MATCH: Model of Atmospheric Transport and Chemistry
METRIC: Metrics of climate change
MLS: Microwave limb Sounder
MM: Meteorological Model
MOZAIC: Measurement of OZone by Airbus In-service airCraft
MTTG: Medium-Term Technology Goals for NO_x
NAFC: North Atlantic Flight Corridor
NAO: North Atlantic Oscillation
NASA: National Aeronautics and Space Administration
NEPAIR: New Emissions Parameter for aircraft
NH: Northern Hemisphere
N_i: Ice Crystal Number Concentration
NOXAR: Nitrogen Oxides and Ozone along Air Routes
OAG: Official Airline Guide
OC–EC: Organic Carbon – Elemental Carbon
OPE: Ozone Production Efficiency
PartEmis: Measurement and predictions of the emission of aerosols and gaseous precursors from gas turbine engines
POLINAT: Pollution from Aircraft Emissions in the North Atlantic Flight Corridor
PSC: Polar Stratospheric Cloud
QBO: Quasi-Biennial Oscillation
QUANTIFY: Quantifying the Climate Impact of Global and European Transport Systems
RF: Radiative Forcing
RFI: Radiative Forcing Index
RHI: Relative Humidity Over Ice
RPK: Revenue Passenger Kilometres
RT: Radiative Transfer
RTK: Revenue Tonne Kilometres
RTM: Radiative Transfer Model
SAD: Surface Area Density
SAGE: System for assessing Aviation's Global Emissions
SARS: Severe Acute Respiratory Syndrome
SCENIC: Scenarios of aircraft emissions and impact studies on chemistry and climate
SCM: Simple Climate Model
SH: Southern Hemisphere
SLIMCAT: Stratosphere-only version of TOMCAT, an offline CTM
SRES: Special Report on Emissions Scenarios
SSBJ: Supersonic Business Jet
STP: Standard Temperature and Pressure
STS: Super-cooled Ternary Solutions
SUB: Subsonic
SUCCESS: Subsonic Aircraft: Contrail and Cloud Effects Special Study
SW: Short-Wave
TAR: Third Assessment Report
TCA: Technology Concept Aircraft
TH100: Time Horizon of 100 years
TH20: Time Horizon of 20 years
TH50: Time Horizon of 50 years
TM3: Chemistry–Transport Model
TOA: Top of Atmosphere
TOMCAT: Three-dimensional (3D) offline CTM
TOVS: TIROS-N (Television Infra-Red Observation Satellite) Operational Vertical Sounder
TRADEOFF: Aircraft emissions: Contributions of various climate compounds to changes in composition and radiative forcing – tradeoff to reduce atmospheric impact
TROCCINOX: Tropical Convection, Cirrus and Nitogen Oxides Experiment
TTL: Tropical Tropopause Layer
UCAM: University of Cambridge
UiO: University of Oslo
ULAQ: University of L'Aquila
UNFCCC: United Nations Framework Convention on Climate Change
UTLS: Upper Troposphere and Lower Stratosphere
UV: Ultraviolet

Some chemical symbols used in this assessment

BrO: Bromine monoxide
$BrONO_2$: Bromine nitrate
Br_x: bromine species
C: atomic carbon
$C_{12}H_{23}$: kerosene
CH_4: methane
ClO: Chlorine monoxide
Cl_x: chlorine species
CO: carbon monoxide
CO_2: carbon dioxide
H: hydrogen
H_2: hydrogen molecule
H_2O: water vapour
H_2O_2: hydrogen peroxide
H_2SO_4: sulphuric acid
HC: hydrocarbon
HNO_2/HONO: nitrous acid
HNO_3: nitric acid
HO_2: hydroperoxy radical
HO_x: the sum of OH and HO_2
HSO_4: Hydrogen sulphate
$h\nu$: ultra violet radiation
N: atomic nitrogen
N_2O: nitrous oxide
N_2O_5: Dinitrogen pentoxide
NAT: nitric acid trihydrate
NMHC: non-methane hydrocarbons
NO: Nitric oxide
NO_2: nitrogen dioxide
NO_x: nitrogen oxides ($NO + NO_2$)
NO_y: Odd reactive nitrogen (NO, NO_2, NO_3, N_2O_5, $ClONO_2$, HNO_4, HNO_3)
O: atomic oxygen
$O(^3P)$: atomic oxygen in the ground state formed from the photodissociation of O_2
O_2: oxygen molecule
O_3: ozone
OH: hydroxyl radical
PAN: peroxy acetyl nitrate
S: atomic sulfur
S^{IV}: Sulphur (oxidation state four)
SO_2: sulphur dioxide
SO_3: sulphur trioxide
SO_x: sulphur oxides
STE^{inf}: ozone influx from the stratosphere
S^{VI}: Sulphur (oxidation state six)